

2-3043 77
①

Resy 100pp

UNLIMITED

AGARD-AR-291

AGARD-AR-291

AGARD

ADVISORY GROUP FOR AEROSPACE RESEARCH & DEVELOPMENT
7 RUE ANCELLE 92200 NEUILLY SUR SEINE FRANCE

AGARD ADVISORY REPORT 291

A

Technical Status Review Appraisal of the Suitability of Turbulence Models Flow Calculations

Revue Technique — L'Evaluation de l'Applicabilité
Modèles de Turbulence dans le Calcul
(Ecoulements)

Processed / not processed by DIMS
.....signed.....date
W. J. ... 8/6/95
NOT FOR DESTRUCTION



NORTH ATLANTIC TREATY ORGANIZATION

UNLIMITED



AGARD

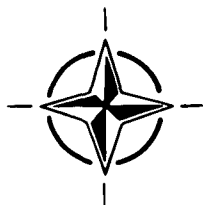
ADVISORY GROUP FOR AEROSPACE RESEARCH & DEVELOPMENT
7 RUE ANCELLE 92200 NEUILLY SUR SEINE FRANCE

AGARD ADVISORY REPORT 291

Technical Status Review Appraisal of the Suitability of Turbulence Models in Flow Calculations

(Revue Technique — L'Evaluation de l'Applicabilité
des Modèles de Turbulence dans le Calcul
des Ecoulements)

This Advisory Report was prepared at the request of
the Fluid Dynamics Panel of AGARD at a Technical Status Review
held in Friedrichshafen, Germany, 26th April 1990.



North Atlantic Treaty Organization
Organisation du Traité de l'Atlantique Nord

The Mission of AGARD

According to its Charter, the mission of AGARD is to bring together the leading personalities of the NATO nations in the fields of science and technology relating to aerospace for the following purposes:

- Recommending effective ways for the member nations to use their research and development capabilities for the common benefit of the NATO community;
- Providing scientific and technical advice and assistance to the Military Committee in the field of aerospace research and development (with particular regard to its military application);
- Continuously stimulating advances in the aerospace sciences relevant to strengthening the common defence posture;
- Improving the co-operation among member nations in aerospace research and development;
- Exchange of scientific and technical information;
- Providing assistance to member nations for the purpose of increasing their scientific and technical potential;
- Rendering scientific and technical assistance, as requested, to other NATO bodies and to member nations in connection with research and development problems in the aerospace field.

The highest authority within AGARD is the National Delegates Board consisting of officially appointed senior representatives from each member nation. The mission of AGARD is carried out through the Panels which are composed of experts appointed by the National Delegates, the Consultant and Exchange Programme and the Aerospace Applications Studies Programme. The results of AGARD work are reported to the member nations and the NATO Authorities through the AGARD series of publications of which this is one.

Participation in AGARD activities is by invitation only and is normally limited to citizens of the NATO nations.

The content of this publication has been reproduced directly from material supplied by AGARD or the authors.

Published July 1991

Copyright © AGARD 1991
All Rights Reserved

ISBN 92-835-0625-1



Printed by *Specialised Printing Services Limited*
40 Chigwell Lane, Loughton, Essex IG10 3TZ

Recent Publications of the Fluid Dynamics Panel

AGARDOGRAPHS (AG)

Experimental Techniques in the Field of Low Density Aerodynamics

AGARD AG-318 (E), April 1991

Techniques Expérimentales Liées à l'Aérodynamique à Basse Densité

AGARD AG-318 (FR), April 1990

A Survey of Measurements and Measuring Techniques in Rapidly Distorted Compressible Turbulent Boundary Layers

AGARD AG-315, May 1989

Reynolds Number Effects in Transonic Flows

AGARD AG-303, December 1988

Three Dimensional Grid Generation for Complex Configurations – Recent Progress

AGARD AG-309, March 1988

REPORTS (R)

Aircraft Dynamics at High Angles of Attack: Experiments and Modelling

AGARD R-776, Special Course Notes, March 1991

Inverse Methods in Airfoil Design for Aeronautical and Turbomachinery Applications

AGARD R-780, Special Course Notes, November 1990

Aerodynamics of Rotorcraft

AGARD R-781, Special Course Notes, November 1990

Three-Dimensional Supersonic/Hypersonic Flows Including Separation

AGARD R-764, Special Course Notes, January 1990

Advances in Cryogenic Wind Tunnel Technology

AGARD R-774, Special Course Notes, November 1989

ADVISORY REPORTS (AR)

Rotary-Balance Testing for Aircraft Dynamics

AGARD AR-265, Report of WG 11, December 1990

Calculation of 3D Separated Turbulent Flows in Boundary Layer Limit

AGARD AR-255, Report of WG10, May 1990

Adaptive Wind Tunnel Walls: Technology and Applications

AGARD AR-269, Report of WG12, April 1990

Drag Prediction and Analysis from Computational Fluid Dynamics: State of the Art

AGARD AR-256, Technical Status Review, June 1989

CONFERENCE PROCEEDINGS (CP)

Vortex Flow Aerodynamics

AGARD CP-494, July 1991

Missile Aerodynamics

AGARD CP-493, October 1990

Aerodynamics of Combat Aircraft Controls and of Ground Effects

AGARD CP-465, April 1990

Computational Methods for Aerodynamic Design (Inverse) and Optimization

AGARD CP-463, March 1990

Applications of Mesh Generation to Complex 3-D Configurations

AGARD CP-464, March 1990

Fluid Dynamics of Three-Dimensional Turbulent Shear Flows and Transition
AGARD CP-438, April 1989

Validation of Computational Fluid Dynamics
AGARD CP-437, December 1988

Aerodynamic Data Accuracy and Quality: Requirements and Capabilities in Wind Tunnel Testing
AGARD CP-429, July 1988

Aerodynamics of Hypersonic Lifting Vehicles
AGARD CP-428, November 1987

Aerodynamic and Related Hydrodynamic Studies Using Water Facilities
AGARD CP-413, June 1987

Applications of Computational Fluid Dynamics in Aeronautics
AGARD CP-412, November 1986

Store Airframe Aerodynamics
AGARD CP-389, August 1986

Unsteady Aerodynamics – Fundamentals and Applications to Aircraft Dynamics
AGARD CP-386, November 1985

Aerodynamics and Acoustics of Propellers
AGARD CP-366, February 1985

Improvement of Aerodynamic Performance through Boundary Layer Control and High Lift Systems
AGARD CP-365, August 1984

Wind Tunnels and Testing Techniques
AGARD CP-348, February 1984

Aerodynamics of Vortical Type Flows in Three Dimensions
AGARD CP-342, July 1983

Missile Aerodynamics
AGARD CP-336, February 1983

Prediction of Aerodynamic Loads on Rotorcraft
AGARD CP-334, September 1982

Wall Interference in Wind Tunnels
AGARD CP-335, September 1982

Fluid Dynamics of Jets with Applications to V/STOL
AGARD CP-308, January 1982

Aerodynamics of Power Plant Installation
AGARD CP-301, September 1981

Computation of Viscous-Inviscid Interactions
AGARD CP-291, February 1981

Subsonic/Transonic Configuration Aerodynamics
AGARD CP-285, September 1980

Turbulent Boundary Layers Experiments, Theory and Modelling
AGARD CP-271, January 1980

Aerodynamic Characteristics of Controls
AGARD CP-262, September 1979

High Angle of Attack Aerodynamics
AGARD CP-247, January 1979

Dynamic Stability Parameters
AGARD CP-235, November 1978

Unsteady Aerodynamics
AGARD CP-227, February 1978

Laminar-Turbulent Transition
AGARD CP-224, October 1977

Preface

The past decade has seen a rapidly accelerating development of computational methods, following the ever increasing computing power offered by modern technology.

The new tool has found immediate and wide application in fluid dynamics initiating a new era in this field by opening unlimited, as we see it at the present time, horizons in research and development with corresponding technical implications for the aerospace industry. In retrospect it appears, that the fluid dynamicist of the sixties or even the seventies, could have hardly imagined that solving problems of considerable complexity as those handled by today's computers, could have been possible within the elapsed short period of time.

During the first part of the past decade the ability of the developed computer codes to produce relatively economically a great amount of information regarding flow characteristics around bodies of complex geometries created a sense of euphoria mainly among users of computational techniques. However, it was soon recognized that in order to produce valid answers to questions related to intricate flow cases by employing CFD methods, more is required than simply developing computer capabilities matching the complexities of the problem. Validation procedures, initiated as early as 1968 with the first Stanford conference, have been gradually introduced as an indispensable part of developing valid computer codes. Equally important, it has been also widely recognized, that suitable modelling of physical processes in flows, such as turbulence transport, constitutes a crucial factor for the development of successful prediction codes. This cannot be achieved without adequate understanding of the underlying physical aspects of these phenomena.

The Fluid Dynamics Panel of AGARD has shown a keen interest in computational fluid dynamics in general and for turbulence modelling in particular, following very closely the developments in these areas, as related to the arising needs, especially in the aerospace industry. As a result, several activities in the form of symposia, specialists' meetings, working groups etc. have been proposed and organized by the panel during the last decade. In this context the FDP has organized a Technical Status Review activity on the "Appraisal of the Suitability of Turbulence Models in Flow Calculations" which took place in Friedrichshafen, Germany on April 26, 1990, resulting in the publication of the present Advisory Report. The general scientific scope within which the present TSR activity was placed, has been defined as follows:

- i) To carry out an in depth appraisal of the suitability of existing turbulence models for use in flow calculations. For this purpose, available information from the existing theoretical and experimental work on the subject should be reviewed and critically evaluated.

In this process, the underlying physical concepts for each particular turbulence model should be considered as they apply to different flow cases, therefore establishing the range of validity of each model for flow calculations. Existing uncertainties, discrepancies, inadequacies and failures in reported results, rising from inherent limitations in the employed model and/or its inappropriate application, should be pointed out and discussed.

- ii) To evaluate the potential of existing knowledge regarding turbulence models, in covering present and future needs in the field of flow calculations.
- iii) Based on the above studies, to issue guidelines for future theoretical and experimental work and propose a number of key experiments and flow calculations cases to be conducted in the future.

Since the capability of a Technical Status Review activity to fulfil such an ambitious scope is rather limited, a subcommittee has been initiated and operates, in order to follow developments on the subject and suggest to the panel future appropriate actions to be taken.

As the chairman of the Technical Status Review I would like to express my gratitude to each and all members of the committee responsible for organizing and implementing this activity. Their interest and enthusiasm has guaranteed the participation of well-known members of the scientific community working on the subject. I would also like to express my appreciation to the executive of the Fluid Dynamics Panel, Dr W. Goodrich for the interest he has shown and the assistance extended to the committee in carrying this effort to its final goal of publishing the present Advisory Report.

D.D. Papailiou
Chairman of the TSR committee

Préface

La dernière décennie a été marquée par le développement fulgurant des méthodes de calcul grâce à l'accroissement de la puissance des ordinateurs offert par les technologies modernes.

Ce nouvel outil a trouvé des applications diverses et immédiates en dynamique des fluides, où il a permis d'ouvrir un nouveau domaine d'intérêt avec, apparemment, des horizons illimités de recherche et développement ayant des implications techniques importantes pour l'industrie aérospatiale. Rétrospectivement, il est certain que le spécialiste en dynamique des fluides des années soixante ou soixante dix aurait eu du mal à imaginer que la résolution de problèmes aussi complexes que ceux qui sont traités par les ordinateurs modernes serait acquise dans un laps de temps si court.

Pendant la première partie de la dernière décennie, la capacité des codes machine évolués pour générer, à faible coût relatif, un volume considérable de données sur les caractéristiques des écoulements autour de corps de géométries complexes a créé l'euphorie, principalement chez les utilisateurs des techniques de calcul. Cependant, il a été vite reconnu que pour obtenir des réponses valables aux questions touchant des cas d'écoulements complexes avec des méthodes d'aérodynamique numérique, il ne suffit pas seulement de développer les capacités de l'ordinateur pour qu'il corresponde aux complexités du problème.

Les procédures de validation, dont les premières datent de 1968, époque de la première conférence de Stanford, se sont révélées peu à peu indispensable au développement de codes machine valables.

Il est également important de noter qu'il a été largement reconnu que la modélisation adéquate de certains processus physiques dans les écoulements, tel que le transport de la turbulence, constitue un facteur critique pour le développement de codes de prédiction performants. Ceci ne peut se faire sans l'acquisition de connaissances appropriées des aspects physiques sous-jacents de ces phénomènes.

Le Panel AGARD de la dynamique des fluides s'intéresse vivement à l'aérodynamique numérique en général et à la modélisation de la turbulence en particulier. Il suit de très près les travaux en cours dans ces domaines, dans la mesure où ils correspondent aux besoins qui se font sentir, en particulier dans l'industrie aérospatiale. Par conséquent, différentes activités telles que symposia, réunions de spécialistes, groupes de travail etc.. ont été proposées et organisées par le Panel au cours de la dernière décennie. Dans ce cadre, le FDP a développé une activité de revue technique de l'état de l'art, intitulée "L'évaluation de l'applicabilité de modèles de turbulence dans le calcul des écoulements" le 26 avril 1990 à Friedrichshafen en Allemagne. Le présent rapport consultatif est le fruit de cette réunion. Le cadre scientifique général de ce rapport est défini comme suit:

- i) Faire une évaluation détaillée de l'applicabilité des modèles de turbulence existants pour le calcul des écoulements. A cette fin, les informations résultant des travaux théoriques et expérimentaux doivent être revus et évalués de façon critique.

Dans ce procédé, les concepts physiques de base pour chaque modèle de turbulence doivent être considérés par rapport à différents cas d'écoulements. Les incertitudes, divergences, insuffisances et échecs dont il est fait mention dans les résultats, et qui proviennent des limitations propres du modèle employé et/ou de son application inopportune doivent être signalées et discutées.

- ii) Evaluer le potentiel des connaissances actuelles en ce qui concerne les modèles de turbulence pour couvrir les besoins actuels et futurs dans le domaine du calcul des écoulements.
- iii) Sur la base de ces études, établir des directives pour de futurs travaux théoriques et expérimentaux et proposer un certain nombre d'expériences clés et de cas de calcul d'écoulements à lancer à l'avenir.

Un programme si ambitieux déborde du cadre d'un tel examen et un sous-comité a donc été créé. Il a pour mandat de suivre les développements dans ce domaine et de recommander des actions futures à prendre par le Panel.

En tant que Président de cette revue technique de l'état de l'art, je tiens à exprimer ma reconnaissance envers tout et chacun des membres du comité responsable de l'organisation et de la mise en oeuvre de cette activité. Grâce à leur motivation et à leur enthousiasme, nous avons pu compter sur la participation de plusieurs membres éminents de la communauté scientifique qui travaillent sur ce sujet. Je tiens enfin à remercier l'Administrateur du Panel de la Dynamique des Fluides, le Dr W. Goodrich, pour l'intérêt qu'il a manifesté pour ce projet et pour l'aide qu'il a bien voulu apporter au comité pour la concrétisation de ces efforts sous la forme du présent rapport consultatif.

D.D. Papailiou

Fluid Dynamics Panel

Chairman: Dr W.J. McCroskey
Senior Staff Scientist
US Army Aero Flightdynamics Directorate
Mail Stop N-258-1
NASA Ames Research Center
Moffett Field, CA 94035-1099
United States

Deputy Chairman: Professor Ir J.W. Slooff
National Aerospace Laboratory NLR
Anthony Fokkerweg 2
1059 CM Amsterdam
The Netherlands

PROGRAMME COMMITTEE

Prof. D. Papailiou (Chairman)
Dept. of Mechanical Engineering
University of Patras
Kato Kostritsi
Patras 26500, Greece

Prof. R. Decuyper
Ecole Royale Militaire
Chaire de Mécanique Appliquée
Avenue de la Renaissance
B-1040 Brussels, Belgium

M. l'Ing. Général B. Monnerie
Directeur Adjoint de l'Aérodynamique
pour les Applications
ONERA
B.P. 72
92322 Châtillon Cedex, France

Dr. W. Schmidt
Messerschmitt-Bölkow-Blohm GmbH
Director, Air Vehicle Engineering
Military Airplane Division
8000 München 80, Germany

Prof. M. Onorato
Dipartimento di Ingegneria
Aeronautica e Spaziale
Politecnico di Torino
C. so Duca degli Abruzzi 24
10129 Torino, Italy

Ir A. Elsenaar
National Aerospace Laboratory NLR
Anthony Fokkerweg 2
1059 CM Amsterdam, The Netherlands

Prof. Dr T. Ytrehus
Division of Applied Mechanics
The University of Trondheim
The Norwegian Inst. of Technology
N-7034 Trondheim — NTH
Norway

Prof. J. Jimenez
Escuela Tecnica Superior de
Ingenieros Aeronauticos
Departamento de Mecanica de Fluidos
Plaza del Cardenal Cisneros 3
28040 Madrid, Spain

Dr Ü. Kaynak
TUSAŞ
Havacılık ve Uzay San. A.S.
P.K. 18 Kavaklıdere
06690 Ankara, Turkey

Prof. A.D. Young
70 Gilbert Road
Cambridge CB4 3PD
United Kingdom

Dr S. Lekoudis
Director (Acting) Mechanics Div.
Code 1132
Office of Naval Research
Arlington, VA 22217-5000
United States

PANEL EXECUTIVE

Dr W. Goodrich

Mail from Europe:
AGARD—OTAN
Attn: FDP Executive
7, rue Ancelle
F-92200 Neuilly-sur-Seine
France

Mail from US and Canada:
AGARD—NATO
Attn: FDP Executive
APO New York 09777

Tel: 33 (1) 47 38 57 75
Telex: 610176F
Telefax: 33 (1) 47 38 57 99

Contents

	Page
Recent Publications of the Fluid Dynamics Panel	iii
Preface	v
Préface	vi
Fluid Dynamics Panel and Programme Committee	vii
	Reference
<i>Presents the following papers:</i>	
Turbulence Modelling: Survey of Activities in Belgium and the Netherlands, an Appraisal of the Status and a View on the Prospects by B. van den Berg	1
Calculation of Turbulent Compressible Flows by J. Cousteix	2
Some Current Approaches in Turbulence Modelling by W. Rodi	3
Turbulence Models for Natural Convection Flows along a Vertical Heated Plane by D.D. Papailiou	4
Turbulent Flow Modelling in Spain. Overview and Developments by C. Dopazo, R. Aliod and L. Valiño	5
Computational Turbulence Studies in Turkey by Ü. Kaynak	6
Appraisal of the Suitability of Turbulence Models in Flow Calculations: A UK View on Turbulence Models for Turbulent Shear Flow Calculations by G.M. Lilley	7
Collaborative Testing of Turbulence Models by P. Bradshaw	8

TURBULENCE MODELLING: SURVEY OF ACTIVITIES IN BELGIUM AND THE NETHERLANDS, AN APPRAISAL OF THE STATUS AND A VIEW ON THE PROSPECTS

B. van den Berg
 National Aerospace Laboratory NLR
 P.O. Box 90502
 1006 BM Amsterdam
 The Netherlands

SUMMARY

Turbulence research proceeding presently at various places in the Netherlands and Belgium is briefly reviewed. Subsequently some experimental results obtained in turbulent boundary layers, as occur on airplane wings, are considered in relation to the usual turbulence model assumptions. The status of turbulence modelling is found not to be satisfactory. To support the development of semi-empirical models of acceptable accuracy, a more extensive base of reliable turbulence data would be desirable.

MAIN SYMBOLS

k constant in mixing length relation
 l mixing length
 p static pressure
 q turbulent kinetic energy
 u,v,w fluctuating velocities
 U,V mean velocities, in x- and y-direction
 x,y coordinates, approximately parallel and normal to the mean flow direction
 δ boundary layer thickness
 δ^* displacement thickness
 π pressure gradient parameter
 τ shear stress

Subscripts

e at boundary layer edge
 tr at transition
 s at shock
 w at wall

1. INTRODUCTION

The need for reasonably accurate turbulence models is becoming more and more pressing due to the progress made with the development of efficient solution procedures for the Reynolds-averaged Navier-Stokes equations. Though turbulent flow research is being done at many places for quite some time now, progress has been slow. The field of research is wide and comprises very different flow types, e.g. turbulent boundary layers along airplanes or ships, atmospheric boundary layers, open water flows, internal flows, flows with chemical reactions, etc. A summary of the research work going on presently in Belgium and the Netherlands will be given here. The main aim of the paper, however, is to review concisely the state of the art in general and to discuss the prospects for accurate turbulence models.

After the summary of local work in section 2, the state of the art in turbulence modelling will be exemplified for a few simple flows in section 3. On the basis of the results of the brief analysis some conclusions will be drawn. Finally in section 4 the author's view on the status and prospects of turbulence modelling will be expressed.

2. SURVEY OF LOCAL ACTIVITIES

At NLR in the Netherlands the activities in 3D turbulent boundary layer research have been taken up again in an extensive measurement program of mean flow and turbulence properties in the shear layers of a swept wing (Fig. 1). This is a European collaborative project with companion measurements in the French F2 wind tunnel (Van den Berg, 1988). Further work at NLR concerns 2D turbulent shear layers, namely turbulence measurements in wakes at strong adverse pressure gradients, as occur on wings with flaps.

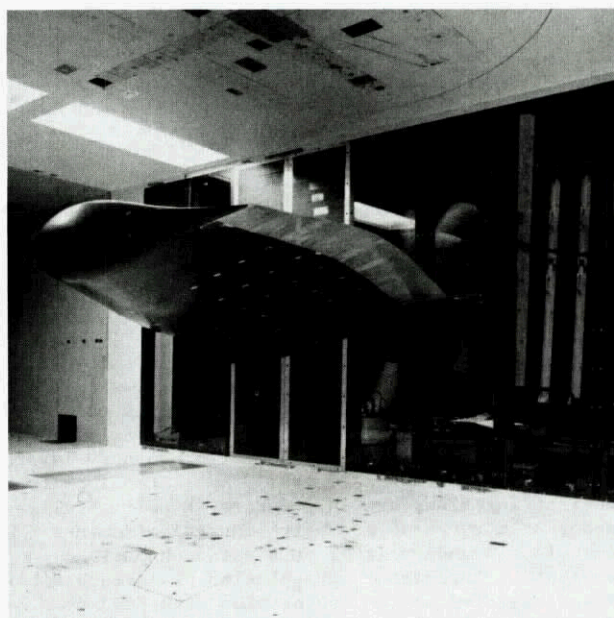


Fig. 1 Garteur swept wing model for 3D turbulent shear layer measurements in the NLR 3 x 2 m² wind tunnel

At Delft University three research groups are active in turbulence research. At the Faculty of Aerospace Engineering an experimental investigation of the flow in the vicinity of an airfoil trailing edge is near completion (Absil & Passchier, 1990). Pitot, Laser-Doppler and hot-wire measurements are carried out on a fine measurement grid to resolve the sudden local changes in the flow near the trailing edge (Fig. 2). At the same Faculty recently measurements have been initiated to obtain turbulence data downstream of a laminar separation bubble, as well as in turbulent wakes at large adverse pressure gradients to supplement the NLR data.

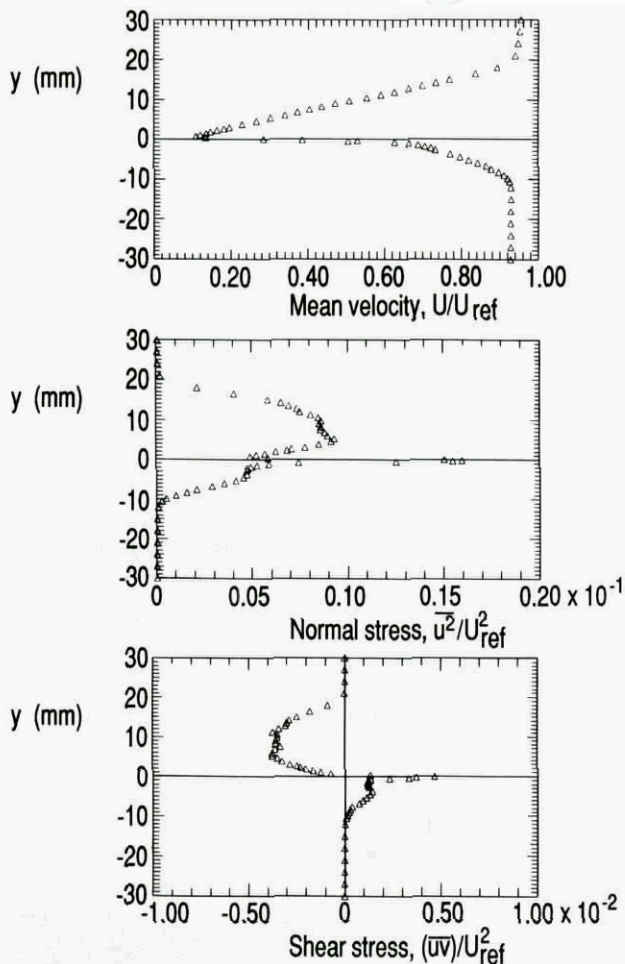


Fig. 2 Laser-Doppler measurement results at 0.5% chord behind an airfoil trailing edge in the Delft University $1.8 \times 2.25 \text{ m}^2$ wind tunnel

At the Fluid Dynamics Division of the Faculty of Mechanical Engineering work on numerical simulation of turbulent flows is going on, modelling the small-scale eddies. The large eddy simulations have been done primarily for atmospheric boundary layers (Van Haren & Nieuwstadt, 1987), but extensions to engineering flows are in progress. Experimentally, coherent structures are being investigated in a turbulent boundary layer in a water channel. A project on turbulence manipulation by surface riblets is carried out in cooperation with Eindhoven University, Faculty of Physics (Pulles et al, 1989). Though the direct objective is here viscous drag reduction, an important byproduct may be a better comprehension of turbulent flow structures near the surface. A new project at Eindhoven University concerns measurements on the decay of swirl in a pipe to support turbulence model development for these flows.

At the Faculty of Physics, Delft University, natural convection boundary layers along a heated vertical plate and in a square cavity with a heated vertical side wall are investigated using different turbulence models (see e.g. Lankhorst, Henkes & Hoogendoorn, 1988). For these calculations a special-purpose processor has been developed to solve efficiently the Navier-Stokes equations: the Delft Navier Stokes Processor.

Turbulence modelling for ship stern flows, using the parabolized Reynolds-averaged Navier-Stokes equations, is studied at the Dutch maritime research institute MARIN (Hoekstra, 1987). At the Delft Hydraulics Laboratory turbulence models for

stratified flows are investigated (Uittenbogaard & Baron, 1989). The application of turbulence models for the prediction of flows with suspended particles is considered at Shell Laboratories in Amsterdam (Roekaerts, 1989).

In Belgium turbulence research work also is going on at several places. At VKI, Rhode-St-Génèse, both the Aerospace Department and the Environmental and Applied Fluid Dynamics Department are active in the field. One research topic is the 3D turbulent flow in ducts of different shapes for Mach numbers up to one. These flows are being computed with the parabolized Reynolds-averaged Navier-Stokes equations, using different turbulence models. Navier-Stokes solutions for 2D airfoils at low Reynolds numbers have also been obtained (Alsalihi, 1989) and extensions of the work employing special low-Reynolds-number turbulence models are in progress.

Further work at the Aerospace Department of VKI comprises the development of a one-equation model for the prediction of the transition from laminar to turbulent flow (Deyle & Grundmann, 1990). Similar work, using modifications of a two-equation turbulence model, is going on at Ghent University. Figure 3 shows the turbulence intensity development in the transition region of a boundary layer as measured and computed with a two-equation model and taking into account the turbulent flow intermittency (Vancouilli & Dick, 1988).

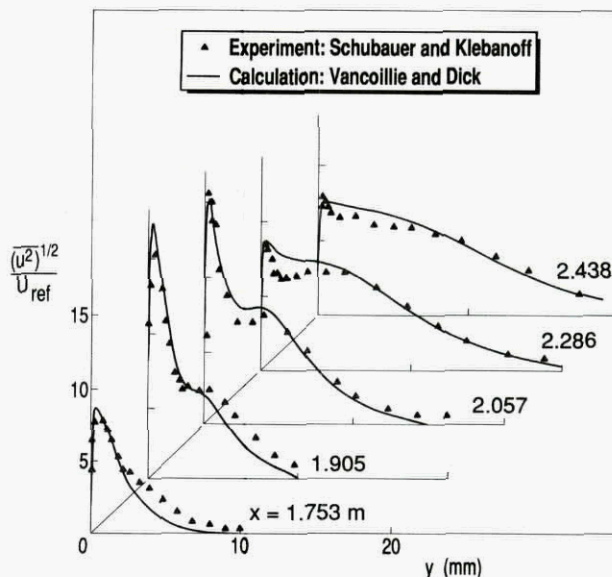
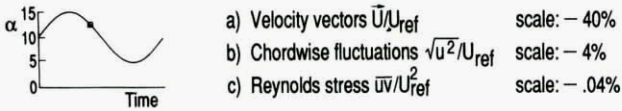


Fig. 3 Turbulence intensity in a boundary layer transition region. Comparison between experiment and calculations at Ghent University based on a turbulence model with an allowance for intermittency

At the Environmental and Applied Fluid Dynamics Department of VKI non-linear algebraic Reynolds stress models have been tested with encouraging results for the prediction of the turbulent flow over a back-ward facing step (Benocci & Skovgaard, 1989). An other direction of research concerns droplet transport in turbulent flows using different turbulence models. Further, large-eddy simulations of turbulent flows are being carried out, first in a 2D channel (Pinelli & Benocci, 1989), while extensions to 3D channels and free-shear layers are under development. Numerical simulations of the large eddies in turbulent flows is also a research topic of Louvain University. Finally, at the Free University of Brussels extensive measurements have been carried out in the shear layers of an oscillating NACA 0012 airfoil (De Ruyk et al, 1988). Figure 4 shows typical results obtained with

a rotating single hot-wire in the partially separated trailing edge region. Work on the validation of turbulence models has been initiated.



Reduced freq. = 0.3

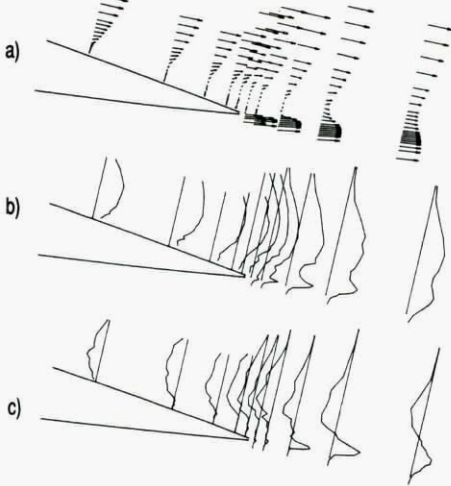


Fig. 4 Some hot-wire measurement results near an oscillating airfoil in the Brussel Free University 1 x 2 m² wind tunnel

It is clear from the foregoing that interesting contributions are being made at various places in Belgium and the Netherlands. One comment may be that, so far work on modelling is being done, it concerns in general earlier applications of existing turbulence models rather than the development of new models or new concepts. Further the survey of work suggests that the various activities seem to progress sometimes rather independently, notwithstanding the small scale of the countries considered. This can be at least partly attributed to a specific interest in a particular type of turbulent flow. Since this review is related to an AGARD activity, the type of turbulent flow on aircraft configurations will be discussed in more detail in the following section.

3. STATUS FOR SOME SIMPLE AIRFOIL FLOWS

In reviews of turbulence modelling attention is often focussed on complex turbulent flows and the deficiencies of turbulence models in these circumstances. However, turbulent shear flows on practical airplanes are for the most part simple boundary layer flows. An accurate prediction of these simple turbulent flows is a prerequisite for satisfactory calculations of the whole flow field. For this reason it was regarded useful to discuss here turbulence models for simple shear flows, and to refer to companion papers in this AGARD report for a discussion of more complex turbulent flows.

To support the discussion a typical pressure distribution on a modern transonic airfoil has been plotted in figure 5. In the first place it may be noted that along a considerable part of the airfoil upper surface the surface pressure gradient is close to zero. The boundary layer development along that part will generally differ little from that along a flat plate at constant pressure. As flow velocities are high, local viscous losses will be comparatively large. Consequently, any turbulence model should at least yield accurate predictions for constant-pressure turbulent boundary layers.

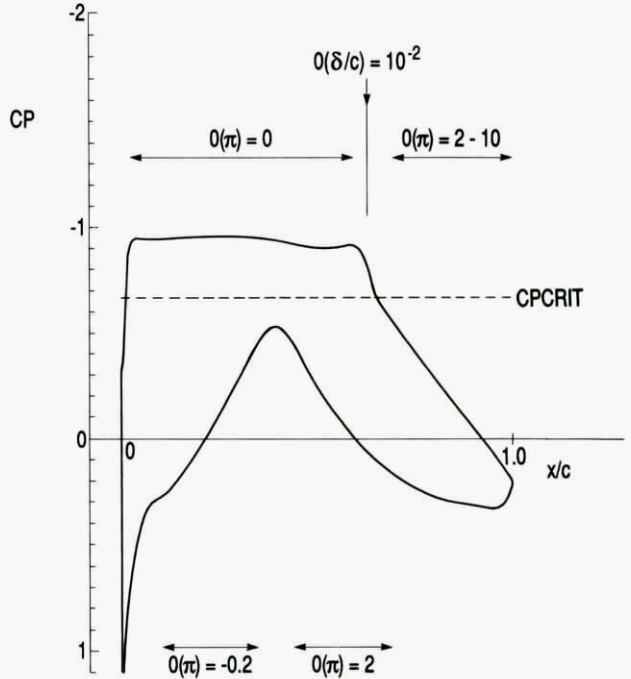


Fig. 5 Typical pressure distribution on a modern airfoil section and associated levels of the B.L. pressure gradient parameter, $\pi = (\delta^*/\tau_w)(dp/dx)$

Large adverse pressure gradients normally occur over the rear part of the airfoil, especially on the upper surface. In figure 5 typical order of magnitudes for the boundary layer pressure gradient parameter, $\pi = (\delta^*/\tau_w)(dp/dx)$, are indicated. Accurate predictions of the turbulent boundary layer development in these adverse pressure gradient regions are a further requirement. On the upper surface moreover a small region with very large pressure gradients often exists due to the presence of a shock wave in the flow. The interaction of the shock with the boundary layer can have a large effect on the viscous flow development and this is an example of a complex region where turbulence modelling requires special attention.

Attached turbulent boundary layers are often computed using algebraic eddy-viscosity or mixing-length models. These models contain at least three empirical constants. In the wall region of the

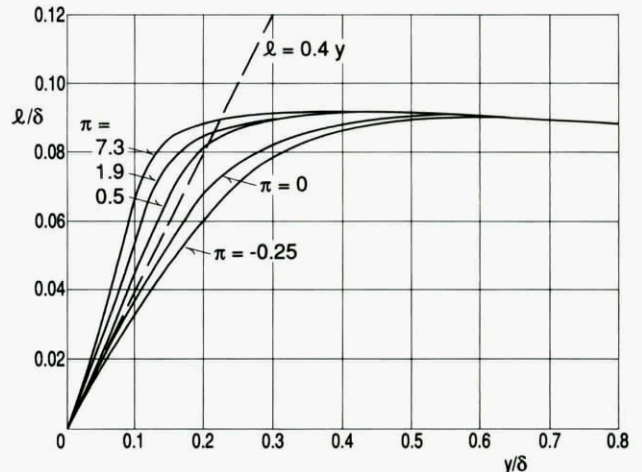


Fig. 6 Mixing lengths deduced from turbulent shear stress measurements in equilibrium boundary layers at various pressure gradients (East et al, 1979)

boundary layer outside the viscous sublayer the turbulent shear stress, τ , is normally expressed in the mixing length relation $\tau = l^2 \rho (\partial U / \partial y)^2$ with $l = k \cdot y$. In this relation is y the distance to the wall and k one of the empirical constants, the so-called Von Karman constant. Evidence is gradually accumulating, however, that the value of k is not a constant, but depends on the surface pressure gradient. Mixing length variations, deduced from turbulence measurements in equilibrium boundary layers at different non-dimensionalized pressure gradients π , have been plotted in figure 6 (East et al, 1979). According to these measurements the value of k varies widely and differs generally substantially from the usually assumed value for the constant, $k = 0.4$.

The measurement data shown were obtained a decade ago, but the point that k varies with the pressure gradient has been made even earlier, amongst others by a group at Cambridge University (Galbraith, Sjolander & Head, 1977). One of their plots has been reproduced in figure 7, completed with the data from figure 6. The turbulent shear stresses were not directly measured in the cases considered initially at Cambridge. Instead, the stresses were derived from the equations of motion and the measured mean velocity profiles, which were represented by a profile family assuming a log law velocity variation in the wall region: $u^+ = (\ln y^+ + A) / k_u$, with $k_u = \text{constant}$. It is easy to see that, if the shear stress variation in the wall region is not negligible, the latter implies that k in $l = k \cdot y$ can not be constant and must vary according to $k = k_u (\tau / \tau_w)^{1/2}$. To a first approximation the shear stress variation near the wall may be written as $\tau / \tau_w = 1 + \pi (y / \delta^*)$. This suggests that if $k_u = \text{constant}$, the average value of k in the wall region will vary globally as $k = k_u (1 + C \cdot \pi)^{1/2}$. This relation with $k_u = 0.4$ and a suitable value of $C = 0.25$ appears to represent the found variation of k with π well. This means also, however, that conclusions about k based on the presumption that $k_u = \text{constant}$, i.e. that the log law velocity variation is preserved in pressure gradient flows, are not convincing.

This objection does not hold, however, for the data of figure 7 based on turbulent shear stress measurements, which support the claimed variation of k with pressure gradient. Further support has come recently from direct numerical simulations of tur-

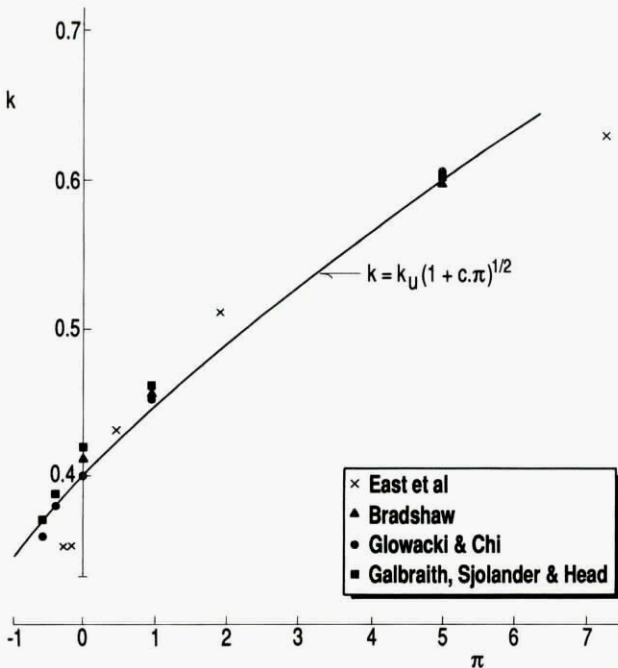


Fig. 7 Effect of pressure gradient on value of k in $l = k \cdot y$ for equilibrium boundary layers

bulent boundary layers at favourable pressure gradients and in three-dimensional boundary layers (Spalart, 1986, 1989). The obtained solutions of the time-dependent three-dimensional Navier-Stokes equations also seem to indicate that the log law velocity variation in the wall region is preserved and that the mixing-length relation is altered.

On the whole, substantial evidence has been accumulated that the value of k in the mixing length relation might not be constant. Yet in the majority of algebraic mixing-length or eddy-viscosity turbulence models now in use, k is assumed constant. The value of k is known to have a comparatively large effect on the calculated boundary layer development. Referring to figure 5, typical adverse pressure gradients on airfoils, $\pi = 2$ or more, would lead according to figure 7 to a k -increment of 20 % or more. The effect of neglecting the variation of k in the calculations is likely, therefore, to be far from negligible.

An other assumed empirical constant in many models is the dimensionless eddy viscosity, $\nu_e / U_e \delta^*$, or mixing length, l / δ , in the outer region of the turbulent boundary layer. However, turbulence history effects are known from several experiments to be very important in this region and to affect the value of the "constant" substantially. To illustrate the severity of history effects, the mixing length development downstream of a laminar-turbulent transition region has been shown in figure 8. The data were obtained at Delft University in a boundary layer at a small adverse pressure gradient (Van Oudheusden, 1985). The value of k is constant here within the measurement scatter, but the mixing length ratio l / δ in the outer region is seen to vary considerably. The ratio l / δ appears to be twice as large at the first measurement station than the ratio at the last station, where the mixing length has relaxed to a more normal level. The last station is situated at nearly 80 boundary layer thicknesses behind the transition region. The relaxation of the transitional flow with high turbulent shear stresses to the lower stresses in equilibrium conditions appears to take a considerable streamwise distance.

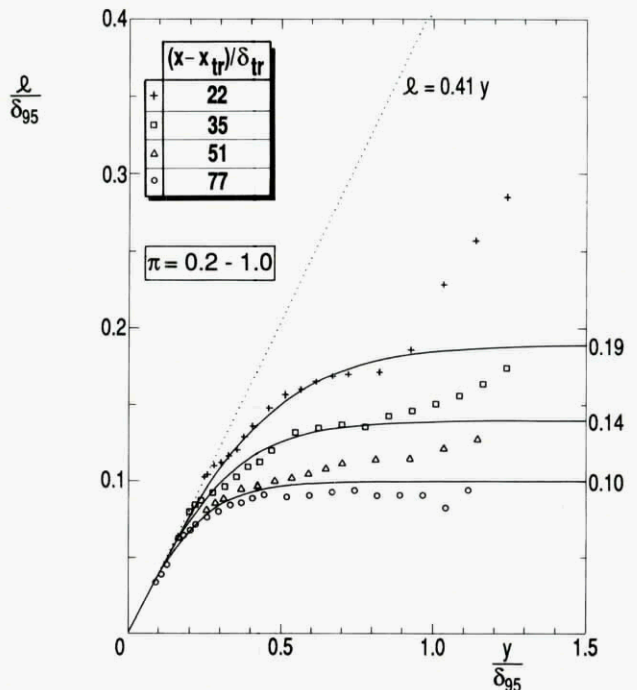


Fig. 8 Mixing lengths deduced from measurements in an adverse-pressure-gradient turbulent boundary layer developing downstream of a transition region (van Oudheusden, 1985)

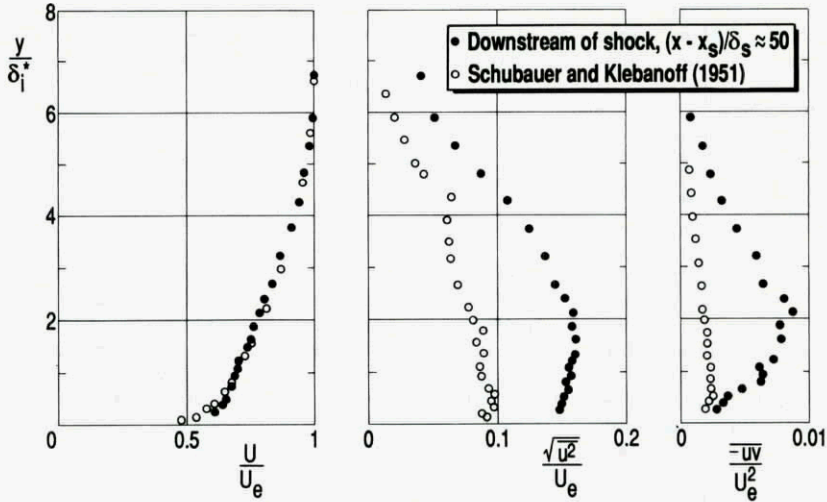


Fig. 9 Boundary layer properties downstream of a shockwave B.L. interaction region. Comparison with data at same H_1 and R_δ in more near-equilibrium conditions (Delery et al, 1986)

On transonic airfoils, shock boundary layer interactions may lead to substantial changes in the turbulence properties, which also relax downstream only slowly. The turbulence intensities and shear stresses measured downstream of a shock at a distance of about 50 boundary layer thicknesses are compared in figure 9 with the corresponding data in a turbulent boundary layer in more near-equilibrium conditions (Delery & Marvin, 1986). Evidently turbulent stresses are still very high at this large distance behind the shock. As indicated in figure 5, the boundary layer thickness on the airfoil upper surface at the position of the shock, say at about mid-chord, is typically of the order of $1 \frac{1}{2}$ chord. Consequently the adverse pressure gradient region behind the shock up to the airfoil trailing edge is likely to be dominated by turbulence history effects of the shock boundary layer interaction.

It is clear that turbulence history effects are not taken into account at all in simple algebraic eddy-viscosity and mixing-length models. However, also more advanced models often fail to predict the correct order of magnitude of turbulence history effects, even if they are based on turbulence transport equations, which they usually are. The turbulence transport equations can be derived by suitable manipulations from the Navier-Stokes equations. The equation for the turbulent kinetic ener-

gy, $q = 1/2(u^2+v^2+w^2)$, reads for two-dimensional mean flows:

$$U \frac{\partial q}{\partial x} + v \frac{\partial q}{\partial y} = \underbrace{(-\overline{uv})}_{\text{turbulence history}} \frac{\partial U}{\partial y} - \underbrace{(\overline{u^2-v^2})}_{\text{turbulence production}} \frac{\partial U}{\partial x} + \text{diffusion - dissipation}$$

In the usual thin shear layer approximation, the spatial derivative in the approximate mean flow direction, $\partial/\partial x = O(L^{-1})$, is supposed to be much smaller than the crosswise derivative, $\partial/\partial y = O(\delta^{-1})$, as $L \gg \delta$ in thin shear layers. In that case turbulence history, as represented by the left-hand side terms of the above equation, would be negligibly small compared to the production term. The large turbulence history effects found in experiment in thin shear layers must come, therefore, from other terms in the turbulence transport equations, most likely the dissipation term responding slowly to flow condition changes. Note that this is one of the terms relying heavily on semi-empirical modelling and therefore not necessarily predicting a history effect of the right amount.

Finally the effect of three-dimensionality of the mean flow on the turbulence properties will be briefly discussed. As turbulence is inherently three-dimensional one might assume that the genera-

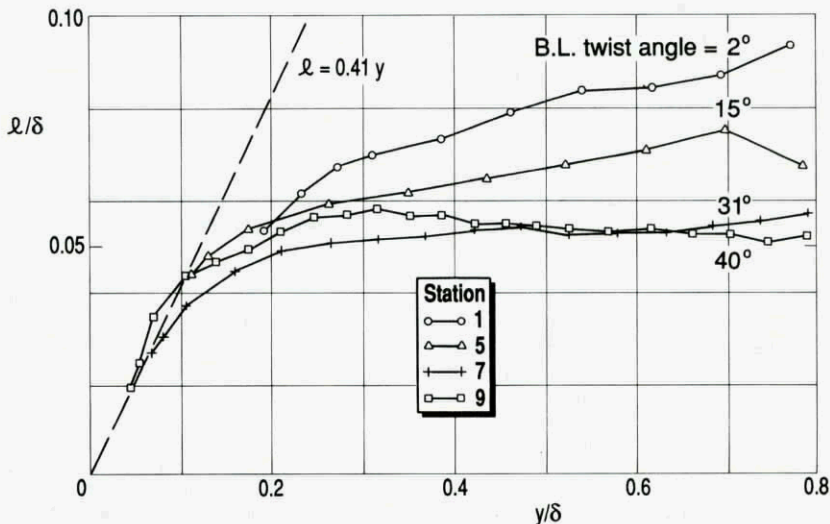


Fig. 10 Mixing lengths deduced from turbulence measurements in a three-dimensional boundary layer (Elsenaar et al, 1975)

lization of turbulence properties in two-dimensional shear flows to three-dimensional flows would be straightforward. Measurements indicate, however, that this is not true and that the three-dimensionality of the mean flow tends to reduce turbulence activity in general and the turbulent shear stresses especially. As an example the mixing length values derived from turbulence measurements in a two-dimensional boundary layer developing into a three-dimensional one are shown in figure 10 (Elsenaar & Boelsma, 1975). The mixing length ratio l/δ in the outer region of the boundary layer is seen to drop substantially, when the amount of twist of the boundary layer velocity profiles becomes significant. Turbulence history effects may play a role again, but it is likely that in addition the velocity profile twist hampers the development of turbulent eddies and so leads to a reduction of turbulence activity (Bradshaw & Pontikos, 1985). Few turbulence models available up to now predict such a decrease of turbulent shear stress magnitude with mean-flow three-dimensionality. The non-alignment of the shear stress and the velocity gradient, i.e. the non-isotropic eddy viscosity observed experimentally, is neither taken into account in most existing turbulence models.

The observations made in this section indicate that even for simple boundary layer flows, available turbulence models will often not meet the accuracy requirements, certainly not those made normally by aerospace industry, i.e. prediction accuracies of the order of 1 % or better. Uncertainties exist even in seemingly well-established data, such as the constant in the mixing length relation for the wall region. Acceptable predictions of the turbulence development are still more remote for complex turbulent flow regions, like shock boundary layer interactions. Due to turbulence history, the downstream effects of such a complex flow region may remain appreciable for quite some distance. On the whole, the position that adequate turbulence models for accurate predictions are available seems still remote.

4. GENERAL VIEW ON TURBULENCE MODELLING

It looks sensible to start with a discussion of the origin of the turbulence modelling problem. In the first place it is important to note that the equations which describe turbulent flows are actually well-known: the time-dependent Navier-Stokes equations. Consequently one can not state that there is any fundamental problem to be solved in turbulence. There is only a practical problem, as it is nearly impossible to solve in reality the full time-dependent Navier-Stokes equations for most turbulent flows. Numerical solutions can not be obtained in general because of the fine computational grid in space and time needed. To circumvent the problem the time-averaged or Reynolds-averaged Navier-Stokes equations are solved as a rule, but these contain extra unknowns, the apparent stresses due to turbulence or Reynolds stresses. This means that the need for turbulence modelling only occurs because the full equations are not being solved.

It should be noted that there is no reason why it would be possible to obtain accurate solutions using a reduced set of equations. Actually in the author's opinion it seems unlikely that solving the full time-dependent Navier-Stokes equations can be really circumvented. This statement amounts to stating that it is unlikely that a truly universal turbulence model exists. The evidence about turbulence available up to now does not support universal properties in various flows. Large eddies play an important role in turbulent flows and the large eddy properties are known to differ essentially for different flow conditions. It is not clear how the large eddies can be predicted for

different flows without taking the time-dependence of the flow into account, or without simulating at least the large eddies in time-dependent calculations.

If a universal turbulence model does not exist, turbulence models with a limited validity, restricted to certain turbulent flow conditions, must be accepted. Then turbulence modelling comes down to approximating for certain flow conditions the Reynolds stress terms by a convenient mathematical model on the basis of available data, usually from experiments. In this view turbulence modelling is much more a semi-empirical art of engineering level than a fundamental scientific problem. Note that even if universal validity can not be attained, it remains useful to attempt to stretch the range of validity of semi-empirical turbulence models, since zonal models valid in parts of the flow may be expected to pose problems at the zone boundaries.

The foundation for any development of a semi-empirical model should be a reliable and extensive data base. The data must come from experiments or from solutions of the full time-dependent Navier-Stokes equations. Although the latter source of data is promising for the future, most turbulence data presently still come from experiment. A data base of sufficient extent and reliability is not yet available, even not for simple turbulent flows, as the examples discussed in this paper indicate.

ACKNOWLEDGEMENT

Thanks are due to those who informed the author about the turbulence research going on at their places, and in particular to Dr. J.A. Essers, who collected the information from Belgium.

REFERENCES

1. Asbil, L.H.J. and Passchier, D.M., 1990 - "LDA measurements in the highly asymmetric trailing edge flow of a NLR 7702 airfoil". Fifth International Symposium on Application of Laser Techniques to Fluid Mechanics, Lisbon.
2. Alsalihi, Z., 1989 - "Compressible Navier-Stokes solutions over low Reynolds number airfoils". Proc. Int. Conf. on Low Reynolds Number Airfoils (Springer).
3. Benocci, C. and Skovgaard, M., 1989 - "Prediction of turbulent flow over a backward facing step". Sixth Conf. on Num. Methods in Laminar and Turbulent Flows, Swansea.
4. Berg, B. van den, 1989 - "A European collaborative investigation of the three-dimensional turbulent shear layers of a swept wing". AGARD Conf. Proc. No. 438.
5. Bradshaw, P., 1966 - "The turbulence structure of equilibrium boundary layers". NPL Aero Report 1184.
6. Delery, J. and Marvin, J.G., 1986 - "Shock-wave boundary layer interactions". AGARDograph No. 280.
7. Deyle, H. and Grundmann, R., 1990 - "Transition model for prediction and calculation of boundary layers". VKI Aerospace Report.
8. East, L.F., Sawyer, W.G. and Nash, C.R., 1979 - "An investigation of the structure of equilibrium turbulent boundary layers". RAE Report TR 79040.
9. Galbraith, R.A.M., Sjolander, S. and Head,

- M.R., 1977 - "Mixing length in the wall region of turbulent boundary layers". Aeron. Quart. 28, 97.
10. Glowacki, W.J. and Chi, S.W., 1972 - "Effect of pressure gradient on mixing length for equilibrium turbulent boundary layers". AIAA Paper 72-213.
11. Haren, L. van and Nieuwstadt, F.T.M., 1989 - "The behavior of passive and buoyant plumes in a convective boundary layer, as simulated with a large eddy model". Journ. Appl. Meteor. 28, 818.
12. Hoekstra, M., 1987 - "Computation of steady viscous flow near a ship's stern". Notes on Num. Fluid Mech. 17, 45 (Vieweg).
13. Lankhorst, A.M., Henkes, R.A.W.M. and Hoogedoorn, C.J., 1988 - "Natural convection in cavities at high Rayleigh numbers, computations and validation". Proc. of Second UK Nat. Conf. on Heat Transfer.
14. Oudheusden, B.W. van, 1985 - "Experimental investigation of transition and the development of turbulence in a boundary layer flow in an adverse pressure gradient". Delft Univ., Dept. Aerospace Eng., Master Thesis.
15. Pinelli, A. and Benocci, C., 1989 - "Large eddy simulation of fully turbulent plane channel flow". VKI Techn. Note 171.
16. Pulles, C., Krishna Prasad, K. and Nieuwstadt, F.T.M., 1989 - "Turbulence measurements over longitudinal micro-grooved surfaces". Appl. Scient. Research 46, 197.
17. Roekaerts, D., 1989 - Sixth Conf. on Num. Methods in Laminar and Turbulent Flows, Swansea.
18. Ruyk, J. de, Hazarika, B. and Hirsch, Ch., 1988 - "Transition and turbulence structure in the boundary layers of an oscillating airfoil". Free Univ. Brussel VUB Report STR-16.
19. Spalart, P.R., 1986 - "Numerical study of sink-flow boundary layers". Journ. Fluid Mech. 172, 307.
20. Spalart, P.R., 1989 - "Theoretical and numerical study of a three-dimensional turbulent boundary layer". Journ. Fluid Mech. 205, 319.
21. Uittenbogaard, R.E. and Baron, F., 1989 - "A proposal: Extension of the $q^2 - \epsilon$ model for stably stratified flows with transport of internal wave energy". Seventh Symp. Turb. Shear Flows, Stanford.
22. Vancoilli, G. and Dick, E., 1988 - "A turbulence model for the numerical simulation of the transition zone in a boundary layer". Journ. Eng. Fluid Mech. 1.

CALCULATION OF TURBULENT COMPRESSIBLE FLOWS

J. COUSTEIX

ONERA/CERT

Complexe scientifique de Rangueil

2 avenue E. Belin

31055 Toulouse Cédex

FRANCE

SUMMARY

This paper discusses the use and the suitability of turbulence models for calculating compressible flows in Aerodynamics. As the compressible form of turbulence models is generally extended from a basic incompressible form, the emphasis is placed on the pertinence of these extensions and on the peculiarities of compressible flows.

1. INTRODUCTION

The calculation of compressible turbulent flows in Aerodynamics has been performed by using more or less empirical methods. These methods include correlations techniques and integral methods for calculating boundary layer flows. Such methods are still in use today but it is clear that more detailed or more accurate methods are needed.

In the seventies a great hope has been placed in the development of transport equation models to represent the effects of turbulence on the mean flow. After a period of enthusiasm where these techniques enabled us to make a decisive step towards a real improvement in the calculation methods of turbulent flows, it appears that the progress is now much slower.

This paper is trying to state where we are with the turbulence models, what is being done and what could or should be done to improve these turbulence models.

2. PECULIARITIES OF TURBULENT COMPRESSIBLE FLOWS

2.1 Averaged equations

2.1.1 Definition of averages

For practical applications, the calculation of turbulent flows is approached by using statistical equations which are :

$$\frac{\partial \langle \rho \rangle}{\partial t} + \frac{\partial \langle \rho u_i \rangle}{\partial x_i} = 0 \quad (1)$$

$$\frac{\partial \langle \rho u_i \rangle}{\partial t} + \frac{\partial \langle \rho u_i u_j \rangle}{\partial x_j} = - \frac{\partial \langle \rho p \rangle}{\partial x_i} + \frac{\partial \langle f_{ij} \rangle}{\partial x_i} \quad (2)$$

$$f_{ij} = 2 \mu \left(s_{ij} - \frac{\delta_{ij}}{3} \frac{\partial u_l}{\partial x_l} \right); \quad s_{ij} = \frac{1}{2} \left(\frac{\partial u_i}{\partial x_j} + \frac{\partial u_j}{\partial x_i} \right)$$

where $\langle \cdot \rangle$ denotes a statistical average.

The main question is to choose how to decompose $\langle \rho u_i \rangle$ and $\langle \rho u_i u_j \rangle$ in equations (1) and (2). The decomposition of $\langle f_{ij} \rangle$ is less important because the viscous stresses are negligible in turbulent flow. A discussion of this problem has been done by CHASSAING, 1985.

The pressure and the density are decomposed as :

$$p = \langle p \rangle + p'; \quad \langle p' \rangle = 0$$

$$\rho = \langle \rho \rangle + \rho'; \quad \langle \rho' \rangle = 0$$

but many possibilities can be used to decompose the velocity.

If we use the decomposition :

$$u_i = \langle u_i \rangle + u''_i; \quad \langle u''_i \rangle = 0$$

we have :

$$\langle \rho u_i \rangle = \langle \rho \rangle \langle u_i \rangle + \langle \rho' u''_i \rangle$$

$$\begin{aligned} \langle \rho u_i u_j \rangle &= \langle \rho \rangle \langle u_i \rangle \langle u_j \rangle + \langle \rho' u''_i \rangle \langle u_j \rangle \\ &\quad + \langle \rho' u''_j \rangle \langle u_i \rangle + \langle \rho \rangle \langle u''_i \rangle \langle u''_j \rangle \\ &\quad + \langle \rho' u''_i u''_j \rangle \end{aligned}$$

Compared with the incompressible case, many additional terms appear and the formulation of equations is very complicated.

Most of the works use a mass-weighted velocity \tilde{u}_i . This type of average has been introduced by FAVRE, 1958, in turbulence studies. We have :

$$\tilde{u}_i = \frac{\langle \rho u_i \rangle}{\langle \rho \rangle}; \quad u_i = \tilde{u}_i + u'_i; \quad \langle \rho u'_i \rangle = 0$$

and

$$\langle \rho u_i \rangle = \langle \rho \rangle \tilde{u}_i$$

$$\langle \rho u_i u_j \rangle = \langle \rho \rangle \tilde{u}_i \tilde{u}_j + \langle \rho u'_i u'_j \rangle$$

The average equations are :

$$\frac{\partial \langle \rho \rangle}{\partial t} + \frac{\partial \langle \rho \tilde{u}_i \rangle}{\partial x_i} = 0 \quad (4)$$

$$\langle \rho \rangle \frac{\partial \tilde{u}_i}{\partial t} + \langle \rho \rangle \tilde{u}_j \frac{\partial \tilde{u}_i}{\partial x_j} = - \frac{\partial \langle \rho p \rangle}{\partial x_i} + \frac{\partial}{\partial x_j} (F_{ij} - \langle \rho u'_i u'_j \rangle) \quad (5)$$

with : $F_{ij} = \langle 2 \mu s_{ij} - \frac{2}{3} \mu \frac{\partial u_l}{\partial x_l} \delta_{ij} \rangle$

Equations (4) and (5) have an "usual" form in the sense that they look like their incompressible counterpart.

The concept of average stream surface has the same meaning as in incompressible flow. In addition, the equations for the Reynolds stresses - $\langle \rho' u'_i u'_j \rangle$ are obtained in a natural way and not too many additional terms are introduced.

The danger is that the equations are too close to the incompressible case and it is tempting to apply them an "incompressible" closure, which is not always justified.

It is worth mentioning that many other decompositions are possible and this problem is not closed.

Nevertheless the mass-weighted averages are used in the rest of this paper.

2.1.2. Equations with mass-weighted averages

To simplify the writing of the averaged equations, $\langle \rho \rangle$ is written $\bar{\rho}$. For example, we have :

$$\bar{\rho} \tilde{u}_i = \langle \rho \tilde{u}_i \rangle$$

but when ρ is combined with a random function inside a sign $\langle \rangle$, the same convention does not apply :

$$\langle \rho u'_i u'_j \rangle \neq \langle \rho \rangle \langle u'_i u'_j \rangle$$

When no confusion is expected, the sign (\sim) is omitted :

$$U_i = \tilde{u}_i \\ h = \tilde{h}$$

Continuity equation

$$\frac{\partial \rho}{\partial t} + \frac{\partial \rho U_k}{\partial x_k} = 0 \quad (6)$$

Momentum equation

$$\rho \frac{DU_i}{Dt} = \frac{\partial}{\partial x_k} (-P \delta_{ik} + F_{ij} - \langle \rho u'_i u'_k \rangle) \quad (7)$$

with :

$$\frac{D}{Dt} = \frac{\partial}{\partial t} + U_k \frac{\partial}{\partial x_k} \\ F_{ik} = \langle 2 \mu \left(s_{ik} - \frac{\delta_{ik}}{3} \frac{\partial u_l}{\partial x_l} \right) \rangle \\ s_{ik} = \frac{1}{2} \left(\frac{\partial u_i}{\partial x_k} + \frac{\partial u_k}{\partial x_i} \right)$$

At high REYNOLDS number, the viscous stress F_{ik} is negligible compared with the turbulent stress - $\rho \langle u'_i u'_k \rangle$. Near a wall, this is no longer true. Even if the fluctuations of viscosity are neglected, the expression of F_{ik} is not simple because :

$$\left\langle \frac{\partial u_i}{\partial x_k} \right\rangle = \frac{\partial U_i}{\partial x_k} - \frac{\partial}{\partial x_k} \left(\frac{\langle \rho u'_i \rangle}{\rho} \right)$$

Kinetic energy equations

The mean value of kinetic energy is decomposed as :

$$\frac{1}{2} \langle \rho u_i u_i \rangle = \frac{1}{2} \rho U_i U_i + \frac{1}{2} \langle \rho u'_i u'_i \rangle = \rho K + \rho k \quad (8)$$

The first part K corresponds to the averaged motion and the second part k to the fluctuations.

The corresponding equations are :

$$\rho \frac{DK}{Dt} = P \frac{\partial U_i}{\partial x_i} - F_{ik} \frac{\partial U_i}{\partial x_k} + \langle \rho u'_i u'_k \rangle \frac{\partial U_i}{\partial x_k} \\ + \frac{\partial}{\partial x_k} [U_i (-P \delta_{ik} + F_{ik} - \langle \rho u'_i u'_k \rangle)] \quad (9a)$$

$$\rho \frac{DK}{Dt} = \langle \rho' \frac{\partial u'_i}{\partial x_i} \rangle - \langle f_{ik} \frac{\partial u'_i}{\partial x_k} \rangle \\ + \langle \rho u'_i u'_k \rangle \frac{\partial U_i}{\partial x_k} + \frac{\langle \rho' u'_i \rangle}{\rho} \frac{\partial P}{\partial x_i} \quad (9b) \\ + \frac{\partial}{\partial x_k} \left(- \langle u'_i p' \rangle \delta_{ik} + \langle f_{ik} u'_i \rangle - \frac{1}{2} \langle \rho u'_k u'_i u'_i \rangle \right)$$

with

$$f_{ik} = 2 \mu \left(s_{ij} - \frac{\delta_{ij}}{3} \frac{\partial u_l}{\partial x_l} \right); \quad s_{ik} = \frac{1}{2} \left(\frac{\partial u_i}{\partial x_k} + \frac{\partial u_k}{\partial x_i} \right)$$

$$F_{ik} = \langle f_{ik} \rangle$$

The dissipation rate of the instantaneous kinetic energy is $\phi = f_{ik} \frac{\partial u_i}{\partial x_k}$. Its averaged value is decomposed as :

$$\langle \phi \rangle = \Phi + \langle \phi' \rangle$$

with

$$\Phi = f_{ik} \frac{\partial U_i}{\partial x_k}$$

$$\Phi = F_{ik} \frac{\partial U_i}{\partial x_k}$$

$$\langle \phi' \rangle = \langle f_{ik} \frac{\partial u'_i}{\partial x_k} \rangle$$

Φ is the dissipation rate of the kinetic energy of the averaged motion which appears in eq. 9a. $\langle \phi' \rangle$ is the dissipation rate of the averaged kinetic energy of the fluctuating motion which appears in eq. 9b. The exchange of energy between K and k is represented by the work of the REYNOLDS stresses - $\langle \rho u'_i u'_k \rangle \frac{\partial U_i}{\partial x_k}$.

In the k-equation, the compressibility appears explicitly through two terms : $\langle \rho' \frac{\partial u'_i}{\partial x_i} \rangle$ and

$\frac{\langle \rho' u'_i \rangle}{\rho} \frac{\partial P}{\partial x_i}$. This does not mean however that

the compressibility cannot influence other terms.

REYNOLDS stress equations

We define T_{ij} as :

$$T_{ij} = \langle \rho u'_i u'_j \rangle / \rho$$

The REYNOLDS stress equation is :

$$\rho \frac{DT_{ij}}{Dt} = \rho P_{ij} - \rho D_{ij} + \rho \Phi_{ij} + \rho C_{ij} + \frac{\partial}{\partial x_k} (\rho J_{ijk}) \quad (10)$$

$$\rho P_{ij} = -\rho T_{ik} \frac{\partial U_j}{\partial x_k} - \rho T_{jk} \frac{\partial U_i}{\partial x_k}$$

$$\rho D_{ij} = \langle f_{ik} \frac{\partial u'_j}{\partial x_k} \rangle + \langle f_{jk} \frac{\partial u'_i}{\partial x_k} \rangle$$

$$\rho \Phi_{ij} = \langle p' \left(\frac{\partial u'_i}{\partial x_j} + \frac{\partial u'_j}{\partial x_i} \right) \rangle$$

$$\rho C_{ij} = \frac{\langle \rho' u'_i \rangle}{\rho} \frac{\partial P}{\partial x_j} + \frac{\langle \rho' u'_j \rangle}{\rho} \frac{\partial P}{\partial x_i}$$

$$\rho J_{ijk} = -\langle \rho u'_k u'_i u'_j \rangle + \langle f_{jk} u'_i \rangle - \langle u'_i p' \rangle \delta_{jk} - \langle u'_j p' \rangle \delta_{ik}$$

The interpretation of this equation is nearly the same as in incompressible flow. ρP_{ij} is the production term ; ρD_{ij} is the destruction term

($\rho \frac{D_{ii}}{2}$ is the dissipation of k) ; $\rho \Phi_{ij}$ is the velocity-pressure correlation ; ρJ_{ijk} is the diffusion due to interactions between velocity fluctuations, due to viscosity and due to interactions between pressure and velocity.

The compressibility appears explicitly only through the term C_{ij} but, once again, the modelled form of the other terms can be influenced by compressibility. For example, the modelling of Φ_{ij} is based on the POISSON equation for p' which is obtained by taking the divergence of the momentum equation. In this equation, many additional terms appear due to the compressibility of the flow :

$$\begin{aligned} -\frac{\partial^2 p'}{\partial x_i \partial x_i} &= 2 \frac{\partial^2}{\partial x_l \partial x_m} (\langle \rho \rangle u'_l U_m) + 2 \frac{\partial^2}{\partial x_l \partial x_m} (\rho' u'_l U_m) + \\ &+ \frac{\partial^2}{\partial x_l \partial x_m} (\rho' U_l U_m) \\ &+ \frac{\partial^2}{\partial x_l \partial x_m} (\langle \langle \rho \rangle + \rho' \rangle u'_l u'_m - \langle \rho u'_l u'_m \rangle) \quad (11) \\ &- \frac{\partial^2 p'}{\partial t^2} - \frac{\partial^2}{\partial x_l \partial x_m} (f_{lm} - F_{lm}) \end{aligned}$$

2.2 Variations of density and temperature

The flows under consideration are characterized by a high Mach number and very often by a heat transfer at walls. Therefore heat is produced by direct dissipation and transferred by the turbulent fluctuations.

These phenomena imply a non uniform averaged temperature and density, which influence the velocity field.

In a boundary layer developing on an adiabatic wall, the large amount of dissipation near the wall leads to a large static temperature in this region. Then the kinematic viscosity is larger than near the external edge of the boundary layer and the local REYNOLDS number is smaller. Compared with an incompressible boundary layer, the viscous sublayer is thicker.

The variation of density in itself does not imply a modification of the turbulence structure. For example, the study by BROWN and ROSHKO of a low-speed mixing layer with a mixing of gases with different densities showed that the spreading rate of the layer is not affected by the variation of density. On the contrary, the spreading rate of a mixing layer of air is significantly reduced in supersonic flow. This means that there is a genuine compressibility effect in this case. It is not clear however if this is due to an effect on the turbulence structure. At least partly, the reduction of the spreading rate can be attributed to an effect of compressibility on the stability properties of the flow which are at the origin of the large scale structures. PAPAMOSCHOU-ROSHKO studied ten configurations of free shear layers obtained by using the flow of various gases (N_2 , Ar, He) at various MACH numbers (between 0.2 and 4). These authors introduced a convective MACH number which is defined in a coordinate system moving with the convection velocity of the dominant waves and structures of the shear layers. The theoretical analysis is performed by studying the stability of a compressible inviscid vortex sheet. PAPAMOSCHOU-ROSHKO showed that the growth rates of the various free shear layers fall nearly onto a single curve. This result indicates that the shear layer question is more related to a stability problem than to a turbulence problem.

2.3 Decomposition of the fluctuating field in three modes

Another feature of compressible flows is that all the flow characteristics are fluctuating : velocity, temperature, density and pressure.

KOVASZNAY showed that these fluctuations can be expressed as a function of three basic modes

(see FAVRE et al.) : fluctuations of vorticity, entropy and pressure (acoustic fluctuations) and when the level of fluctuations is low, the equations describing the evolution of vorticity and pressure are separated. (The correlation coefficients between the various modes are not necessarily low).

When the fluctuations are no longer low, a second order theory predicts various possible interactions between modes. In supersonic flows, a strong interaction is the vorticity-vorticity interaction which is at the origin of the aerodynamic noise.

These flows are also characterized by the pressure fluctuations (which are isentropic) which can be transmitted over long distances as MACH waves. The loss of turbulent energy by sound radiation is low but the radiated energy can have a strong effect on the laminar-turbulent transition. In supersonic and hypersonic wind tunnels, the transition on a flat plate or on a cone is strongly dependent on the noise generated by the turbulent boundary layers developing on the test section walls. The transition location is correlated with the test section size because the noise affecting the transition depends on the distance between the model and the tunnel walls.

The role played by the pressure fluctuations in the turbulence modelling can be very different in compressible or incompressible flows. For example, the influence of compressibility on the $\langle p' \frac{\partial u'_i}{\partial x_i} \rangle$ term appears through the

POISSON equation for the pressure which contains much more terms in a compressible flow.

The averaged pressure gradient can also modify the processes of turbulence generation or destruction in supersonic flows. The pressure gradient can be very strong (through a shock wave or an expansion fan) and the interaction with the term $\frac{\langle \rho' u'_i \rangle}{\rho}$ in the turbulent kinetic

energy equation can be significant. This also means that the wall curvature is an important parameter because it implies the existence of a normal pressure gradient and an effect on the turbulence.

2.4 The MORKOVIN hypothesis

Let us go back to the decomposition of the turbulent field into three modes : vorticity, entropy and acoustic pressure. At low MACH numbers in an isothermal flow, only the vorticity mode remains. In a compressible flow, if the vorticity generation by interactions between modes is negligible, the turbulence structure is unaffected by compressibility (the

possible vorticity generation interactions are vorticity-entropy, vorticity-acoustic pressure, entropy-acoustic pressure).

From experimental data, MORKOVIN, 1961, showed that the acoustic mode and the entropy mode are negligible in boundary layers with usual rates of heat transfer and $M_e < 5$.

According to MORKOVIN, these flows are such as :

$$\frac{p'}{\rho} \ll 1 ; \frac{T'_i}{T_i} \ll 1$$

Using the state law and assuming that the velocity fluctuations u'/U are not too large, we have :

$$\frac{p'}{\rho} \approx - \frac{T'}{T} \approx (\gamma - 1) M^2 \frac{u'}{U}$$

The following relationships are deduced :

$$\frac{\langle p'^2 \rangle^{1/2}}{\rho} = \frac{\langle T'^2 \rangle^{1/2}}{T} = (\gamma - 1) M^2 \frac{\langle u'^2 \rangle^{1/2}}{U} \quad (12a)$$

$$r_{u'T'} = \frac{\langle u'T' \rangle}{(\langle u'^2 \rangle \langle T'^2 \rangle)^{1/2}} = -1 \quad (12b)$$

This is the so-called strong REYNOLDS analogy. In fact, the basic hypotheses presented above are not very well founded and improvements of the analysis have been proposed by GAVIGLIO, 1987. Nevertheless, practical results such as formulae (12) can give reasonable orders of magnitude. For example, in a boundary layer on an adiabatic wall in supersonic flow, $r_{u'T'}$ is of order - 0.8.

The use of the strong REYNOLDS analogy should be done with care, in particular when the flow undergoes rapid variations.

It should also be noticed that some of the formulae deduced from the strong REYNOLDS analogy are not galilean invariant ; this is the case of the formula (12a) because M^2/U is not galilean INVARIANT.

BRADSHAW, 1977, associated the validity of the MORKOVIN hypothesis with low values of $\frac{\langle p'^2 \rangle^{1/2}}{\rho}$. For boundary layers with an external MACH number lower than 5, the condition is fulfilled as $\frac{\langle p'^2 \rangle^{1/2}}{\rho}$ is smaller than 0.1.

BRADSHAW noticed that at higher MACH numbers, the total temperature fluctuations are no longer negligible but when the wall is cooled, the level of temperature and density fluctuations increases only slowly with the MACH number. At these higher MACH numbers, the pressure fluctuations increase and the turbu-

lence structure can be affected (pressure-vorticity and pressure-entropy interactions can generate vorticity fluctuations).

BRADSHAW also noticed that in free mixing layers, the level of velocity fluctuations $\langle u'^2 \rangle^{1/2}/U$ can reach 0.3 so that the density fluctuations are larger. This implies that the limit of validity of the MORKOVIN hypothesis ($\langle \rho'^2 \rangle^{1/2}/\rho < 0.1$) is limited to external MACH number less than 1.5. This is in rough agreement with experimental data but as already said, it is not clear if the effect of Mach number on the spreading rate of the mixing layer is due to an alteration of the turbulence structure or to an effect on the stability of the flow (which is at the origin of the large structures).

The "incompressible" behaviour of boundary layers in supersonic flow can be illustrated by examining shear stress profiles (figure 1). MAISE and McDONALD, 1968, determined the evolution of the shear stress in a flat plate boundary layer at $M_e = 0$ and $M_e = 5$ for a REYNOLDS number $R_\theta = 10^4$ and an adiabatic wall. The comparison of the profiles $-\langle \rho u'v' \rangle / \tau_w$ shows that the effect of compressibility is small. Similar results have been obtained by SANDBORN up to $M_e = 7$. In the same way, quantities like $\langle \rho u'^2 \rangle / \tau_w$ are not affected by compressibility (SANDBORN, 1974).

MAISE and McDONALD also showed that the mixing length distribution is nearly independent of MACH number. This means that the turbulent shear stress is expressed as :

$$-\langle \rho u'v' \rangle = \rho l^2 \left(\frac{\partial U}{\partial y} \right)^2 \quad (13)$$

where l/δ has the same evolution of y/δ as in incompressible flow (figure 2). This formula can be used to calculate equilibrium or near equilibrium boundary layers, but no shock wave-boundary layer interaction for example.

Many features of supersonic boundary layers are close to the incompressible case but some effects of compressibility on turbulence structure can be noticed. For example, the intermittency function defined as the fraction of time that the flow is turbulent is sharper in supersonic flow ; this means that the region with intermittent turbulence is narrower in supersonic flow (figure 3).

The entrainment coefficient is also affected by the MACH number. Compared to an equivalent boundary layer in incompressible flow, the entrainment coefficient of a boundary layer on an adiabatic wall is approximately doubled at $M_e = 5$.

2.5 Compressibility transformations

The idea that compressible flows behave like incompressible flows led many authors to look for transformations which reduce the study of compressible boundary layers to that of an equivalent incompressible boundary layer.

In fact, there is no method which enables us to transform exactly the equations of a compressible boundary layer into incompressible equations.

Among the various problems, we can cite the presence of large temperature gradients normal to the wall, the dissipation effects, the fluctuating density terms, ... which have no counterpart in incompressible flow.

The idea of compressibility transformation is however used for specific purposes, for example the study of the law of the wall or the construction of a skin friction law.

2.6 Transition and low REYNOLDS number effects

To study this problem, BUSHNELL et al., 1975, characterized the boundary layer with the parameter δ^+ based on the thickness δ :

$$\delta^+ = \frac{\delta (\tau_{\max}/\rho_w)^{1/2}}{v_w}$$

where the index "max" refers to the maximum shear τ in the boundary layer.

Qualitatively, the importance of low REYNOLDS numbers are given in a (δ^+, R_x) plane (figure 4).

This diagram shows that the effects of low REYNOLDS numbers can be important even if the REYNOLDS number $R_x = \frac{\rho_e U_e x}{\mu_e}$ is large.

BUSHNELL et al. observed that the level of the mixing length in the outer region can be doubled or more when δ^+ is of order 100 (figure 5a). However this increase is a function of distance downstream of transition (compare figures 5a and 5b) ; it takes about a distance of 30-50 δ to wash out the low REYNOLDS number effects.

The transition onset is greatly affected by compressibility effects : influence of MACH number, influence of wall to boundary layer edge temperatures ratio. ARNAL used the e^n -transition criterion to evaluate these effects. Let us recollect the principle of this technique. The stability properties of laminar boundary layers are determined by solving the ORR-SOMMERFELD equations. These solutions indicate whether small perturbations are stable or unstable (the perturbations are waves charac-

terized by their frequency and wave length). Another result of these solutions is the amplification rate of the unstable waves. Then, it is possible to calculate the total amplification rate A/A_0 of the most amplified waves. The transition criterion introduced by VAN INGEN, 1956, and SMITH-GAMBERONI, 1956, tells that transition occurs when A/A_0 reaches a critical level e^n . The factor n is an empirical input which characterizes the quality of the external flow : when the external flow is noisy, the value of n is small (in noisy supersonic or hypersonic wind tunnels, $n = 2-4$) ; in a clean environment, n is of order 8-10 (BUSHNELL et al., 1988).

The calculated effects of MACH number (adiabatic wall) and of the wall to edge temperature ratios are shown in figures 6 et 7. Let us notice that these results are at least in qualitative agreement with experimental data. For a boundary layer developing on an adiabatic wall, an increase in MACH number stabilizes the transition (the transition REYNOLDS number is larger) except in the range $2 < M < 3.5$, where the opposite effect is observed (figure 6). Figure 7 shows that, for a given MACH number, a cooling of the wall increases the transition REYNOLDS number compared to the case of an adiabatic wall at the same MACH number. It is also noted that the beneficial effect of wall cooling is less pronounced as the MACH number increases.

2.7 Turbulent heat flux

The diffusion of heat in a turbulent boundary layer is due to the molecular diffusivity and to the transport by turbulence. The corresponding fluxes are :

$$Q_l = -\lambda \frac{\partial T}{\partial y} \quad \text{and} \quad Q_t = \langle \rho v' h' \rangle$$

When the flow is fully turbulent, the ratio Q_t/Q_l is large and the thermal transfer is mainly due to turbulence.

As already seen, the correlation between velocity and temperature fluctuations is good. The coefficient $|\langle v'T' \rangle| / (\langle v'^2 \rangle \langle T'^2 \rangle)^{1/2}$ can be of the order 0.6. Then, the order of magnitude of Q_t/Q_l is :

$$\frac{Q_t}{Q_l} \sim \frac{u \ell}{\nu} \mathcal{P} \frac{\langle T'^2 \rangle^{1/2}}{\Delta T}$$

where \mathcal{P} is the PRANDTL number ; ΔT is a characteristic temperature difference within the boundary layer ; u is a characteristic velocity of turbulence ; ℓ is a characteristic length scale of turbulence.

Thus the thermal turbulence is characterized

by the PECLET number :

$$\mathcal{P}_e = R_l \mathcal{P}$$

For air, the PRANDTL number is close to unity so that the thermal field is fully turbulent for the same range of REYNOLDS numbers as the velocity field.

Then the turbulent heat fluxes are often analyzed by using the turbulent PRANDTL number \mathcal{P}_t defined as :

$$\mathcal{P}_t = \frac{\langle \rho u' v' \rangle}{\frac{\partial U}{\partial y}} / \frac{\langle \rho u' T' \rangle}{\frac{\partial T}{\partial y}} \quad (14)$$

In certain analyses, the value $\mathcal{P}_t = 1$ is taken. This is the so-called REYNOLDS analogy (which is different from the strong REYNOLDS analogy).

For flat plate boundary layers in air, the turbulent PRANDTL number is of order $\mathcal{P}_t = 0.8-0.9$ with a tendency to increase near the wall and to decrease near the outer edge.

No systematic effects of MACH number, low REYNOLDS number or blowing have been observed (BUSHNELL et al, 1977).

The data of BLACKWELL et al. show a decrease in \mathcal{P}_t when the pressure gradient is positive (see LAUNDER, 1976).

The value of the PRANDTL number can be influenced by boundary conditions. For example, on a rough wall compared with a smooth wall, the increase in heat flux is less than the increase in the skin friction.

On the other hand, the value of the PRANDTL number depends on the type of flow. In free flows, \mathcal{P}_t is significantly different from unity in the central part of the flow. For round jets, \mathcal{P}_t is of order 0.7. For wakes, values of order 0.5 have been measured. This means that calculating a compressible turbulent flow with a turbulent PRANDTL number is a simple solution but not the best. (figure 8).

The analogy between the fluctuations of velocity and temperature has been extensively studied by FULACHIER and ANTONIA. They found that there is a good analogy for the energy-containing part of the spectra of the temperature fluctuations and of the total velocity fluctuations ; this result has been obtained for different types of flows.

These authors also showed that the spectral distribution of the PRANDTL number is not at all uniform. The analogy between velocity and temperature fluctuations is analyzed by using the parameter B :

$$B = \frac{\langle q'^2 \rangle^{1/2}}{\langle T'^2 \rangle^{1/2}} \frac{\frac{\partial T}{\partial y}}{\frac{\partial U}{\partial y}}$$

where q' is the fluctuation of the total velocity.

FULACHIER and ANTONIA observed that B varies from flow to flow but is nearly constant within a given flow. In addition, the spectral distribution of B is nearly uniform (except for high values of frequency).

2.8 Other problems

As already seen, the compressibility of the flow adds many complexities as compared to the incompressible flow. The list of problems discussed in this section is not complete and many other effects could be cited.

The hypersonic vehicles often have a blunt shape so that a bow shock wave exists in front of them. Then, the streamlines which cross this shock wave do not have the same entropy jump and the boundary layer is fed with variable entropy streamlines ; the associated variations of free stream characteristics normal to the wall can be large. The influence on the turbulence structure is not known.

Instability like GÖRTLER vortices can develop in supersonic or hypersonic flow. This has been observed in the flow on a compression ramp for example.

The shock wave-boundary layer interaction is obviously a problem of prime importance in transonic, supersonic and hypersonic flow. This topic has been reviewed by DELERY, 1988, in great details.

3. EXAMPLES OF CALCULATION OF TURBULENT COMPRESSIBLE FLOWS

3.1 Flat plate boundary layers

An integral method has been used (COUSTEIX et al, 1974) to determine the effects of MACH number and wall temperature on the skin friction of the flat plate boundary layer. The integral method is based on the solution of the global equations of continuity, momentum and energy. The closure relationships are obtained from self-similarity solutions calculated with a mixing length scheme.

Figures 9 and 10 show the comparisons of numerical results with the VAN DRIEST II results. These latter results are in good agreement with the experimental data and are recommended as references at the 1980-81 STANFORD

Conference. The integral method gives right trends in the range of parameters investigated ($M_e < 5$; $0.2 < T_w / T_{ad} < 1$).

CEBECI-SMITH also presented comparisons of experimental skin friction coefficients for adiabatic flat plate boundary layers by using results obtained with their method. The calculations have been performed with the CEBECI-SMITH mixing length model. In the range $0.4 < M_e < 5$, $1\ 600 < R_\theta < 702\ 000$, figure 11 shows that the calculations reproduce the experiments very well.

Another application of the integral method proposed by COUSTEIX et al. is shown on figure 12. In the experiments performed by HASTINGS-SAWYER, the MACH number is nearly constant ($M_e = 4$) and the wall is adiabatic. Good results are obtained on boundary layer thickness and skin friction.

The following application concerns a flat plate boundary layer with heat transfer (COLEMAN et al.). The calculations have been first performed in turbulent flow with a mixing length scheme (figure 13). It seems that the quality of results is poor as the MACH number increases. Calculations have also been performed by ARNAL by taking into account transition effects. In the transition region, the shear stress is calculated by :

$$-\langle \rho u'v' \rangle = \hat{\epsilon} \mu_t \frac{\partial U}{\partial y}$$

The eddy viscosity is given by a mixing length scheme. In incompressible flow, the intermittency function $\hat{\epsilon}$ is described according to figure 14 (θ is the momentum thickness calculated at the current point and θ_T is the value determined at the transition point). In compressible flow, the intermittency function $\hat{\epsilon}$ is expressed

by the same function but $\frac{\theta}{\theta_T} - 1$ is replaced by

$$\left(\frac{\theta}{\theta_T} - 1 \right) / (1 + 0.02 M_e^2)$$

to take into account the lengthening of the transition region at high speeds. In the application shown on figure 15, the transition point is prescribed according to the experiments. Qualitatively, well behaved computational results are obtained but the level of heat fluxes is slightly overestimated in the turbulent region.

3.2 Boundary layer with pressure gradient

In the experiments of CLUTTER-KAUPS, the boundary layer is studied along a body of revolution with different conditions of velocity, pressure gradient and wall temperature. In the example presented, the MACH number is

around 2.5, the pressure gradient is slightly negative and the ratio T_w/T_{ad} is around 0.6.

The calculations have been performed using three methods : the integral method proposed by COUSTEIX et al., a mixing length scheme and the k- ϵ JONES-LAUDER model. This case does not pose special difficulties and all the methods are in good agreement with experiments (figure 16).

In the experiments of LEWIS et al., 1972, the boundary layer is studied along the inner wall of a cylinder and a centerbody placed along the axis generates the pressure gradient. The wall is adiabatic. The calculations shown in figure 17 have been performed by CEBECI with his mixing length model. The calculated results reproduce the effects of adverse and favorable pressure gradient very well.

3.3 Boundary layer with variable wall temperature

Extensive studies of boundary layers with pressure gradient, heat fluxes and blowing and suction have been performed by MORETTI-KAYS, MOFFAT-KAYS. The case presented in figure 18 deals with a negative pressure gradient and a variable wall temperature. The calculations by CEBECI-SMITH follow the experimental data remarkably well.

3.4 Calculations with heat flux transport equations

FINSON and WU, 1979, developed a REYNOLDS stress transport equation model which also includes transport equations for the turbulent heat fluxes. This model has been applied with the boundary layer approximation. FINSON-WU used their model to calculate boundary layers on rough wall. To do this, they added roughness functions in the momentum equation, in the turbulent kinetic energy equation and in the dissipation equation.

Figures 19 and 20 show the results of their calculation at low speed and comparisons with measurements by HEALZER et al.. The calculations reproduce the increase in the skin friction coefficient and in the STANTON number ($St = \phi_w / \rho_e u_e (h_{ic} - h_w)$). It is interesting to notice that the increase in the heat flux is less than the increase in skin friction. This means that the REYNOLDS analogy is not preserved. This case illustrates the interest in using a model with heat flux transport equations.

In incompressible flow, several models have been proposed for calculating a scalar field with scalar flux equations. The scalar can be temperature. Such a model has been developed

by JONES-MUSONGE, 1988. Figure 21 shows the application of this model to the experimental data obtained by TAVOULARIS and CORRISIN in a nearly homogeneous shear flow with a linear temperature gradient. The results represented in figure 26 are the turbulent PRANDTL number and the ratio of heat fluxes. Here again, this case illustrates the value of a model with heat flux transport equations.

JONES-MUSONGE applied their model with the same success to a thermal mixing layer downstream of a turbulence grid and to a slightly heated plane jet in stagnant surrounds.

3.5 Shock wave-boundary layer interactions

BENAY et al., 1987, performed a critical study of various turbulence models applied to the calculation of shock wave-boundary layer interaction in transonic flow. This study has been performed by using the boundary layer equations solved in the inverse mode (the displacement thickness distribution is introduced as a datum in this calculation method). The authors verified the validity of this approach by comparison with NAVIER-STOKES solutions. They tested mixing length models (from MICHEL, ALBER and BALDWIN-LOMAX) and models with transport equations (the JOHNSON-KING model which includes an equation for the maximum shear stress, the k- ϵ JONES-LAUDER model, the Algebraic Stress Model which is obtained from the RODI proposal applied to the HANJALIC-LAUDER three equation model). In a general way, the authors concluded that the models with transport equations behave better than the other models. The best results are obtained with the Algebraic Stress Model (figures 22b-c-d). It is noticed that the mean velocity profiles are well calculated with this model whereas the turbulence characteristics are not. However the experiment reveals that the flow is not strictly steady and the unsteadiness can interact with turbulence ; on the other hand, the experimental data are not analysed by taking into account this unsteadiness.

Another example is provided by calculations performed at NASA with NAVIER-STOKES equations (see MARVIN-COAKLEY). The experimental configuration is depicted in figure 23a. The results obtained with three models are compared with the experimental data : the CEBECI-SMITH model, the BALDWIN-LOMAX and a q- ω model which has been proposed by COAKLEY, 1983 ; this model has been modified to take into account compressibility corrections and finally a heat transfer correction is included (in the eddy viscosity, the length scale becomes $l = \min(2.4y, q/\omega)$ in order to reduce the heat transfer in the region of reattachment). The results are given in figures 23b and 23c

for two angles of the corner : $\theta = 15^\circ$ and $\theta = 38^\circ$. A reasonable agreement is obtained with the three models for $\theta = 15^\circ$; for the case $\theta = 38^\circ$, the results obtained with the CEBECI-SMITH model have not been given because of the difficulties in computing the displacement thickness distribution. It should also be noticed that the overshoot of the heat flux near the reattachment is not predicted by any model.

3.6 Calculation of the free shear layer

The free shear layer is a flow where the inadequacy of "incompressible" models has been attributed to compressibility terms. Indeed the models extended from the incompressible case without compressibility effects predict practically no effect of the MACH number on the rate of expansion of the free shear layer whereas the experimental results indicate a decrease in the expansion as the MACH number increases. The results shown in figure 24 are concerned with a shear layer with a zero velocity on one side and a non zero velocity U_e on the other side. The thickness δ is defined as the distance between the points where the velocity is $\sqrt{0.1} U_e$ and $\sqrt{0.9} U_e$. The computed results have been produced by BONNET for the 1980-81 STANFORD Conference. To calculate this flow, BONNET tried to include compressibility terms in the modelling of the pressure-velocity correlation term. He argued that the pressure equation in a steady compressible two-dimensional thin shear flow suggests that compressibility affects mainly the return-to-isotropy term. Accordingly, the modelled form of this term is multiplied by a compressibility dependent factor. Improvements of the same quality have been obtained by VANDROMME and by DUSSAUGE-QUINE who also introduced compressibility effects. These compressibility corrections lead to improved results (as compared with experimental data) but it is not sure if the effects of MACH number are attributable to modifications of the turbulence structure or to a problem of stability which modifies the large structures of the shear layer in which case it is not justified to accuse the turbulence model.

CONCLUSION

The calculations of classical compressible turbulent boundary layers not too far from equilibrium have often been approached with rather simple models extended in a straightforward manner from the incompressible case. For these cases, this approach is justified even at MACH numbers as high as 10 except perhaps for the calculation of wall heat flux where some uncertainty is still present. Indeed, in most of the calculations, the turbulent heat flux is evaluated by using a turbulent PRANDTL num-

ber which is assumed essentially to be a constant. This hypothesis influences directly the calculation of the wall heat fluxes. In many situations, the value of the PRANDTL number is not the value determined in a flat plate boundary layer. Therefore, it is certainly valuable to try to develop transport equations for the turbulent heat fluxes. This work is often performed when the temperature can be considered as a passive scalar which is a first approach to the more general problem of compressible flow. Useful information can be gained from the studies of the mixing of non reactive gases and from the study of homogeneous compressed turbulence (REYNOLDS, 1987).

The question of including compressibility corrections in the transport equations is not solved because these terms have been used for flows such as the free shear layer or shock wave-boundary layer interaction. It seems that the inclusion of such terms has often been beneficial but it is not clear if these compressibility terms are completely justified or if they mask other problems. In the case of the shock wave-boundary layer interaction, models are available which give reasonable agreement on pressure distribution for example, but none of them give the viscous parameters with the required accuracy.

A third important problem is the near wall treatment (which is not specific of the compressible flows). In most of the applications, a simple model is used (for example a mixing length or a one-equation model) but efforts are devoted to develop more general models valid in the fully turbulent region and in the near wall region (LAUNDER-TSELEPIDALIS, 1988).

Indeed the near wall model is very important because not only it influences the prediction of the skin friction for example, but also it has an important effect on the numerical behaviour of the model. The numerical properties of the models are rather rarely studied, although they are of great practical relevance ; indeed it is not very useful to have a well physically founded model which leads to untractable numerical difficulties.

The evaluation of turbulence models is based on comparisons with experimental data but it appears that accurate data are not very numerous in compressible flows. Surprisingly good data are available for complex flows like shock-wave/boundary layer interactions but for simpler boundary layer flows the data are limited. Good and detailed data are needed to evaluate the effects of MACH number, wall temperature, pressure gradient. For this latter case (effect of pressure gradient), simple experiments are difficult because the generation of streamwise pressure gradient induces the presence of a pressure gradient normal to the wall. Now, when boundary layer codes are used the

presence of normal pressure gradient is not accounted for. Then it could be instructive to develop second order boundary layer codes to analyze the validity of turbulence models in such cases.

Another direction which is being worked on to improve turbulence models is the use of full numerical simulations. In incompressible flow, the results of these simulations have led to improvements (for example for the study of rotation effects) and it is believed that the numerical simulations are useful to generate complete sets of data for basic flows and the analysis of these data is certainly a precious guide to improve turbulence models.

It is also worth mentioning the problem of laminar-turbulent transition. The accurate prediction of the transition location and of the transition length are obviously very important parameters for the description of the flow but the influence on the characteristics of the downstream turbulent flow is not very well known.

REFERENCES

ARNAL D. "Laminar-turbulent transition problems in supersonic and hypersonic flows" AGARD FDP VKI Special Course on Aerothermodynamics of Hypersonic Vehicules (30 May-3 June 1988)

BALDWIN B.S., LOMAX H. "Thin layer approximation and algebraic model for separated turbulent flows" AIAA Paper N° 78-0257 (1978)

BENAY R., COET M.C., DELERY J. "Validation de modèles de turbulence appliqués à l'interaction onde de choc-couche limite transsonique" La Rech. Aérop. N°1987-3 (1987)

BLACKWELL B.F., KAYS W.M., MOFFAT R.J. Rept. HMT-16, Mech. Eng. Dept., Stanford University (1972)

BONNET J.P. "Comparison of computation with experiment" 1980-81 AFOSR-HTTM STANFORD Conference on Complex Turbulent Flows, Ed. S.J. KLINE, B.J. CANTWELL, G.M. LILLEY

BRADSHAW P. "Compressible turbulent shear layers" Annual Review of Fluid Mechanics, (1977)

BROWN G.L., ROSHKO A. "On density effects and large structures in turbulent mixing layers" J.F.M. Vol. 64 part 4 (1974)

BUSHNELL D.M., WATSON R.D., HOLLEY B.B. "MACH and REYNOLDS number effects on turbulent skin friction reduction by injection" J. Spacecraft Vol. 12 N°8 (1975)

BUSHNELL D.M., CARY A.M., HOLLEY B.B. "Mixing length in low REYNOLDS number compressible turbulent boundary layers" AIAA Journal Vol. 13 N° 8 (1975)

BUSHNELL D.M., CARY A.M., HARRIS J.E. "Calculation methods for compressible turbulent boundary layers" VKI Lecture Series LS86 (1976) NASA SP-422 (1977)

BUSHNELL D.M., MALIK M.R., HARVEY W.D. "Transition prediction in external flows via linear stability theory" IUTAM Symp. Transonicum III, Göttingen (may 1988)

CEBECI T., SMITH A.M.O. "Analysis of turbulent boundary layers" Academic Press (1974)

CHASSAING P. "Une alternative à la formulation des équations du mouvement d'un fluide à masse volumique variable" Journal de Mécanique Théorique et Appliquée Vol. 4 n° 3 (1985)

CHAMBERS A.J., ANTONIA D.A., FULACHIER L. "Turbulent Prandtl number and spectral characteristics of a turbulent mixing layer" Int. J. Heat Mass Transfer, Vol. 28 n° 8 (1985)

CLUTTER D.W., KAUPS K. "Wind tunnel investigations of turbulent boundary layers on axially symmetric bodies at supersonic speeds" DOUGLAS Aircraft Division Rep. N° LB 31425 (1964)

COAKLEY T.J. "Turbulence modelling methods for the compressible NAVIER-STOKES equations" AIAA 83 1693, DANVERS, MA (JULY 1983)

COLEMAN G.T., ELESTROM G.M., STOLLERY J.L. "Turbulent boundary layers at supersonic and hypersonic speeds" AGARD CP 93 (1971)

COUSTEIX J., HOUEVILLE R., MICHEL R. "Couches limites turbulentes avec transfert de chaleur" La Rech. Aérop. N° 1974-6 (1974)

DELERY J. "Shock/shock and shock wave/boundary layer interactions in hypersonic flows" AGARD FDP VIK Special Course on Aerothermodynamics of Hypersonic Vehicles (1988)

DUSSAUGE J.P., QUINE C. "A second order closure for supersonic turbulent flows - Application to the supersonic mixing" Workshop on "the Physics of Compressible Turbulent Mixing" Princeton, N.J. (1988) To be published in "Lecture notes in engineering" Springer Verlag

FAVRE A., KOVASZNAY L.S.G., DUMAS R., GAVIGLIO J., COANTIC M. "La turbulence en mécanique des fluides" Ed. GAUTHIER-VILLARS (1976)

FINSON M.L., WU P.K.S. "Analysis of rough wall turbulent heating with application to blunted flight vehicles" AIAA Paper 79-0008 (1979)

FULACHIER L., ANTONIA R.A. "Spectral relationships between velocity and temperature fluctuations in turbulent shear flows" Phys. Fluids 26(8) pp. 2105-2108 (1983)

GAVIGLIO J. "Reynolds analogies and experimental study of heat transfer in the supersonic boundary layer" Int. J. Heat Mass Transfer Vol. 30 N° 5, pp. 911-926 (1987)

HANJALIC K., LAUNDER B.E. "A Reynolds stress model of turbulence and its application to thin shear flows" J.F.M. Vol. 52, Part 4 (1972)

HANJALIC K., LAUNDER B.E. "Contribution towards a Reynolds stress closure for low Reynolds number turbulence" J.F.M. Vol. 74 n° 3 (1976)

HASTINGS R.L., SAWYER W.G. "Turbulent boundary layers on a large flat plate at $M = 4$ " RAE TR 70040

HEALZER J.M., MOFFAT R.J., KAYS W.M. "The turbulent boundary layer on a rough porous plate : experimental heat transfer with uniform blowing" Thermosciences Division, Dept. of Mech. Eng., STANFORD University Report n° HMT-18 (1974)

JONES W.P., LAUNDER B.E. "The prediction of laminarization with a two-equation model of turbulence" Int. J. of Heat Mass Transfer Vol. 15 (1972)

JONES W.P., MUSONGE P. "Closure of the Reynolds stress and scalar flux equations" Phys. Fluids 31 (12) pp. 3589-3604 (1988)

LAUNDER B.E. "Heat and mass transport" in "Turbulence" Ed. P. BRADSHAW - Topics in Applied Physics - Vol. 12 Springer Verlag, BERLIN-HEIDELBERG-NEW YORK (1976)

LAUNDER B.E., TSELEPIDAKIS D.P. "Contribution to the second-moment modelling of sublayer turbulent transport" Zoran Zaric Memorial, BELGRAD (1988)

LEWIS J.E., GRAN R.L., KUBOTA T. "An experiment in the adiabatic compressible turbulent boundary layer in adverse and favorable pressure gradients" J. Fluid Mech. 51 (1972)

MAISE G., McDONALD M. "Mixing length and kinematic eddy viscosity in a compressible boundary layer" AIAA J. 6, 73 (1968)

MARVIN J.G., COAKLEY T.J. "Turbulence modelling of hypersonic flows" The Second Joint EUROPE/US, Short Course in Hypersonics, Colorado Springs (1989)

MEIER H.U., ROTTA J.C. "Temperature distributions in supersonic turbulent boundary layers" AIAA J. 9, 2149 (1971)

MICHEL R. "Couches limites - Frottement et transfert de chaleur" Cours de l'Ecole Nationale Supérieure de l'Aéronautique (1967)

MOFFAT R.J., KAYS W.M. "The turbulent boundary layer on a porous plate ; experimental heat transfer with uniform blowing and suction" Int. J. Heat Mass Transfer 11 (1968)

MORETTI B.M., KAYS W.M. "Heat transfer to a turbulent boundary layer with varying free stream velocity and varying surface temperature : an experimental study" Int. J. Heat Mass Transfer 8 (1965)

MORKOVIN M.V. "Effects of compressibility on turbulent flows" Coll. Intern. CNRS N° 108, Mécanique de la Turbulence, Ed. CNRS (1961)

PAPAMOSCHOU D., ROSHKO A. "The compressible turbulent shear layer : an experimental study" J.F.M. Vol. 197, pp. 453-477 (1988)

REYNOLDS W.C. "Fundamentals of turbulence for turbulence modelling and simulation" AGARD Report n° 755 (1987)

RODI W. "The prediction of free boundary layers by use of a two-equation model of turbulence" Ph. D. Thesis, University of LONDON (1972)

SANDBORN V.A. "A review of turbulence measurements in compressible flow" NASA TM X-62, 337 (1974)

SMITH A.M.O., GAMBERONI N. "Transition, pressure gradient and stability theory" DOUGLAS Aircraft Co. Report ES26 388, EL SEGUNDO, CALIFORNIA (1956)

TAVOULARIS S., CORRISIN S. "Experiments in nearly homogeneous turbulent shear flow with a uniform mean temperature gradient" J.F.M. Vol. 104 (1981)

VAN DRIEST E.R. "Turbulent boundary layer in compressible fluids" J. Aeron.Sci. 18, 145 (1951)

VANDROMME D. "Contribution à la modélisation et à la prédiction d'écoulements turbulents à masse volumique variable" Doctorat d'Etat - Université de LILLE (1983)

VAN INGEN J.L. "A suggested semi-empirical method for the calculation of the boundary layer transition region" Univ. of Technology, Dept. of Aero. Eng., Rept. UTH-34, DELFT (1956)

FIGURES

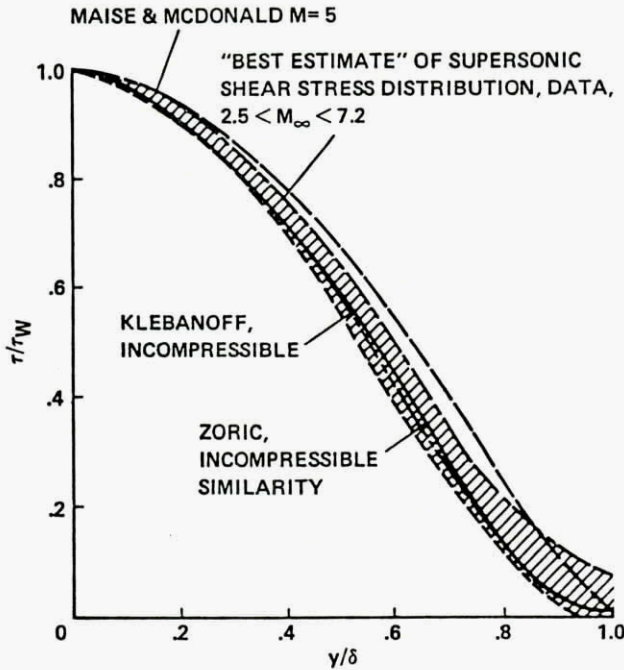


Figure 1 : Effect of Mach number on the shear stress distribution in a flat plate boundary layer
Figure taken from MARVIN-COAKLEY

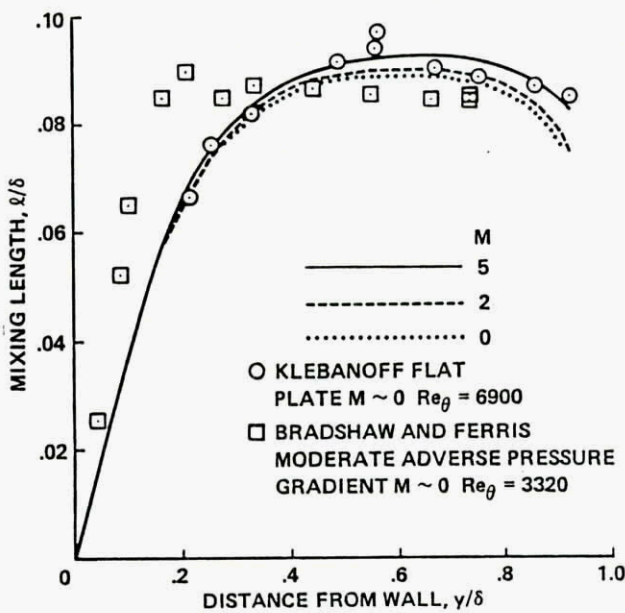


Figure 2 : Effect of Mach number on the mixing length distribution from MAISE and McDonald.
Figure taken from MARVIN-COAKLEY

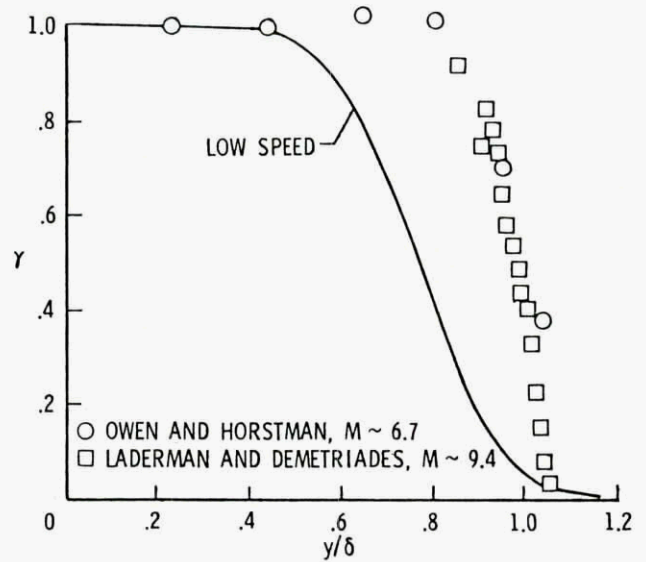


Figure 3 : Effect of Mach number on the intermittency function from SANDBORN.
Figure taken from BUSHNELL et al., 1976

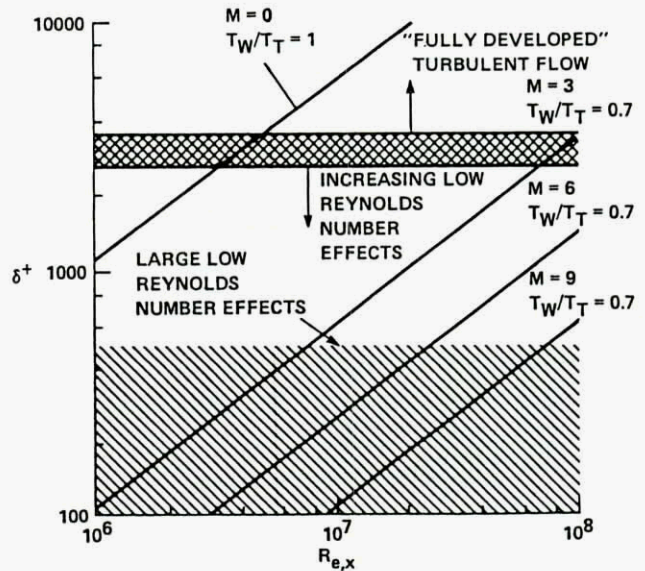


Figure 4 : Importance of low Reynolds number effects at high Mach number
From BUSHNELL et al., 1976

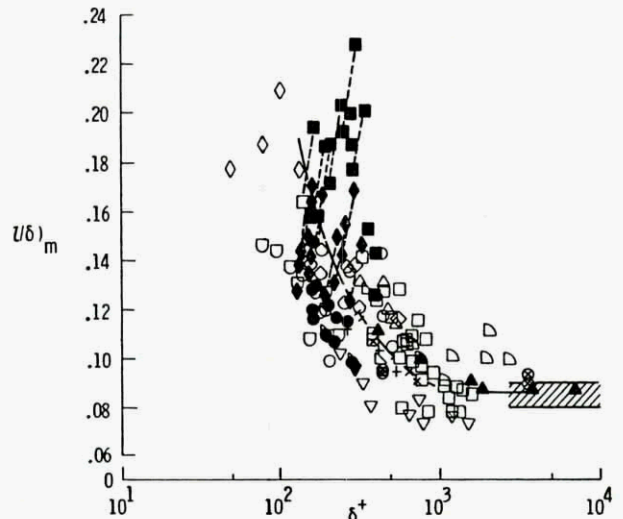


Figure 5a : Variation of the outer level of the mixing length downstream of natural transition on plates, cones and cylinders
From BUSHNELL et al.

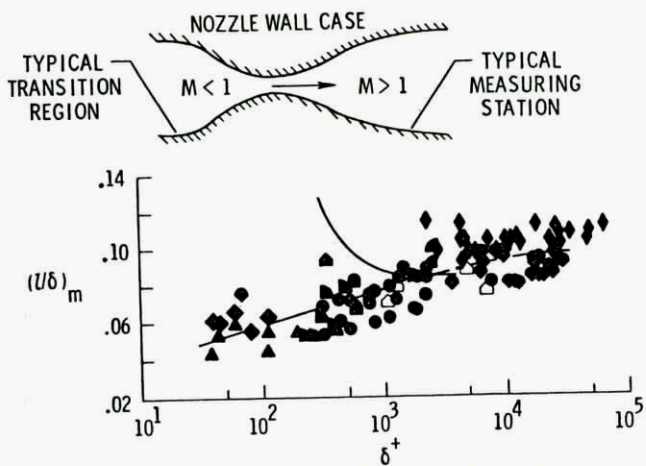


Figure 5b : Effects of low boundary layer Reynolds number on the outer level of the mixing length for flows on nozzle walls without laminarization-retransition
 From BUSHNELL et al.

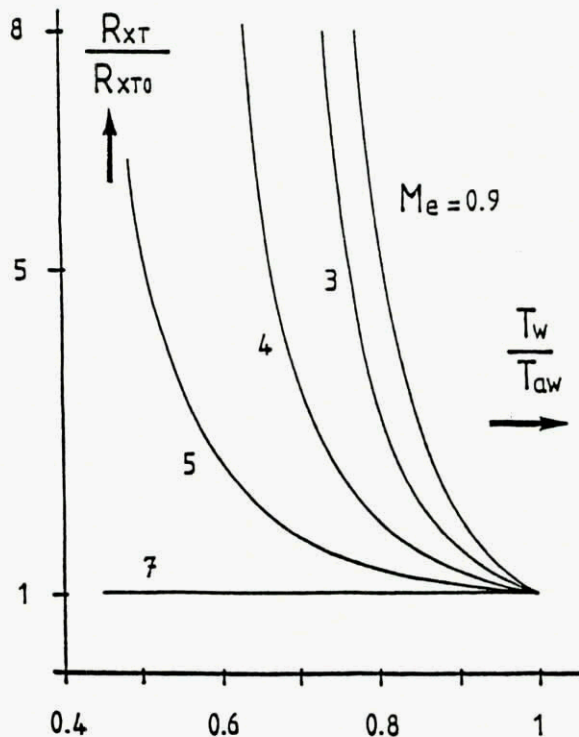


Figure 7 : Theoretical effect of wall cooling on the flat plate transition Reynolds number as calculated by the e^n method ($n=9$)
 From ARNAL, 1988

R_{xT0} is the transition Reynolds number for $T_w/T_{aw} = 1$ (adiabatic wall). R_{xT0} depends on the value for the Mach number

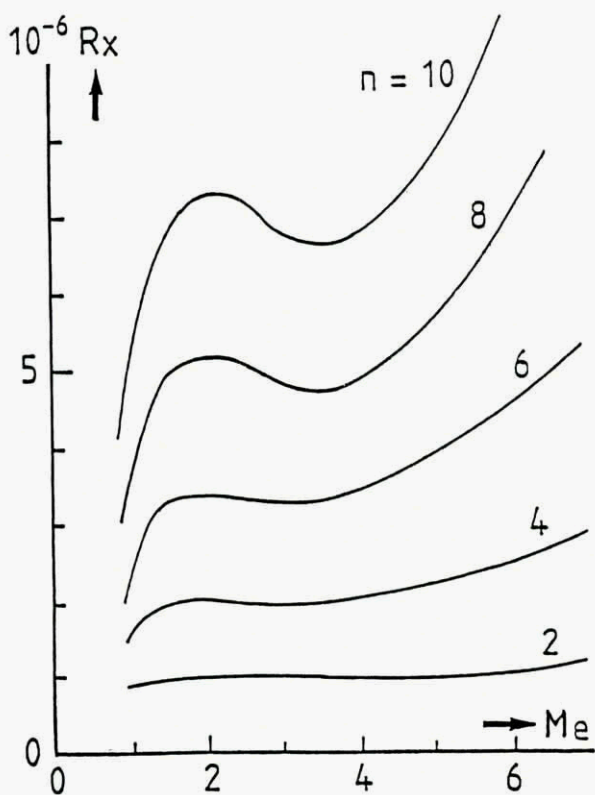


Figure 6 : Application of the e^n method to the boundary layer transition on a sharp cone with an adiabatic wall
 From ARNAL, 1988

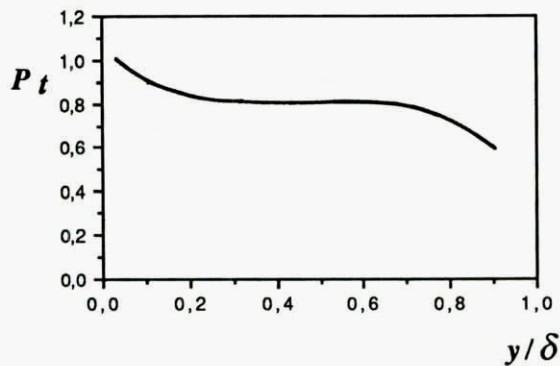


Figure 8a : Prandtl number in a boundary layer
 From MEIER-ROTTA

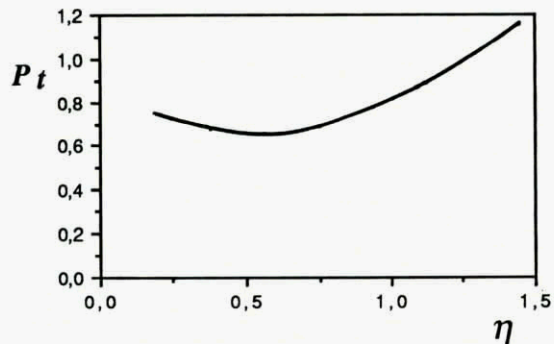


Figure 8b : Prandtl number in a plane jet
 From FULACHIER-ANTONIA

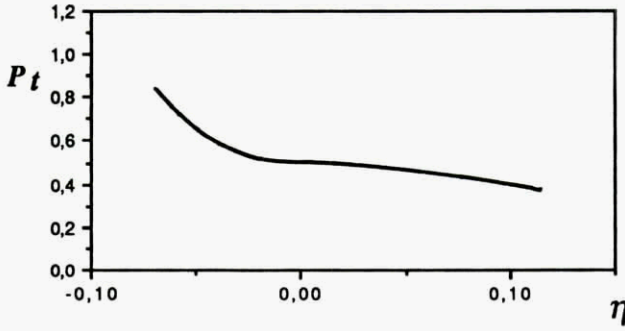


Figure 8c : Prandtl number in a mixing layer
 From CHAMBERS et al.

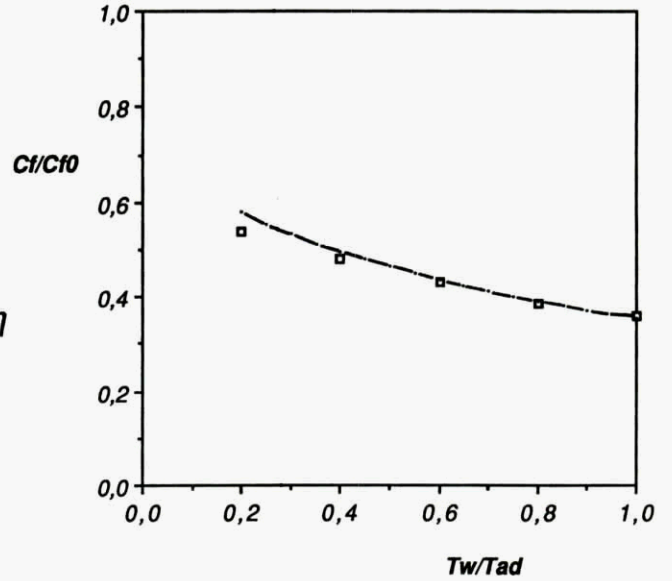


Figure 10 : Effect of wall temperature on the skin friction of a flat plate boundary layer ($M_e=5$)

T_w = wall temperature - T_{ad} = adiabatic wall temperature
 Free flight at 15000 m
 $R\theta = 10\ 000$ $Cf_0 = 2.634 \cdot 10^{-3}$

From VAN DRIEST II applied to KARMAN-SCHÖNHERR equation

□ Integral method

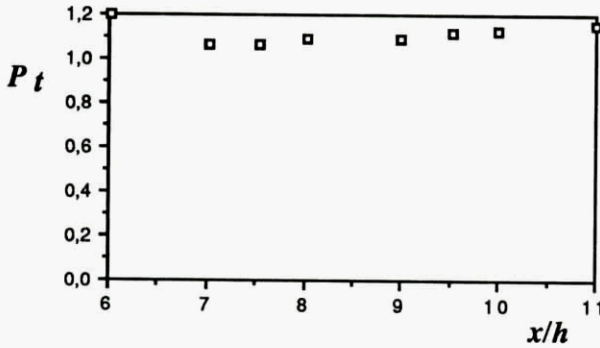


Figure 8d : Prandtl number in a homogeneous shear flow
 From TAVOULARIS-CORRSIN

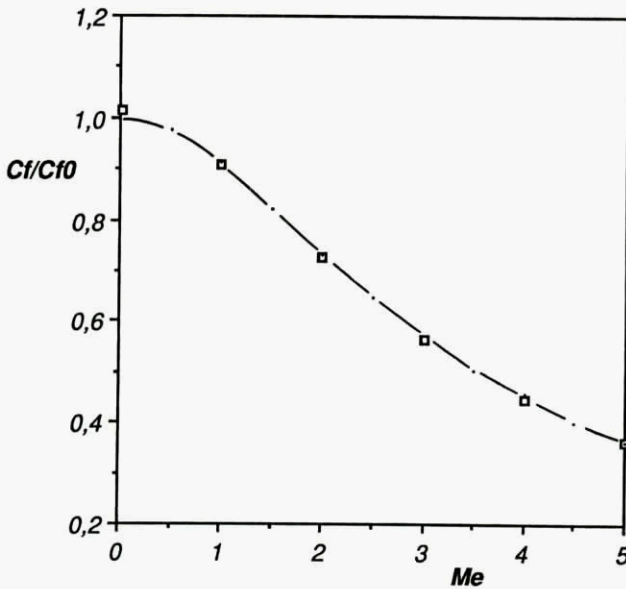


Figure 9 : Effect of Mach number on the skin friction of a flat plate boundary layer (insulated wall)

Free flight at 15000 m
 $R\theta = 10\ 000$ $Cf_0 = 2.634 \cdot 10^{-3}$

From VAN DRIEST II applied to KARMAN-SCHÖNHERR equation

□ Integral method

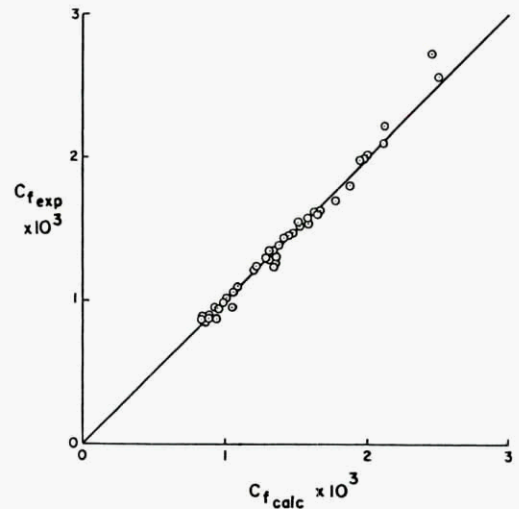


Figure 11 : Comparison of calculated and experimental local skin friction values for adiabatic flat plates

Calculations from CEBECI-SMITH

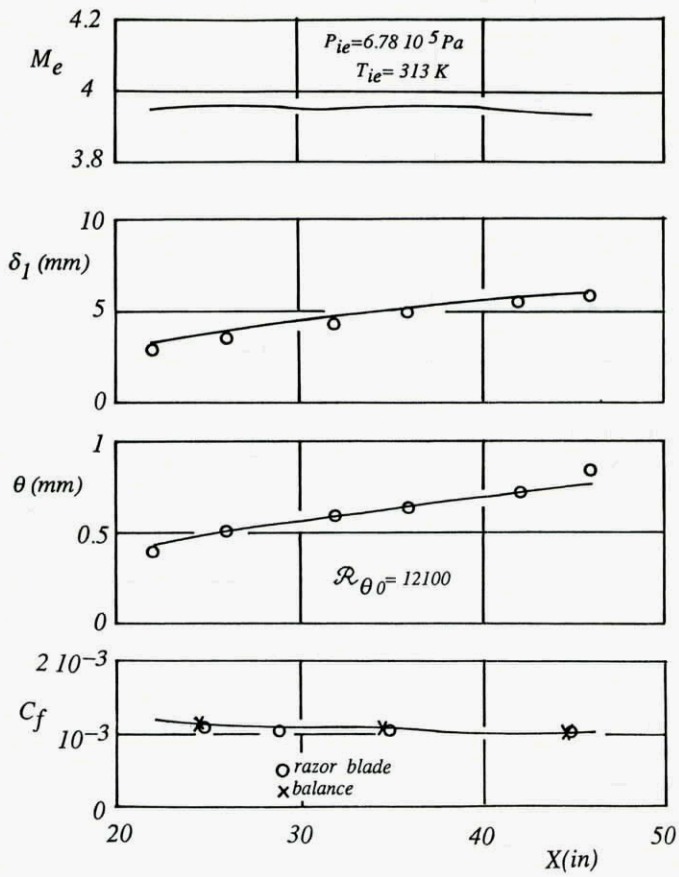


Figure 12 : Calculation of the experiments of HASTINGS-SAWYER with an integral method

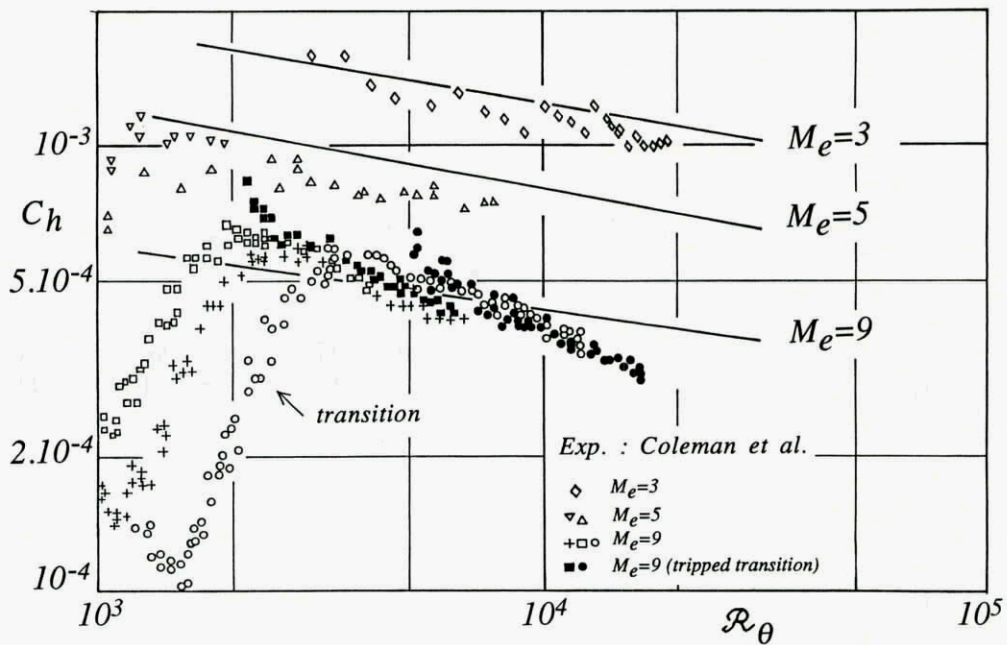


Figure 13 : Calculations of COLEMAN et al. experiments with a mixing length scheme

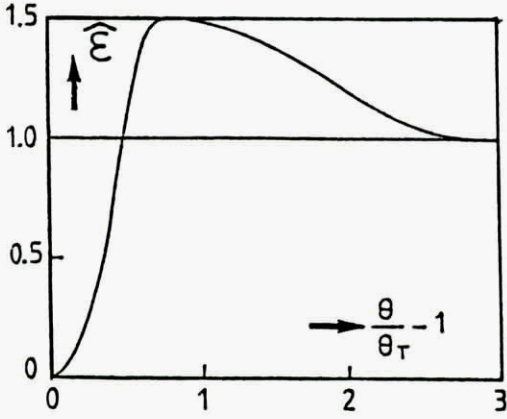


Figure 14 :Intermittency function used by ARNAL in incompressible flow

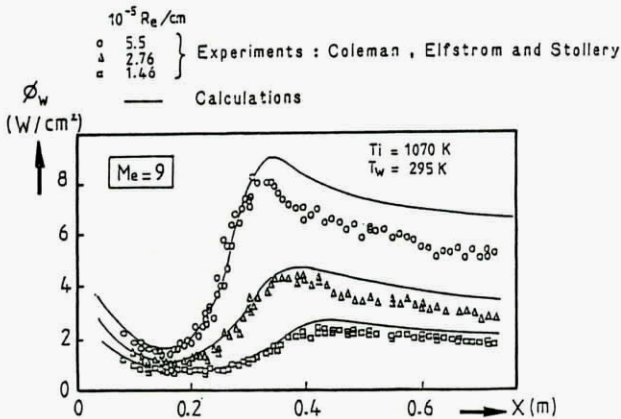


Figure 15 : Calculations of COLEMAN et al. experiments taking into account the transition region
 From ARNAL

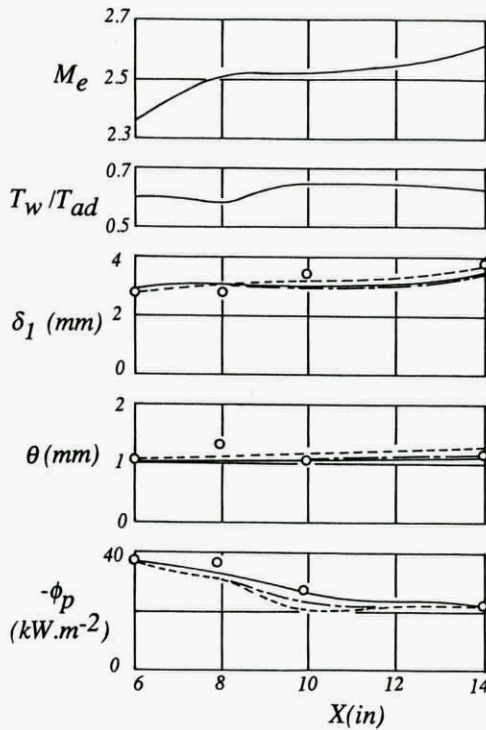


Figure 16 : Calculation of CLUTTER-KAUPS experiments

- integral method
- mixing length
- k - ε model (JONES-LAUNDER)

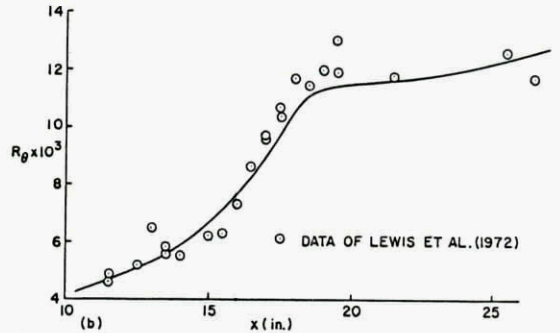
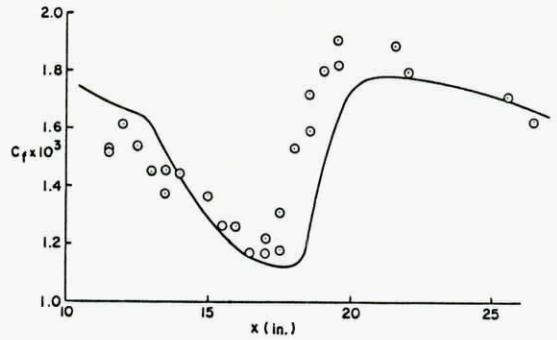
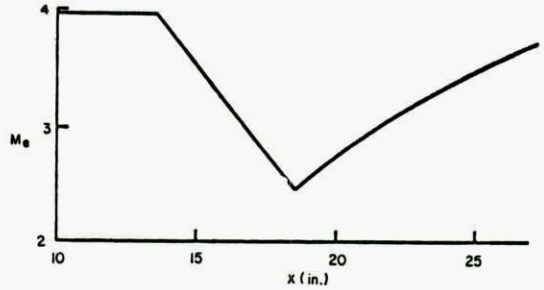


Figure 17 : Calculations of LEWIS et al. experiments by CEBECI-SMITH

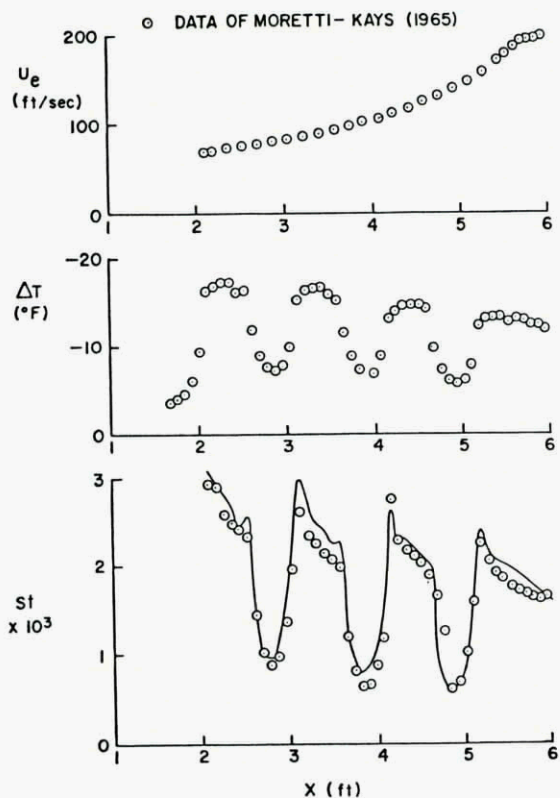


Figure 18 : Boundary layer with variable wall temperature
 ○○○○ Experiments : MORETTI-KAYS
 ——— Calculations : CEBECI-SMITH

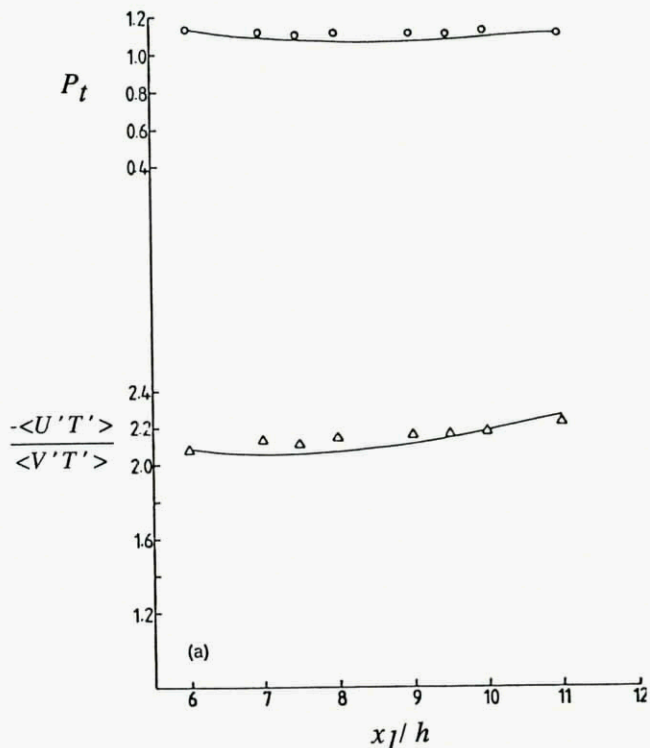


Figure 21 : Scalar turbulence in a nearly homogeneous shear flow with a linear mean temperature gradient ΔT Experiment : TAVOULARIS-CORRSIN
 ——— Calculations : JONES-MUSONGE

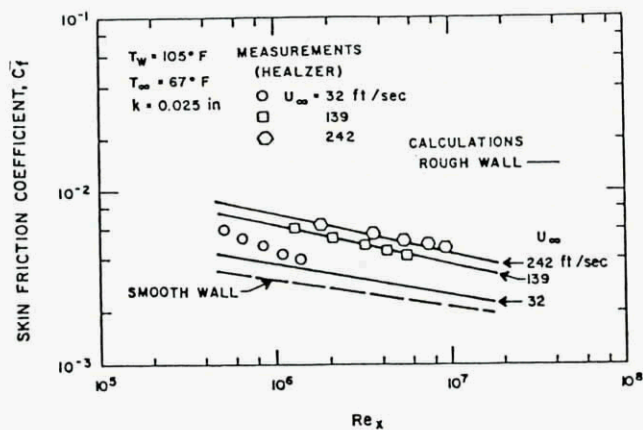


Figure 19 : Calculations of the skin friction coefficient on a roughened flat plate
 By FINSON-WU

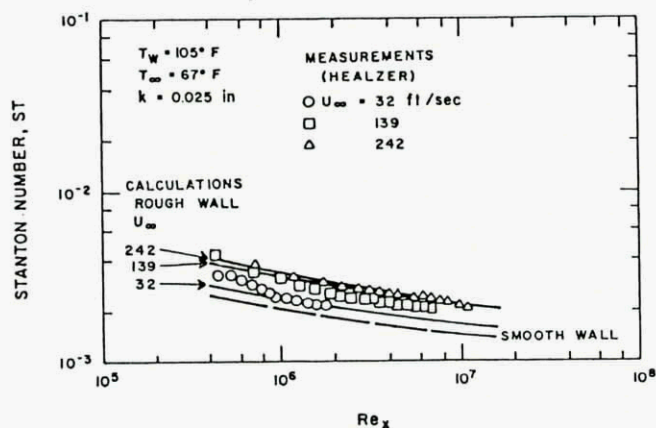


Figure 20 : Calculations of the heat transfer coefficient on a roughened flat plate
 By FINSON-WU

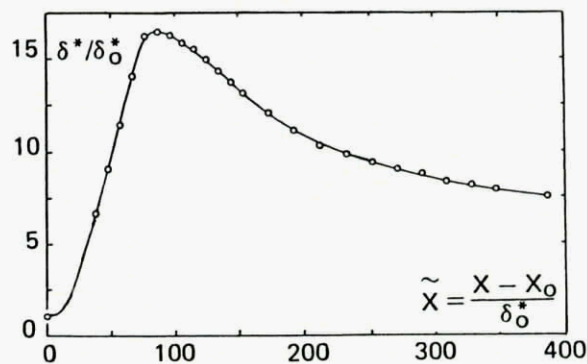


Figure 22a : Calculations of a boundary layer/shock-wave interaction with an inverse boundary layer method - $M_{e0} = 1.36$
 The experimental displacement thickness distribution is used as an input of the method
 From BENAY et al.

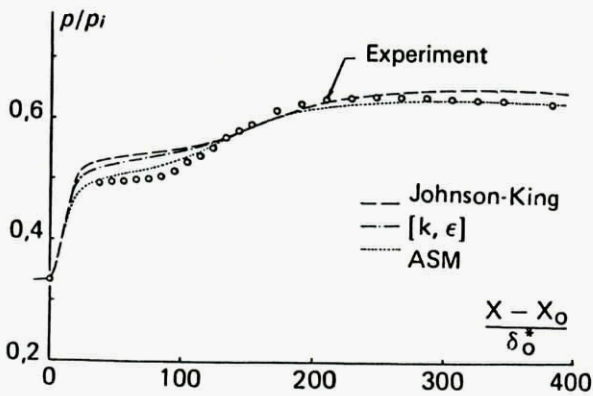
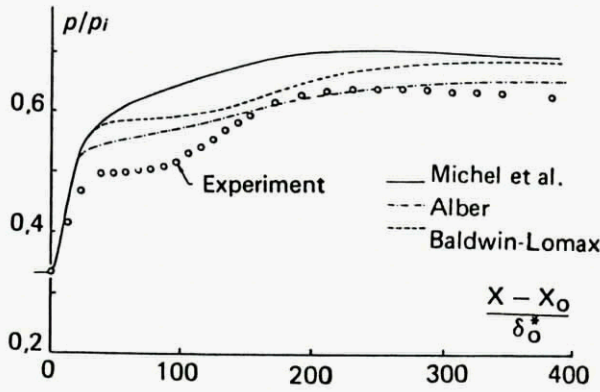


Figure 22b : Comparison between calculated and experimental pressure distribution

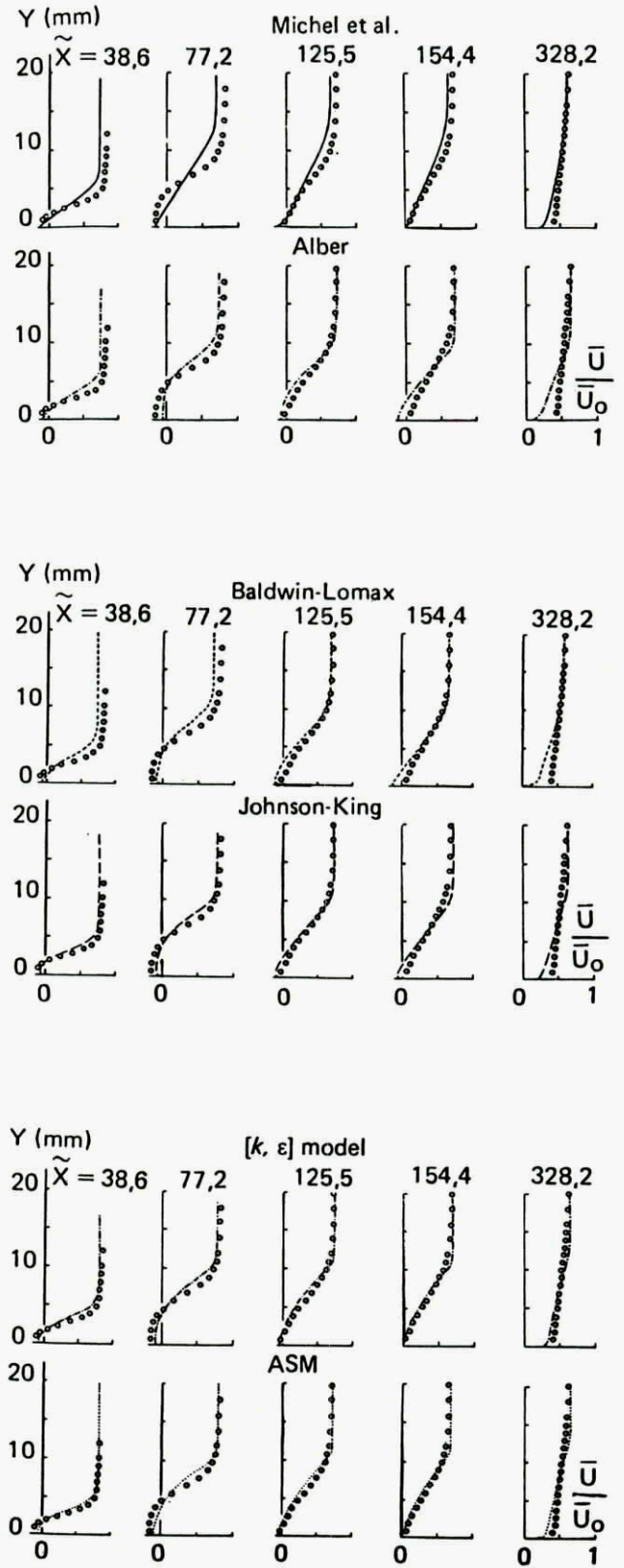


Figure 22c : Comparison between calculated and experimental boundary layer velocity profiles

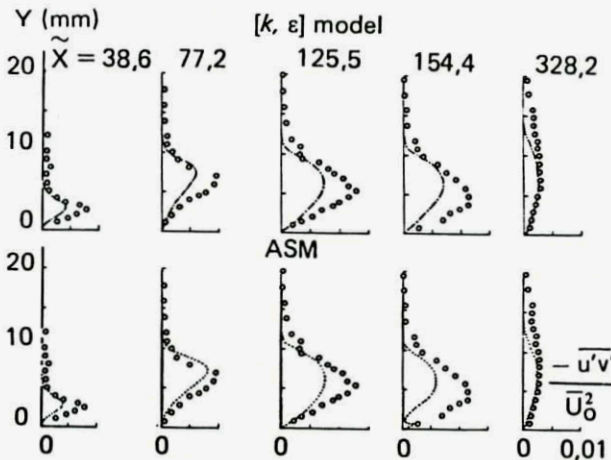
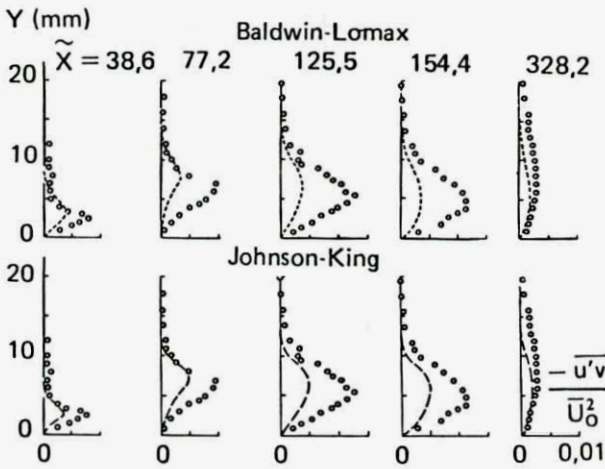
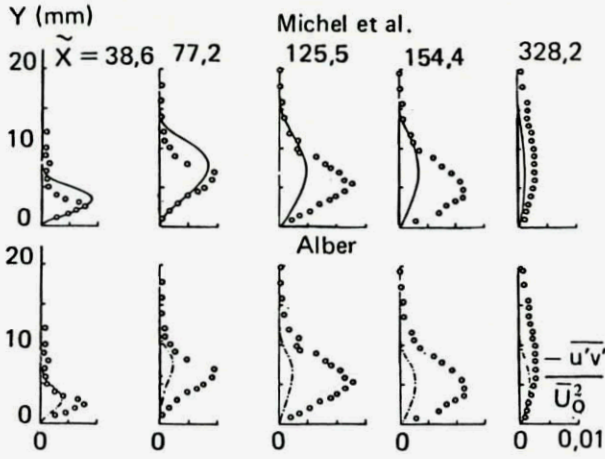


Figure 22d : Comparison between calculated and experimental boundary layer shear stress profiles

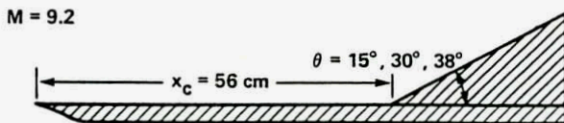


Figure 23a : Study of a compression corner flow
 From MARVIN-CAOKLEY

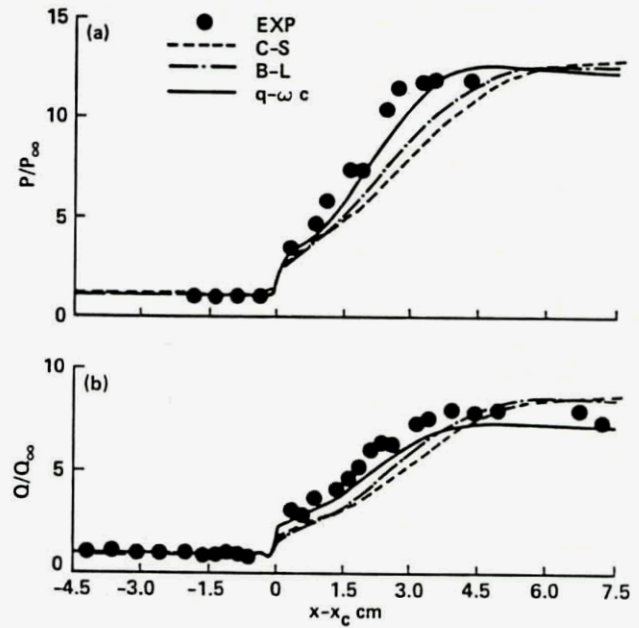


Figure 23b : Comparison between calculated and experimental data on a compression corner flow
 - $\theta = 15^\circ$ - Pressure and heat transfer distributions

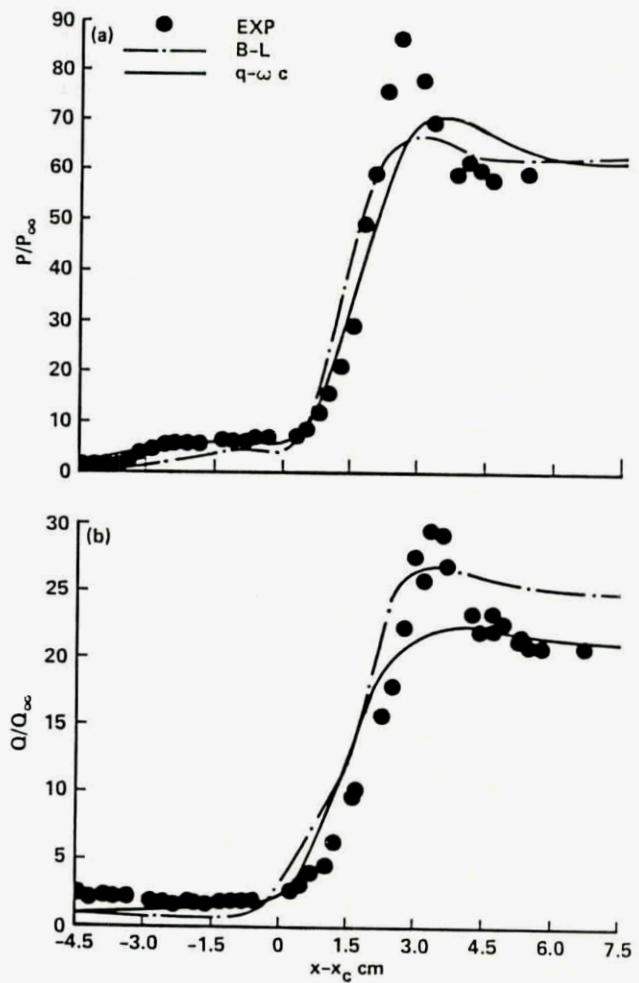


Figure 23c : Comparison between calculated and experimental data on a compression corner flow
 - $\theta = 38^\circ$ - Pressure and heat transfer distributions

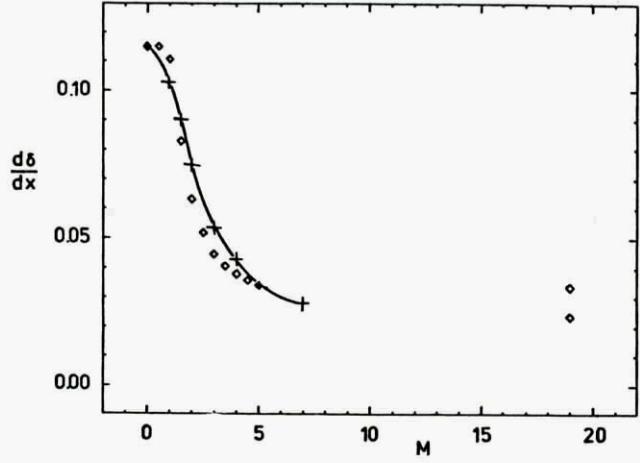


Figure 24 : Calculation of the free shear layer expansion rate
◇ experimental data
—+— Calculations (J.P. BONNET)

SOME CURRENT APPROACHES IN TURBULENCE MODELLING

W. Rodi
 Institute for Hydromechanics
 University of Karlsruhe
 7500 Karlsruhe, F.R. Germany

SUMMARY

The paper reviews some recent work in the area of modelling turbulence in near-wall regions and by Reynolds-stress-equation models. Various low-Reynolds-number versions of the $k-\epsilon$ model and their damping functions are examined with the aid of results from direct numerical simulations and they are compared with respect to their performance in calculating boundary layers under adverse and favourable pressure gradients. A two-layer model is presented in which near-wall regions are resolved with a one-equation model and the core region with the standard $k-\epsilon$ model. Various applications of this model are shown. The ability of the various models to simulate laminar-turbulent transition in boundary layers is discussed. Recent applications of a fairly simple, standard Reynolds-stress-equation model to two complex flows of practical interest are presented. Finally, the paper reports on some recent proposals for improved Reynolds-stress-equation models and provides an outlook on possible future turbulence-model developments.

1. INTRODUCTION

In conventional turbulence modelling, whose task it is to provide models for calculating the turbulent stresses appearing in the Reynolds-averaged equations, three main approaches have emerged:

- (i) Fairly simple eddy-viscosity models, which are either entirely algebraic and of the mixing-length-model type (Cebeci-Smith [1], Baldwin-Lomax [2]) or employ an ordinary differential equation for the maximum shear stress (Johnson and King [3]) are used extensively for calculating the flow over airfoils and turbomachinery blades at all speeds. The usefulness of the various models depends on the degree of flow separation. While the entirely algebraic models cannot simulate transport and history effects, the Johnson-King model can account for such effects and therefore appears to perform best in the presence of separation regions. However, this model was designed for external aerodynamic flows with relatively small separation zones and is not so suitable for other situations with massively separated flow.
- (ii) The second main class of turbulence models in practical use today are the $k-\epsilon$ -type models employing two differential equations for calculating the eddy viscosity, one for the velocity scale and the other for the length scale of the turbulent fluctuations. $k-\epsilon$ -type models are widely used for practical calculations and are built into many commercial general-purpose CFD codes. They can handle situations with massive separation; yet there is no guarantee for good accuracy. The use of an isotropic eddy viscosity, establishing a close link between the turbulent stresses and the strain rate, is probably too simple for highly non-isotropic situations prevailing in flows with complex strain fields. Most practical $k-\epsilon$ model calculations are still carried out with wall functions bridging the viscous sublayer, but recently also low-Reynolds-number versions resolving this sublayer have become popular, and these versions must be used whenever the flow is transitional. Considerable research activity has been going on in the area of near-wall modelling.
- (iii) The third class of models in use are Reynolds-stress-equation (RSE) models also known as second-order closure schemes. They do not employ the eddy-viscosity concept but solve model-transport equations for the individual Reynolds stresses. They are better suited for complex strain

fields as well as for simulating transport and history effects and the anisotropy of turbulence, and they automatically account for certain extra effects on turbulence such as due to streamline curvature, rotation, buoyancy and flow dilatation. RSE models have recently been subjected to fairly wide testing and are presently built into commercial CFD codes. However, the main testing and application has been restricted to fairly basic versions of RSE models which do not satisfy certain theoretical requirements like the realisability conditions and compatibility with the limiting 2D state of turbulence near walls. Another active area of research is the development of more refined models which do satisfy these requirements. Further, RSE models were applied so far mainly in connection with wall functions, but recently research has focused also on near-wall RSE modelling.

Much of the recent turbulence modelling activities described briefly under (ii) and (iii) was prompted by the increase in computing power. This also triggered another development in turbulence research, as direct numerical simulations are now possible, at least for moderate Reynolds numbers. The direct simulations performed to-date already provide a wealth of data that allow the checking of each and every detail of the model proposals and may form the basis for devising improved models. Hence, turbulence-model development and testing benefits increasingly from the direct numerical simulation data, but since these are so far restricted to fairly low Reynolds numbers, the greatest impact of the direct simulations was so far on near-wall modelling.

The present paper describes some recent developments in areas where research is particularly active, namely the areas of near-wall modelling and the application of basic RSE models to complex flows. Further, trends in the development of more refined Reynolds-stress closures are briefly discussed. Of necessity, only some areas of recent turbulence-modelling work can be covered, and the paper focuses on incompressible flow and on the modelling of Reynolds stresses (rather than turbulent heat and mass fluxes).

2. NEAR-WALL MODELLING

The simple eddy-viscosity models listed in the Introduction under (i) resolve the viscous sublayer near walls by relying on the van Driest damping model for the eddy viscosity. The application of these models is restricted mainly to external aerodynamic flows without massive separation. Dictated by the limitations of computer resources, most practical calculations with more complex turbulence models such as $k-\epsilon$ - and Reynolds-stress-equation models were carried out so far by bridging the rather thin, viscosity-affected near-wall layer by wall functions. The areas of steep gradients in this layer were thereby not resolved as the first grid point away from the wall was placed outside the viscous sublayer. As described in some detail in [4] for the $k-\epsilon$ model, the wall functions relating the velocity and turbulence quantities at the first grid point mainly to the friction velocity lean heavily on the assumption of a logarithmic velocity distribution and of local equilibrium of turbulence. These assumptions are certainly not generally valid, for example not when strong secondary flows extend into the sublayer [5] and also not in separated flows. The wall functions are of course particularly unsuited for separation and reattachment regions. Due to recent increases in computing power, the necessity to use wall functions is now much reduced, and considerable activity was recently directed towards testing and developing low-Reynolds-number models for simulating the turbulent processes very near walls. In the following, some of these activities will be described for $k-\epsilon$ -type models. It should be mentioned in this context that for

strongly compressible aerodynamic flows, there is some trend in the opposite direction, namely to use specially developed wall functions [6]. For various transonic and supersonic flows, Marvin [7] reports superior k-ε model predictions with these wall functions over the use of a low-Re version.

2.1 Low-Re k-ε Models

Various near-wall versions of the widely used k-ε turbulence model have been proposed, and the pre 1984 models have been reviewed by Patel et al. [8]. These versions employ the eddy-viscosity concept and determine the eddy viscosity ν_t from

$$\nu_t = f_\mu c_\mu \frac{k^2}{\tilde{\epsilon}} \quad (1)$$

where f_μ is a damping function and k and ϵ are determined from the following equations:

$$U_j \frac{\partial k}{\partial x_j} = \frac{\partial}{\partial x_j} \left[\left(\nu + \frac{\nu_t}{\sigma_k} \right) \frac{\partial k}{\partial x_j} \right] + \underbrace{\nu_t \left(\frac{\partial U_i}{\partial x_j} + \frac{\partial U_j}{\partial x_i} \right) \frac{\partial U_i}{\partial x_j}}_{P_k} - \epsilon \quad (2)$$

$$U_j \frac{\partial \tilde{\epsilon}}{\partial x_j} = \frac{\partial}{\partial x_j} \left[\left(\nu + \frac{\nu_t}{\sigma_\epsilon} \right) \frac{\partial \tilde{\epsilon}}{\partial x_j} \right] + c_{\epsilon 1} f_1 \frac{\tilde{\epsilon}}{k} P_k - c_{\epsilon 2} f_2 \frac{\tilde{\epsilon}^2}{k} + E \quad (3)$$

In some model versions, $\tilde{\epsilon}$ is equal to the actual dissipation ϵ , while in others it is $\tilde{\epsilon} = \epsilon - D$, where D depends on the version considered and is non-zero only in the viscosity-affected region. Equation (3) for the variable $\tilde{\epsilon}$ contains the additional damping functions f_1 and f_2 and in some versions an extra term E . The versions published before 1984, their damping functions and the extra terms involved have been discussed in detail by Patel [8]. Here, three more recent versions [9, 10, 11] are included and three issues are addressed, namely the f_μ -function, comparison with direct simulation data, and the performance for boundary layers under adverse and favourable pressure gradients. As was pointed out already in [8], the damping of the turbulent momentum transfer near walls is due to both viscous effects and the reduction of velocity fluctuations normal to the wall by the pressure-reflection mechanism. The second mechanism is, to first approximation, independent of viscosity, but since it is difficult to separate the two effects they are usually both modelled by the viscosity-dependent f_μ -function although they are properly correlated only for the viscosity effects. This must be considered a pragmatic approach which is physically not very sound [12], but a proper delineation of the two processes is possible only in the context of a Reynolds-stress-equation model where the behaviour of the normal fluctuating component and its damping are simulated directly by the model.

From the high-Re stress-equation model of Gibson and Launder [13] applied to a local-equilibrium shear layer follows that the shear stress is related to the velocity gradient by $-\overline{uv} = 0.263 \nu^2 k^2 / \epsilon \partial U / \partial y$ while low-Re k-ε models use $-\overline{uv} = \nu_t \partial U / \partial y$ with ν_t from (1). Thus $f_\mu = 2.92 \nu^2 / k$, if the formula from the Gibson-Launder model is applicable to the low-Re region. This relationship derived by Launder [14] is compared in Fig. 1 with the f_μ -distribution deduced in [8] from experimental data, taking over the bars for the ν^2/k -data from [14]. This comparison suggests that the near-wall damping expressed by f_μ is mostly due to the reduction of the normal fluctuations, which is mainly controlled by non-viscous wall effects. It therefore appears reasonable to correlate f_μ with a parameter involving the wall distance, e.g. y^+ , as was done in the more recent proposals [10, 11]. It should be noted, however, that y^+ defined in the usual way via the friction velocity U_τ is suitable only for attached flows. Fig. 1 also includes the f_μ -distribution deduced by Gilbert [15] from his direct simulation of channel flow. First, however, his results for the product $f_\mu c_\mu$ reproduced in Fig. 2 are considered which show that this quantity is not really constant outside the viscosity-affected region. These results do however confirm that $c_\mu = 0.09$ in the region of local equilibrium, i.e. where $P_k/\epsilon \approx 1$. In the central portion of the channel, where P_k/ϵ decreases towards zero, c_μ increases as derived already by Rodi [16] from algebraic stress modelling.

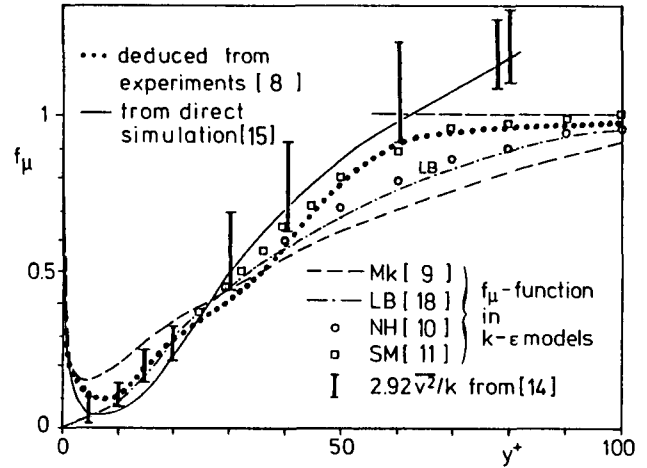


Fig. 1: f_μ -function in low-Re k-ε models

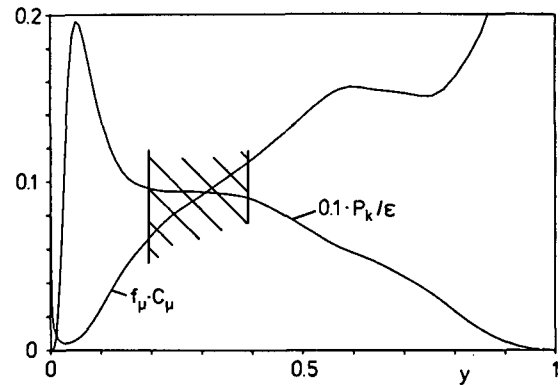


Fig. 2: Distribution of $c_\mu f_\mu$ and P_k/ϵ in channel from direct simulation [15]

When c_μ is chosen as 0.09 and the actual dissipation rate ϵ is taken for $\tilde{\epsilon}$ in (1), there follows the f_μ -distribution shown in Fig. 1 from Gilbert's direct simulation which is in surprising accord with the distribution deduced by Patel et al. [8] from experimental data. As ϵ has a finite value at the wall, f_μ has to increase very near the wall where it behaves as $f_\mu \sim 1/y$ as pointed out by Chapman and Kuhn [17]. The data also follow this trend, and Myong and Kasagi [9] have actually used a f_μ -function in their k-ε model which exhibits this behaviour while the f_μ -function used in the rather popular model of Lam and Bremhorst [18] goes to zero at the wall. On the other hand, when an $\tilde{\epsilon}$ is used in (1) which goes to zero at the wall, f_μ behaves as $f_\mu \sim y$. The models of Nagano and Hishida, NH [10], and Shih and Mansour, SM [11], follow this approach. Their strictly y^+ -dependent f_μ -functions are also included in Fig. 1. SM determined their function with the aid of the direct simulation results of Kim et al. [19]. It is therefore not surprising that their f_μ -function agrees closely with the f_μ -curve in Fig. 1 which was deduced from direct simulation, albeit a different one [15]. Very close to the wall agreement is also good, but this is not obvious from Fig. 1 because, as was mentioned already, different $\tilde{\epsilon}$ definitions have been used. It should be noted here that SM used $\tilde{\epsilon} \neq \epsilon$ only in (1) but solved equation (3) for ϵ . Also, they employed an additional pressure-diffusion term in the k-ε equation (2) which is effective very near walls.

After all the above discussion it must be said that the exact distribution of f_μ very near the wall has little effect on the predictions because in this region viscous stresses dominate over turbulent ones. This is borne out by a comparison of kinetic energy and eddy-viscosity profiles obtained with various model versions for channel flow in Fig. 3. The Reynolds number of the flow was rather low (3300 based on channel half-width and mean velocity) and direct simulation results are also available for comparison [19]. It is clear from Fig. 3 that very near the wall the various predictions are hardly distinguishable, but further away there are significant differences owing to the different functions and additional terms used in the various models. For example, the Jones-Launder [22] model underpredicts the peak in the k-

distribution and also gives too low eddy viscosity at intermediate wall distances, while the Lam-Bremhorst [18] model yields too large eddy viscosities towards the centre of the channel.

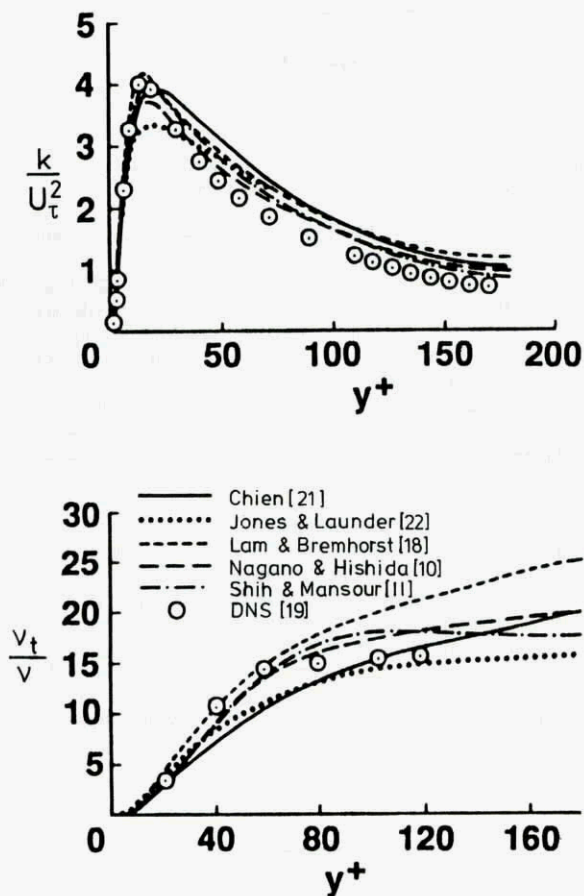
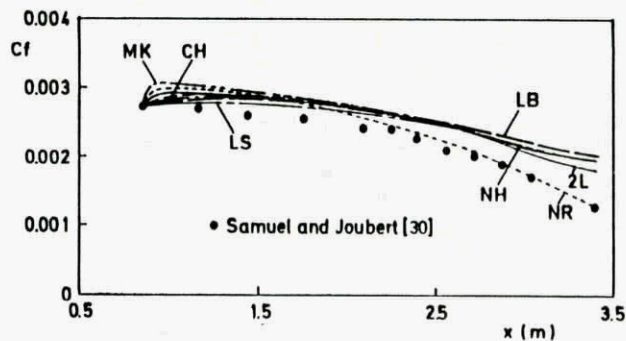
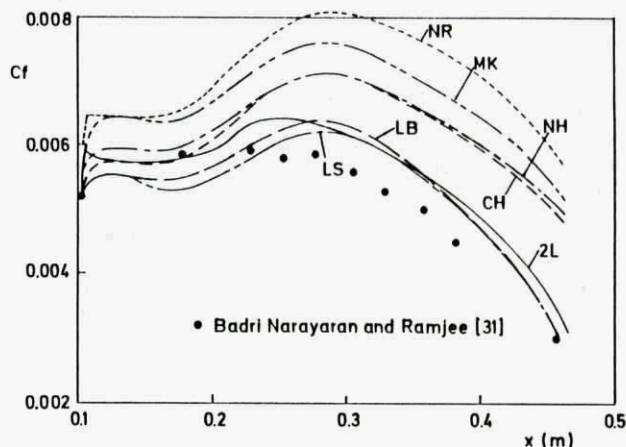


Fig. 3: Near-wall kinetic energy (k) and eddy-viscosity (v_t) distributions in low Re channel flow, from [20]

Although correct near-wall and low-Reynolds-number behaviour of a model is an important feature, it does not necessarily guarantee good performance in engineering calculations. In these, one of the most important parameters to be calculated is the friction coefficient c_f , and Figs. 4a and b show respectively how various models perform in calculating this coefficient in boundary layers under adverse and favourable pressure gradients. The calculations shown were carried out by Fujisawa [25, 26]. It should perhaps be mentioned first that all models succeed in predicting correctly the c_f behaviour under zero pressure-gradient conditions. Fig. 4a shows that all low-Re versions of the k - ϵ model overpredict the friction coefficient under adverse pressure-gradient conditions. This behaviour was traced by Rodi and Scheuerer [23] to the high-Re-form of the ϵ -equation (and in particular to the value of the coefficient $c_{\epsilon 1}$ in this equation) employed which leads to a too steep increase of the turbulent length scale under adverse pressure-gradient conditions. Fig. 4a also includes a prediction with the Norris-Reynolds [24] one-equation model, which only solves an equation for k but uses the usual linear length-scale prescription. It can be seen that with this length-scale specification the friction-coefficient distribution in boundary layers with adverse pressure gradient can be predicted correctly. The situation is quite different for boundary layers under favourable pressure gradient, for which predictions with various models are shown in Fig. 4b. Here the Norris-Reynolds one-equation model (without any modification) performs rather poorly while the Launder-Sharma (LS) and Lam-Bremhorst (LB) versions of the k - ϵ model do fairly well. On the other hand, the Chien (CH), Myong and Kasagi (MK) and Nagano and Hishida (NH) models also overpredict c_f considerably. From these calculations it appears that the low-Re functions in the latter models are not very suitable for favourable pressure-gradient conditions.



a) Adverse-pressure-gradient situation of Samuel and Joubert [30]



b) Favourable-pressure-gradient situation of Badri Narayanan and Ramjee [31]

Fig. 4: Friction coefficient in boundary layers with streamwise pressure gradient, from [25, 26]; NR = Norris-Reynolds [24] one-equation model, LB = Lam-Bremhorst [18], LS = Launder-Sharma [36], CH = Chien [21], NH = Nagano-Hishida [10], MK = Myong-Kasagi [9] low-Re- k - ϵ models, 2L = two-layer model,

At the end of this section it should be emphasized once more that it is of course desirable for a model to have the correct near-wall behaviour, but also that the details of this behaviour very near the wall have in fact little influence on the overall model performance and in particular on the mean-flow quantities of engineering interest. The judgement of the performance of the model for engineering calculations can only be based on test calculations for as wide a variety of flows as possible. Further substantiation on this point will be made in the section on transition modelling.

2.2 Two-Layer Models

Low-Re k - ϵ models have the undesirable feature of requiring very high numerical resolution near the wall, and it was shown above that they perform rather poorly in adverse-pressure-gradient boundary layers. Further, the damping functions in these models were developed for attached boundary layers and are not always well behaved in separated flows. Hence, in order to save grid points and therefore computing time and also to introduce the fairly well established length-scale distribution very near the wall into the model, one recent trend in practical calculations is to use the k - ϵ model only away from the wall and to resolve the near-wall viscosity-affected layer with a simpler model involving a length-scale prescription.

At the University of Karlsruhe, a two-layer model is under examination which uses near walls the one-equation model due to Norris and Reynolds [24] because this has been found to perform well in adverse-pressure-gradient boundary layers [23]. This model determines the eddy viscosity from the relation:

$$v_t = f_\mu c_\mu \sqrt{k} L \text{ with } f_\mu = 1 - \exp(-0.0198 R_y \frac{25}{A^+}), R_y = \frac{\sqrt{k} y}{\nu} \quad (4)$$

involving the damping function f_μ . In this, the parameter A^+ is usually given a value of 25 except for accelerating and transitional boundary layers as described below. The distribution of k is obtained by solving the k -equation (2). The dissipation rate ϵ appearing in this is determined from

$$\epsilon = \frac{k^{3/2}}{L} \left(1 + \frac{13.2}{\sqrt{k} L / \nu} \right) \quad (5)$$

which also involves a viscosity influence. The length scale L is assumed proportional to the wall distance y in the near-wall layer to which the application of this model is restricted. The model is matched with the high-Re k - ϵ model at a location where either the damping function f_μ or the ratio of turbulent to laminar viscosity, ν_t/ν , has a prescribed value (e.g. $f_\mu = 0.95$ or $\nu_t/\nu = 36$) ensuring that the matching takes place in a region where viscosity effects are small.

The model was tested by Fujisawa et al. [26] for various boundary-layer flows. For a boundary layer with zero pressure gradient, the mean-flow behaviour was predicted in good agreement with experimental data and so was the shear-stress distribution, but the predicted near-wall peak in k is too low (similar to that in Fig. 3 for the Jones-Laundier model). Predictions of the friction coefficient for boundary layers with adverse and favourable pressure gradients are included in Figs. 4a and b, respectively. The first figure shows that the two-layer model is only slightly better than the k - ϵ model under adverse-pressure-gradient conditions; here it is again the ϵ -equation used in the outer part of the boundary layer which yields too high a length scale and in turn also too high a turbulent shear stress and

friction coefficient. The two-layer-model prediction included in Fig. 4b for the favourable-pressure-gradient case shows fairly good agreement with the data. It should be mentioned, however, that this good performance could be achieved only by making the parameter A^+ in the damping function f_μ (4) a function of the pressure gradient as recommended by Crawford and Kays [27]:

$$A^+ = 25(30.175 p^* + 1), \quad p^* = \frac{\nu}{\rho U_\tau^2} \frac{dP}{dx} \quad (6)$$

A constant value of $A^+ = 25$ was adopted for zero and adverse-pressure-gradient boundary layers and is also used for the separated flow calculations reported below.

Cordes [28] tested the two-layer model for the flow over a backward-facing step as studied experimentally in [29]. Fig. 5 compares his calculations obtained with this model and with the standard k - ϵ model employing wall functions with measurements. The two-layer model predicts the reattachment length in much better agreement with the experiments and also produces a small second corner eddy which is absent in the calculation with the standard k - ϵ model. Also, the velocity and shear-stress distributions improve and are in generally good accord with the data. Fig. 6 shows similar test calculations performed by Bührle [32] for the flow over a T-configuration as studied experimentally by Jaroch and Fernholz [33, 34]. Although these authors point out the basically three-dimensional nature of the flow in their experiment, a two-dimensional calculation was performed for the flow in the symmetry plane. It can be seen from Fig. 6 that again the two-layer model predicts the reattachment length in much better agreement with measurements than the standard k - ϵ model employing wall functions. On the other hand, the velocity profiles indicate that the separation zone is predicted too thin by both models. This then leads to a shift in the shear-stress distribution towards the wall. It can further be seen that the shear-stress level

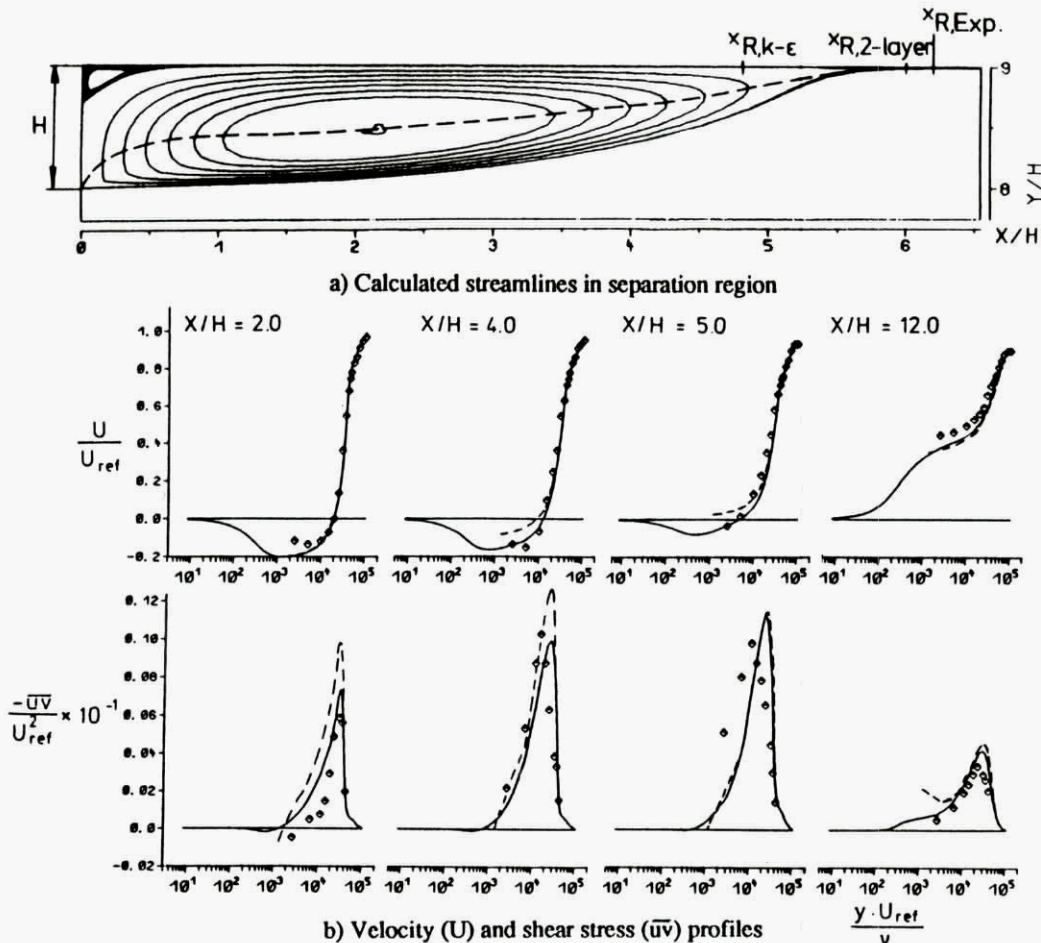


Fig. 5: Flow over backward-facing step with aspect ratio of 1.125
 — Calculations with 2-layer model [28],
 ---- Calculations with standard k - ϵ model [28], \diamond experiments [29]

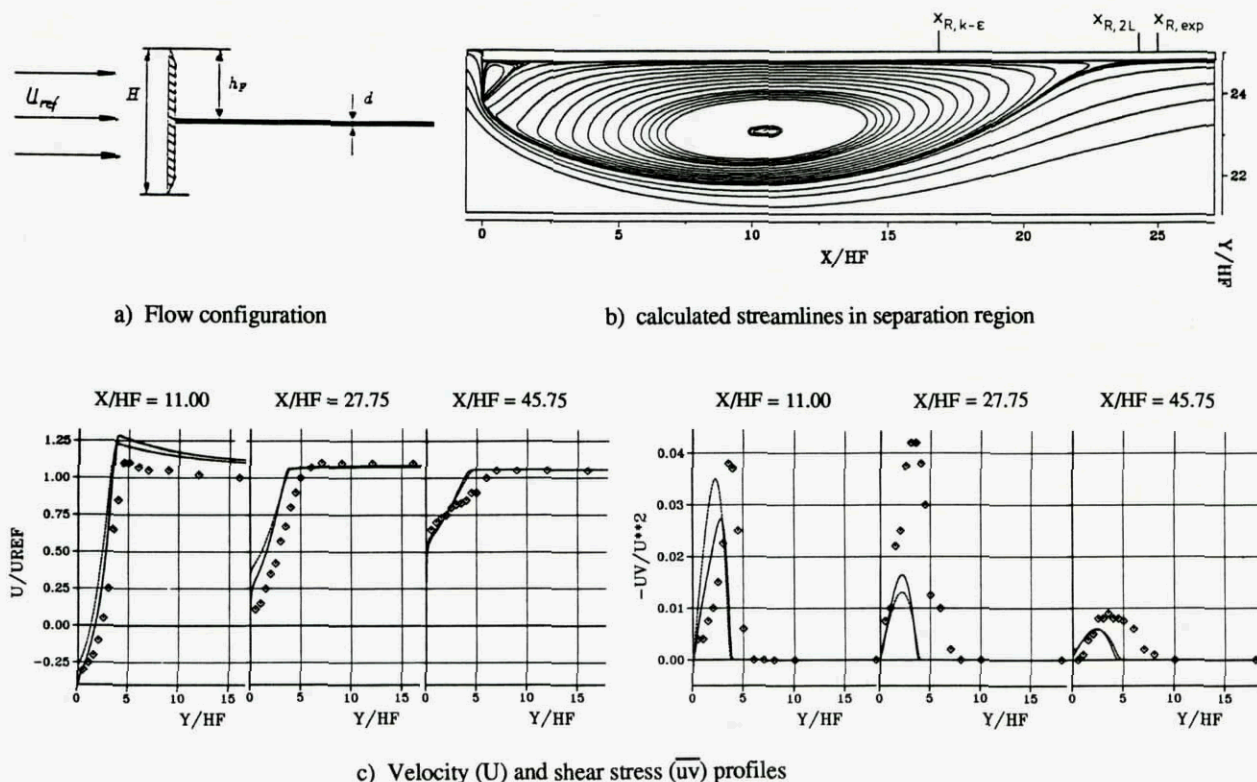


Fig. 6: Flow over T-configuration; — Calculations with 2-layer model [32],
 --- Calculations with standard k- ϵ model [32], \diamond experiments [33]

is underpredicted, and it is not entirely clear at present whether the higher shear stress in the experiments is associated with the basically three-dimensional nature of the flow. However, for practical purposes the overall features of the flow are fairly reasonably predicted by the two-layer model. Further testing of the two-layer model is in progress, also in three-dimensional situations.

2.3 Transition Modelling

For the prediction of laminar-turbulent transition occurring for example on airfoils and turbine blades, the use of a low-Reynolds-number model is an absolute necessity. With k- ϵ -type models, natural transition occurring at low free-stream turbulence levels (say below 1%) via Tollmien-Schlichting waves cannot be simulated but requires artificial triggering. At higher free-stream turbulence levels, which are common in turbomachinery flows, transition occurs in a bypass situation due to the turbulent free-stream disturbances. This mechanism can be simulated by k- ϵ -type models which mimic the diffusion of free-stream turbulence into the laminar boundary layer. However, in order to start the boundary-layer calculations near the leading edge, initial k- and ϵ -profiles must be specified in the laminar boundary layer, and some low-Re-versions of the k- ϵ model have been found to be sensitive to this specification. Usually, the kinetic-energy distribution is related to the velocity distribution by

$$k/k_e = (U/U_e)^2 \quad (7)$$

where "e" relates to values in the free stream. The ϵ -distribution is expressed by the following equilibrium approximation:

$$\epsilon = a_1 k \partial U / \partial y \quad (8)$$

where a_1 is an empirical structure parameter ($= -\overline{uv}/k$) for which Rodi and Scheuerer [35] proposed a correlation with the free-stream turbulence level Tu for use in the Lam-Bremhorst model. Fujisawa [25] examined the sensitivity of various low-Re k- ϵ model versions to the coefficient a_1 and hence to the prescription of the initial ϵ -profile. He found that the Lam-Bremhorst model is most sensitive, which was the reason for Rodi and Scheuerer to introduce the above mentioned function for a_1 . The Launder-

Sharma [36] model, which is a successor to the Jones-Launder [22] model, was found to be less sensitive, but there is still some influence of the a_1 -value on the transition location. For boundary layers with zero pressure gradient, the usual value of the structure parameter, $a_1 = 0.3$, was found to give the correct transition location. The models of Chien [21] and Myong and Kasagi [9] were found to be insensitive to the value of a_1 , but transition was predicted by these models to occur considerably too early when compared with the data of Abu Ghannam [37] for Tu = 1.9%.

For transition calculations with the two-layer model described in 2.2, the parameter A^+ occurring in the damping function in equation (4) is made a function of the boundary-layer state. In laminar boundary layers, a large value is chosen for A^+ (here 300) so that a small v_t results, and for fully turbulent boundary layers A^+ is made a function of the pressure gradient according to (6), with a value of 25 for zero and adverse pressure gradients, as was described above. In the region of laminar to turbulent transition, A^+ is assumed to vary between these two limiting values according to the following formula

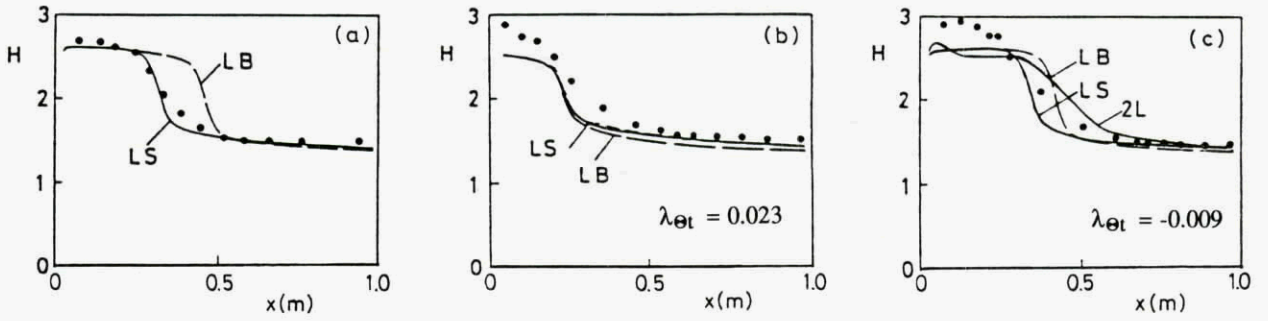
$$A^+ = A_1^+ (300 - A_1^+) \left(1 - \sin \left(\frac{\pi}{2} \frac{Re_\theta - Re_{tr}}{Re_{tr}} \right) \right)^3 \quad (9)$$

which is applied whenever the local momentum thickness Reynolds number Re_θ is larger than the critical transition Reynolds number Re_{tr} but is smaller than twice this number. For the critical Reynolds number, the following empirical dependence on free-stream turbulence level and pressure gradient due to Abu Ghannam and Shaw [38] is taken:

$$Re_{tr} = 163 + \epsilon xp \left(F(\lambda_2) - \frac{F(\lambda_2) \cdot Tu}{6.91} \right) \quad (10)$$

$$F(\lambda_2) = \begin{cases} 6.91 + 12.75\lambda_2 + 63.64\lambda_2^2 & \lambda_2 \leq 0 \\ 6.91 + 2.48\lambda_2 - 12.27\lambda_2^2 & \lambda_2 > 0 \end{cases} \quad \lambda_2 = -\frac{\theta^2 \frac{dp}{dx}}{\mu \cdot U_e}$$

where θ is the momentum thickness.



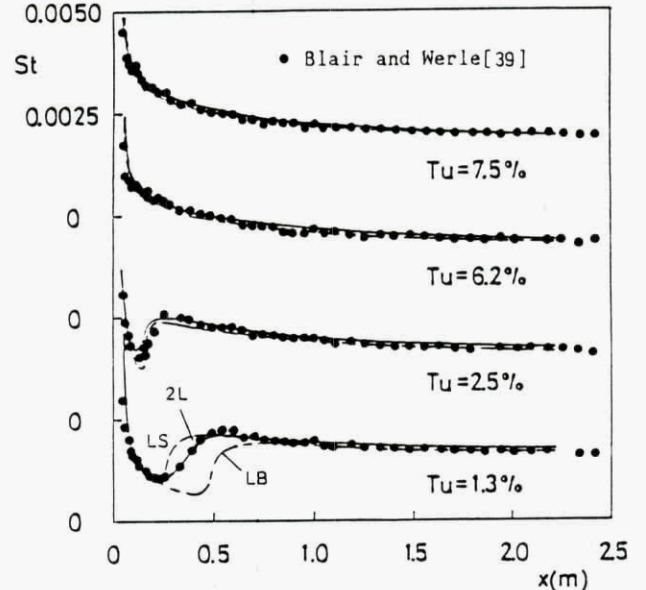
a) Zero pressure gradient, $T_u = 1.9\%$ b) Favourable pressure gradient, $T_u = 3.5\%$ c) Adverse pressure gradient, $T_u = 1.8\%$

Fig. 7: Shape factor H in transitional boundary layers, from [25, 26], ● experiments [37], key to model see Fig. 4

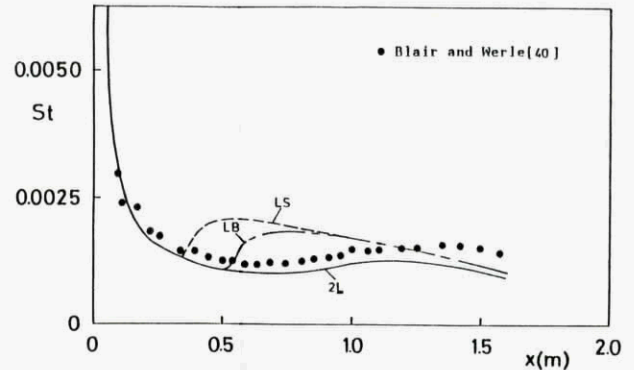
Fujisawa [25, 26] has tested the ability of the Lam-Bremhorst (LB) model, the Launder-Sharma (LS) model and the two-layer (2L) model described above for calculating the transition of boundary layers. For the LS model he used a constant value of $\alpha_1 = 0.3$ in (8), while for the LB-model calculations he used the Tu-dependent correlation of Rodi and Scheuerer [35]. For boundary layers with zero pressure gradient as studied experimentally by Abu Ghannam [37], Fujisawa found that at $T_u = 1.2\%$, the LB model produced no transition while the LS model predicted transition correctly. When the turbulence level is increased, both models lead to transition but at intermediate T_u -levels the LB model produces late transition while the LS model predicts the correct location. At higher T_u -levels (3.3% in the calculation example) both models yield roughly the same results and the correct transition behaviour. For the intermediate turbulence level the results for the shape factor are given in Fig. 7a. Similar conclusions can also be drawn from heat transfer calculations. Fig. 8a presents the variation of the Stanton number predicted with various models for boundary layers with zero pressure gradient and various free-stream turbulence levels and provides comparisons with the data of Blair and Werle [39]. At the lowest turbulence level (1.3%), the LB model predicts transition too late and the LS model slightly too early while the two-layer model yields very good agreement with the data. When the turbulence level is raised to 2.5%, transition moves forward and is predicted fairly well by all three models. For the higher turbulence levels (6.2% and 7.5%) transition occurred before the first measurement station in the unheated-wall part very close to the leading edge. This very early transition is predicted by all the models.

Fig. 7b compares predicted shape factors with the measurements of Abu Ghannam [37] for a boundary layer with mild favourable pressure gradient and $T_u = 3.5\%$. In this case, both the LB and the LS model yield a satisfactory prediction of transition. However, for a strongly accelerated boundary layer, for which the distribution of the Stanton number is given in Fig. 8b, the situation is different. Here the strong acceleration at modest free-stream turbulence level (2.1%) causes a delay in the onset of transition and also transition to take place over a larger distance than in the zero-pressure-gradient case (see Fig. 8a). Both the LB and the LS model predict transition to occur too early and too abruptly and only the two-layer model appears to do justice to the observed transition process. Finally, in Fig. 7c the shape factor variation for a situation with adverse pressure gradient and $T_u = 1.8\%$ is shown. Here, all three models do a fairly good job, but the two-layer model predicts a gentler transition which is closer to the observed behaviour.

From the test calculations carried out so far, it appears that the Launder-Sharma model is somewhat superior to the Lam-Bremhorst model with regard to transition simulation and it has the advantage that it is considerably less sensitive to the prescribed initial ϵ profile in the laminar boundary layer. The two-layer model, which involves an empirical transition correlation, appears also very promising and is presently tested under unsteady conditions for boundary layers on turbine blades subjected to passing wakes generated by the preceding blade row [41].



a) Zero pressure gradient



b) Favourable pressure gradient
 $(k = \nu/U_e \cdot dU_e/dx = 0.75 \times 10^{-6})$, $T_u = 2.1\%$

Fig. 8: Stanton number St in transitional boundary layers, from [25, 26], key to models see Fig. 4

3. REYNOLDS-STRESS-EQUATION MODELLING

Due to increased computing power and improved numerical techniques, models employing transport equations for the individual Reynolds stresses $u_i u_j$ have recently undergone extensive testing and are now applied also to relatively complex flow situations involving recirculation and to 3D flows. Considerable experience is now available with these models, and this has been summarised in various review articles, e.g. [42, 43]. So far, all the applications reported for practically relevant flows have been obtained with relatively simple versions of stress-equation models developed more than 10 years ago [44, 13]. The model equation for $u_i u_j$ used most frequently (and also in the application examples given below) is the following:

$$\underbrace{\frac{\partial \overline{u_i u_j}}{\partial t}}_{\text{rate of change}} + \underbrace{U_k \frac{\partial \overline{u_i u_j}}{\partial x_k}}_{\text{convection}} = c_s \underbrace{\frac{\partial}{\partial x_k} \left(\frac{k}{\epsilon} \overline{u_k u_l} \frac{\partial \overline{u_i u_j}}{\partial x_k} \right)}_{\text{diffusion}} - \underbrace{\overline{u_i u_l} \frac{\partial U_j}{\partial x_k} - \overline{u_j u_l} \frac{\partial U_i}{\partial x_k}}_{P_{ij} = \text{production}}$$

$$- c_1 \underbrace{\frac{\epsilon}{k} \left(\overline{u_i u_j} - \frac{2}{3} \delta_{ij} k \right)}_{\Phi_{ij,1}} - c_2 \underbrace{\left(P_{ij} - \frac{2}{3} \delta_{ij} P_k \right)}_{\Phi_{ij,2}} - \underbrace{\frac{2}{3} \epsilon \delta_{ij}}_{\text{diss}}$$

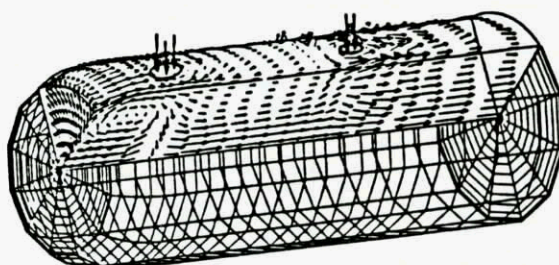
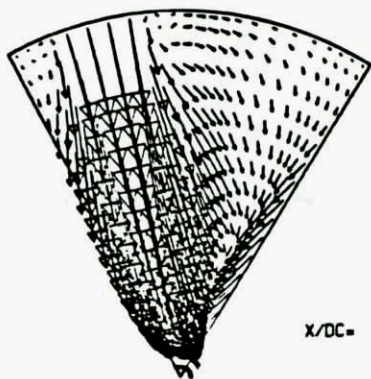
$$\underbrace{\hspace{10em}}_{\Phi_{ij} = \text{pressure-strain}} \quad (11)$$

which, together with a model equation for determining the dissipation rate ϵ , is model 2 of Launder, Reece and Rodi [44]. Local isotropy of the turbulence was assumed to model the dissipation rate of the individual stress components $\overline{u_i u_j}$ and the diffusive transport of $\overline{u_i u_j}$ is simulated by a simple gradient diffusion model. The return to isotropy part of the pressure-strain mechanism is simulated with Rotta's linear model assuming this part to be proportional to the anisotropy of the turbulence. The

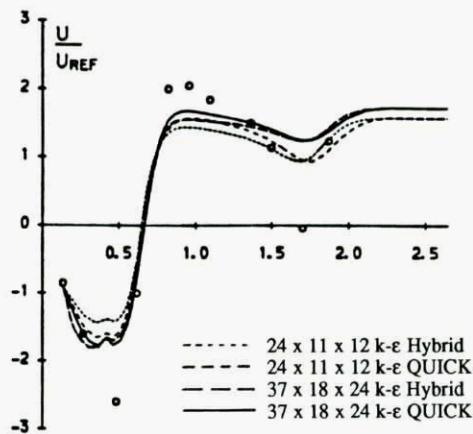
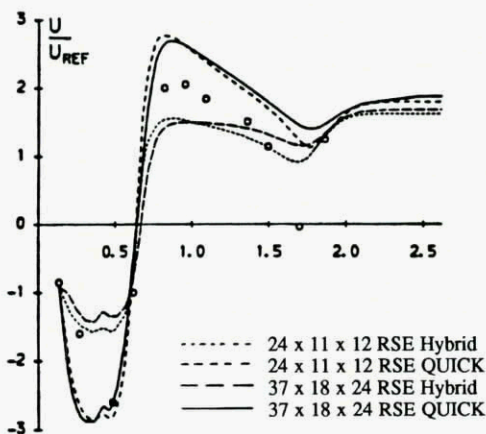
so-called rapid part of the pressure-strain term is simulated with the analogous isotropation of production model. Near walls, the damping of the normal fluctuations due to the presence of the wall is accounted by an extra surface correction to the pressure-strain model e.g. the one due to Gibson and Launder [13]. Further, the near-wall region is either bridged by using wall functions or is resolved with the aid of simpler near-wall models (two-layer approach discussed above).

3.1 Application Examples

In their review papers on second-moment-closure modelling, Launder [42] and Leschziner [43] provide a number of calculation examples where the use of a Reynolds-stress-equation model leads to markedly improved predictions compared with those obtained with the $k-\epsilon$ model. Among the examples are the flow through an axisymmetric annular diffuser involving two bends with strong curvature effects, rotating channel flow, strongly swirling flows with separation (coaxial swirling jets in a pipe),

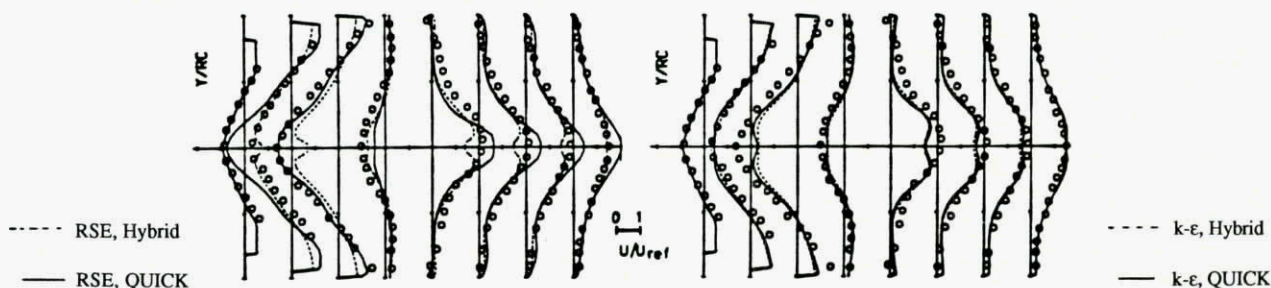


a) Geometry and velocity field predicted with RSE model



b) Variation of centre-line velocity

$x/DC = .135 \ .270 \ .486 \ .621 \ .824 \ .959 \ 1.094 \ 1.364$ $x/DC = .135 \ .270 \ .486 \ .621 \ .824 \ .959 \ 1.094 \ 1.364$



c) Radial profiles of axial velocity

Fig. 9: 3D flow in combustor model, lines are calculations [46], o experiments [45]

flow in a plenum chamber and flow around a square-sectioned U-bend. Reynolds-stress-equation models are now used increasingly for solving more complex flows, which will be demonstrated in the following by providing two calculation examples.

The first example concerns the very complex three-dimensional flow in a combustor, which was studied experimentally under isothermal conditions by Koutmos [45]. A swirling jet with relatively small flow rate enters the combustor at the left and dilution jets from two rows of holes (introducing 83% of the total flow rate) enter radially. Lin [46] carried out calculations for this flow using both the basic RSE and the k-ε model and also both the hybrid central/upwind differencing scheme and the more accurate QUICK scheme. Because of periodicity, the calculations could be restricted to a 60° segment as shown in Fig. 9a, and this figure also gives an indication of the boundary-fitted grid used and the very complex flow evolving in this situation. Fig. 9b compares calculated and measured distributions of the centre-line velocity. The fairly large negative velocity value indicated by one measurement point at $x/D \approx 0.5$ is not reproduced by the k-ε model; with the RSE model such large negative velocities can be obtained, but only when the numerically more accurate QUICK scheme is used. Fig. 9c shows the development of the axial velocity profiles. Altogether the agreement of both models with experiments is only modest, but the flow behaviour predicted by the RSE model is somewhat closer to reality.

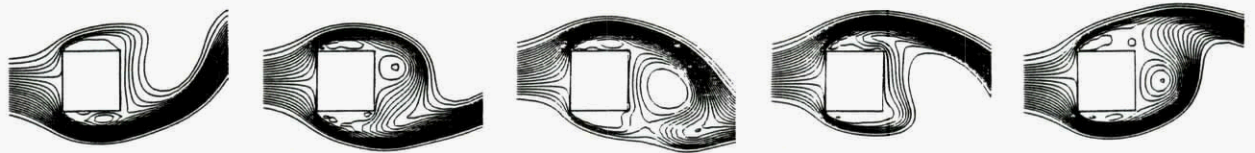
The next example has a simple geometry but the flow is very complex due to its unsteady nature involving periodic vortex shedding. As the latter motion is not turbulence, it cannot be simulated by turbulence models and the flow cannot be calculated by solving time-averaged equations but only by resolving the periodic shedding motion in an unsteady calculation. For this purpose, equations for ensemble-averaged quantities need to be solved; in these ensemble-averaged stresses appear which need to be simulated by a turbulence model. For the flow around a square cylinder at $Re = 22000$, Franke [47] performed calculations with the k-ε model and the basic RSE model, in both cases with wall functions as well as with the one-equation Norris-Reynolds model [24] for resolving the viscous sublayer. In the calculation using the k-ε model and wall functions, a steady solution resulted and no vortex shedding was obtained. In the calculations with the other three model variants, unsteady motion with periodic

vortex shedding was obtained, and a sequence of streamlines covering approximately one period is shown in Fig. 10a. Values of the dimensionless shedding frequencies (Strouhal number St) and time-averaged drag coefficients \bar{c}_D are compared in Table 1 with experimental values. The k-ε model yields too low values for both Strouhal number and drag coefficient, while the two-layer RSE model produces too high values; the RSE model with wall functions yields results in closest agreement with the measurements, at least as far the parameters St and \bar{c}_D are

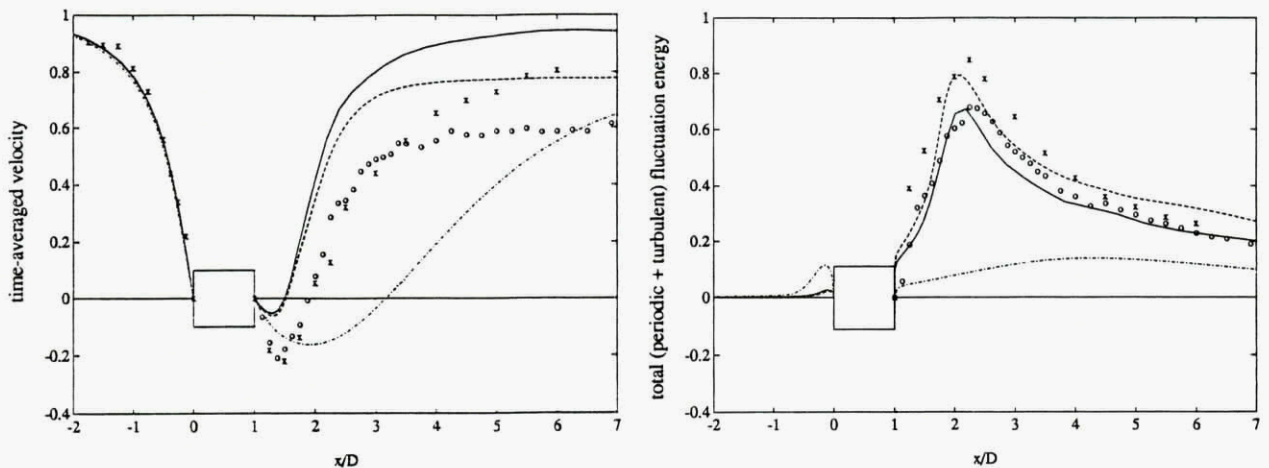
Table 1 Global parameters for vortex-shedding flow past square cylinder [47]

		St	\bar{c}_D
Calculations	2 layer k-ε model	.124	1.79
	RSE model with wall functions	.136	2.15
	2 layer RSE model	.159	2.43
Experiments		.135-.139	2.05-2.23

concerned. Fig. 10b displays the distribution of the time-averaged velocity along the centre-line. It is clear from this figure that the k-ε model produces too long a separation region. This indicates that the model generates not enough mixing and hence not enough momentum exchange due to the unsteady vortex shedding which is too weak in these calculations. The RSE model calculations yield too short a separation zone and hence this model seems to generate too much vortex-shedding motion. This finding is supported by the distribution of the total (periodic plus turbulent) fluctuating energy along the centre-line shown in Fig. 10c. The RSE calculations agree fairly well with the measurements, but the turbulent contribution of the total energy (not shown here) is underpredicted so that the periodic contribution must be too large. On the other hand, the k-ε model grossly underpredicts the fluctuation level behind the cylinder. In front of the cylinder, however, the k-ε model leads to unnaturally high turbulent fluctuations. This problem with the k-ε model in stagnation flows is now well known and can be traced to the fact that the turbulent energy production in this flow is due to normal stresses (not shear stresses) and these cannot be simulated correctly with an



a) Streamlines calculated with RSE model and wall functions for phases $t/T = 1/20, 5/20, 9/20, 13/20, 17/20$



b) Distribution of time-averaged velocity and total kinetic energy of fluctuations (periodic + turbulent) along centre line. Calculations [47]: -.- 2 layer k-ε model, — RSE model with wall functions, --- 2 layer RSE model; experiments: o Lyn [48] $Re = 22000$, x Duraó et al. [49] $Re = 14000$

Fig. 10: Vortex-shedding flow past a square cylinder; calculations [47] are for $Re = 22000$

isotropic eddy-viscosity model, leading to excessive energy production. This problem does not arise when an RSE model is used. Overall, the RSE model leads to significantly improved predictions for vortex-shedding flows compared with the k- ϵ model predictions because it can account for the anisotropy, history and transport effects which are important in these flows.

3.2 Advanced Reynolds-Stress-Equation Models

The model approximations that have entered the Reynolds-stress-equation (11) are fairly simple and do not satisfy certain theoretical constraints such as the realisability conditions due to Schumann [50], and they are also not compatible with the limiting two-dimensional behaviour of turbulence very near walls. Hence, considerable effort has gone into the development of improved models. Launder [42] has recently given a summary on these developments. Here only the main trends are briefly outlined.

Most important is the modelling of the pressure-strain term in the Reynolds-stress-equation, and hence most research effort has gone into this modelling, with the return to isotropy part $\phi_{ij,1}$, and the rapid part $\phi_{ij,2}$ being treated separately. Rotta's linear model for $\phi_{ij,1}$ (given in equation 11) has the incorrect behaviour that $\phi_{ij,1}$ does not vanish in 2D turbulence as it should. This was remedied by introducing more elaborate forms involving second and third invariants of the anisotropy tensor $a_{ij} = (\overline{u_i u_j} / k - 2/3\delta_{ij})$, see e.g. [42]. The isotropization of production model for the rapid part $\phi_{ij,2}$ given in equation (11) is also incompatible with 2D turbulence and shows an incorrect response in homogeneous shear layers to the variation of the ratio of production to dissipation of kinetic energy, P_k/ϵ . Also for this part more elaborate models have been proposed [42, 52], involving quadratic and cubic terms. The more refined pressure-strain models were tested for relatively simple shear layers and were found superior to the model given in (11), but further testing of the somewhat complex models is certainly necessary before their general validity can be established.

The assumption of local isotropy leading to the dissipation model in (11) is also not compatible with 2D turbulence. Hence, more elaborate relations for the dissipation rate of the individual stress components near walls were proposed, e.g. in [53]. More elaborate diffusion models have also been suggested in the literature, but in his review paper Launder [42] argues that in general their use is not really warranted, if only because the weaknesses of model predictions can seldom be traced to weaknesses of the diffusion model.

In the practical applications of standard RSE models such as the one given by eq. (11), the near-wall layer was not resolved and the damping of the normal fluctuations was accounted for by wall corrections to the pressure-strain model. The new, more complex pressure-strain models just discussed, which are consistent with the limiting 2D behaviour of turbulence at the wall, should help to simulate this damping effect. However, experience gained with these models so far [42] indicates that the use of these models alone seems not sufficient and that wall-correction terms, although reduced in magnitude, may still be necessary. In some near-wall RSE models which appeared in the literature, viscosity-dependent functions were introduced to simulate the damping effect, which appears to be mainly a pressure-reflection effect and is therefore not really affected by viscosity. However, some influence of viscosity may have to be brought in. Work on near-wall RSE modelling is in progress at various research institutions (e.g. at UMIST, Manchester, Arizona State University and Stanford University / NASA Ames), but it is fair to say that at present no thoroughly tested near-wall RSE model is available.

4. CONCLUSIONS AND OUTLOOK

Simple turbulence models involving no differential equations or only an ordinary differential equation for the maximum shear stress will continue to be used in many practical calculations, especially for external aerodynamic flows, and they will be refined further. The k- ϵ model will also continue for some time to play a key role in engineering calculations, and most of these calculations will be carried out with wall functions for many years to come. However, near-wall models will be used increasingly to replace the wall functions, at least in incompressible flows. A fairly large variety of different low-Reynolds-number k- ϵ models

is now available, and the most recently developed ones show the correct near-wall behaviour as demonstrated by comparison with direct simulation data. However, the various model versions were tested mainly for simple boundary layers and their predictive ability, including that for transition, has yet to be established for a wider range of flows, especially for the newly proposed models. As the various damping functions in the low-Re k- ϵ models were designed for use in boundary layers, the performance of these models in separated flows is not clear and has to be examined before the models can also be used with some confidence for these flows. For both boundary layers and 2D separated flows, encouraging results were obtained with a two-layer model, which employs the k- ϵ model only in the outer part of the flow but resolves the near-wall region with a one-equation model. This model also needs further testing, in particular for three-dimensional situations. Here the question arises whether the computer resources available now and in the near future are sufficient for resolving the viscous sublayer with such a model also in 3D situations.

Reynolds-stress-equation models will be used more and more for practical calculations in place of the k- ϵ model, particularly for situations with complex strain fields and special effects on turbulence like due to streamline curvature, rotation etc. Slowly, the more refined of the RSE models will come to be used, but considerable testing is still necessary before these models are ready for practical application; the same is true also for near-wall RSE models. The importance of direct numerical simulation data for testing the turbulence models and as basis for the development of new model assumptions will increase dramatically. However, as the Reynolds numbers possible in direct numerical simulations will go up only slowly, the resulting data will be restricted to fairly low Reynolds numbers and the main impact will remain in the area of near-wall modelling. For high Reynolds numbers, perhaps results from large-eddy simulations can be exploited in a similar way, but these simulations are of course themselves dependent on model assumptions entering the subgrid-scale model, and sometimes they may rather be used directly as a predictive tool; in complex flow situations where the structure of turbulence is important or 3D time-dependent calculations have to be carried out anyway, large-eddy or very-large-eddy simulations are likely to become the methods to be used in a few years' time [54]. However, in many application areas, conventional turbulence models will still be used and needed for many years to come.

5. ACKNOWLEDGEMENTS

The work reported here was supported partly by the Deutsche Forschungsgemeinschaft. The author is grateful to J. Cordes, R. Franke and D. Lyn for providing unpublished calculation results and to R. Zschernitz for the efficient typing of the manuscript.

6. REFERENCES

1. Cebeci, T. and Smith, A.M.O., "Analysis of Turbulent Boundary Layers", Academic Press, New York, 1974.
2. Baldwin, W.S. and Lomax, H., "Thin-layer approximation and algebraic model for separated turbulent flows", AIAA Paper 87-257, 1978.
3. Johnson, D.A. and King, L.S., "A mathematically simple turbulence closure model for attached and separated turbulent boundary layers", AIAA J., 23, 1985, pp. 1684-1692.
4. Launder, B.E. and Spalding, D.B., "The numerical computation of turbulent flow", Comp. Meth. in Appl. Mech. and Eng., 3, 1974, pp. 269-289.
5. Iacovides, H. and Launder, B.E., "The numerical simulation of flow and heat transfer in tubes in orthogonal-mode rotation", Proc. 6th Symp. on Turbulent Shear Flows, Toulouse, France, 1987.
6. Viegas, J.R., Rubesin, M.W. and Horstman, C.C., "On the use of wall functions as boundary conditions for two-dimensional separated compressible flows", AIAA Paper 85-0180, 1985.
7. Marvin, J.G., "Progress and challenges in modeling turbulent aerodynamic flows", in Proc. Int. Symp. on Engineering Turbulence Modelling and Measurements, ed. W. Rodi, Elsevier Publishers, 1990.
8. Patel, V.C., Rodi, W. and Scheuerer, G., "Turbulence models for near-wall and low-Reynolds-number flows: A review", AIAA J., 23, 1985, pp. 1308-1319.

9. Myong, H.K. and Kasagi, N., "A new approach to the improvement of k-e turbulence model for wall-bounded shear flows", *JSME Int. Journal, Series II*, **33**, 1990, pp. 63-72.
10. Nagano, Y. and Hishida, M., "Improved form of the k-e model for wall turbulent shear flows", *ASME J. Fluids Eng.*, **109**, 1987, pp. 156-160.
11. Shih, T.H. and Mansour, N.N., "Modelling of near-wall turbulence", *Proc. Int. Symp. on Engineering Turbulence Modelling and Measurements*, ed. W. Rodi, Elsevier Publishers, 1990.
12. Hanjalic, K., "Practical predictions by two-equation and other fast methods", *Proc. Zoric Memorial Int. Seminar on Wall Turbulence*, Dubrovnik, Yugoslavia, Hemisphere Publishing Corp., 1988.
13. Gibson, M.M. and Launder, B.E., "Ground effects on pressure fluctuations in the atmospheric boundary layer", *J. Fluid Mech.*, **86**, 1978, pp. 491-511.
14. Launder, B.E., "Low-Reynolds number turbulence near walls", UMIST Manchester, Dept. of Mech. Eng. Rept. TFD/86/4, 1986.
15. Gilbert, N., "Numerische Simulation der Transition von der laminaren in die turbulente Kanalströmung", Report DFVLR - FB 88-55, DLR Göttingen, F.R. Germany, 1988.
16. Rodi, W., "The prediction of free turbulent boundary layers by use of a two-equation model of turbulence", Ph.D. Thesis, University of London, 1972.
17. Chapman, D.R. and Kuhn, G.D., "The limiting behaviour of turbulence near a wall", *J. Fluid Mech.*, **170**, 1986, pp. 265-292.
18. Lam, C.K.G. and Bremhorst, K.A., "Modified form of the k-e model for predicting wall turbulence", *ASME J. Fluids Eng.*, **103**, 1981, pp. 456-460.
19. Kim, J., Moin, P. and Moser, R., "Turbulence statistics in fully developed channel flow at low Reynolds number", *J. Fluid Mech.*, **177**, 1987, pp. 123-166.
20. Shih, T.H., "Turbulence modelling: Near-wall turbulence and effects of rotation on turbulence", *CTR Annual Research Briefs*, Centre for Turbulence Research, NASA Ames Research Centre and Stanford University, 1989, pp. 12-26.
21. Chien, T.-Y., "Predictions of channel and boundary-layer flows with a low-Reynolds-number turbulence model", *AIAA J.*, **20**, 1982, pp.33-38.
22. Jones, W.P. and Launder, B.E., "The calculation of low-Reynolds-number phenomena with a two-equation model of turbulence", *Int. J. Heat Mass Transfer*, **16**, 1973, pp. 1119-1130.
23. Rodi, W. and Scheuerer, G., "Scrutinizing the k-e model under adverse pressure gradient conditions", *J. Fluids Eng.*, **108**, 1986, pp. 174-179.
24. Norris, L.H. and Reynolds, W.C., "Turbulent channel flow with a moving wavy boundary", Rept. No. FM-10, Stanford University, Dept. Mech. Eng., 1975.
25. Fujisawa, N., "Calculations of transitional boundary-layers with a refined low-Reynolds-number version of a k-e model of turbulence", *Proc. Int. Symp. on Engineering Turbulence Modelling and Measurements*, ed. W. Rodi, Elsevier Publishers, 1990.
26. Fujisawa, N., Rodi, W. and Schönung, B., "Calculation of transitional boundary layers with a two-layer model of turbulence", *Proc. 3rd Int. Symp. on Transport Phenomena and Dynamics of Rotating Machinery*, Honolulu, April 1990.
27. Crawford, M.E. and Kays, M.W., "STAN 5 - a program for numerical computation of two-dimensional internal and external boundary-layer flows", NASA CR-2742, 1976.
28. Cordes, J., private communication, 1988.
29. Driver, D.M. and Seegmiller, H.L., "Features of a reattaching turbulent shear layer in divergent channel flow", *AIAA J.*, **23**, 1985, pp. 163-171.
30. Samuel, A.E. and Joubert, P.M., "A boundary layer developing in an increasingly adverse pressure gradient", *J. Fluid Mech.*, **66**, 1974, pp. 481-505.
31. Badri Narayanan, M.A. and Ramjee, V., "On the criteria for reverse transition in a two-dimensional boundary layer flow", *J. Fluid Mech.*, **35**, 1969, pp. 225-241.
32. Bührle, P., "Numerische Berechnung der abgelösten Strömung über eine senkrechte ebene Platte mit einer zur Anströmung parallelen Trennplatte in der Symmetrieebene", Studienarbeit am Institut für Hydromechanik, Universität Karlsruhe, 1989.
33. Jaroch, M., "Eine kritische Betrachtung der Methode diskreter Wirbel als Modell für eine abgelöste Strömung mit geschlossener Ablöseblase auf der Basis experimenteller Erkenntnisse", *Fortschrittsberichte VDI, Reihe 7*, **127**, 1987.
34. Jaroch, M.P. and Fernholz, H.H., "The three-dimensional character of a nominally two-dimensional separated turbulent shear flow", *J. Fluid Mech.*, **205**, 1989, pp. 523-552.
35. Rodi, W. and Scheuerer, G., "Calculation of laminar-turbulent boundary layer transition on turbine blades", *Proc. AGARD-PEP 65th Symp.*, Bergen, Norway, May 1985.
36. Launder, B.E. and Sharma, B.I., "Application of the energy-dissipation model of turbulence to the calculation of flow near a spinning disk", *Letters in Heat and Mass Transfer*, **1**, 1974, pp. 131-138.
37. Abu Ghannam, B.J., "Boundary-layer transition in relation to turbomachinery blades", Ph.D. Thesis, University of Liverpool, Liverpool, U.K., 1979.
38. Abu Ghannam, B.J. and Shaw, R., "Natural transition of boundary layers - the effects of turbulence, pressure gradient and flow history", *J. Mech. Eng. Sci.*, **22**, 1980, pp. 213-228.
39. Blair, M.F. and Werle, M.J., "The influence of free-stream turbulence on the zero pressure gradient fully turbulent boundary layer", *UTRC Rept. R80-914388-12*, 1980.
40. Blair, M.F. and Werle, M.J., "Combined influence of free-turbulence and favourable pressure gradients on boundary-layer transition and heat transfer", *UTRC Rept. R81-914388-17*, 1981.
41. Rodi, W., Liu, X. and Schönung, B., "Transitional boundary layers with wake-induced unsteadiness", *Proc. 4th Symp. on Numerical and Physical Aspects of Aerodynamic Flows*, Long Beach, California, January 1989.
42. Launder, B.E., "Second-moment closure: present... and future?", *Int. J. Heat and Fluid Flow*, **10**, 1989, pp. 282-300.
43. Leschziner, M.A., "Second-moment closure for complex flows", *Proc. Int. Forum on Mathematical Modelling of Processes in Energy Systems*, Int. Centre for Heat and Mass Transfer, Sarajevo, March 1989.
44. Launder, B.E., Reece, G.C. and Rodi, W., "Progress in the development of a Reynolds-stress turbulence closure", *J. Fluid Mech.*, **68**, 1975, pp. 537-566.
45. Koutmos, P., Ph.D. Thesis, University of London, 1985.
46. Lin, C.A., Ph.D. Thesis, Faculty of Technology, University of Manchester, 1989.
47. Franke, R., private communication, 1990.
48. Lyn, D., private communication, 1989.
49. Durao, D.F.G., Heitor, M.V. and Pereira, J.C.F., "Measurements of turbulent and periodic flows around a square cross-sectioned cylinder", *Experiments in Fluids*, **6**, 1988, pp. 298-304.
50. Schumann, U., "Realisability of Reynolds-stress turbulence models", *Physics of Fluids*, **20**, 1977, pp. 721-725.
51. Lumley, J.L., "Computational modelling of turbulent flows", in *Advances in Applied Mechanics*, **18**, 1978, pp. 123-176, Academic Press, New York.
52. Shih, P.H. and Lumley, J.L., "Modelling of pressure-correlation terms in Reynolds stress and scalar flux equations", Rept. FDA-85-3, Sibley School of Mech. and Aerospace Eng., Cornell University, 1985.
53. Launder, B.E. and Reynolds, W.C., "Asymptotic near-wall stress-distribution rates in turbulent flow", *Physics of Fluids*, **26**, 1983, pp. 1157-1158.
54. Reynolds, W.C., "The potential and limitations of direct and large-eddy simulations", Position Paper at Conference "Whither Turbulence? or Turbulence at the Cross Road", Cornell University, March 22-24, 1989, to be published by Springer in the Lecture Notes in Physics Series.

**TURBULENCE MODELS FOR NATURAL CONVECTION FLOWS
 ALONG A VERTICAL HEATED PLANE**

by

D.D. Papailiou

Laboratory of Applied Thermodynamics,
 Dept. of Mechanical Engineering, University of Patras
 Kato Kostritsi, Patras 26500, Greece

Introduction:

The present work has been prepared for presentation in the Technical Status Review on "Appraisal of the Suitability of Turbulence Models in Flow Calculations", organized by the Fluid Dynamics Panel of AGARD (Friedrichshafen, April 26, 1990). Its objective is to review the state of development of turbulent models currently employed in the computation of turbulent free convection flows along heated plane surfaces. In this context some experimental results recently obtained in the Laboratory of Applied Thermodynamics, University of Patras, are also compared with corresponding computations in which existing turbulence models were used.

Although free convection flows such as plumes, buoyant jets, thermals and those originated from heated surfaces, find wide application in various fields of science and technology including aeronautics, the understanding of turbulence transport processes in these cases is lagging behind as compared to other flows. This is generally due to the currently existing lack of sufficient knowledge regarding the effects of buoyancy on the turbulence structure of these flows and also its participation and role in the corresponding transport processes. The reasons causing this inadequacy of necessary information will be discussed in the following. As a consequence, in computing buoyancy induced flows, turbulent transport models are adopted from forced convection or ordinary flows, mostly in modified forms.

By reviewing the existing experimental evidence and computational methods currently in use for predicting the simple case of free convection turbulent flow along heated planes, it becomes possible to appreciate the difficulties presented in developing turbulence models for buoyancy driven flows. It also becomes possible to identify the sources of existing problems and limitations and finally, to suggest a course for future research activities in this particular area.

Most of the reported in the literature experimental and computational work on turbulent free convection, refers to Grashof or Rayleigh numbers corresponding to fully developed turbulent flow conditions. However, apart from the fact that both transitional and non-fully developed turbulence states are important on their own merits, their closer investigation might substantially help in improving free convection computational schemes. The study of these states of flow development could for instance result to the selection of more representative initial conditions and/or a more effective method for introducing turbulence action in the computations. More important, conditions prevailing in these states is known to affect the physical processes occurring in the following state of fully developed turbulence. The combined experimental and computational effort in the region of Grashof numbers between 10^7 and 10^{10} , presented in this work aims at exploring some of the above mentioned possibilities.

Turbulence Models for Free Convection Flow Along a Vertical Heated Plane:

The problem of turbulent free convection along a vertical heated wall, has been the subject of investigation for the past several decades. Numerous experiments have been reported in the literature (1-14), the majority of which has been limited to measurements of overall and local heat transfer coefficients and mean temperature distributions in the turbulent boundary layer. This is caused by existing inherent difficulties in measuring velocity in buoyant flows, especially near a heated wall where a combination of very low velocities and very steep temperature gradients dominate.

The lack of sufficient experimental information, which exist in abundance for most of the ordinary flows, appears to be mainly responsible for the inadequate understanding of buoyancy dominated free convection turbulent transport phenomena. As a consequence, this prevents the development of convincing theoretical arguments on which the modelling of turbulence transport terms will be based. At the present, almost all the theoretical efforts on the subject are based on analogies "borrowed" from forced convection flows.

The turbulence models which are presently employed in free convection boundary layer computations fall into three categories namely, algebraic (15, 16), standard κ - ϵ (17, 18) and low Reynolds number κ - ϵ (19-26). Algebraic models are using the concept of eddy diffusivity in forms either directly transferred from forced convection or modified for free convection. The latter two categories employ two equation κ - ϵ models describing turbulent kinetic energy and dissipation dynamics.

In the case of standard κ - ϵ modelling the use of wall functions is necessary to avoid the steep gradients prevailing near the wall and to provide boundary conditions for the κ and ϵ differential equations. Since no wall functions exist for turbulent free convection boundary layer, logarithmic wall functions, appropriate for forced convection boundary layer with small pressure gradients, are commonly used in computations (27).

In the case of low-Reynolds κ - ϵ models, the diminishing presence of turbulence near the wall is modelled by the introduction of a number of functions in the differential equations for κ and ϵ (27). It should be noticed that, here again, low-Reynolds number models used in free convection, with the exception of the model developed by To and Humphrey (26), have been originally developed for forced convection boundary layers.

Henkes and Hongendoorn (28) have conducted a systematic comparison of turbulence models of the three categories, by employing a selected number of them in the computation of a free convection turbulent boundary layer along a vertical plate. Their calculations covered the range $10^{10} < Gr_x < 10^{12}$ corresponding to a fully developed flow. According to the methodology followed by the authors, calculations started at $Gr_x = 10^9$, where laminar similarity velocity and temperature profiles were employed. The selected turbulence models were introduced at $Gr_x = 2 \cdot 10^9$. An amount of turbulence kinetic energy was also introduced at the edge of the boundary layer when κ - ϵ models were employed. Their calculations ended at $Gr_x = 10^{12}$.

The conducted comparison included heat transfer rates at the wall and also, velocity and temperature profiles. A sensitivity study was also carried, regarding the choice of the wall function for the standard κ - ϵ model as well as the influence of the parameters of the low-Reynolds number κ - ϵ models on the obtained results.

The conclusions reached by the investigators are summarized in the following: The calculated heat transfer rates by the selected algebraic turbulence model of Cebeci -Khattab (15) are too low. This model is also producing laminar-like velocity profiles due to serious underestimation of turbulence viscosity. The standard κ - ϵ model calculates too high values of wall-heat transfer which, as the sensitivity studies indicated, depend on the choice of the wall functions. The low-Reynolds number models of Lam and Bremhorst (21), Chien (23) and Jones and Launder (20) perform best up to $Gr_x = 10^{11}$. Beyond this value the first two models predict heat transfer rates which are higher than the experimental, while the model of Jones and Launder gives more accurate results. However, the latter model exhibits a late transition to turbulence as shown in fig. 1. It should be noted, that all low-Reynolds number models produce velocity and temperature distributions which fall above the experimental at the outer region of the boundary layer. Finally, the authors suggest that an accurate low-Reynolds number κ - ϵ model for turbulent free convection boundary layer computations can be constructed by replacing wall functions by zero wall conditions for κ and ϵ and by adding certain functions of the Chien's model to the standard κ - ϵ model equations.

Regarding the computations conducted by using the low-Reynolds number κ - ϵ models, difficulties can arise in achieving turbulent transition. According to the authors, the solution of the low-Reynolds number models is not unique. Assuming that the solution for large Gr_x is independent of the starting profile, both laminar and turbulent solutions exist for large Gr_x , if homogeneous boundary conditions for κ and ϵ are applied at the wall and the outer edge of the boundary layer. Similar problems regarding transition to turbulence and uniqueness of solution, have been reported to exist in other configurations of free convection computations (29).

An interesting work offering some physical insight in the structure of a fully developed turbulent natural convection boundary layer forming along a heated vertical surface, has been reported by George and Capp (30). For the case under consideration the authors correctly recognized the necessity of treating the flow in two parts namely, an inner part next to the wall in which viscous and conduction effects are dominant while mean convection of momentum and heat are negligible and an outer part, in which the opposite conditions prevail. They employed momentum and energy equations for these parts in which, according to the above stated arguments, only appropriate for each part terms were retained. By using classical scaling methods of analysis, were able to reach some useful conclusions regarding the structure of the layer and to obtain relations for the velocity and temperature distribution as well as heat transfer rates.

According to their analysis the inner part is characterized by constant heat flux and consists of two sublayers and a buffer layer between them. More specifically, next to the wall there exist conductive and viscous sublayers with linear velocity and temperature distributions, their relative thickness depending on the Prandtl number. The outer part of the constant heat flux inner layer is occupied by a buoyant sublayer characterized by velocity and temperature distributions varying as the cube root and the inverse cube root of the distance from the wall respectively, that is:

$$\frac{T-T_w}{T_1} = K_2 \left(\frac{y}{n_t}\right)^{-\frac{1}{3}} + A(Pr) \quad , \quad \frac{U}{U_1} = K_1 \left(\frac{y}{n_t}\right)^{\frac{1}{3}} + B(Pr) \quad (1)$$

where, K_1 , K_2 , are universal constants, $A(Pr)$, $B(Pr)$ universal functions of the Prandtl number, U_1 , T_1 , inner velocity and temperature scales and n_t , inner length scale which, for constant temperature wall,

$$n_t = \left[\frac{\alpha^2}{g\beta(T_w - T_\infty)} \right]^{\frac{1}{3}} \quad (2)$$

These theoretical predictions are well supported experimentally as will be further discussed in the following. Heat transfer and friction laws have also been derived in this work which, as in the case of the velocity and temperature profiles, contain as yet unspecified functions of the Prandtl number. The authors point out in their concluding remarks, that additional experimental and theoretical work is needed to supply missing information regarding the physics of the problem and also, to make possible the calculation of the unknown Prandtl functions mentioned above. This is important in developing new computational models, since the velocity and temperature distributions of the experimentally confirmed buoyant sublayer could be utilized as inner boundary conditions, therefore avoiding the difficulties presented in modelling turbulence in the inner part of the boundary layer.

Finally, the work of Siebers, Moffatt and Schwind (14) should be mentioned, in which extensive measurements of heat transfer coefficients and temperature profiles in air are presented, for Grashof numbers up to $2 \cdot 10^{12}$. Regarding the measured temperature

distributions, they found that in the outer region, beyond the buoyant sublayer, they obey a logarithmic relation of the form:

$$\theta = \frac{T_w - T}{T_w - T_\infty} = 0.8 \ln\left(\frac{y}{\delta_t}\right) + 0.81 \quad (3)$$

where δ_t is the thermal boundary layer thickness,

$$\delta_t = \int_0^{\infty} \frac{T - T_\infty}{T_w - T_\infty} dy \quad (4)$$

The preceded survey on the suitability of the turbulence transport models, presently employed in computations of natural convection flows along vertical heated planes, leads to the conclusion that, those models are not capable of accurately predicting heat transfer rates and/or velocity and temperature distributions, within a sufficiently extended range of Grashof and Prandtl numbers. It is therefore evident that, as will be discussed in the following, further experimental and theoretical work is needed.

From the experimental point of view, as already mentioned, an abundance of mean temperature distribution and wall heat transfer measurements exist in the literature although for a restricted range of Grashof and Prandtl numbers. Also, the statistical characteristics of the turbulent thermal field have been measured to a certain extent (3,4,9,10,31-34). However, measurements of the mean and statistical character of the corresponding turbulent velocity field are very limited (35-38), for reasons already explained. Especially, the present lack of direct measurements of momentum and heat turbulent transport terms of the form $u'_i u'_j$ and $u'_i \theta'$, impose severe limitations in the understanding of these processes in the different parts of the boundary layer. It is evident, that without such knowledge, the development of turbulent models offering adequately accurate predictions cannot be expected. Recent attempts to conduct velocity measurements by using laser velocimetry, appear promising in providing such information in the near future (31).

Further experimentation is also needed, in order to establish firmly the mathematical form of mean temperature and velocity distribution in the various parts of the turbulent boundary layer as well as the skin friction and wall heat transfer. In this direction the already discussed findings and suggestions contained in reference (30), might form the basis for further investigation. It should be added that future experiments regarding both mean and statistical turbulent flow characteristics should be planned to be conducted in an extended range of Prandtl and Grashof numbers.

In buoyancy generated flows where the velocity field is initiated and sustained by the corresponding thermal field, a strong interaction exists between the two fields. Although this interdependence probably dominates the turbulence dynamics as well as the transport processes in these flows, it has not been adequately investigated. Addressing this question will certainly enhance the understanding of the physical aspects of turbulent transport mechanisms in buoyant flows, resulting to improved modelling of the corresponding terms in the conservation equations. It could also provide physically founded relations between them, to replace the empirical Prandtl number dependent formulas currently in use.

The conducted survey has shown the limitations of the presently employed turbulence models in free convection computations, strongly indicating that suitable models for these flows cannot be developed by modifying existing ones corresponding to ordinary or forced convection flows. This task demands adequate understanding of the buoyancy influenced turbulence structure and related transport mechanisms not presently existing. To supply the needed information the widely accepted procedure of comparing carefully selected experiments, conducted along the discussed directions, with corresponding computations should be adapted. However, the method of interplay between experiment and computation cannot produce the sought knowledge if confined to comparing only overall quantities, as the trend has been in the past few years. This methodology should be used as a tool for a detailed investigation of the structure of the various parts of the turbulent velocity and temperature fields, in which different physical processes prevail. In the case of a heated vertical plane these parts have been identified to correspond to an inner layer consisting of a viscous, conduction and buoyant sublayers and an outer layer, as already mentioned. The described approach is also expected to help in selecting appropriate boundary conditions in order to avoid a number of computational difficulties as for instance, handling the low turbulence region near the wall.

Experiments in the non-fully developed turbulent state:

The history of flow development towards a fully developed turbulence state is generally known to affect both the structure of turbulence and the occurring in this state physical processes. In turbulent free convection, studying turbulence in its developing stages and comparing experimental results with computational predictions, is expected to allow a better understanding of turbulence transport processes and especially the influence of buoyancy on them. It will also assist in recognizing existing shortcomings in the presently employed turbulence models and in acquiring useful information for the development of suitable ones for free convection flow.

In the conducted preliminary investigation reported in the following the experimental results obtained in a non-fully developed turbulent free convection thermal layer formed along a heated vertical plane are compared with corresponding computational predictions. The experimental apparatus, consisting of a stainless steel plate of dimensions 1000x500x12 mm heated by ten uniformly spaced resistance elements, has been described in reference (34). By controlling the power delivered to each element, a uniform temperature over the surface of the plate was achieved. The obtained measurements covered both mean and statistical

characteristics of the turbulent temperature field by using a hot-wire anemometer with the sensor operating as a resistance thermometer. Heat transfer rates were also estimated from the obtained temperature distributions and from wall temperature and heat flux measurements by using Newton's law. In the present work only mean temperature distributions and heat transfer rates are reported.

As already discussed, Henkes and Hoongendoorn (28) have computed heat transfer rates by using different turbulence models as shown in figure 1 in which, corresponding measurements obtained in the present experiments, are added. It can be seen in this figure that the majority of the turbulence models fail dramatically to predict heat transfer rates in the mentioned range of Grashof numbers.

As a next step, the form of the inner and outer parts of the measured mean temperature distributions were examined as shown in figures 2 and 3. The measured distributions corresponding to the inner part (fig. 2) exhibit a gradual development with increasing Grashof number towards the theoretically predicted inverse cube root form, characteristic of the buoyant sublayer in a fully developed state. Furthermore, computations were carried for two Grashof numbers namely, $Gr_x = 2.7 \cdot 10^6$ and $Gr_x = 9.7 \cdot 10^6$ and for three different turbulence models as shown in figures 4 and 5. These, were compared with measured in the present experiments temperature distributions at the same Grashof numbers, corresponding to non-fully and fully developed flows. It is evident that none of the computed profiles agrees with the experiment and that in the case of the higher Grashof number only the model of Jones and Launder predicts the inverse cube root form in a small part of the buoyant sublayer. Equally significant none of the employed turbulence models appears capable to produce computed distributions following the trend exhibited by the measured profiles, in the range of Grashof numbers corresponding to non-fully developed flow conditions.

The comparison of the form of the outer part of the measured temperature profiles with the logarithmic expression suggested in (14) leads to similar remarks as those made for the inner part (fig. 3). Although not as dramatic, there is again a gradual approach to the logarithmic form with increasing Grashof numbers.

In conclusion, the present state of development of turbulence models employed in free convection flow computations appears unsatisfactory. Existing efforts, mainly attempting to use turbulence models "borrowed" from ordinary or forced convection flows in modified forms, have produced only limited results. To develop turbulence models suitable for this category of complicated flows it is suggested, that research efforts should be directed towards understanding the effects of buoyancy on turbulence transport processes and the mechanism of the existing strong interaction between the flow field and the sustaining it thermal field. The known methodology of interplay between experiment and computation consists a most valuable approach to the problem. However, this should not be used only for validation purposes, but as a tool for the study of the turbulence structure and transport processes in the various parts consisting the velocity and temperature fields associated with these flows. Finally, the reported experiments suggest, that studying the development of turbulence towards a fully developed state offers valuable information assisting in the clarification of a number of questions discussed in this work.

References

- 1.- E.R.G. Eckert and T.W. Jackson "Analysis of a Turbulent Boundary Layer on a Flat Plate" NACA TN 1015, 1950.
- 2.- C.Y. Warner and V.S. Arpaci "An Experimental Investigation of Turbulent Natural Convection in Air at Low Pressure Along a Vertical Heated Flat Plate" Int. J. of Heat and Mass Transfer, Vol 11, pp 397-406, 1968.
- 3.- G.C. Vliet and C.K. Liu "An Experimental Study of Turbulent Natural Convection Boundary Layers" J. Heat Transfer, Vol. 91, p. 511, 1969.
- 4.- R. Cheeswright "Turbulent Natural Convection from a Vertical Plane Surface" J. Heat Transfer, Vol. 90, pp 1-8, 1968.
- 5.- F.J. Bayley "An Analysis of Turbulent Free Convection Heat Transfer" Proc. Inst. Mech. Engrs, Vol. 169 (20), p. 361, 1955.
- 6.- S.S. Kutateladze, A.G. Kiriyaskin and P.V. Ivakin, "Turbulent Natural Convection on a Vertical Plate and in a Vertical Layer" Int. J. Heat and Mass Transfer, Vol. 15, pp 193-202, 1972.
- 7.- J. Countanceau "Convection Naturelle Turbulence sur une Plaque Verticale Isotherme, Transition, Echange de Chaleur et Frottement Parietal Lois de Repartition de Vitesse et de Temperature" Int. J. Heat and Mass Transfer, Vol. 12, pp 753-769, 1969.
- 8.- J.M. Piau "La Convection Naturelle en Regime Turbulent, Aux Grandes Nombres de Grashof", C.R. Hebd. Seanc. Acad. Sci. Paris, Ser. A294, pp. 420-423, 1972.
- 9.- R.R. Smith, "Characteristics of Turbulence in Free Convection Flow Past a Vertical Plate" Ph. D. Thesis, University of London, 1972.
- 10.- D.D. Papailiou, P.S. Lykoudis "Turbulent Free Convection Flow" Int. J. Heat Mass Transfer, Vol. 17, pp 161-172, 1974.
- 11.- K. Noto and R. Matsumoto "Turbulent Heat Transfer by Natural Convection Along an Isothermal Vertical Flat Surface", J. Heat Transfer, Vol. 97, pp 621-624, 1975.
- 12.- J.W. Elder "Turbulent Free Convection in a Vertical Slot", J. Fluid Mech. Vol 23 (1), pp 99-111, 1965.
- 13.- Z.H. Qureshi and B. Gebhart "Transition and Transport in a Buoyancy Driven Flow in Water Adjacent to a Vertical Uniform Flux Surface" Int. J. Heat Mass Transfer, Vol 21, pp 1467-1479, 1978.
- 14.- D.L. Siebers, R.F. Moffatt and R.G. Schwind "Experimental, Variable Properties Natural Convection From a Large, Vertical, Flat Surface", Transactions of ASME, Vol. 107, pp 124-132, 1985.
- 15.- T. Cebeci and A. Khatib "Prediction of Turbulent Free Convective Heat Transfer From a Vertical Flat Plate", J. Heat Transfer, Vol. 97, pp. 469-471, 1975.
- 16.- H. Mason and R.A. Seban "Numerical Predictions For Turbulent Free Convection from Vertical Surfaces", Int. J. Heat and Mass Transfer, Vol. 17, pp1329-1336, 1974.

- 17.- O.A. Plumb and L.A. Kennedy "Application of a κ - ϵ Turbulence Model to Natural Convection from a Vertical Isothermal Surface", *J. Heat Transfer*, Vol. 99, pp 79-85, 1977.
- 18.- S.J. Lin and S.W. Churchill "Turbulent Free Convection from a Vertical, Isothermal Plate", *Numer. Heat Transfer*, Vol 1, pp 129-145, 1978.
- 19.- S. Hassid and M. Poreh "A Turbulent Energy Dissipation Model for Flows with Drag Reduction", *J. Fluids Eng.*, Vol 100, pp 107-112, 1978.
- 20.- W.P. Jones and B.E. Launder "The Prediction of Laminarization with a Two-Equation Model of Turbulence", *Int. J. Heat and Mass Transfer*, Vol. 15, pp. 301-314, 1972.
- 21.- C.K.G. Lam and K. Bremhorst "A Modified form of the κ - ϵ Model for Predicting Wall Turbulence", *J. Fluids Engng*, Vol 103, pp 456-460, 1981.
- 22.- K.Y. Chien, "Predictions of Channel and Boundary Layer Flows with a Low-Reynolds number Two-Equation Model of Turbulence" AIAA-80-0134, 1980.
- 23.- K.Y. Chien, "Predictions of Channel and Boundary Layer Flows with a Low-Reynolds number Turbulence Model", *AIAA J.*, Vol.20, pp 33-38, 1982.
- 24.- W.C. Reynolds, "Computation of Turbulent Flows", *Ann. Rev. Fluid Mech.*, Vol.8, pp 83-208, 1976.
- 25.- G.H. Hoffman, "Improved Form of the Low Reynolds Number κ - ϵ Turbulence model", *Physics of Fluids*, Vol.18, pp 309-312, 1975.
- 26.- W.M. To and J.A.C. Humphrey, "Numerical Simulation of Buoyant Turbulent Flow-1. Free Convection Along a Heated Vertical Flat Plate", *Int. J. Heat and Mass Transfer*, Vol. 29, pp 513-592, 1986.
- 27.- V.C. Patel, W. Rodi and G. Scheuerer "Turbulence Models for Near-Wall and Low-Reynolds number Flows a Review", *AIAA J.*, Vol. 23, pp 1308-1319, 1985.
- 28.- R.A.W.M. Henkes and C.J. Hoogendoorn "Comparison of Turbulence Models for the Natural Convection Boundary Layer Along a Heated Vertical Plate", *Int. J. Heat and Mass Transfer*, Vol.32, pp. 151-169, 1989.
- 29.- H. Ozoe, A. Mouri, M. Ohmuro, S.W. Churchill and N. Lior "Numerical Calculations of Laminar and Turbulent Natural Convection in Water in Rectangular Channels Heated and Cooled Isothermally on the Opposing Vertical Walls" *Int. J. Heat and Mass Transfer*, Vol.28, pp. 125-138, 1985.
- 30.- W.K. George and S.P. Capp "A theory for natural convection turbulent Boundary Layers Next to Heated Vertical surfaces", *Int. J. Heat and Mass Transfer*, Vol.22, pp. 813-826, 1969.
- 31.- M. Miyamoto, H. Kajino, J. Karima and I. Takanami "Development of Turbulence Characteristics in a Vertical Free Convection Boundary Layer", *Proc. 7th Int. Heat Transfer Conf.*, Vol.2, pp. 323-328, 1982.
- 32.- D.D. Papailiou "Statistical Characteristics of a Turbulent Free-Convection Flow in the Absence and Presence of a Magnetic Field", *Int. J. Heat and Mass Transfer*, Vol. 23, pp. 889-895, 1980.
- 33.- K. Kitamura, M. Koike, I. Fukuoka and T.S. Saito "Large Eddy Structure and Heat Transfer of Turbulent Natural Convection Along a Vertical Flat Plate", *Int. J. of Heat and Mass Transfer*, Vol. 28, pp 837-850, 1985.
- 34.- T.J. Tsirikoglou and D.D. Papailiou "The Structure of the Turbulent Temperature Field Above Heated Planes". Published in the "Advances in Turbulence", Editors: G. Comte-Bellot and J. Mathieu, Springer-Verlag, pp 300-309, 1987.
- 35.- R. Cheesewrite and E. Ierokipiotis "Velocity Measurements in a Natural Convection Boundary Layer", Queen Mary College, Faculty of Engineering Research, Report EP 5022, 1981.
- 36.- R. Cheesewrite and E. Ierokipiotis "Velocity measurements in a Turbulent Natural Convection Boundary Layer" *Proc. 7th Int. Heat Transfer Conf.*, Vol. 2, pp 305-309, Munich, F.R.G., 1982.
- 37.- C.J. Hoogendoorn and H. Euser, "Velocity Profiles in the Turbulent Free Convection Boundary Layer", *Proc. 6th Int. Heat Transfer Conf.*, Vol. 2, pp 193-198, 1978.
- 38.- M. Hishida, Y. Nagamo, T. Tsuji and I. Kaneko, "Turbulent Boundary Layer of Natural Convection Along a Vertical Flat Plate", *Trans. Japan Soc. Mech. Engrs*, Vol. 47, pp 1260-1268, 1981.

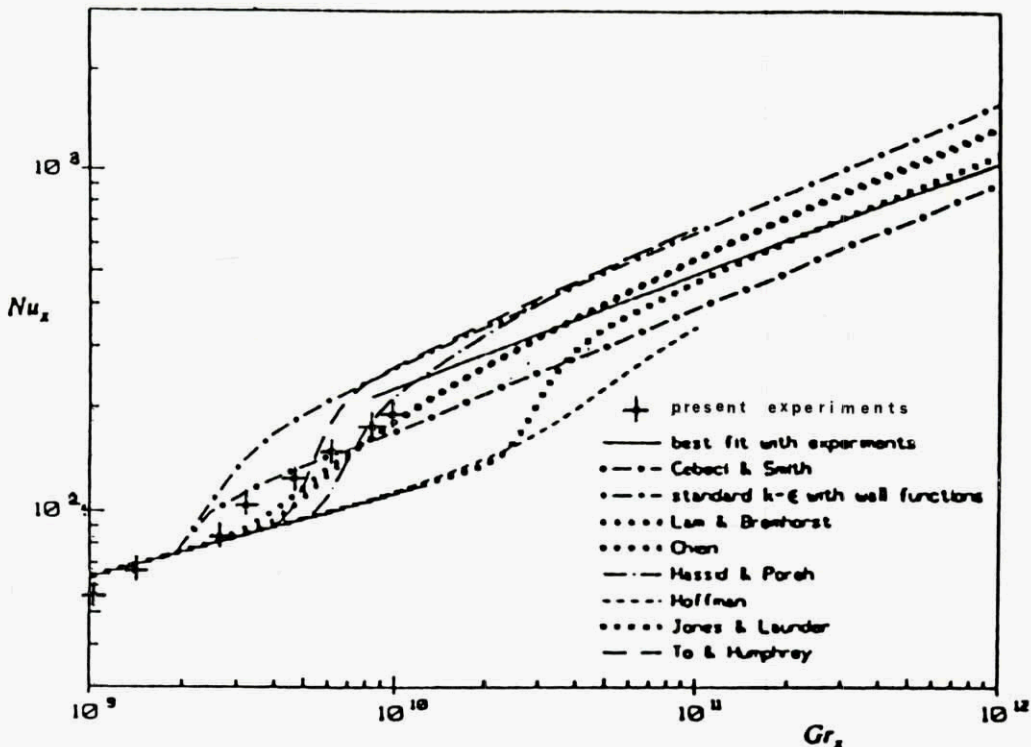


Fig. 1. Computed and measured wall heat transfer for air.
 Henkes and Hoogendoorn ref. (28)

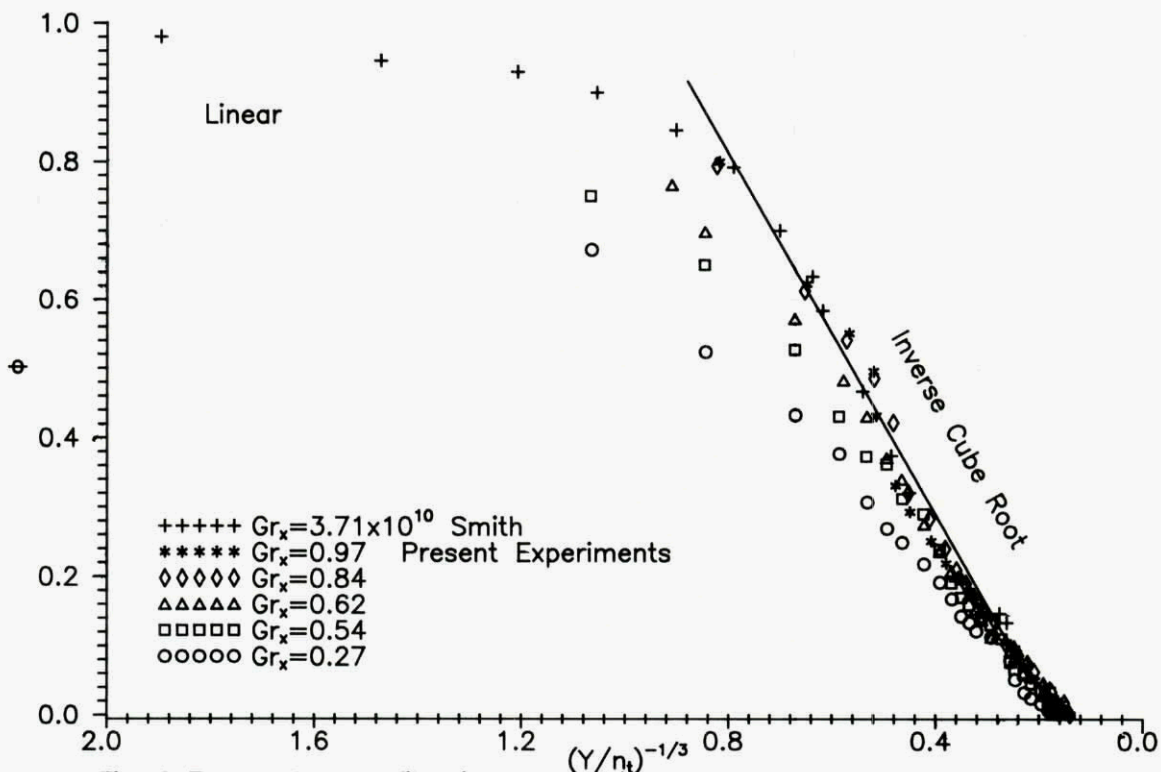


Fig. 2 Temperature profiles in a developing turbulent natural convection boundary layer along a vertical surface - inner part.

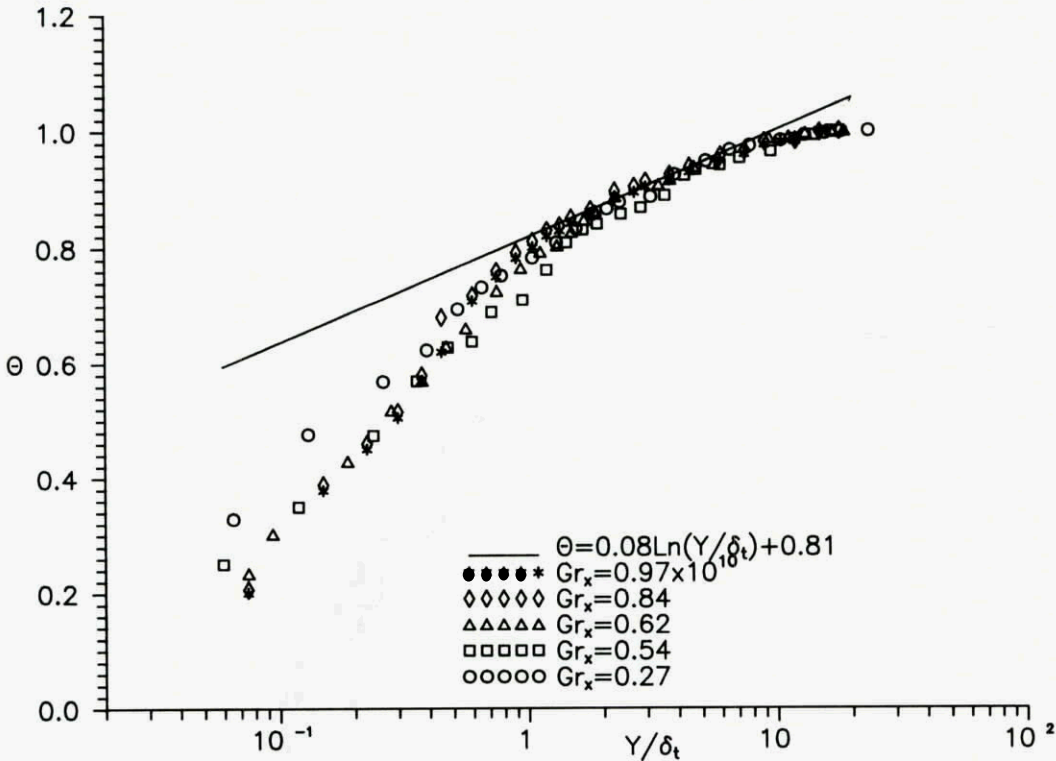


Fig. 3 Temperature profiles in a developing turbulent natural convection boundary layer along a vertical surface - outer part.

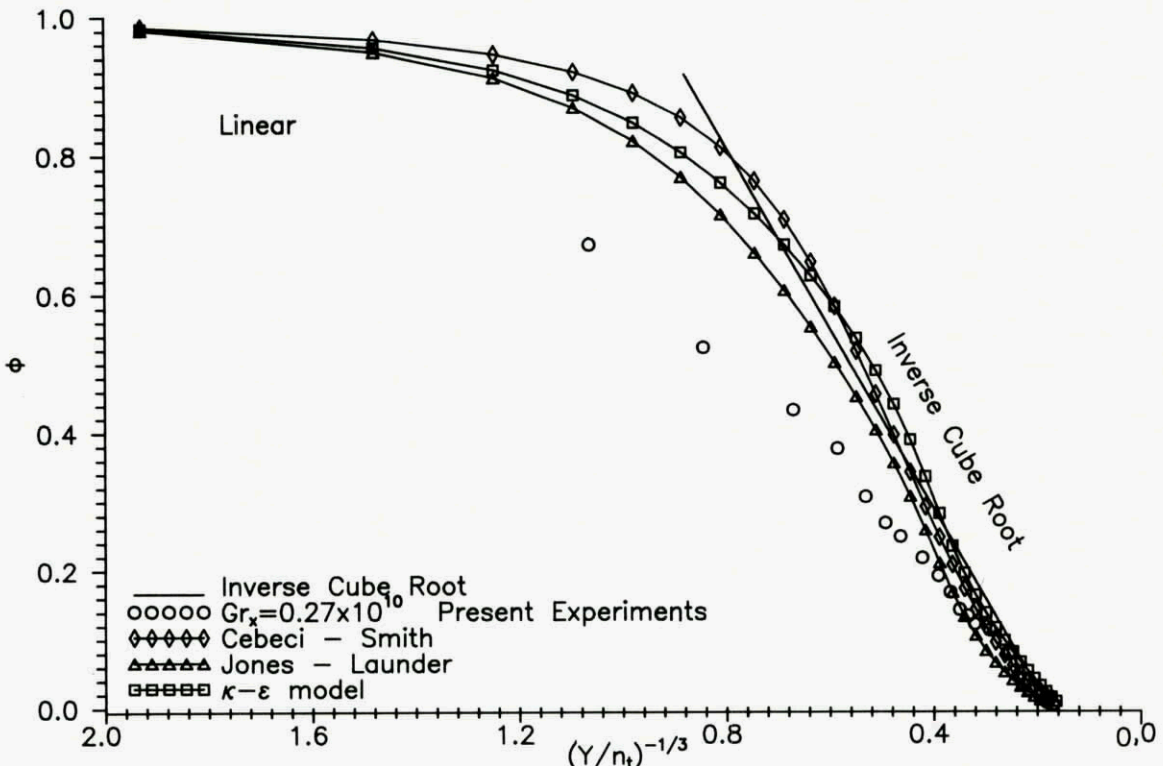


Fig. 4 Comparison of computed and measured temperature profiles. Non-developed flow.

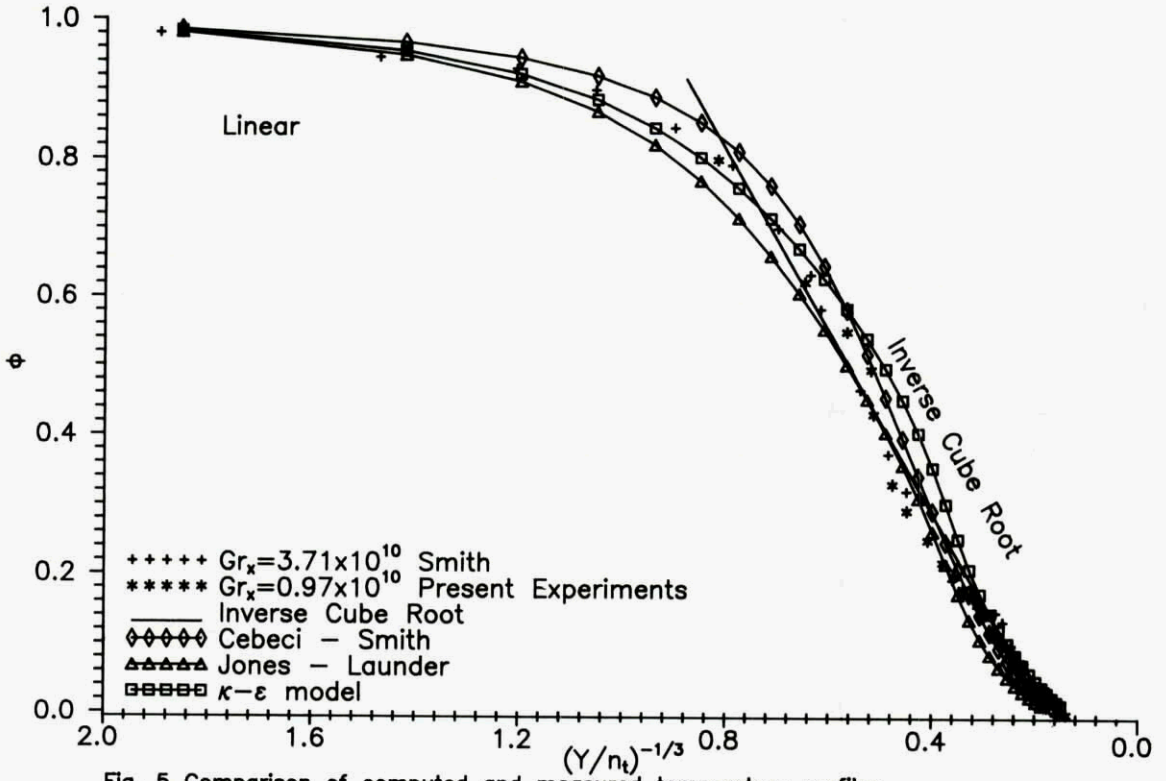


Fig. 5 Comparison of computed and measured temperature profiles.
Fully developed flow.

TURBULENT FLOW MODELLING IN SPAIN. OVERVIEW AND DEVELOPMENTS.

C. Dopazo, R. Aliod and L. Valiño
Fluid Mechanics Group, School of Engineering
University of Zaragoza
M. Luna, 3, 50015 Zaragoza
Spain

ABSTRACT

A brief overview of ongoing flow modelling activities in Spain in the fields of turbulent boundary layers, two-phase flows and turbulent reactive flows is presented.

Turbulent shear flows laden with small solid particles and the turbulent isothermal mixing of two chemical species undergoing a second order irreversible chemical reaction are discussed in more detail. An eulerian approach is followed in the former, employing a phase indicator function conditioning technique for the continuous phase and a Boltzmann type velocity distribution function for the dispersed phase. The latter is treated via a probability density function (pdf) formalism where the joint statistics of concentrations and concentration-gradients is investigated. Predictions are compared with available experimental results in both cases.

Some concluding remarks on the specific needs on modelling or turbulent two-phase and reacting flows are listed.

1. INTRODUCTION

As in most fields of scientific research, the ultimate goal in the investigation of turbulent flows is to develop a quantitative tractable predictive theory. This objective is hampered by the existence of a wide spectrum of length and time scales, ranging from the characteristic sizes and frequencies of the large turbulent structures to the Kolmogorov length and time microscales. This prevents direct numerical simulation (DNS) of turbulent flows in most cases of practical interest. DNS^{13, 16, 31, 36} of some idealized and limit cases can provide useful information on the asymptotic behavior of turbulent fields.

Existing computers set a limit on the length and time scales that can be numerically resolved. Large eddy simulation (LES) methodology²¹ filters the contribution to a fluctuating variable coming from large structures averaging the effects of small scales below a given threshold. The latter introduce unknown terms in the resulting equations. Models or closure hypothesis must be proposed in order to proceed further to the numerical simulation. In some instances, dumping the small scale contributions into a collective pool may yield good results. This can be the case of the turbulence modelling where most energy production and energy transfer processes are dominated by large/intermediate size eddies, while the overall small-scale action upon the flow can be simulated and quantified as a diffusive-like irreversible mechanism. However, if a process is tied to the small fluctuating scales the closure difficulties might render LES strategies useless. This is the case of chemically reacting turbulent flows.

Reynolds averaging techniques consider the contribution to a fluctuating variable coming from the whole spectrum of length and/or time scales²⁵. The closure problem can be more severe and difficult to solve than the equivalent one in LES for the velocity field or of the same order to complexity for a reactive scalar in a turbulent flow. Moment and probability density function (pdf) equations have been obtained after Reynolds-averaging the corresponding local-instantaneous conservation equations. Most modelling activity has revolved around moment-equations^{18,19}. Pdf transport equations condense the information equivalent to an infinite hierarchy of moment equations^{9,10,25}. It has been shown that the pdf formalism is the natural one for turbulent reactive flows¹⁰ and that pdf models can be proposed based on second order closure models²⁹.

An overview of ongoing activities on turbulent flow modelling in Spain is presented in Section 2. Modelling work on turbulent boundary layers, two-phase flows and turbulent reactive flows is briefly described. More details with emphasis on closure models are provided in Section 3 for two selected cases: Turbulent shear flows laden with small solid particles and turbulent isothermal mixing of an acid and a base undergoing a second order irreversible chemical reaction; these cases exemplify two areas in which significant modelling efforts are required. In the former even the basic equations and methodologies to be used as a starting point are being questioned. The latter is adequate to illustrate the difference between what seems to be the natural pdf approach and what most moment modellers in the field are doing. Section 4 contains some concluding remarks on the two selected cases.

2. OVERVIEW

The following ongoing turbulent flow modelling activities in Spain have been brought to the attention of the authors:

2.1 Turbulent Boundary Layers

2.1.1 Asymptotic Expansion Techniques^{7,26}

Turbulence modelling is being conducted via the asymptotic techniques originated within the framework of "periodic homogenization theory". The flow variables are asymptotically expanded and the model can, thus, be formally justified. The averaged partial differential equations have a structure analogous to that of the compressible Navier-Stokes equations.

The starting point is the so called MPP turbulence models²⁰, valid for incompressible flows of ideal or weakly viscous fluids. These models have been generalised in a first attempt⁷ to inviscid compressible

isentropic flows. No closure hypothesis are required at this level. The Reynolds stress tensor is obtained from the solution of a non-linear differential equation. The gradient of the inverse lagrangian coordinate associated to the mean velocity field, the average turbulent kinetic energy and the average helicity appear as parameters in that equation. The unclosed terms can then be tabulated and it is to be expected that the corresponding table has a universal character²⁶. These models do not take into account the flow behavior near solid walls. On the other hand, mechanisms for turbulence generation are not considered and models are typically non-stationary.

As a first step, a reformulation of asymptotic models for moderately high Reynolds number and moderate Mach number compressible isentropic flows has been achieved. Non-standard boundary conditions adding new non-linearities to the problem and based on the well known logarithmic law of the wall have been introduced to take into account the existence of boundary layers. The methodology followed to numerically solve the problem is described in detail in Reference 26 where a large number of numerical results are presented.

In a second step, new models describing the turbulent motion of the fluid over the whole domain, including the regions near solid walls, have been formulated. The flow domain is decomposed into a turbulent boundary layer and an inviscid outer zone. Small parameters are introduced and asymptotic expansions for the flow variables are hypothesized for the different zones. Formal manipulation of the equations, identifying the coefficients of the various powers of the small parameters, lead to averaged variable equations for the inner and outer zones. The original initial and boundary conditions are supplemented with those obtained from "matching" the inner and outer variables. The use of these models allows, among other things, to rigorously justify, from the asymptotic point of view, the laws of the wall.

The numerical solution rest upon semi-implicit time discretization schemes and finite element type approximation for the space variables. A least square type formulation is utilized followed by an algorithm of the Buckley-Le Nir conjugate gradient⁶. Finally, the numerical problem is reduced to the solution of a "cascade" of linear problems, some of them analogous in nature to the Stokes problem, which can be solved using, for example, the Glowinski-Pironneau method, and others of the Poisson type.

These techniques are being developed within the framework of the HERMES Project of the European Space Agency (ESA) in order to predict the thermal behavior of this space aircraft during its reentry into the earth's atmosphere.

2.1.2 Algebraic Model of Turbulence¹

The two-dimensional (2D) compressible laminar Navier-Stokes equations are considered in a non-dimensional form,

$$\frac{\partial \mathbf{U}}{\partial t} + \frac{\partial \mathbf{F}}{\partial x} + \frac{\partial \mathbf{G}}{\partial y} = 0 \quad (1)$$

where the flux vectors \mathbf{F} and \mathbf{G} can be expressed as $\mathbf{F} = \mathbf{F}^I + \mathbf{F}^V$, $\mathbf{G} = \mathbf{G}^I + \mathbf{G}^V$. The superscripts I and V denote inviscid and viscous contributions, respectively, and

$$\mathbf{U} = \begin{bmatrix} \rho \\ \rho u \\ \rho v \\ \rho e \end{bmatrix} \quad \mathbf{F}^I = \begin{bmatrix} \rho u \\ \rho u^2 + p \\ \rho uv \\ \rho uh \end{bmatrix} \quad \mathbf{G}^I = \begin{bmatrix} \rho v \\ \rho uv \\ \rho v^2 + p \\ \rho vh \end{bmatrix}$$

$$\mathbf{F}^V = \frac{1}{Re} \begin{bmatrix} 0 \\ -\tau'_{11} \\ -\tau'_{12} \\ -u \tau'_{11} - v \tau'_{12} + \frac{\mu}{Pr} \frac{\partial T}{\partial x} \end{bmatrix}$$

$$\mathbf{G}^V = \begin{bmatrix} 0 \\ -\tau'_{12} \\ -\tau'_{22} \\ -u \tau'_{12} - v \tau'_{22} + \frac{\mu}{Pr} \frac{\partial T}{\partial y} \end{bmatrix} \quad (2)$$

Here Re and Pr denote the Reynolds and Prandtl numbers respectively, u and v the two components of the velocity vector and ρ , e , p , h and T are the dimensionless density, specific total energy, pressure, specific total enthalpy and temperature of the fluid. The Sutherland relation is used to take into account the dependence of the molecular viscosity coefficient, μ , on temperature and Mach number. The non-dimensional components of the stress tensor, τ'_{11} , τ'_{12} and τ'_{22} are assumed to follow the Navier-Poisson relation for laminar flows. The equation of state complete the problem specification.

For turbulent flows μ is replaced by " $\mu_l + \mu_t$ ". μ_l is the laminar viscosity. For the "eddy viscosity coefficient", μ_t , the Baldwin-Lomax algebraic model⁴ is used. The variables in Equ. (2) stand then for average values. Cebeci's modifications avoid the calculation of the boundary layer edge.

In this two-layer model the turbulent viscosity is given by,

$$\mu_t = \begin{cases} \mu_{ti} & \text{for } y \leq y_{co} \\ \mu_{to} & \text{for } y > y_{co} \end{cases} \quad (3)$$

where μ_{ti} and μ_{to} stand for inner and outer values of μ_t , y is the normal distance to the wall and y_{co} is the cross-over value, the minimum y for which the inner and outer values of μ_t are equal.

Van-Driest formulation is followed for μ_{ti} ,

$$\mu_{ti} = C_i \rho l^2 w \quad (4)$$

where C_i is a constant, and

$$l = k y [1 - \exp(-y^+/A^+)] \quad (5)$$

w is the mean vorticity module given by,

$$w = \sqrt{\left(\frac{\partial u}{\partial y} - \frac{\partial v}{\partial x}\right)^2} \quad (6)$$

and $y^+ = y u_* / \nu$, with u_* being the friction velocity and ν the kinematic viscosity.

Clauser formulation is used to express μ_{to} ,

$$\mu_{to} = K C_{cp} F_w F_K(y) \quad (7)$$

K is Clauser constant, C_{cp} is an additional constant and

$$F_w = \min(y_{max} F_{max}, C_{wk} y_{max} u_{dif}^2 / F_{max}) \quad (8)$$

F_{max} is the maximum value of

$$F(y) = y [1 - \exp(-y^+/A^+)] \quad (9)$$

and y_{max} is the value of y at which $F(y) = F_{max}$. $F_K(y)$ is the Klebanoff intermittency factor,

$$F_K(y) = [1 - 5.5 (C_K y / y_{max})] \quad (10)$$

u_{dif} is the difference between the maximum and minimum values of the velocity for a profile. The standard values are assigned to the constants.

The solution is obtained by advancing the unsteady non-dimensional form of the equations to steady state by means of a hybrid timestepping scheme. The convergence is accelerated by the use of local timestepping and the incorporation of implicit residual averaging. Spatial discretization is accomplished by means of a Galerkin finite element method assuming a general unstructured grid of linear three-noded triangular elements. In the code, this is achieved by the equivalent process of computing the element contributions from a loop over all the element sides in the mesh. To ensure complete vectorisation of this procedure, the element sides are automatically coloured by the mesh generator¹. The resulting scheme is stabilised by the application of an artificial dissipation operator which is formed as a blended combination of second and fourth differences.

2.2 Two-Phase Flows

2.2.1 Dispersed Phase as a Continuum¹⁵

A monodispersed cloud of rigid spheres suspended in an incompressible isothermal viscous gas is considered. No mass transfer between the phases is included. The dynamic behavior of the particles is characterized by continuous velocity, pressure and concentration fields. For a distribution of particle sizes, as many velocity, pressure and concentration fields are required as the number of size families to be treated.

The particle/particle and particle/fluid interactions are simulated by the introduction of a "pressure" and a "viscosity" of the particle cloud and an inter-phase force taking into account the momentum transfer between the phases.

Should the particle cloud viscosity be ignored no macroscopic mechanism exists to set a limit to strong gradients. A discrete system of particles has been analysed in order to find a strong-gradients limiting mechanism for the continuum model. The inviscid flow around an ensemble of spherical particles has been investigated. None of the microscopic terms can prevent the development of strong gradients in the particle concentration. The consideration of the cloud viscosity seems thus to be necessary in order to describe small wavelengths.

On the other hand, the functional dependence of the particle cloud pressure is important and has significant macroscopic consequences upon the flow development¹⁵.

The specification of the particle cloud viscosity and pressure are therefore open topics. The viscosity data measured by Schürge³² for glass spherical particles of various diameters have been analysed. The viscosity increases considerably when the fluidised bed concentration approaches the maximum packing concentration; on the other hand, it has been observed that a dimensionless viscosity can be obtained by scaling the experimental data with the particle density, the fluidization velocity and a characteristic length which is a function of the particle diameter and Reynolds number. A universal curve of the dimensionless viscosity as a function of the volume concentration can then be plotted. More experiments are however necessary in order to ascertain the suspension rheological behavior.

At moderately high loads the particles interact mainly with the surrounding fluid and the stresses of the cloud are mostly due to particle/fluid interactions. On the other hand, for high cloud concentrations the frequency of collisions between particles increases and the pressure of the particle cloud should substantially grow, preventing the cloud from attaining concentrations above that of maximum packing. Neither experimental data nor theoretical developments exist to model the cloud pressure at high concentration. However, the correct modelling of the pressure is essential, as this is an important mechanism limiting the maximum value of particle concentration.

2.2.2 Eulerian Formulation of Average Equations^{2,3}

In the theoretical derivation of two-phase flow equations, extensive use is made of conditioned averaging techniques^{8,11}. Spatial, temporal, or ensemble average and double/mixed average operators are frequently found in the literature. Two consecutive averages are also encountered in turbulent two-phase flow modeling. Nevertheless the existing formalisms are not quite satisfactory, specially in dealing with turbulent flows. Volume or time averaging produce filtering of small-scale turbulent structures or large fluctuating frequencies. To avoid that filtering effect, dispersed elements must be much smaller than Kolmogorov scales and the number of elements inside the probe volume large enough to get stable values. Those situations rarely occur in practice and are impossible to satisfy in dilute flows. Ensemble averages

avoid these problems but the interaction terms have no straightforward meaning and must be interpreted by comparison with other averages. Applying two consecutive averages lead to equations with a large number of terms with no direct physical meaning and include high order fluctuation correlations, creating some serious closure problems.

Following the usual conditioning technique based on a phase-indicator function³ and properly defining a joint probability density function to describe the dispersed phase dynamics, some of the ideas pointed out by Herczynski and Pienkowska¹⁴ are generalized. Theorems and associated properties are given allowing a general, rigorous and systematic treatment of the continuous phase of a dispersed two-phase flow system. The conditioned mean value of any variable derivative can be expressed as the derivative of the variable conditioned mean value, plus an extra interface source term, which will introduce in the equations information about the action of the second phase. The formalism employed, shares some features in common with those previously developed. The difficulties mentioned above are however overcome. Using those results conditioned average continuity, momentum turbulent kinetic energy and turbulence dissipation rate equations for the continuous phase can be obtained. The main characteristics of these equations are:

- General applicability. In principle no restrictions are placed on the sizes of dispersed elements or their concentrations.
- Continuous phase variables appear statistically averaged. Therefore no spatial or temporal filtering is performed.
- Continuous phase equations are obtained in a single-step averaging operation.
- Continuous phase equations are formally identical to those in classical turbulent single-phase flows, with similar terms and the same order of fluctuation correlations.
- A few additional interaction terms, with direct physical interpretation and mathematical properties which help in modeling them, enter the continuous phase equations.

General eulerian equations for the moments of the particle velocity are next obtained. This is done from a "Boltzmann type" probability density function transport equation which is assumed to correctly represent the particle cloud dynamics^{3,22}. Dispersed phase average continuity, momentum and fluctuating kinetic energy equations are then generated. Neither a particle cloud pressure nor viscosity appear in the average equations. Particle fluctuating velocity correlations and phase interaction terms are unknowns.

A k- ϵ turbulence model is used for the continuous phase. The dispersed phase is modelled via a gradient transport approximation where the particle turbulent diffusivity is rephrased in terms of a root mean square particle fluctuating velocity and, in the case of a dilute dispersed phase, a particle relaxation length. Closure hypothesis are also proposed for the phase interaction terms.

An axisymmetric turbulent jet configuration has been chosen to validate the model for both single phase and two-phase flows. A classical finite volume four-node formula space-marching fully-implicit scheme has been used. Validation has been conducted by comparing the model predictions with available experimental data^{12,24}. Preliminary predictions indicate a reasonably good agreement^{2,3}.

2.3 Turbulent Reacting Flows³⁴

The mixing of dynamically passive inert and reactive scalars convected by a field of nearly homogeneous turbulence is being investigated. The transport equation for the joint probability density function (pdf) of scalars and their gradients is used. Exact treatment is possible of the processes of the straining by mean velocity gradients, the chemical reaction and the dissipation of scalar fluctuations. Closure approximations are required for the non-closed terms describing the straining of scalar gradients by fluctuating velocity gradients and the dissipation of scalar/scalar-gradient and of scalar-gradient correlations by molecular diffusion.

A cumulant expansion technique^{17,23} is used to treat the turbulent straining term. The limit of large Kubo or Reynolds number ("strong perturbation limit") is identified. Furthermore, the "small time limit" allows to truncate the cumulant function operator series expansion at the second-order level. This small time pdf behavior is all that is required in order to derive a scalar-gradient increment random equation. For isotropic turbulent velocity gradients the straining is inversely proportional to the square of the Kolmogorov time micro-scale. The scalar gradients display a tendency to grow and to become isotropic.

A binomial sampling model^{33,34} is used to close the molecular dissipation terms. This model has features in common with the LMSE closure approximation^{9,10} and with Langevin models²⁹. This closure model leads to a qualitatively reasonable relaxation process and produces correct asymptotic results¹³.

A stochastic scalar-gradient straining model is proposed in terms of products of two random vectors. This simulation also implies a model for the turbulent velocity gradient and, therefore, for the turbulent strain rate tensor and for the fluctuating vorticity. Only the consequences of this model on scalar gradients have been explored until now.

A Monte Carlo simulation²⁷ of the molecular dissipation processes is performed considering non-interacting particles. During a time step, all the particles are affected by a LMSE process, while only a fraction acquire new values via a binomial or gaussian sampling technique. Scalar mixing frequencies can be calculated as a part of this joint pdf formulation. The ratio of scalar-gradient to scalar characteristic mixing frequencies is assumed to be a constant greater than one²³.

The previous formulation is then applied to study the evolution of an inert scalar in grid generated turbulence. In particular, the prediction of the concentration

variance and the characteristic mixing frequency displays an excellent agreement with the experimental data for the evolution of dilute ClNa injected at the grid into a main water flow⁵. The flatness factor of the concentration gradient grows to values significantly greater than 3. The latter can be taken as an indication of the internal intermittency of the scalar field.

The reaction between sodium hydroxide diluted in the main flow and methyl formate injected as a dilute solution at the grid generating the turbulence has been investigated in detail by Bennani et al.⁵. Predicted means and variances agree very well with experimental data. The experimentally determined segregation coefficient stabilizes at about -0.7, and it is accurately predicted. The coefficient of skewness of the injected species is positive while that of the species diluted in the main flow are negative, both increasing downstream. Large values of the flatness factors of both species clearly suggest the spatial segregation of reactants. The computation of characteristic mixing frequencies for both species shows how moderately fast chemical reaction (Damköhler number of order unity) can significantly modify the time and length scales of the scalar fields. This is a call of attention on some extended practices in turbulent combustion modeling which overlook this fact. The coefficients of skewness and the flatness factors of the magnitude of the concentration gradients increase downstream reaching high positive values. This is a clear sign of the small scale intermittency. The predicted pdf of the concentration gradient magnitude for both reactants display a log-normal behavior. The dissipation of the injected scalar fluctuations, is significantly faster than that of the reactant diluted in the main flow, due most probably to the initial structure of the injected field that favors the action of the stretching mechanisms and enhances molecular effects.

Information on the statistics of length scales defined as the ratio of concentration and concentration gradients could be obtained from the formulation. The sensitivity of the strain-rate/scalar-dissipation correlation coefficient to changes in the Schmidt or Prandtl numbers could also be evaluated. The same formalism could probably be extended to investigate the fluctuating vorticity dynamics in nearly homogeneous shear flows with constant mean velocity gradients.

3. PRESENTATION OF TWO SELECTED CASES

The following two cases have been selected for a more detail description:

3.1 Eulerian Formulation of Two-Phase Flow Average Equations³

3.1.1 Fluid Phase Conditioning Technique

A phase indicator function, I , is defined such that^{8,11},

$$I(\mathbf{x}, t) = \begin{cases} 1 & \text{if } (\mathbf{x}, t) \text{ is inside the continuous phase} \\ 0 & \text{otherwise} \end{cases}$$

In the process of averaging the Navier-Stokes equations conditioned upon the presence of the fluid phase the indicator function appears as a factor of time and space

derivatives. The following relation holds¹¹,

$$\langle I \phi, \lambda \rangle = \langle I \phi \rangle, \lambda - \langle \phi I, \lambda \rangle \quad (11)$$

ϕ stands for any continuous phase variable and, λ for the derivative with respect to λ (time or space). $\langle \rangle$ is meant for statistical average. The last term in equ. (11) represents the phase interaction. Should the characteristic length of the dispersed elements be much smaller than the mean overall flow characteristic length, this interaction term can be expressed as³

$$\langle \phi I, \lambda \rangle = \frac{\alpha^d}{V^d} \overline{\phi}_{S_p} \overline{\phi_{n, \lambda}}^* + \epsilon_{\phi \lambda} \quad (12)$$

where α^d is the "particle concentration", the overbar followed by a star denotes statistical average conditioned to the center of the dispersed elements being positioned at point \mathbf{x} at time t , $\overline{\phi}_{S_p}^*$ is the dispersed element average volume, the surface integral extends over the interface, S_p , $\epsilon_{\phi \lambda}$ is a residue usually much smaller than the first term on the right side of equ. (12) and

$$n_{\lambda} = \begin{cases} -\mathbf{v}^s \cdot \mathbf{n} & \text{if } \lambda = t \\ n_k & \text{if } \lambda = x_k \end{cases} \quad (13)$$

\mathbf{v}^s and \mathbf{n} are the interface velocity and the unit vector perpendicular to the interface element located at \mathbf{x} , pointing towards the continuous phase, respectively. The subscript k designates the k component of the corresponding vector.

3.1.2 Continuous Phase Conditioned Equations and Modeling

The instantaneous conservation equations multiplied by I and averaged, after making use of Equ. (12) yield the continuity, momentum, turbulent kinetic energy and dissipation rate averaged equations.

A k - ϵ model is used to represent the turbulence. The following expressions are used for the unclosed terms,

$$-\alpha \overline{u'_i u'_j} = -\alpha \frac{2}{3} k \delta_{ij} + v_T \left[(\alpha U_i)_{,j} + (\alpha U_j)_{,i} \right] \quad (14)$$

$$-\alpha \left(\overline{u'_i k'} + \frac{1}{\rho} \overline{u'_i p'} \right) = \frac{v_T}{\sigma_k} (\alpha k)_{,i} \quad (15)$$

where α is the void fraction, U and u' are the mean and fluctuating velocity, respectively, k and k' are the average and the instantaneous-fluctuating turbulent kinetic energy, respectively, δ_{ij} is the Kronecker delta, p' is the fluctuating pressure, σ_k is set equal to one and $v_T = C_D(\mathbf{P}, \epsilon) k^2 / \epsilon$ is the turbulent viscosity. \mathbf{P} and ϵ stand for the turbulent kinetic energy production and dissipation rates, respectively.

The weakest point in the model is the ϵ -transport equation, which is replaced by

$$(\alpha \epsilon)_{,t} + (\alpha U_j \epsilon)_{,j} = \left[\left(v + \frac{v_T}{\sigma_\epsilon} \right) (\alpha \epsilon)_{,j} \right]_{,j} + \alpha \frac{\epsilon}{k} (C_{\epsilon_2} P - C_{\epsilon_1} \epsilon) + I_\epsilon \quad (16)$$

where the constants σ_ϵ , C_{ϵ_1} and C_{ϵ_2} are assigned the values corresponding to single-phase flows and the phase interaction term is designated by I_ϵ . Based on dimensional considerations and order of magnitude estimates the following model is proposed,

$$I_\epsilon = \frac{\rho^d}{\rho} a \frac{\epsilon}{k} \left\{ -C_{\epsilon_3} (k - k^d) + C_{\epsilon_4} \left[K (U_i - V_i)^2 + k (1 - \theta) \right] \right\} \quad (17)$$

where ρ^d and k^d are the dispersed phase density and fluctuating kinetic energy, respectively, a is the inverse of the particle relaxation time, $K = (R/\eta) + a \tau_L$, with R and η being the particle radius and Kolmogorov length microscale respectively and $\tau_L = 0.5 (k/\epsilon)$, V is the mean dispersed phase velocity and $\theta = \tau_L / (\tau_L + 1/a)$. C_{ϵ_3} and C_{ϵ_4} are both tentatively taken equal to one.

The phase interaction terms in the momentum and turbulent kinetic energy equations are modelled as,

$$I_{U_i} = -\frac{\rho^d}{\rho} a (U_i - V_i) \quad (18)$$

$$I_k = \frac{\rho^d}{\rho} a (1 - \theta) - \frac{\rho^d}{\rho} a (k - k^d) \quad (19)$$

Should mass transfer at the interface be negligible and for solid particles the I_U , I_k and I_ϵ include all the significant phenomena taking place at the solid/fluid interface.

A rigorous presentation of the equations and closure assumptions is contained in Reference 3.

3.1.3 Dispersed Phase Average Equations and Closures

A Boltzmann type equation is assumed to accurately describe the particle cloud dynamics^{3,22}. The generalised transport equation for the particle velocity distribution function can be multiplied by any function of the velocity field and integrated over the phase-space in order to generate moment equations. For clouds of solid non-diffusive particles undergoing elastic collisions and allowing neither disgregation nor agglomeration, average continuity, momentum and fluctuating kinetic equations are easily obtained^{2,3}.

The unknown terms are then modelled as,

$$-\alpha^d \overline{v'_i v'_j}^* = -\alpha^d \frac{2}{3} k^d \delta_{ij} + v^d \left[(\alpha^d v_i)_{,j} + (\alpha^d v_j)_{,i} \right] \quad (20)$$

$$-\alpha^d \overline{k' v'_j}^* = \frac{v^d}{\sigma_k^d} (\alpha^d k^d)_{,j} \quad (21)$$

where v' is the dispersed phase fluctuating velocity and v^d is the particle turbulent diffusivity, which for a dilute dispersed phase is given by, $v^d = C_p k^d / a$. σ_k^d has been set equal to one.

The phase interaction terms to be modelled in the dispersed phase equations are identical to those entering the fluid phase equations and closure assumptions have already been proposed.

A detailed derivation of the equations and a justification of the models are presented in References 2 and 3.

3.1.4 Numerical Results

An axisymmetric turbulent jet configuration has been chosen to validate this model for both single phase and two-phase flows. The pressure is assumed constant throughout the flow field.

A classical finite volume, four node formula, space marching, fully implicit scheme has been used .

Due to this particular methodology applied to a parabolic shear flow, the radial momentum equation is not solved. An additional closure assumption is required for $W_r = U_r - V_r$ (the radial relative velocity) namely

$$W_r = C_\alpha \frac{v^d}{\alpha^d} \frac{\partial \alpha^d}{\partial r} \quad (22)$$

with $C_\alpha = 0.5$. Justification for this hypothesis is provided in Reference 3.

The standard values for the single-phase $k - \epsilon$ model coefficients are used:

$$C_D = 0.09 (1 - 0.44 G), C_{\epsilon_1} = 1.44 \\ C_{\epsilon_2} = 1.92 (1 - 0.035 G), \sigma_k = 1.0, \sigma_\epsilon = 1.3$$

G is the deceleration parameter, modifying the traditional C_D and C_{ϵ_2} values, introduced by Rodi³⁰ in order to get the proper single phase jet spreading rate.

Based on a few initial runs, the preliminary values for the additional two-phase model coefficients are:

$$C_p = 0.1, \sigma_{k^d} = 1.0, C_{\epsilon_3} = 1.0, C_{\epsilon_4} = 1.0$$

3.1.5 Model Predictions

Available experimental data for turbulent jets of air, laden with solid particles or liquid droplets in highly dilute concentrations, were scrutinized. Restrictions setting the range of applicability for the model, are not fully satisfied by most of the published works. Furthermore, only a few publications supply direct measurement of each individual phase, and on measured turbulent parameters and boundary conditions required for proper model calibration. Nevertheless, the experimental data from References 12 and 24 have been selected to test the model predictions. Three basic cases have been documented:

Case	2R(μm)	φ ₀	R/η	R W ₀ /Δy
1	50	0.32	0(1)	0(10)
2	50	0.85	0(1)	0(10)
3	200	0.80	0(1)	0(100)

where φ₀ stands for the initial particle mass loading ratio.

Comparison between model predictions and experiments are shown in Figures 1 to 6. Comments are self-explanatory. r and x represent the radial and axial coordinates, respectively. x = 0 is located at the nozzle exit. The nozzle diameter is D. In order to make clear the dispersed phase influence upon the flow, single phase jet measurements and predictions are included in each figure. Single phase jet data were taken from References 24 and 35.

Figures 1 to 3 relate to case 1, the best documented one. Predicted and measured mean velocity, turbulence intensity and turbulent shear stress profiles are presented for both phases. The agreement is reasonable.

Figures 4 and 5 refer to case 2. The values of the variables at the centerline are slightly underpredicted. The turbulent axial velocity is accurately estimated. Centerline velocity values have been shown to be very sensitive to the value of C_p.

Figure 6 belongs to case 3. Centerline particle and fluid velocity are correctly predicted. However, the computed profile for the dispersed phase seems to be sharper than what the few experimental points available suggests.

3.2 Turbulent Mixing and Chemical Reactions³⁴

It seems now clear that neither large-eddy simulation (LES) nor direct numerical simulation (DNS) can be successfully applied at present to solve general turbulent reacting flow problems²⁸. Some investigators advocate the presumed pdf method in order to evaluate the average chemical source terms entering the moment equations²⁸. However, the use of a pdf transport equation^{9,10} is by far the most rigorous methodology to cope with the non-linear chemical rate terms. These terms are close in the pdf formulation. Should a transport equation for the joint pdf of velocity, kinetic energy dissipation rate, concentration and scalar

dissipation rate be used, the closure problem associated with the turbulent transport can also be avoided²⁸. Here some preliminary ideas on the use of the joint pdf of scalar fields and their gradients are presented³⁴.

3.2.1 Basic Equations

The isothermal turbulent mixing of two scalar fields undergoing a second order chemical reaction obeys the local instantaneous equation,

$$L C_{\alpha} = S_{\alpha} (C) \quad (23)$$

where

$$L = \frac{\partial}{\partial t} + v_j \frac{\partial}{\partial x_j} - D \nabla^2 \quad (24)$$

is the convection/diffusion operator. v_j(x,t) is the local instantaneous velocity field at point x and time t, which can be decomposed into a mean field, U_j(x,t), and fluctuation, u_j(x,t). D is the molecular diffusivity assumed identical for the two species. C = {C_α}, for α=1,2, stands for the concentrations of the two chemical species. C_α(x,t) can also be decomposed into a mean, <C_α(x,t)>, and a fluctuating field, c_α(x,t). For a second order irreversible chemical reaction the chemical source term is expressed as S_α(C) = -K_c C₁ C₂, for α=1,2, where K_c is the chemical rate constant.

Let the gradient C_α be defined as C_{α,i} = ∂C_α/∂x_i. Its evolution follows the equation,

$$L C_{\alpha,i} = - \frac{\partial v_j}{\partial x_i} C_{\alpha,j} + \frac{\partial S_{\alpha}}{\partial C_{\beta}} C_{\beta,i} \quad (25)$$

Summation over repeated latin and greek indexes is implied. A transport equation for the joint pdf of the scalar and scalar-gradient fields can readily be derived³⁴,

$$\begin{aligned} \frac{\partial P}{\partial t} + \frac{\partial}{\partial \Gamma_{\alpha}} [S_{\alpha}(\Gamma) P] + \frac{\partial}{\partial \chi_{\alpha i}} \left[\frac{\partial S_{\alpha}(\Gamma)}{\partial \Gamma_{\beta}} \chi_{\beta i} P \right] + \\ D \frac{\partial^2}{\partial \Gamma_{\alpha} \partial \Gamma_{\beta}} (\chi_{\alpha i} \chi_{\beta i} P) = \frac{\partial}{\partial \chi_{\alpha i}} \left(\left\langle \frac{\partial u_j}{\partial x_j} \middle| \Gamma, \chi_{\approx} \right\rangle \chi_{\alpha j} P \right) \\ - 2D \frac{\partial^2}{\partial \Gamma_{\alpha} \partial \chi_{\beta j}} \left(\left\langle \frac{\partial C_{\beta,j}}{\partial x_i} \middle| \Gamma, \chi_{\approx} \right\rangle \chi_{\alpha i} P \right) \\ - D \frac{\partial^2}{\partial \chi_{\alpha j} \partial \chi_{\beta k}} \left(\left\langle \frac{\partial C_{\alpha,j}}{\partial x_i} \frac{\partial C_{\beta,k}}{\partial x_i} \middle| \Gamma, \chi_{\approx} \right\rangle P \right) \end{aligned} \quad (26)$$

where P d Γ d χ = P(Γ, χ; t) d Γ d χ is the probability of the joint event Γ_α ≤ C̃_α(x,t) < Γ̃_α + d Γ_α and

$\chi_{\alpha i} \leq C_{\alpha i}(\mathbf{x}, t) < \chi_{\alpha i} + d \chi_{\alpha i}$. Equ. (26) has been restricted to the case of statistically homogeneous turbulence and scalar fields. $\langle \mathbf{V} | \Gamma, \chi \rangle$ stands for the expectation of the variable \mathbf{V} conditional upon $C(\mathbf{x}, t) = \Gamma$ and $\nabla C(\mathbf{x}, t) = \chi$.

All the terms on the left hand side (LHS) of Equ. (26) are closed and physically represent the accumulation of probability, the probability transport in concentration and concentration-gradient spaces due to chemical reaction and due to molecular mixing of concentrations, respectively. The terms on the right hand side (RHS) of Equ. (26) are not closed. The phenomenon of turbulence straining of scalar-gradients (similar to the vortex stretching mechanism of turbulence²⁵) is ascribed to the first term on the RHS. The last two terms represent the cross-dissipation of scalars/scalar-gradients and the dissipation of scalar-gradient/scalar-gradient correlations due to molecular mixing, respectively. In order to use Equ. (26) the three terms on its RHS must be approximated.

3.2.2 Turbulence Straining of Scalar-Gradients

Since a sequential Monte Carlo (MC) simulation²⁷ of Equ. (26) will be conducted hereafter, the effect on P of the terms on the RHS can be separately treated.

In the limit of large turbulent Reynolds number and of small time, Kubo technique¹⁷ leads to the following representation of the first term on the RHS of Equ. (26),

$$\left(\frac{\partial P}{\partial t} \right)_1 = t \left\langle \frac{\partial u_j}{\partial x_i} \frac{\partial u_i}{\partial x_k} \right\rangle \frac{\partial}{\partial \chi_{\alpha i}} \left[\chi_{\alpha j} \frac{\partial}{\partial \chi_{\beta k}} (\chi_{\beta i} P) \right] \quad (27)$$

The subscript 1 on the LHS of Equ. (27) indicates that the P variation is due only to the first term on the RHS of Equ. (26). It is pertinent to remark that Equ. (27) implies only mathematical approximations but no closure hypothesis in the classical sense.

For statistically homogeneous and isotropic fluctuating velocity-gradient fields and incompressible flows Equ. (27) finally becomes,

$$\left(\frac{\partial P}{\partial t} \right)_1 = t \frac{\langle \epsilon \rangle}{30 \nu} (4 \chi_{\alpha k} \chi_{\beta k} \delta_{ij} - \chi_{\alpha i} \chi_{\beta j} - \chi_{\alpha j} \chi_{\beta i})$$

$$\frac{\partial^2 P}{\partial \chi_{\alpha i} \partial \chi_{\beta j}} \quad (28)$$

where $\langle \epsilon \rangle$ is the average turbulent kinetic energy dissipation rate²⁵ and ν is the kinematic viscosity.

3.2.3 Monte Carlo Simulation

Due to the high dimensionality of P , Equ. (26) is simulated via a sequential MC technique²⁷. Every physical process represented by the various terms in Equ. (26) is then considered to act separately and sequentially upon N stochastic particles which

approximate $P(\Gamma, \chi; t)$. A stochastic particle n is defined by its concentration and concentration-gradient values, $\{C_{\alpha}^{(n)}, (\nabla C)^{(n)}\}$.

3.2.3.1 Turbulence Straining

Equ. (28) can be formally transformed into a finite-increment equation by using the definition of the P derivative and a Taylor series expansion. After a few algebraic manipulations, the following stochastic model (equivalent to a closure assumption) is proposed³⁴,

$$\Delta_{\delta t} C_{\alpha, i}^{(n)}(t) = \left(\frac{\langle \epsilon \rangle}{60 \nu} \right)^{1/2} (\delta t) \left(x \eta_i^{(n)} \xi_j^{(n)} + y \eta_j^{(n)} \xi_i^{(n)} + z \eta_k^{(n)} \xi_k^{(n)} \delta_{ij} \right) C_{\alpha, j}^{(n)}(t) \quad (29)$$

The LHS is the change experienced during a time step, δt , by the i^{th} component of the gradient of the scalar α for the stochastic particle n at time t . x , y and z are constants with analytically determined values, $x = -0.35634$, $y = 2.8059$, $z = -0.8165$

η and ξ are statistically independent random vectors with zero mean and unity correlation matrix.

3.2.3.2 Molecular Mixing

A recently developed binomial sampling model^{33,34} is used to close the last two terms on the RHS of Equ. (26). Although the last term on the LHS of Equ. (26) is closed, it is also treated in this manner. It has been shown that this model produces a qualitatively reasonable evolution and the correct asymptotically gaussian relaxation for large times.

3.2.3.3 Chemical Reaction

The change of scalar and scalar-gradient in a time step, δt , due to chemical reaction are exactly given by,

$$\Delta_{\delta t} C_{\alpha}^{(n)}(t) = (\delta t) S_{\alpha} [C^{(n)}(t)] \quad (30)$$

$$\Delta_{\delta t} C_{\alpha, i}^{(n)}(t) = (\delta t) \frac{\partial S_{\alpha} [C^{(n)}(t)]}{\partial C_{\beta}^{(n)}} C_{\beta, i}^{(n)}(t) \quad (31)$$

3.2.4 Numerical Results

The mixing and chemical reaction of an acid and an alkali diluted in water in a field of grid generated turbulence have been investigated by Bennani et al⁵. The acid is injected at the grid and the base is convected by the main flow. These experiment has been predicted using the previously explained pdf methodology. The evolution of concentration means and variances is presented in Figure 7 showing a good agreement with the experimental data. The segregation coefficient in Figure 8 also shows a reasonable agreement with the measured constant experimental value of -0.7. The skewness and flatness factors for the concentration and concentration-gradients are presented in Figures 9 and

10; no experimental data are available. The large values of the flatness factors of the concentrations are a clear indication of the spatial segregation of the reactants, while those of the concentration-gradients might also reflect the internal intermittency of the scalar fields. The evolution of the characteristic turbulent frequencies for both reactants is plotted in Figure 11. Due probably to the difference in the initial condition of the acid and the base the frequencies for both reactants evolve in a different way. This is not taken into account in present combustion models.

4. CONCLUDING REMARKS

An overview of turbulent flow modelling activities in Spain have been presented. Two selected examples have been described in detail: turbulent two-phase flows and turbulent reactive flows. While there seems to be a consensus that a moderately significant progress in the last two decades has been achieved in the field of turbulence models using moment equations, there are not reasons to be so optimistic in the two cases described. The following comments seem then pertinent:

4.1 Turbulent Two-Phase Flows

- No agreement has been reached on the local instantaneous basic equations to be used as a starting point, in particular for the dispersed phase. While some investigators treat the dispersed phase as a continuum, defining a particle cloud pressure and viscosity, others prefer to describe the particle cloud dynamics in terms of moments of a Boltzmann type equation.

- The type of average employed to generate moment equations also leads to significantly different transport equation structure.

- Classical $k - \epsilon$ or Reynolds stress models can be used for the fluid phase. However, the unknown terms in the dispersed phase equations and the phase interaction terms deserve special and careful consideration.

- LES or vortex dynamics techniques can help to gain significant knowledge on peculiar phenomena influencing the particle dynamics.

- DNS of some simplified two-phase flow systems can provide rational basis to the asymptotic behavior of the proposed models.

- Reliable experimental data for simple flow configurations to validate model predictions are scarce.

4.2 Turbulent Reactive Flows

- The non-linearities in the chemical source terms introduce important difficulties in moment formulations. Even for some idealized situations (diffusion controlled limit, premixed systems, etc.) existing models are not as accurate as desirable.

- The pdf formalism overcomes the closure problem associated with the chemical source terms. The closure of the molecular diffusion effects has proved however to be a very difficult one.

- The conceptually different framework of the pdf methodology makes it appear somehow unnecessarily cumbersome to some investigators.

- Moreover the inclusion of the velocity and/or dissipation rates or gradients into the formulation leads to a pdf with a large number of independent variables. Non-standard Monte Carlo simulations must be used to obtain numerical solutions.

- Since reaction takes place at the molecular level, LES or vortex dynamics techniques are also confronted with closure problems identical to those present in moment formulations.

- DNS of simplified chemical kinetics in simple flows can be of some help as a guidance for the asymptotic behavior of models.

- Most available experimental data pertain to the field of turbulent combustion. Experiments on irreversible bimolecular chemical reactions in incompressible grid-generated turbulence where the interactions among turbulent straining, molecular mixing and chemical reaction can best be evaluated are badly needed in order to validate model predictions.

In summary, in the foreseeable future significant effort will be required to model turbulent two-phase and reactive flows. A judicious combination of physical insight, theoretical developments, analysis via LES and/or DNS of simplified flows and examination of reliable experimental data is the best support for successful modelling endeavors.

ACKNOWLEDGEMENTS

The authors wish to express their gratitude to Professors Fernández-Cara and Chacón and Drs. Abbas and Hernández for supplying excellent summaries of their modelling activities. Thanks are due to Ms. P. Ezquerro for patiently and carefully typing the manuscript.

REFERENCES

1. Abbas, A.S., CASA Technical Report, 1989
2. Aliod, R. and Dopazo, C., "Modelling and Numerical Computation of Turbulent Axisymmetric Jets Containing Dilute Suspensions of Solid Particles", Sixth Symposium on Turbulent Shear Flows, Toulouse (France), September 1987.
3. Aliod, R. "Formulation and Numerical Treatment of Mathematical Models for Turbulent Two-Phase Flows" (in Spanish), PhD Dissertation, University of Zaragoza, February 1990.
4. Baldwin, B.S. and Lomax, H., "Thin Approximation and Algebraic Model for Separated Turbulent Flows", AIAA 16th Aerospace Sciences Meeting, Huntsville, Alabama, January 1978, pp. 78-257.

5. Bennani, A., Gence, J.M. and Mathieu, J., "The Influence of a Grid-Generated Turbulence on the Development of Chemical Reactions", *AIChe J.* **31**, 7, 1985, pp. 1157-1166.
6. Buckley and Le Nir, *Math. Programm.* **27**, 2, 1984, pp. 155-175.
7. Chacón, T., PhD Dissertation, Univ. P. and M. Curie, Paris VI, 1985.
8. Delhaye, M. and Achard, J.L. "On the Averaging Operators Introduced in Two-Phase Flows Modeling", *OECD/NEA Specialists Meeting on Transient Two-Phase Flow*, Toronto (Canada), 1976.
9. Dopazo, C. and O'Brien, E.E., "An Approach to the Autoignition of a Turbulent Mixture", *Acta Astronautica* **1**, 1974, pp. 1239-1266.
10. Dopazo, C., "Non-Isothermal Turbulent Reactive Flows: Stochastic Approaches", PhD Dissertation, State University of New York, Stony Brook, June 1973.
11. Dopazo, C., "On Conditioned Averages for Intermittent Turbulent Flows", *J. Fluid Mechanics* **81**, 3, 1977, pp. 438-443.
12. Elgobashi, S.E., Abou-Arab, T., Rizk, M. and Mostafa, A., "A Two-Equation Turbulence Model for Two-Phase Jets", *Proc. 4th Symp. Turbul. Shear Flows*, Karlsruhe (W. Germany), September 1983, pp. 12.9-12.14.
13. Eswaran, V. and Pope, S.B., "Direct Numerical Simulations of the Turbulent Mixing of a Passive Scalar", *Phys. Fluids* **31**, 1988, p. 506.
14. Herczynski, R. and Pienkowska, J., "Toward a Statistical Theory of Suspensions", *Ann. Rev. Fluid Mech.* **12**, 1980, pp. 237-269.
15. Hernandez, J.A., "Analytical and Numerical Study of Instabilities in Two-Phase Flows", (in Spanish), PhD Dissertation, Universidad Politécnica de Madrid, 1990.
16. Kida, S. and Murakami, Y., "Statistics of Velocity Gradients in Turbulence at Moderate Reynolds Numbers", *Fluid Dynamics Res.*, **4**, 1989, pp. 347-370.
17. Kubo, R., "Stochastic Liouville Equations", *J. Mathematical Physics* **4**, 2, 1963, pp. 174-183.
18. Launder, B.E., Reece, G.J. and Rodi, W.J., "Progress in the Development of a Reynolds Stress Turbulent Closure", *J. Fluid Mechanics* **68**, 1975, pp. 537-566.
19. Lumley, J.L., "Computational Modeling of Turbulent Flows", *Adv. Appl. Mech.*, **18**, 1978, pp. 123-176.
20. MacLaughlin, D., Papanicolau, G and Pironneau, O., *SIAM J. Appl. Math.* **45**, 1985, pp. 780-797.
21. Mansour, N.N., Moin, P. Reynolds, W.C. and Ferziger, J.H., "Improved Methods for large Eddy Simulations of Turbulence", in *Turbulent Shear Flows I*, F. Durst et al, eds., Springer Verlag, Berlin, 1979, pp. 386-401.
22. Marble, F.E., "Dynamics of a Gas Containing Small Solid Particles", *Proceedings 5th AGARD Combustion and Propulsion Symp.*, Pergamon, New York 1963.
23. Meyers, R.E. and O'Brien, E.E., "The Joint PDF of a Scalar and its Gradient at a Point in a Turbulent Fluid", *Combust. Sci. Technol.* **26**, 1981, pp. 123-134.
24. Modares, D., Than, H. and Elgobashi, S.E., "Two Component LDA Measurements in a Two-Phase Turbulent Jet", *AIAA J.* **22**, 5, 1983, pp. 624-630.
25. Monin, A.S. and Yaglom, A.M., "Statistical Fluid Mechanics", Vol. 2, MIT Press, Cambridge, 1975.
26. Ortégón, F., PhD. Dissertation, Univ. P. and M. Curie, Paris VI, 1989.
27. Pope, S.B., "A Monte Carlo Method for the PDF Equations of Turbulent Reactive Flow", *Combustion Sci. Technology* **25**, 1981, pp. 159-174.
28. Pope, S.B., "Computations of Turbulent Combustion: Progress and Challenges", Plenary Lecture, 23rd. Symp. (Internat.) on Combustion, Orleans (France), July 1990.
29. Pope, S.B., "PDF Methods for Turbulent Reactive Flows", *Prog. Energy Combust. Sci.* **11**, 1985, pp. 119-192.
30. Rodi, W., "The Prediction of Free Turbulent Boundary Layers by Use of a Two-Equation Model of Turbulence, Ph D Dissertation, Imperial College of London, U.K., 1972.
31. Rogallo, R.S. and Moin, P. "Numerical Simulation of Turbulent Flows", *Ann. Rev. Fluid Mech.* **16**, 1984, pp. 99-137.
32. Schügerl, K., "Rheological Behavior of Fluidized Systems", in "Fluidization", Academic Press, London, 1971.
33. Valiño, L. and Dopazo, C., "A Binomial Sampling Model for Scalar Turbulent Mixing", to appear *Phys. Fluids A*, 1990.
34. Valiño, L., "Computation of Homogeneous Turbulent Flows with Chemical Reaction: Monte Carlo Numerical Simulation of Velocities, Concentrations and Concentration-Gradients", (in Spanish), PhD Dissertation, University of Zaragoza, October 1989.

35. Wynanski, I. and Fiedler, H., "Some Measurements in the Self-Preserving Jet", *J. Fluid Mechanics*, **38**, 3, 1969, pp. 577-612.

36. Yeung, P.K. and Pope, S.B., "Lagrangian Statistics from Direct Numerical Simulations of Isotropic Turbulence", *J. Fluid Mechanics* **207**, 1989, pp. 531-586.

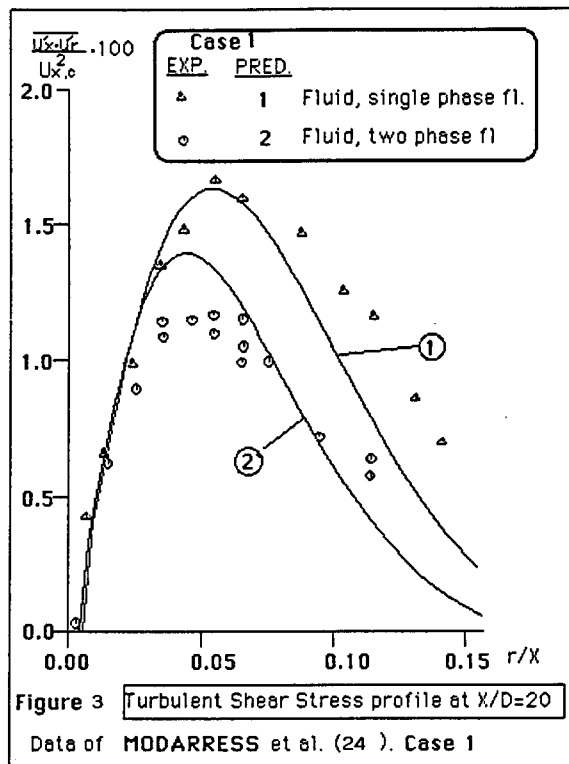
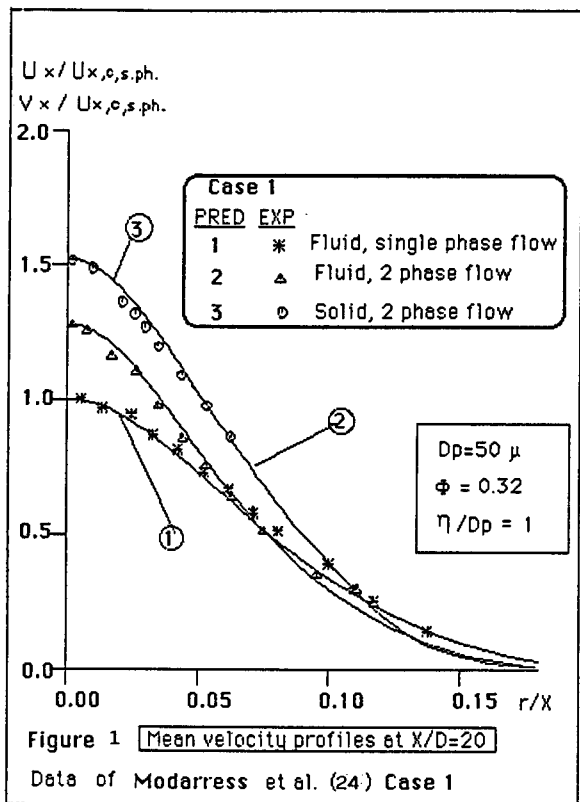


Figure 3 Turbulent Shear Stress profile at $x/D=20$
 Data of MODARRESS et al. (24). Case 1

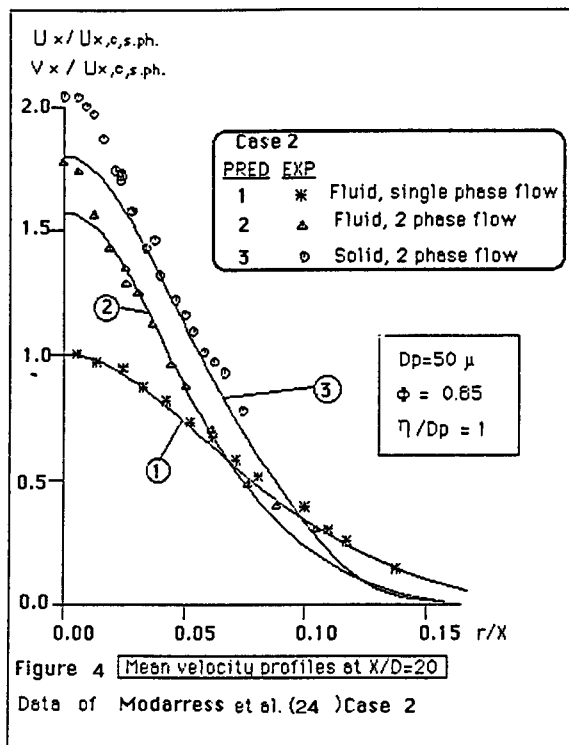
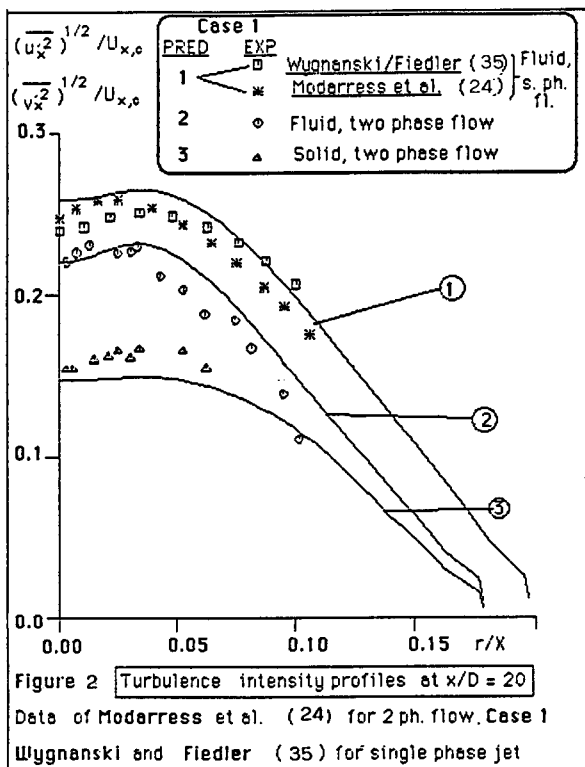
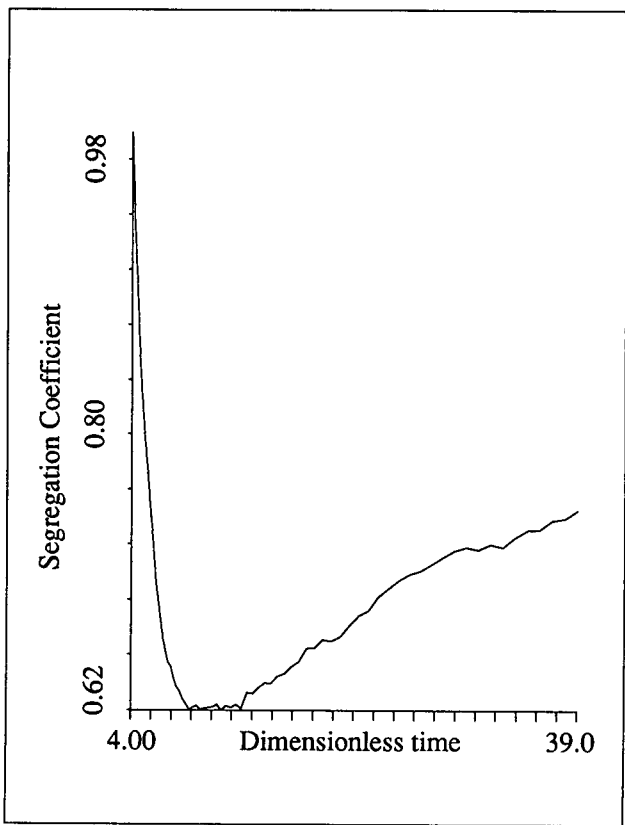
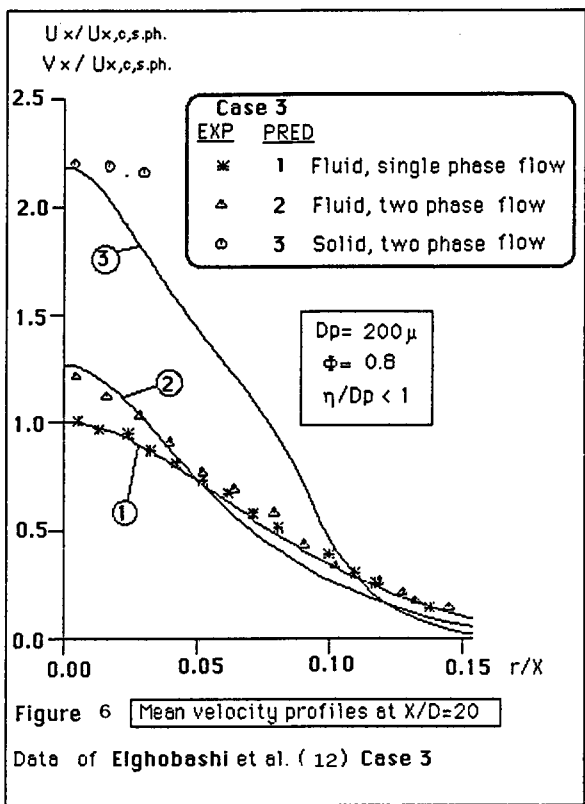
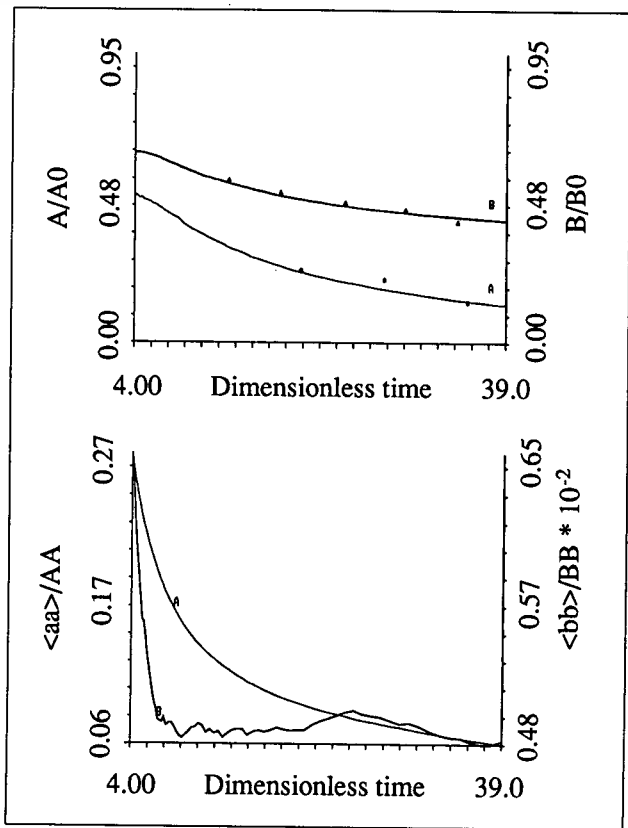
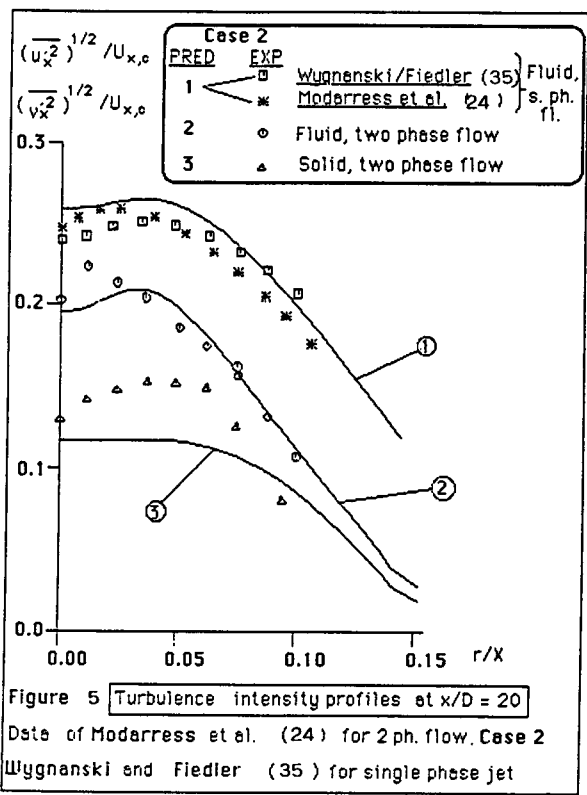


Figure 4 Mean velocity profiles at $x/D=20$
 Data of MODARRESS et al. (24) Case 2

Figure 2 Turbulence intensity profiles at $x/D=20$
 Data of MODARRESS et al. (24) for 2 ph. flow. Case 1
 Wynanski and Fiedler (35) for single phase jet



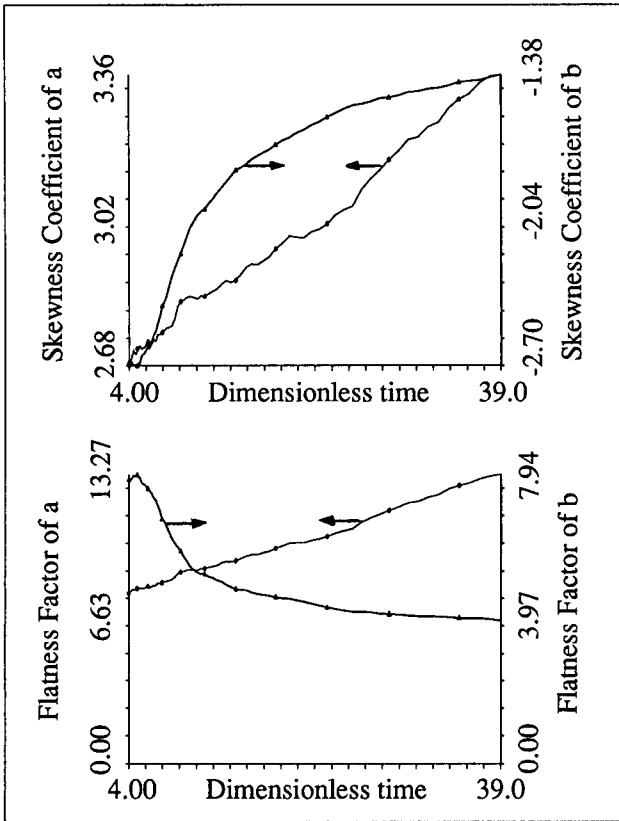


Figure 9. Evolution of the skewness coefficients and flatness factor of two reactive scalars ($Kc = 47.5$ l/mol s).

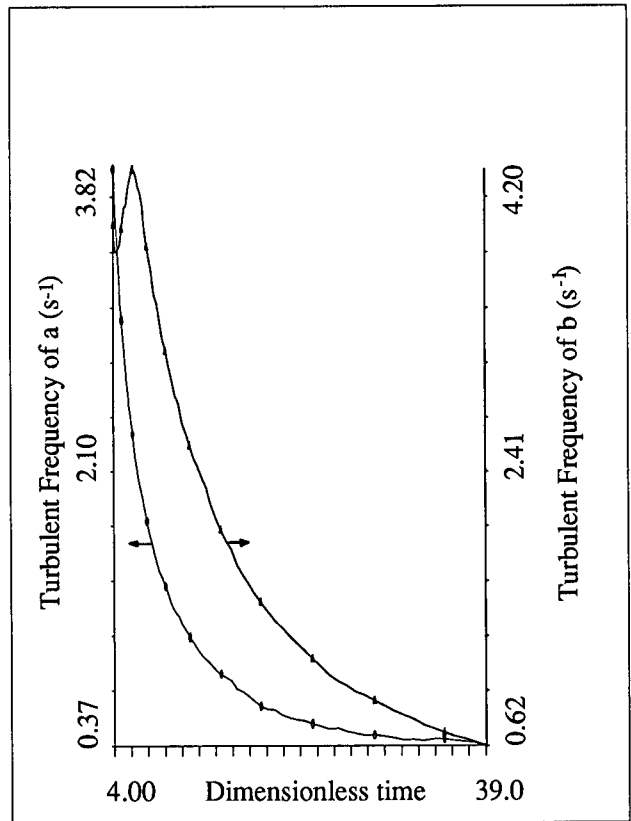


Figure 11. Evolution of the characteristic turbulent frequencies of two reactive scalars ($Kc = 47.5$ l/mol s).

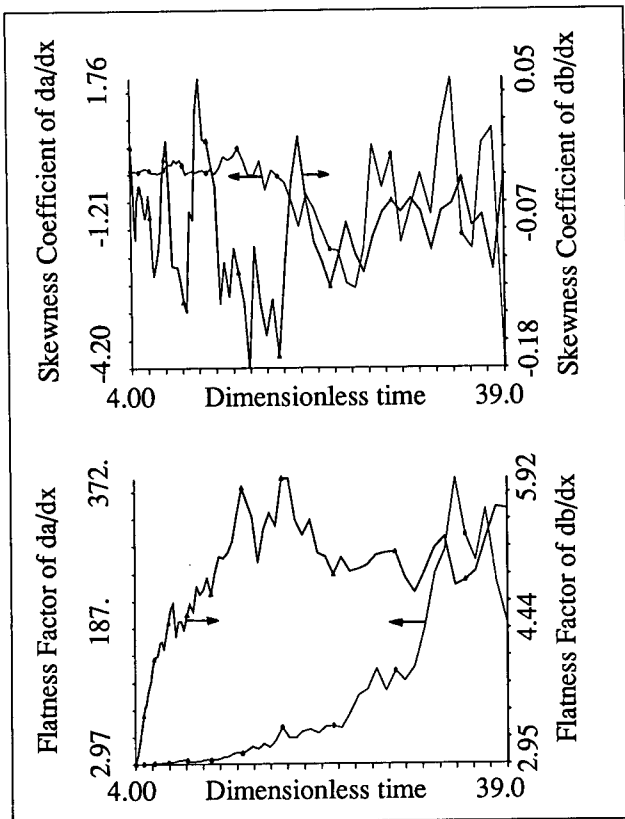


Figure 10. Evolution of the skewness coefficients and flatness factor of two reactive scalar gradients (downstream direction derivative) ($Kc = 47.5$ l/mol s).

COMPUTATIONAL TURBULENCE STUDIES IN TURKEY

Ünver Kaynak
 TUSAS Aerospace Industries (TAI), Inc.
 P.K. 18, 06690, Kavaklıdere
 Ankara, TURKEY

SUMMARY

In this paper, applications of various turbulence models to different flow problems that have recently been carried out in Turkey are presented. Navier-Stokes, boundary layer and vorticity-stream function methods are used to solve two- or three-dimensional steady/unsteady flow problems. Examples are given in low-speed and transonic flow regimes for axisymmetric bodies, airfoils, rigid ripples and jet flows. Different turbulence models are used such as algebraic, half-equation and $k-\epsilon$ models. It has been demonstrated that improved accuracies can be obtained by using the so-called half-equation (nonequilibrium) turbulence model for some three-dimensional configurations. Suitability of different turbulence models is explored for a variety of flow cases such as dynamic stall, jets-in-crossflow and oscillatory boundary layers.

INTRODUCTION

Turbulence modeling and grid generation seem to be the most important issues for computational fluid dynamics today. Although the algorithms have reached to a relative state of maturity in some areas, turbulence modeling remains as a major difficulty for many flow problems. Recognizing this fact, in parallel to the efforts going on in the world, there have been some efforts in Turkey to contribute to our understanding of turbulence. The activities are generally concentrated on the computational side of the turbulence modeling. Two of the major centers for increased activity in turbulence are the TUSAS Aerospace Industries (TAI), Inc. and the Middle East Technical University (METU). In this paper, firstly the following model problems that have been studied at TAI are considered: calculation of a low-speed infinite swept wing flow using the boundary-layer equations, calculation of an axisymmetric bump problem in transonic flow using the Thin-Layer Navier-Stokes (TLNS) equations, calculation of the dynamic stall of a NACA0012 airfoil using the TLNS equations, and numerical simulation of the jets-in-crossflow problem using the TLNS equations. In all these problems, zero- or half-equation models have been used. The main theme of the research conducted at TAI has been the extension of the half-equation turbulence model of the Johnson and King¹ into three-dimensions. This model is particularly attractive because, in the past, much improved accuracies have been obtained for two-dimensional flow problems at a little extra cost. Three-dimensional extension of this model was successfully tested for the first two of the problems enumerated above. Secondly, two more examples are given related with the research done at METU: computation of the unsteady turbulent flow over rough surfaces using a vorticity-stream function formulation with a $k-\epsilon$ model, and extension of the law-of-the-wall for conduits having sharp corners. In the following lines, each of these model problems will be presented:

RESULTS

1) Calculation of a Low-Speed Infinite Swept-Wing Flow

The Berg and Elsenaar² incompressible turbulent boundary layer experiment under infinite swept wing conditions was chosen to compare the performances of the zero-equation algebraic model of the Cebeci and Smith³ and the half-equation turbulence model of the Johnson and King¹ as extended to three-dimensions. The Johnson-King model which includes the non-equilibrium effects in a developing turbulent boundary layer was found to significantly improve the predictive quality of a direct boundary layer method. The improvement was especially visible in the computations with increased three-dimensionality of the mean flow, larger integral parameters, and decreasing eddy-viscosity and shear stress magnitudes in the streamwise direction; all in better agreement with the experiment than simple mixing-length methods. The Johnson-King model accounts for the convection and diffusion effects by solving an ordinary differential equation (o.d.e.) governing the streamwise development of the maximum shear stress derived from the turbulent kinetic energy (t.k.e.) equation. The o.d.e. was originally derived in two-dimensions. For three-dimensions, this o.d.e. was simply interpreted as an equation governing the development of the maximum shear stress on a local streamline. This offers a lot of simplicity and economy in three dimensions.

In the Berg-Elsenaar² experiment, an adverse pressure gradient is applied on a 35° swept flat plate. In the leading edge, the turbulent boundary layer is very nearly two dimensional. Downstream it becomes three-dimensional due to the sweep angle and the adverse pressure gradient (Fig. 1). The difference between the wall flow angle (ϕ_w), and the flow angle at the boundary-layer edge (α_e) that is (β_w) is seen to increase fast in the downstream direction. Near measuring station 9 the wall flow angle exceeds $\phi_w = 55$, which means that the flow is parallel to the plate leading edge showing separation.

Calculations were done on a grid with dimensions $50 \times 10 \times 50$ in streamwise, spanwise and normal directions respectively, using the Van Dalsem and Steger⁴ time-relaxation algorithm in the direct mode. On the IBM 3090 Model 150E scalar computer installed at TAI, the CPU time for the Johnson-King model was only 20% higher than the Cebeci-Smith model and about the same number of iterations were required for convergence. Figure 2 shows the angle β_w between the wall shear stress vector and the external streamline of the boundary layer. The baseline Cebeci-Smith model departs from the experiment after the fifth station. The integral method of Cousteix⁵ doesn't fare better as it departs after the third station. The NLR method⁶ lies very close to the Cebeci-Smith model. On the other hand, the present method goes as far

as the seventh station, than nearing the separation fails to go any further.

In fact, it is known that an indirect procedure is needed to handle the separation, but in this instance the success of the turbulence model is measured by how far downstream it can go before diverging from the experiment. As for the integral parameters, Fig. 3 shows the streamwise displacement thickness for the various models compared with the experiment. The nonequilibrium model yields thicker displacement thicknesses than the baseline³ (and other) models. A turbulent eddy viscosity profile (at Station 7) is presented in Fig. 4 which shows that the nonequilibrium model cuts down the outer portion of the eddy viscosity significantly in a better agreement with the experiment. Finally, Figs. 5 and 6 show the streamwise and crossflow velocity profiles inside the boundary layer. Again, the nonequilibrium model gives closer results to the experiment than the baseline model. For further details, the reader is referred to Ref. 7 on this subject.

2) Turbulence Modeling Studies for Transonic Separated Flows

The aerodynamic characteristics of aircraft in the transonic regime are very sensitive to the viscous effects, and the selection of the turbulence model is no less important than the selection of the numerical algorithm. It is well known that turbulence is slow to respond to changes in the mean strain field. The so-called equilibrium models that are widely used in Navier-Stokes computations fail to model this aspect of the turbulence and exaggerate the turbulent boundary layer's ability to produce the turbulent Reynolds shear stresses in regions of adverse pressure gradient. As a consequence, too little momentum loss within the boundary layer is predicted in the region of the shock wave and along the aft part of the aerodynamic body. This in turn causes the equilibrium models to predict the shock waves too far aft of the experiment.

Recognizing the shortcomings of the equilibrium turbulence models, a collaborative research project between the TAI and NASA/Ames Research Center was started. The purpose of the project was to explore the possibilities of the extension of the Johnson-King model into three-dimensions for use in the Navier-Stokes flow solvers. Under this project, a computer program was written for the Navier-Stokes flow solvers in general curvilinear coordinates using the streamwise integration of the governing o.d.e. for nonequilibrium effects. The streamwise integration idea was provoked by the fact that the t.k.e. equation upon which the present o.d.e. was derived describes the time rate of change of the turbulent kinetic energy *following a fluid particle*.

In this study, the NASA-Ames ARC3D⁶ finite-difference Thin-Layer Navier-Stokes flow solver was used. The preliminary calculations using the newly written turbulence model were done on the axisymmetric bump flow experiment of Bachalo and Johnson.⁹ In this experiment, a thin walled cylinder (15.2 outer diam.) with an axisymmetric circular bump attached 61 cm. from the cylinder leading edge. The bump has a thickness of 1.9 cm. and a chord length of 20.3 cm. The model was specifically designed to simulate

the type of viscous-inviscid interactions that can develop on airfoil sections at transonic conditions, and the model was tested in Ames 2-by-2 foot transonic wind tunnel and 6-by-6 foot supersonic wind tunnel. A finite-difference grid was algebraically generated to simulate the arc bump (Fig. 7). It has dimensions 61 x 5 x 41 in the streamwise, circumferential and normal directions respectively. Since the experiment is axisymmetric, only 5 planes were used in the circumferential direction in a 90 deg. pie. The preliminary runs were done at TAI's IBM 3090 150E computer using the ARC3D⁶ flow solver. The computations were also repeated at the NASA-Ames Research Center using the Cray Y-MP and Cray-2 supercomputers. The fine grid size was 136 x 5 x 45. The Mach number in the experiment was 0.875 and the Reynolds number was 13.6 x 10⁶/m.

Results of the axial bump simulation are shown in Figs. 8-11. In Fig. 8, coefficients of pressure for the equilibrium models of Cebeci and Smith³ (C-S) and Baldwin and Lomax¹⁰ (B-L) and the nonequilibrium model of Johnson and King¹ (J-K) are compared against the experimental data. As seen, the equilibrium models predict shocks too aft of the experimental one in result of the rapid rise in the shear stress and lesser boundary layer growth. The pressure plateau that forms because of the shock induced separation is just nonexistent. On the other hand, using the J-K model correctly predicts the exact shock location as well as the pressure plateau after the shock. Figure 9 compares the displacement thicknesses around the trailing edge and again demonstrates the ability of the J-K model to produce a more accurate viscous layer growth. Figure 10 shows the streamwise variation of the maximum shear stress for the experiment and computations. The C-S model predicts a rapid rise in the shear stress typical of that model, whereas the J-K model predicts a smoother rise. Also, the C-S model displays a faster decay rate for the shear stress than for the J-K model. In Fig. 11, the boundary layer mean velocity profiles are given at the trailing edge of the bump. The J-K model is clearly superior over the equilibrium models inside the boundary layer. The axial bump experiment was a model problem to check the performance of the new turbulence model. Work is underway to test the new model for a truly three-dimensional problem such as a finite wing.

3) Calculation of the Dynamic Stall

In parallel to the efforts going on in the steady three-dimensional low-speed or transonics area as described above, unsteady motion of airfoils including dynamic stall is also investigated. The purpose of this research is to assess the importance of the turbulence model for the dynamic stall phenomenon, and explore the suitability of the J-K model for this type of flow. Majority of the numerical simulations encountered in the literature seems to be conducted for laminar flows.¹¹ For turbulent flows, a computational study was recently made by Rumsey Anderson¹² for unsteady airfoil motion. In their study, significant differences between the B-L model and J-K model were found which showed a need for further studies on this line. The light and deep dynamic stall regimes are considered in the present research. Especially, the light stall is probably the one that most war-

rants concentrated research efforts.¹³ Thin-Layer Navier-Stokes (TLNS) equations are solved using the implicit approximate factorization algorithm of the LU-ADI type due to Obayashi and Kuwahara.¹⁴ An unsteady version was developed by including the time metrics in the program and using the unsteady normal momentum equation for the surface pressure computation while imposing the boundary conditions. A steady grid of a NACA0012 airfoil is harmonically oscillated around the quarter chord with an angular velocity determined from the nondimensional pitch rate.

Firstly, a light-stall case was run without using any turbulence model. Fig. 12 shows the $C_L - \alpha$ curve of the Case-7 of the Ref. 13. The prescribed motion is $\alpha(t) = 10^\circ + 5^\circ \sin(2M_\infty kt)$, where $k = \omega c/2U_\infty$ is the reduced frequency and taken as 0.1. The flow conditions are $M_\infty = 0.3$ and $Re_\infty = 4 \times 10^6$. This laminar result is far off from the experiment as might be expected. In fact such a highly oscillatory lift hysteresis curves were also produced in Ref. 11 using a block-pentadiagonal scheme. On the contrary, Fig. 13 shows the turbulent flow computation using the Baldwin-Lomax model. In this computation, dynamic stall break could not be obtained with the nominal conditions. The reason for this is not clear at the moment. One reason may be the wind tunnel wall effects. Free air grid in the present simulation may not be capable of producing the necessary conditions for the stall break. Transition or the turbulence model may be other reasons. However, when a deep stall case was tried, the airfoil stalled as shown in Fig. 14. The prescribed motion was $\alpha(t) = 15^\circ + 5^\circ \sin(2M_\infty kt)$. Work is in progress in this area, and beside trying to answer the above questions, the suitability and performance of the J-K model for dynamic stall will also be explored.

4) Numerical Simulation of Jets-in-Crossflow

Accurate prediction of jet flows is very important in designing V/STOL aircraft in which jet flows from vectored nozzles provide the lift for take-off as well as the thrust for manoeuvring during the flight or hover. Especially important are the events when the aircraft is close to the ground in which the ground effect takes place. Turbulence modeling plays a very important role in numerical simulation of jets. Without an adequate turbulence model the mixing in the separation and circulation behind the jet in crossflow is underestimated. This causes a larger recirculation region and the calculated surface pressures are lower than the actual values, thus the lift loss below the wing of a V/STOL aircraft may be overestimated. In order to improve our understanding of jets in crossflow and develop a computational tool for such predictions, a cooperative research project was started between the TAI and the General Dynamics Ft. Worth Division. Under the agreement, some jets-in-crossflow problems such as a slot jet or circular jet ejecting from a flat plate were numerically studied. Data are available for these configurations by Kavsaoglu and Schetz.¹⁵ The NASA-Ames ARC3D⁸ program was used as the flow solver.

In the simulations, the Baldwin-Lomax¹⁰ model was used in regions close to the solid boundary and Prandtl mixing length model¹⁶ was used for the jets. No turbulence model was used in the

large recirculation region behind the jets. The experimental conditions were the free stream Mach number $M_\infty = 0.05$, jet exit Mach number $M_j = 0.2$, and the Reynolds number $Re_\infty = 25700$ (based on the jet diameter and freestream velocity). In the computations, twice the velocity values of the experiment ($M_\infty = 0.1$, $M_j = 0.4$) were used keeping the jet to crossflow velocity ratio the same ($R = M_\infty/M_j = 4$). This was done for running the compressible code more efficiently. Results of the computations are presented in Figs. 15 and 16. Figure 15 shows the velocity vectors of the experiment and computation for the circular jet. The grid ($59 \times 21 \times 45$) was rather coarse in the computations due to computer limitations. Only 7 points were used for half of the jet orifice. Figure 16 shows the top view of the jet comparing the surface pressures of the experiment and computation side by side. The agreement is quite encouraging despite the complexity of the flow and the coarse grid used. It is quite possible to use algebraic models for such simple configurations, but for more complex or realistic configurations it should become exceedingly difficult to determine the velocity and length scales. In that case, using a local model such as $k - \epsilon$ model appears to be inevitable.

5) Calculation of Oscillatory Boundary Layers Over Rigid Ripples Using a $k - \epsilon$ Model

For a correct prediction of the time-dependent turbulent structure in unsteady flows, the partial differential equations (p.d.e.) of the motion should be solved from surface to the outside of the boundary layer. In this case, the p.d.e.'s need to be modified for the viscous stresses and wall proximity where extra dissipation terms appear. Also another modification is necessary to account for the surface roughness effect. Such models are usually called low-Reynolds number models since the viscous effects become more significant when the Reynolds number is not high enough. A vorticity-stream function formulation coupled with the $k - \epsilon$ equations was used to solve the unsteady turbulent flow field over rigid ripples with roughened surfaces.¹⁷ Comparison of measurement and calculation for the velocity vectors is shown in Fig. 17. The velocity fields agree well as far as the temporal development of flow field is concerned. However the measured vortex structure is more elongated in the streamwise direction whereas the computed one is more round. It seems that important sources of discrepancy between the measurement and the computation are the assumption of isotropic turbulence and the effect of unsteadiness.

6) Extention of the the Law-of-the-Wall to Conduits Having Sharp Corners

A study¹⁸ has been done by Prof. Çiray and his students at Aero. Eng. Dept., METU, for enlarging the range of applicability of the law-of-the-wall to conduits having sharp corners. It was shown that the mixing length formulation of turbulent shear stress and the ensuing assumptions leading to logarithmic portion of the law-of-the-wall for two-dimensional attached boundary layers may be used to obtain velocity distributions in the conduits. These conduits have rectangular or triangular cross sections in which flow can be confined or unconfined. It was found that the developed formulas are capable of producing wall shear stresses close to 5% of the measured values, except at deep corners where deviations are less than 19%.

CONCLUSION

Implementation of the Johnson-King model in three-dimensions improves the predictive accuracies of the boundary-layer and Navier-Stokes solutions for low-speed and transonic flows respectively. Work now is in progress to implement this model for transonic separated wing flows using the TLNS equations. Suitability of the Johnson-King model for dynamic stall simulation is also being explored. Algebraic models have been found to perform reasonably well for simple jet-in-crossflow problems, but more sophisticated situations or realistic configurations seem to call for a higher order model such as the $k-\epsilon$ model.

REFERENCES

- [1] Johnson, D.A. and King, L. S., "A New Turbulence Closure Model for Boundary Layer Flows with Strong Adverse Pressure Gradients and Separation," AIAA 84-0175, Jan. 1984.
- [2] Van der Berg, B. and Elsenaar, A., "Measurements in a Three Dimensional Incompressible Turbulent Boundary Layer in an Adverse Pressure Gradient Under Infinite Swept Wing Conditions," NLR-TR-72092U, Netherlands, 1972.
- [3] Cebeci, T. and Smith, A.M.O., *Analysis of Turbulent Boundary Layers*, Academic Press, New York, 1974.
- [4] Van Dalsem, W.R. and Steger, J.L., "Efficient Simulation of Separated Three-Dimensional Viscous Flows Using the Boundary Layer Equations," *AIAA Journal*, Vol. 25, March 1987, pp.395-400.
- [5] Cousteix, J., "Three-Dimensional Boundary Layers. Introduction to Calculation Methods," in AGARD Report No. 741: Calculation of Three-Dimensional Boundary Layers Including Separation (1987).
- [6] Wesseling, P. and Lindhout, J.P.F., "A Calculation Method for Three-Dimensional Turbulent Boundary Layers," AGARD Conf. Proc. No. 93 (1971).
- [7] Kavsaoğlu, M. Ş., Kaynak, Ü. and Van Dalsem, W. R., "Three-Dimensional Application of the Johnson-King Turbulence Model For a Boundary-Layer Direct Method," Proceedings of the International Symposium on Computational Fluid Dynamics (ISCFD), P29-34, Nagoya, Japan, Aug. 28-31, 1989.
- [8] Pulliam, T.H. and Steger, J.L., "Implicit Finite Difference Simulations of Three-Dimensional Compressible Flow," *AIAA Journal*, Vol. 18, 1980, pp. 159-167.
- [9] Bachalo, W.D. and Johnson, D.A., "An Investigation of Transonic Turbulent Boundary Layer Separation Generated on an Axisymmetric Flow Model," AIAA 79-1479, 1979.
- [10] Baldwin, B.S. and Lomax, H., "Thin-Layer Approximation and Algebraic Model for Separated Turbulent Flows," AIAA 78-257, Jan. 1978.
- [11] Shida, Y., Takami, H., Kuwahara, K. and Ono, K., "Computation of Dynamic Stall of NACA0012 Airfoil by Block Pentadiagonal Matrix Scheme," AIAA Paper 86-0116, 1986.
- [12] Rumsey, C. L. and Anderson, W. K., "Parametric Study of Grid Size, Time Step, and Turbulence Modeling on Navier-Stokes Computations over Airfoils," AGARD Symposium on Validation of Computational Fluid Dynamics, May 2-5, 1988, Lisbon, Portugal.
- [13] McCroskey, W. J. and Pucci, S. L., "Viscous-Inviscid Interaction on Oscillating Airfoils in Subsonic Flow," *AIAA Journal*, Vol. 20, No.2, Feb. 1982, pp. 167-174.
- [14] Obayashi, S. and Kuwahara, K., "LU Factorization of an Implicit Scheme for the Compressible Navier-Stokes Equations," AIAA Paper 84-1670, June 1984.
- [15] Kavsaoğlu, M. Ş. and Schetz, J. A., "Effects of Swirl and High Turbulence on a Jet in Crossflow," *Journal of Aircraft*, Vol. 26, No.6, June 1989.
- [16] Schetz, J. A., *Injection and Mixing in Turbulent Flow*, Progress in Astronautics and Aeronautics, Vol. 68, AIAA, New York, New York.
- [17] Aydın, İ and Shuto, N., "An Application of the $k-\epsilon$ Model to Oscillatory Boundary Layers," *Coastal Eng. in Japan*, Vol. 30, No.2, 1988.
- [18] Sari, A., "Determination of Wall Shear Stress in a Rectangular Open Channel," M.Sc. Thesis, METU, Ankara, TURKEY, 1987.

FIGURES

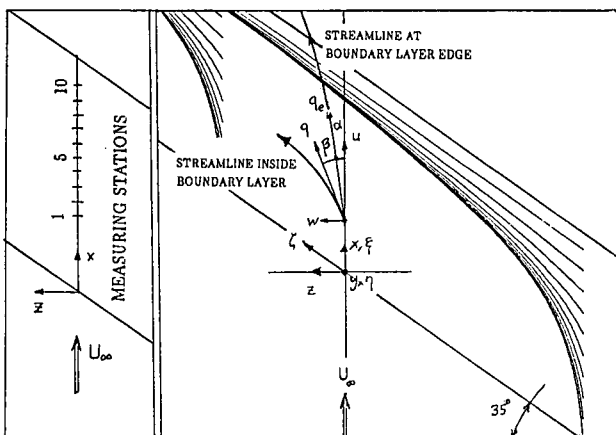


Fig. 1) The wall streamlines and related angles for the infinite swept wing experiment of Berg and Elsenaar.²

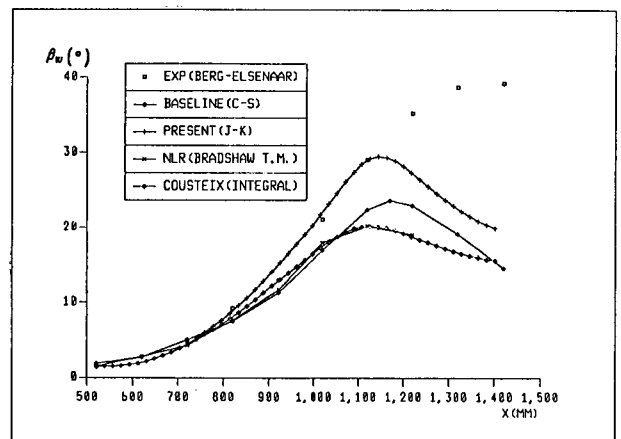


Fig. 2) The wall streamline angle relative to the boundary-layer edge streamline.

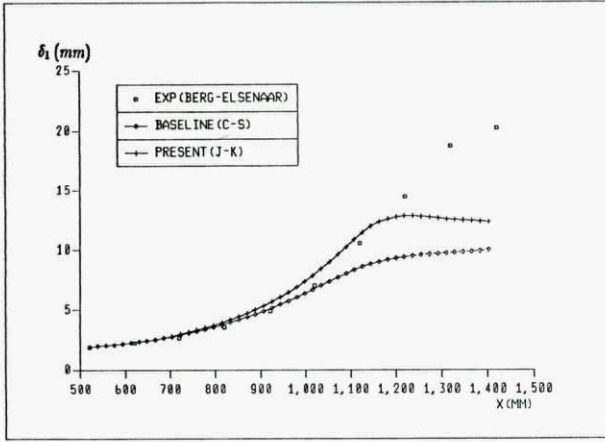


Fig. 3) The streamwise displacement parameter in the streamline co-ordinate system.

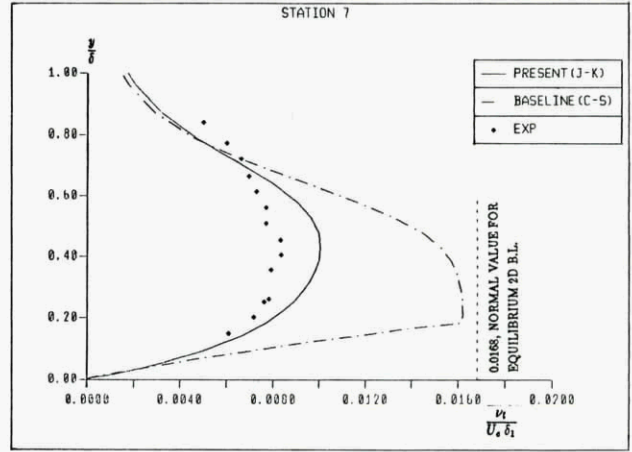


Fig. 4) Comparison of the eddy-viscosity profiles at Station 7.

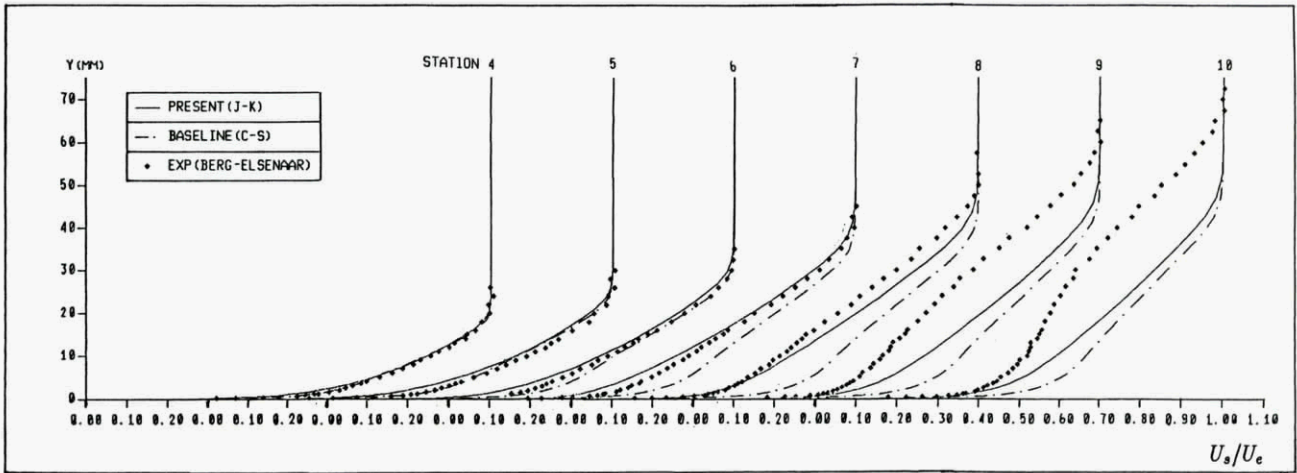


Fig. 5) The streamwise velocity profiles of the computation and measurement.

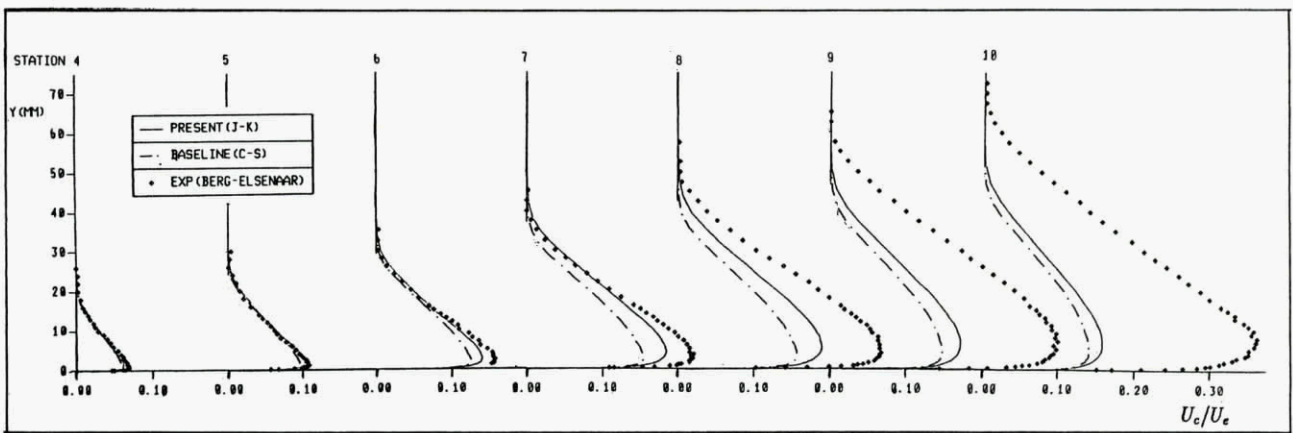


Fig. 6) The crossflow velocity profiles of the computation and measurement.

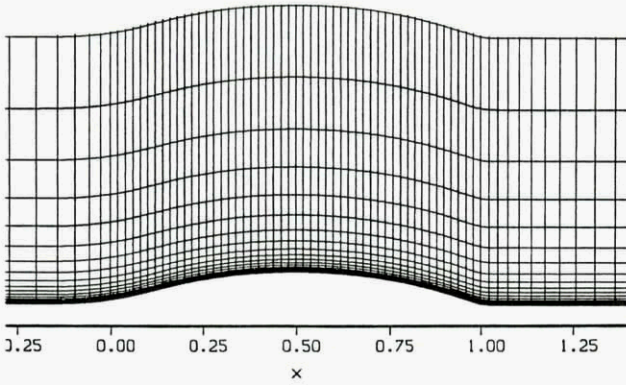
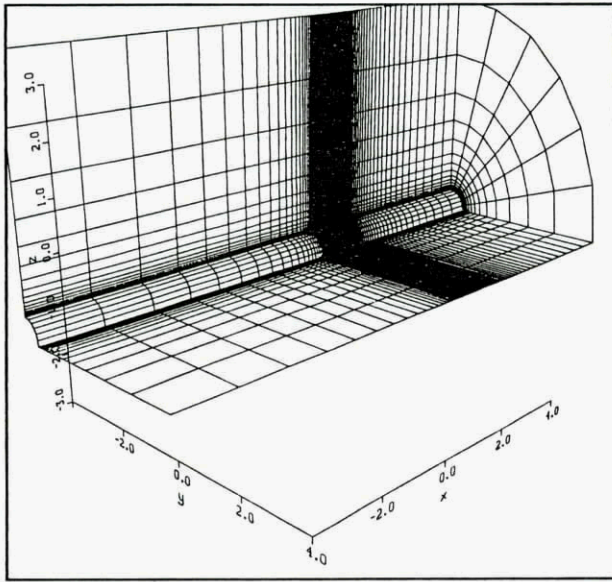


Fig. 7) The finite-difference grid (61 x 7 x 41) for simulating the Bachalo and Johnson⁹ axisymmetric bump experiment.

COEFFICIENT OF PRESSURE
 AXIAL BUMP, $M=0.875$

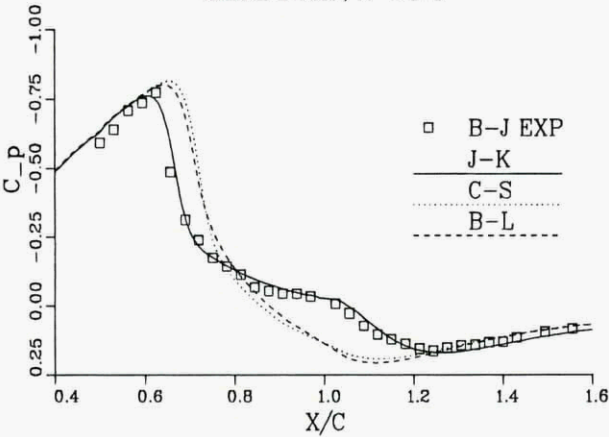


Fig. 8) The coefficient of pressure: $M_\infty = 0.875$, $Re_\infty = 13.6 \times 10^6/m$ (B-L, Baldwin-Lomax, C-S, Cebeci-Smith, J-K Johnson-King models).

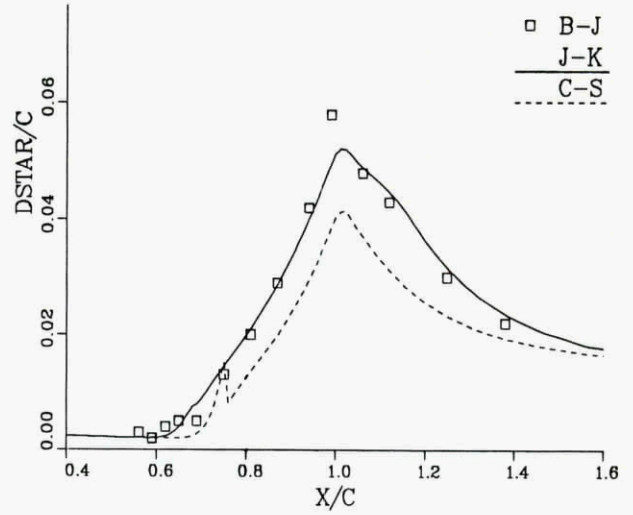


Fig. 9) The displacement thicknesses.

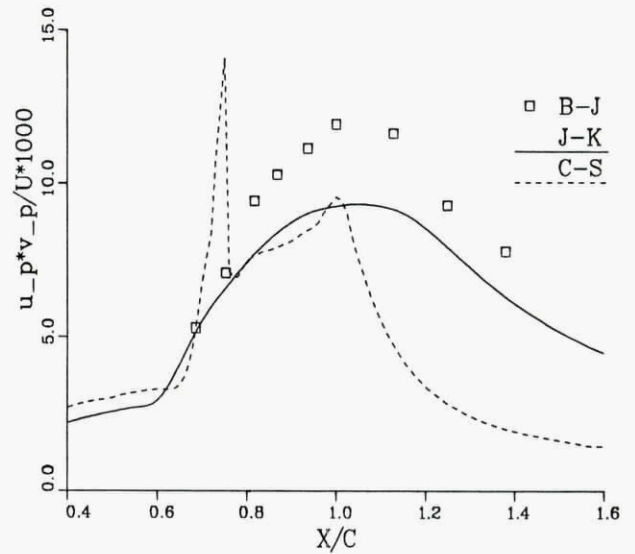


Fig. 10) The streamwise variation of the maximum shear stress.

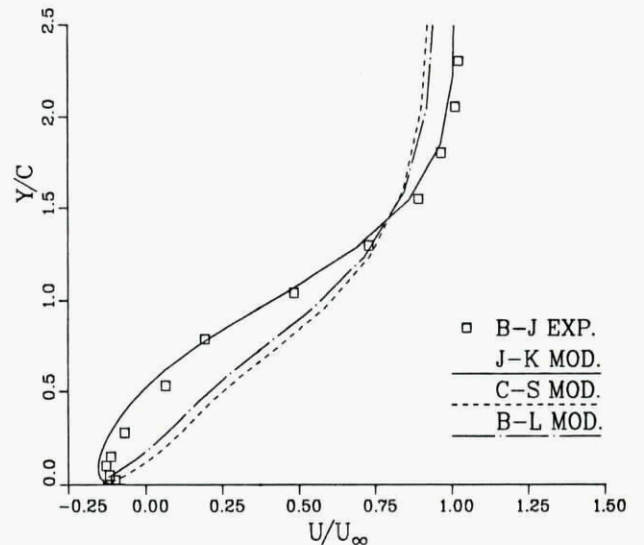


Fig. 11) The boundary-layer mean velocity profiles at the trailing-edge $x/c = 1.0$.

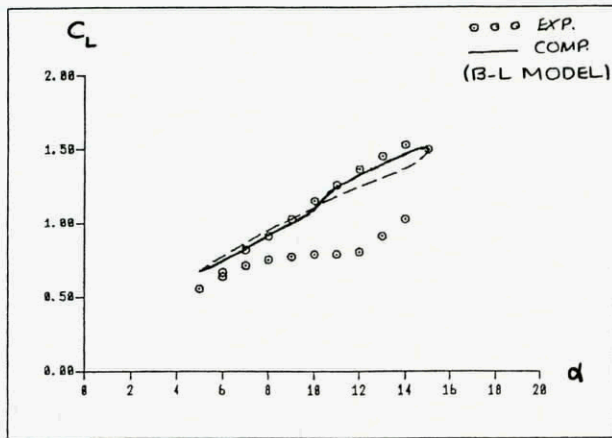
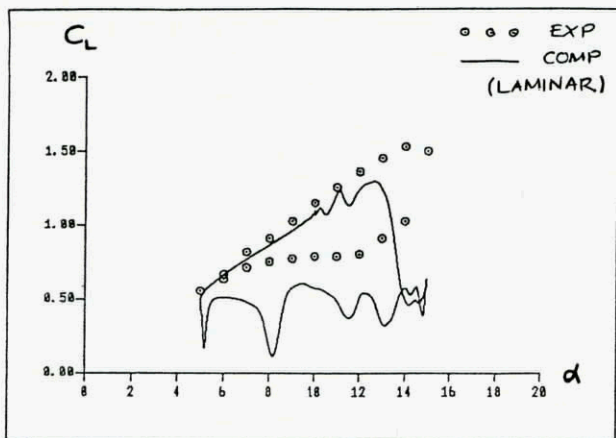


Fig. 12) Coefficient of lift hysteresis for the laminar flow over the NACA0012 airfoil, $\alpha(t) = 10^\circ + 5^\circ \sin(2M_\infty kt)$ ($k = 0.1$, $M_\infty = 0.3$, $Re_\infty = 4 \times 10^6$).

Fig. 13) Coefficient of lift hysteresis using the Baldwin-Lomax turbulence model, light stall: $\alpha(t) = 10^\circ + 5^\circ \sin(2M_\infty kt)$ ($k = 0.1$, $M_\infty = 0.3$, $Re_\infty = 4 \times 10^6$).

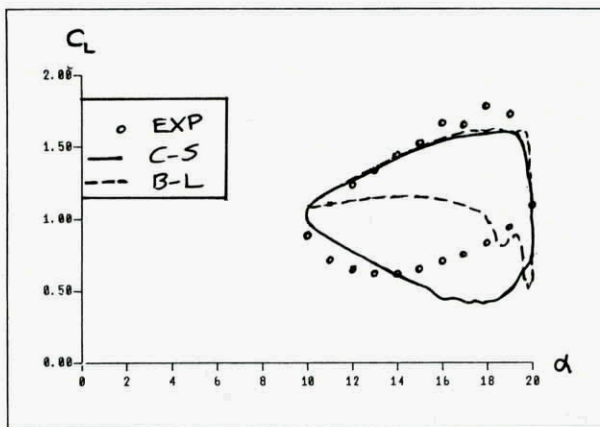


Fig. 14) Coefficient of lift hysteresis using the Baldwin-Lomax and Cebeci-Smith turbulence models, deep stall: $\alpha(t) = 15^\circ + 5^\circ \sin(2M_\infty kt)$ ($k = 0.15$, $M_\infty = 0.3$, $Re_\infty = 4 \times 10^6$).

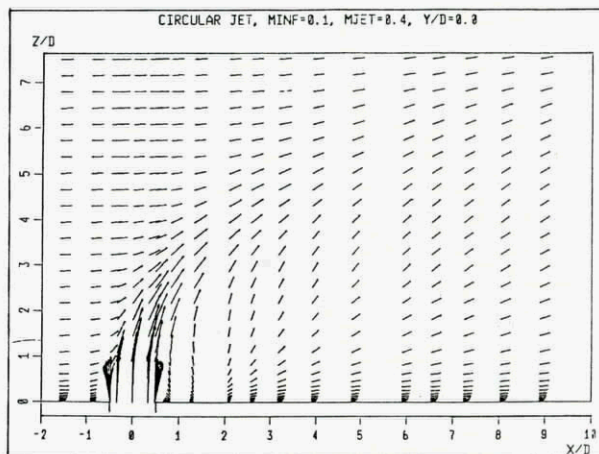
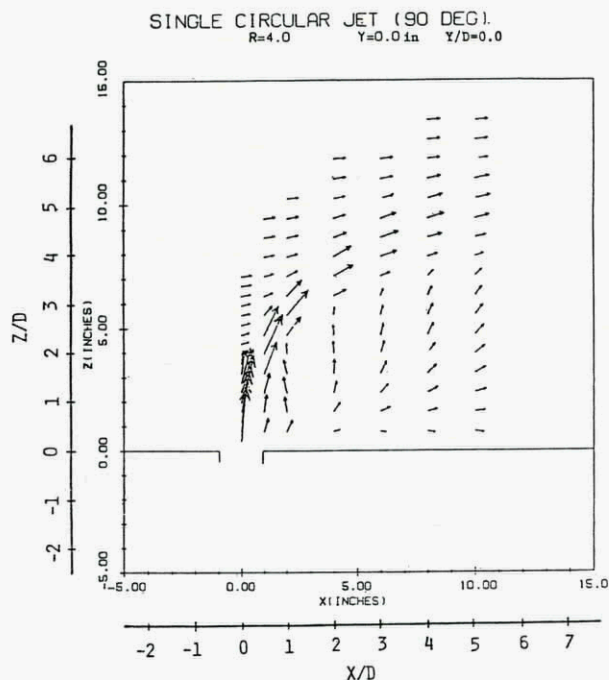


Fig. 15) Comparison of the experimental and computational velocity vectors for a circular jet (Exp: $M_\infty = 0.05$, $M_j = 0.2$; Comp: $M_\infty = 0.1$, $M_j = 0.4$).

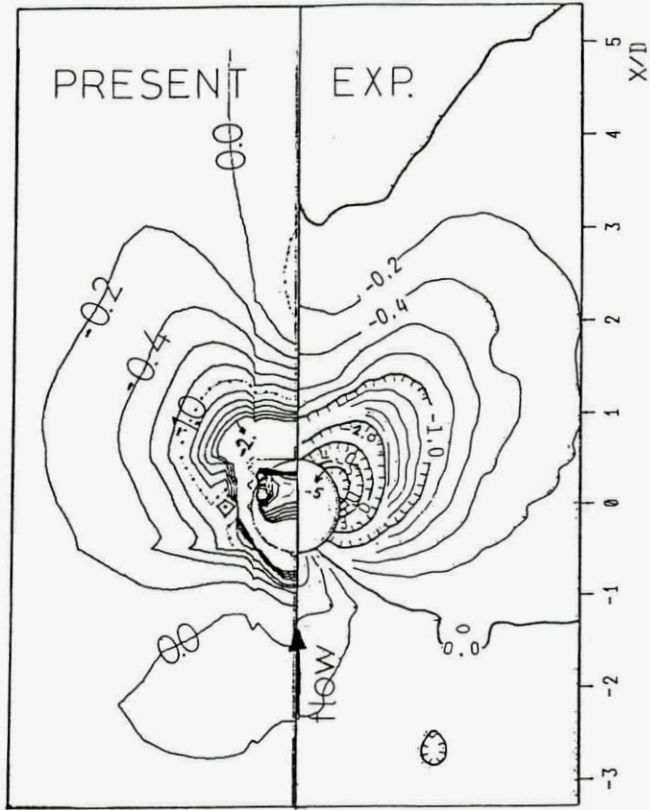


Fig. 16) Top view of the jet orifice comparing the experimental and computational surface pressure coefficients on the plate.

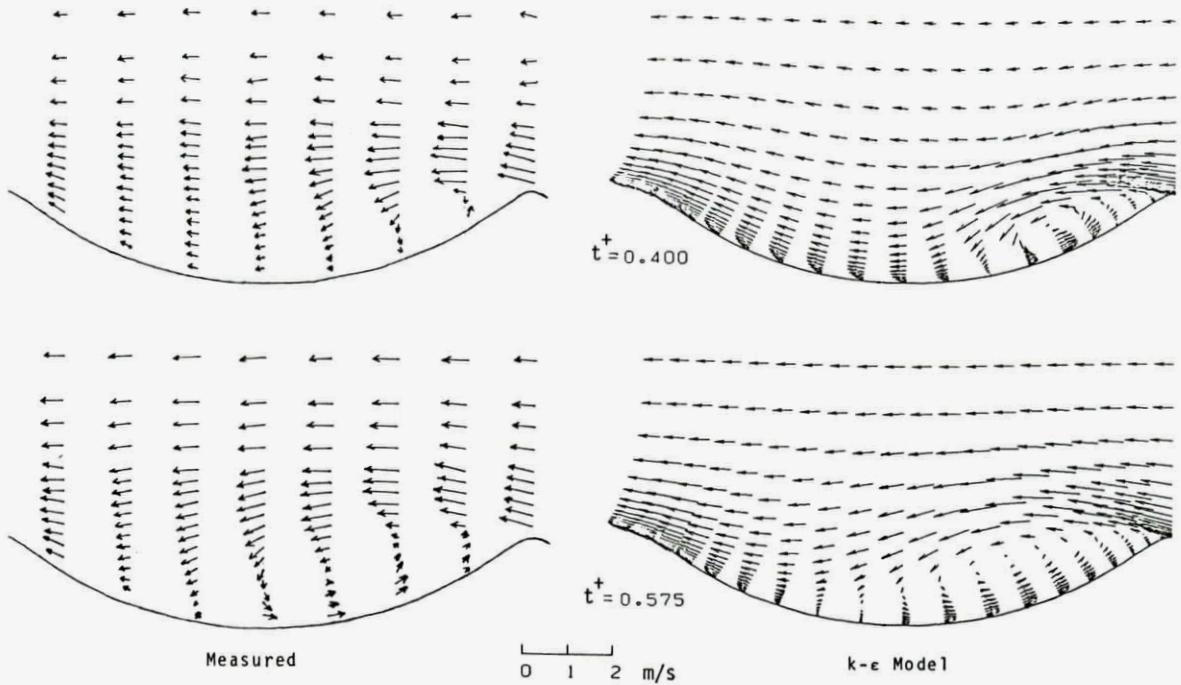


Fig. 17) Comparison of the computed and measured velocity field of the oscillatory boundary layers.

APPRAISAL OF THE SUITABILITY OF TURBULENCE MODELS IN FLOW
CALCULATIONS

A UK VIEW ON TURBULENCE MODELS FOR TURBULENT SHEAR FLOW
CALCULATIONS

G.M.LILLEY

DEPARTMENT OF AERONAUTICS AND ASTRONAUTICS
UNIVERSITY OF SOUTHAMPTON
SOUTHAMPTON SO9 5NH
ENGLAND.

ABSTRACT.

This paper is prepared as a contribution to the discussion by the Fluid Dynamics Panel of AGARD (Friedrichshafen April 1990) on the suitability of turbulence models in flow calculations. The views expressed are those of the author alone.

However a number of groups in UK have supplied information to the author giving views on the status of the methodology currently in use. The paper cannot, however, be regarded as a definitive statement on the overall methodology in respect of turbulence models currently in use in UK at the present time, and the success or otherwise groups have had with respect to these models. To obtain this information was beyond the resources of the author and would inevitably have led to a duplication of effort, since part of this work is already the subject of International meetings and planned conferences and workshops. It was a prime aim of the 1980-1981 Stanford Conference, and will be in the Stanford Workshop planned for next year, to investigate the reliability of the several turbulence models in predicting the properties of certain complex turbulent flows for which good, reliable and independently assessed experimental data was available. Each of these flows was complex, in the sense that it involved more than one rate of strain, and yet these flows were far simpler than the majority of flows which are currently being exposed to CFD codes at the present time.

1. INTRODUCTION.

During the past decade the interest in Computational Fluid Dynamics involving turbulent flows, which had always been a major activity in the Aeronautical Industry, has been expanded from sporadic use in Mechanical, Chemical and Nuclear Engineering, by way of example, to major user interest in both external and internal fluid flow problems. The number of users of CFD codes, including turbulent flow models, in UK alone is very large and they cover a very wide variety of different fluid flow interests and problems. In many of these flow cases good reliable experimental data does not exist, and there is no yardstick which can be used to establish if the results obtained from a given code are reliable, either qualitatively or quantitatively. Thus in this review the author mainly concentrates on the strengths and weaknesses of the various turbulence models in use at present.

A subject of major importance, and one which is not addressed in detail in this paper, is that concerning the numerical methods employed in solving the turbulent flow equations. In the calculations of inviscid codes high levels of numerical diffusion are used to obtain converged results. The direct extension of these techniques to the Reynolds-averaged Navier-Stokes equations, which include turbulent flow models, has often masked the performance of the turbulence model. Major attention needs to be directed towards numerical methods which obtain results from the Reynolds-averaged equations using very small values of numerical diffusion, in order to be confident that a judgement can be made on the performance of a given turbulence model. Coupled with this is the problem of grid generation and the type of grid employed, especially in regions of curved walls and in flows involving two and three-dimensional separation. At the 1980-1981 Stanford Conference one of the

areas of greatest uncertainty in the results received from the various turbulence modelling groups was that concerning numerical errors. The UK groups have also, more recently, had experience where different numerical methods, using the same turbulence model, have led to wide differences in the final results for such basic quantities as mean wall shear and mean velocity distributions. Obviously such discrepancies, arising from numerical errors can be corrected, but until they are done, it is pointless to attempt an appraisal of the different turbulence models in use and to draw definitive conclusions as to which model performs best in which flow, and whether one model performs satisfactorily over a range of turbulent flows.

A further problem concerns what is usually referred to as 'engineering accuracy'. There are certainly available today many commercial turbulent flow field codes which are widely used and which produce answers to a wide variety of turbulent flows, both two and three-dimensional. Most of these results are found to be qualitatively correct and physically significant. They are useful in various stages of design and their usefulness outweighs any errors that may arise in these methods, from either the inadequacy of the turbulence model or the numerics employed in the code. They provide more information about a flow field than can possibly be achieved by experimental means. They also possess the capability of providing new and important information about the flow, which would otherwise not be known. Thus it is often quoted that these codes produce results to good 'engineering accuracy'. Thus one major goal of this 'Technical Status Review' and the forthcoming International Review Workshops and Meetings, and especially the Stanford Workshop, must surely be to spell out the Test Cases against which all Codes should be calibrated, and with the knowledge that a given turbulence model, and a given numerical scheme will in a specified number of different flow domains generate results of a certain quotable accuracy.

2. BACKGROUND

From the earliest of times observations of fluid flow have shown that the normal state of fluid motion is turbulent. However the descriptive term 'dynamics of turbulent motion' is due to Lord Kelvin. It was however the work of Osborne Reynolds and others that proposed that the dynamics of turbulent motion can be described by an eddy viscosity which augments the dynamic viscosity of the fluid, but which unlike it is a function of the flow rather than of the fluid. Indeed Reynolds(1) proposed that turbulent motion be described as a random rapidly fluctuating velocity $q'(x,t)$, about a local, and slowly varying mean velocity,

$Q(x,t)$, with the instantaneous velocity being $q(x,t) = Q(x,t) + q'(x,t)$. In the case of steady, or stationary mean flow, the slowly varying mean velocity, $Q(x,t)$, is independent of time. The long time average of q' is zero.

Reynolds further noted that the long time average of the non-linear inertial terms in the equations of fluid flow, generate a product of the mean flow velocity components plus the mean of the product of the fluctuating velocity components. Thus in a stationary mean compressible flow,

$\overline{\rho q q} = \rho \overline{Q Q} + \rho \overline{q' q'}$, if density fluctuations are ignored, and hence the Reynolds-averaged conservation equations of mass and momentum may be written:

$$\nabla \cdot \rho Q = 0$$

$$\rho(Q \cdot \nabla) Q = -\nabla P + \nabla \cdot (T - \overline{\rho q' q'})$$

where T is the viscous stress tensor, which for a Newtonian fluid is:

$T = -2/3\mu I\theta + \mu(\nabla q + q\nabla)$, and θ is the rate of dilatation, which is equal to $\nabla \cdot q$. The mean pressure is P . The dynamic viscosity is μ , and I is the unit tensor.

3. THE REYNOLDS STRESS.

The term $-\overline{\rho q' q'}$ is called the Reynolds stress tensor since it augments the viscous stress tensor, and represents the effects of turbulent mixing on the flow. It has six independent components, three normal stress components and three shear stress components. It is referred to as a stress simply as a result of it entering the equation of motion as supplementary to the viscous stress tensor. The physical nature of these separate stresses is quite different. The viscous stress arises from a diffusion process which is proportional to the fluid viscosity. In a high Reynolds number turbulent flow it has an extremely small influence on the mean motion except close to solid boundaries where the no-slip boundary condition applies to both the mean and turbulent velocity components. On the other hand the effects of the Reynolds stress are the result of turbulent mixing by eddying motions that act over the entire turbulent shear flow. It is the result of dynamic motion and its overall influence on the mean motion is best expressed, as we will discuss below, as

a turbulent force per unit volume, equal to $-\nabla \cdot (\overline{\rho q' q'})$.

4. THE EDDY VISCOSITY.

Following Boussinesq(2) the Reynolds stresses have been described by an eddy viscosity, μ_T , which augments the dynamic viscosity, μ , such that in incompressible flow:

$$-\overline{\rho q' q'} = (\mu + \mu_T)(\nabla Q + Q\nabla), \text{ where}$$

$1/2(\nabla Q + Q\nabla)$ is the rate of strain tensor in the mean flow. This over-simplified approach to the prediction of turbulent flows replaces the complex physical processes of

turbulent mixing by a single scalar parameter, μ_T , representing the turbulent motion. At best μ_T can be found experimentally, but this presents difficulties since μ_T is flow dependent and varies in magnitude throughout the turbulent shear flow. In general the concept of an eddy viscosity is applied only to the shear stress components and not to the normal stress components. The sum of the normal stress components is proportional to the mean kinetic energy of the turbulent motion, and if k is the mean kinetic energy of the turbulent flow per unit mass then:

$$-\overline{\rho q q} = -2/3 \rho k I + \mu_T (\nabla Q + Q \nabla).$$

In the k - ϵ model $\mu_T = C_\mu \rho k^2 / \epsilon$, noting that $k^{3/2} / \epsilon$ is a length scale of the turbulence.

5. MODELLING OF THE REYNOLDS STRESSES.

Since in the early part of this century the Reynolds stresses had not been measured the only way open to model turbulent flows and thereby to effect predictions, was to use dimensional analysis and physical arguments in the determination of μ_T . If $\nu_T = \mu_T / \rho = O\{l\}$, where q and l are characteristic scales of turbulent velocity and eddy size, and ν_T is a positive quantity, then according to Prandtl(3)'s mixing length theory of turbulence, in which the characteristic turbulent velocity was put equal to l times the local mean shear, $\nu_T = l^2 dU/dy$ in a flow dominated by a mean shear dU/dy . Prandtl and others found this model of turbulence satisfactory in many simple practical flows, provided the mixing length, l , was suitably chosen. In the region close to the wall of a turbulent boundary layer von Karman proposed that $l = Ky$, whereas in the outer region of the boundary layer, l is a fraction of the mean boundary layer thickness. In free shear flows, such as wakes, jets and mixing regions Prandtl proposed that the characteristic turbulent velocity should be proportional to the velocity difference across the shear layer and l was proportional to the local mean width of the shear layer. All these results were supported by flow visualisation and observation. The aim throughout was to predict the mean velocity distribution, although in most cases this became a post-diction since the empirical constants in the mixing length formulas had to be pre-determined from

experiment. Other forms of the mixing length theory of turbulence were introduced, such as the vorticity transport theory of G.I.Taylor(4), with similar success.

Following the introduction of the hotwire, measurements became available of the components of the Reynolds stress tensor. A summary of the measurements in wall-bounded flows and free shear flows can be found in Townsend(5) and Hinze(6). However the greater understanding of the structure of turbulent flows arose from the determination of the space covariances

of two and three components of the turbulent velocity, from which could be derived the wave-number spectrum of the turbulence and integral length scales of the turbulence, together with the Reynolds stresses and the diffusion stress components. These measurements were made in support of the statistical theory of turbulence, Taylor(7), and the theoretical foundations of von Karman and Howarth(8), and later by Batchelor(9), based on the concept of homogeneous turbulence. Kolmogoroff(10) introduced the idea of locally isotropic turbulence in the smallest scales of turbulence, and by dimensional analysis proposed the laws for the characteristic velocity and length scales in the dissipation range and the inertial sub-range in terms of the dissipation function.

The work of Townsend showed that in all practical shear flows the turbulent flow is governed by a large scale structure, which is flow dependent, and which is anisotropic, and a smaller scale structure which is more universal in character and which contains the smallest eddies in the flow, which are responsible for the dissipation. Energy is transferred from the mean flow to the large eddies, which in turn pass their energy through a cascade of eddy scales, without loss, down to the eddies in the dissipation range. From the work of Grant(11), Townsend showed that large eddies although generated at random in respect of space and time, were nevertheless organised and similar in structure, and followed a simple representation, such as a double roller inclined in the direction of flow. Later Townsend found that the theory of rapid distortion introduced by G.I.Taylor, and later by Batchelor and Proudman(12), proved highly successful in the prediction of the space correlations of the Reynolds stress components. In that theory the near isotropic fluid, entrained by the large eddies, is strained by the mean shear in a time small compared with the characteristic flow time. The theory of rapid distortion not only predicts the shape of the space correlation but also the ratios of the final values of the Reynolds stress as achieved after strain. Thus turbulence, except in its largest scales, is found to be elastic and reversible. The more recent developments in Rapid Distortion Theory are reviewed by Savill(13).

6. THE COMPUTATION OF TURBULENT FLOWS.

However since the end of World War 2, the most robust, and consistent way to find the properties of turbulent shear layers, has been via the momentum integral equation of von Karman. In the integral equations the properties of the Reynolds stress are not required, since on integrating across the flow, the force exerted by the Reynolds stress, which is a true divergence, makes no contribution to the integral, except as a small correction to allow for the non-uniform variation in the mean

pressure across the boundary layer, especially in curved flows and in boundary layers in regions of separation. Reference to the proceedings of the Stanford Conferences in 1968(14), and 1980-1981(15) gives details of the many forms of the integral equations and the results achieved. The integral methods are basically post-dictive in that the constants and the expressions for the skin friction, the form parameters, and the entrainment coefficient, are all obtained from comparison with simple flows with the expectation that the same parameters and constants will hold for more complex flows. A major problem in the solution of the integral equations is that the equations are singular at separation where the skin friction vanishes. The singular behaviour can be avoided by using the indirect method of solution, using given distributions for the boundary layer displacement thicknesses over the region of separation rather than specifying the external velocity distribution as in the direct methods of solution. Nevertheless the solutions using the direct and indirect methods do not always match as shown by Cousteix(16).

The advent of high-speed computers in the 1960's led the way towards an attack on the Reynolds-averaged equations of turbulent motion involving various turbulent models. A major advance was the inclusion of the turbulent kinetic equation in the set of equations to be solved. Thus in addition to the mean velocity components the distribution of one of the Reynolds stress components could be obtained provided a length scale of the turbulence could be specified. Reynolds(17) defined the various schemes for solving these equations according to the type of turbulence model and the number of additional partial differential equations required by the model. The turbulence model morphology employed at the 1980-1981 Conference as described by Ferziger et al.(18) is as follows:

LEVEL

1. Correlations.
2. Integral Methods.
3. One-Point Closures.
4. Two-Point Closures.
5. Large Eddy Simulation.
6. Full Simulation.

The Integral methods use the Momentum Integral Equation, as discussed above, plus an additional equation, such as the Energy Integral Equation, the Moment of Momentum Integral Equation, or an Entrainment Correlation. Other choices in the method involve lags for the entrainment and shape factor.

The One-Point Closure schemes specify the treatment of the Reynolds stresses, and the number of additional equations required. Thus the Reynolds stresses are defined according to their specification as Boussinesq (eddy viscosity), algebraic, differential, and full Reynolds stress. For the Boussinesq and

Algebraic Stress Models the methods are sub-classified according to:

Zero-equation models.

- (1) prescribed, (2) 1 from ODE,

One-equation models.

- (1) k equation : 1 prescribed
- (2) k equation : ODE for 1
- (3) 1 prescribed : ω equation

Two-equation models.

- (1) k, ϵ
- (2) k, ω
- (3) k, 1
- (4) k^2 , 1, ϵ

The Differential models are sub-classified according to the number of additional equations employed. Thus

we have four equations for \overline{k} , $\overline{\epsilon}$, \overline{uv} , \overline{vw} , and five equations if $\overline{\epsilon}$, \overline{uv} , $\overline{u^2}$, $\overline{v^2}$, $\overline{w^2}$, are used.

The Full Reynolds stress models are classified according to the inclusion of an extra equation for ϵ or 1, or otherwise.

Two-Point Closures involve spectral methods, but no results for these methods were submitted at the Stanford 1980-1981 Conference.

Large Eddy Simulation provides a three-dimensional time-dependent description of the large eddy structure and its associated small scale structure, limited by the grid size and the flow Reynolds number. A low-order turbulence model is required to model the sub-grid scales in the turbulence.

At the Stanford 1980-1981 Conference the majority of methods submitted were Level 2 and 3.

7. THE DIMENSIONS OF TURBULENT SHEAR FLOW STRUCTURE.

Let us define U_0 and L_0 as the characteristic velocity and length scales of the flow. We define a flow time $T_0 = L_0/U_0$ and the flow Reynolds number is $U_0 L_0/\nu \gg 1$. In our turbulent flow, is assumed to exist, a continuous distribution of all scales of turbulence from the largest, being typically of the flow itself, to the smallest scales responsible for the dissipation. We introduce L as the integral scale of the turbulence and the Lagrangian time scale $T_L = L/q$, where q is the characteristic

velocity of the turbulence equal to say, the root mean square of the turbulent velocity. We assume that at high Reynolds numbers $qL/\nu \gg 1$, although $q \ll U_0$ and $L \ll L_0$. Now the mean dissipation function $\epsilon = \overline{v^2}$, to a good approximation in a high Reynolds number turbulent shear flow. However if we define q_g and l_g as the typical velocity and length scale of the dissipating eddies, then according to Kolmogoroff $q_g l_g/\nu = 1$, and the dissipation is $\epsilon = \nu q_g^2/l_g^2$. Hence $\omega = q_g/l_g$, where for convenience we have written ω^2 as the mean square vorticity equal to ϵ/ν . We find also that

$\epsilon = q_s^3/l_s$, and $q_s = (v\epsilon)^{1/4}$ and $l_s = v^{3/4}/\epsilon^{1/4}$. The circulation around the dissipating eddies is $\gamma_s = q_s l_s = v$. Thus both ϵ and w are functions of the dissipating scales of turbulence. But the mean dissipation rate, ϵ , must equal the rate of supply of energy from the mean flow, and this is equal to q^2/T_L . Hence, $\epsilon = q^3/L$ since $T_L = L/q$. If we define the Reynolds number of the turbulence $R_T = qL/v$ then

$$q/q_s = R_T^{1/4}, \text{ and}$$

$$L/l_s = R_T^{3/4}.$$

Thus the scale of the energy containing eddies relative to that of the dissipating eddies increases with Reynolds number to the power 3/4, and the velocities by the power 1/4. Some further deductions immediately follow.

In a steady shear flow in equilibrium we find, $\epsilon = -\overline{uv} dU/dy$. But $-\overline{uv}/q^2$ is $O(1)$ and therefore, since $\epsilon = q^3/L$ we find dU/dy is $O(q/L) = O(1/T_L)$. Thus the mean rate of strain in the turbulence is equal to the mean flow rate of strain, and the characteristic time of the energy containing eddies is $O(T_L) = O(1/dU/dy)$. If we define the mean flow vorticity as $\Omega = |dU/dy|$, then the above results show that,

$$\omega = \Omega R_T^{1/2},$$

and the characteristic turbulent vorticity increases with increase in Reynolds number to the power 1/2.

A further important result is the circulation around the energy containing eddies. If this is defined as, γ_T , then $\gamma_T = qL$ and $q^2 = \gamma_T \Omega$. We can therefore deduce that,

$$-\overline{uv} = \text{const.} \gamma_T dU/dy$$

which is similar to the result derived by Boussinesq. The difference is that whereas Boussinesq introduced an eddy viscosity ν_T our result is given in terms of the eddy circulation, a characteristic of large scale eddy mixing. Of course this interpretation is not surprising since eddy viscosity and circulation have the same dimensions. Thus whereas the normal interpretation of the Boussinesq approximation is regarded as having questionable physical significance, we see that with ν_T replaced by γ_T , we have a relationship which physically makes sense and moreover is closely related to the results of Rapid Distortion Theory. In

RDT it is found that the relation between $-\overline{uv}$ and q^2 depends on the accumulation of the mean flow strain rate along a streamline, Mathieu(19), and this is in agreement with a broad interpretation of the Boussinesq result expressed above. Savill has also suggested that where in a complex flow several strain rates act simultaneously they prevent extreme Reynolds stress levels, it being unlikely that a large fraction of the resultant turbulence stress is directed into one component only. This effective damping of anisotropy is given by Launder and Rodi

as one of the reasons that the $k-\epsilon$ model of turbulence often gives such good results.

Let us continue this argument that γ_T , which is the characteristic circulation of the big eddies containing most of the kinetic energy of the turbulence, is a measure of the large scale mixing. On our hypothesis it is not a gradient diffusion. We put $N_T = \gamma_T/v$ which is the ratio of the circulation around eddies of order scale, L , and those in the dissipation range. But $\gamma_T/v = R_T$ so $N_T = R_T$. Thus the ratio of the circulation around the big eddies to that around the dissipating eddies, $\gamma_T/\gamma_s = R_T = N_T$, and so N_T represents the number of dissipating eddies present in a big eddy. For any given flow the changes in the global picture of the large eddies may appear small, but the structure in the small scales changes dramatically. This suggests we define an effective Reynolds number of the turbulence as $R_T^* = qL/v_T = \gamma_T/v_T = \text{const.}$ of $O(1)$, a result found by Townsend and others. Thus whereas when the flow Reynolds number increases the Reynolds number of the turbulence, R_T , increases also, the effective Reynolds number, R_T^* , of the turbulence in the large scales is independent of Reynolds number at sufficiently high Reynolds numbers. However the small scale structure of the turbulence, especially in the dissipating range, is strongly dependent on Reynolds number as is evidenced by the proportional increase in the number of small scale structures in the flow. We may interpret this as the fractal character of the flow in the smaller scales.

The radian frequency of the big eddies in a Lagrangian frame is $\omega_0^* = q/L = \Omega$, where Ω is the mean flow vorticity. The characteristic radian frequency of the dissipating eddies is $\omega_s^* = q_s/l_s$. Thus $\omega_s^* = \omega_0^*/R_T$, showing that the largest frequencies increase with Reynolds number to the power 1/2. The same inference may be drawn in respect of the wave-numbers in the turbulence.

These simple dimensional relationships of the structure of the turbulent flow in its energy containing and dissipating ranges have important consequences in respect of the flow in an attached boundary layer close to the wall. Close to the wall the mean velocity satisfies the law of the wall.

Thus $\Omega = u_\tau/Ky$ for $y^* > 10$ and $\Omega = u_\tau^2/v$ for $y^* < 5$. But we have shown that $\Omega = q/L$ and so, noting that $q = O(u_\tau)$ and $L = O(Ky)$, the Reynolds number of the turbulence $R_T = Ky^*$, where $y^* = yu_\tau/v$. Hence between the wall and $y^* = 15$, say, R_T changes from zero to 6, assuming K , the von Karman constant, is equal to 0.4. But the value of the Reynolds number of the dissipating eddies is unity, and we see that the Reynolds numbers of the energy containing eddies and the dissipating eddies overlap in this region close to the wall. In the turbulent energy spectrum the inertial sub-range will be absent in this region.

This region is in fact the region where the maximum values of $-\overline{uv}$ and $\overline{q^2}$ are generated, and, as far as the turbulence is concerned, is one of the more important regions of the boundary layer. Nevertheless it is that region where the Reynolds number of the turbulence is small, even at high values of the flow Reynolds number, and where, as we have shown above, we expect large changes to take place in the small scale structure of the turbulence with increase in Reynolds number. But the large scale structure, containing most of the energy is of similar scale to that of the dissipating eddies, suggesting that the region of greatest energy production is also the region of greatest dissipation. This accords with experimental evidence Townsend(5). But we have noted that in the regions of turbulent flow not close to a solid boundary, and in all cases of free shear flow turbulence, the large scale structure is more or less Reynolds number independent at sufficiently high Reynolds numbers, in spite of the large changes that occur in the structure of the small scale turbulence. In the region of a wall both the large scale and the small scale structure are more or less independent of flow Reynolds number. Thus in the region close to a wall, in an attached boundary layer at a high flow Reynolds number, the structure of the turbulent flow is almost universal in character, and possesses a similarity governed by the characteristic scales of velocity, u_τ , or q_s , and length, ν/u_τ , or l_s , in the region of the wall. Again this is in accord with flow visualisation, and experiment. (see Cantwell(20), and Townsend).

In an attached boundary layer the structure of the turbulence in the region of a wall must therefore be governed mainly by the presence of the wall and less on the constraints imposed on the flow outside the boundary layer. These constraints naturally govern the values of u_τ and ν/u_τ , but u_τ may vary widely from one flow to another, such as from favourable to unfavourable pressure gradients. Throughout this section u_τ is the so-called shear velocity, given by $\sqrt{(\tau_w/\rho)}$.

Our conclusion is that models of turbulence must reflect the presence of the wall and the change in turbulence structure which must change from a near universal character close to the wall,

to a structure more related to that associated with free shear flow turbulence further away from the wall. The structure of turbulence close to the wall will be highly anisotropic and almost certainly defies simple description in a turbulence model. (see Kline and Robinson(21)). It would appear more profitable to describe it locally close to the wall in terms of given universal functions. At lower flow Reynolds numbers the constants in these universal functions will be functions of the flow Reynolds number, and would need to be found empirically, or from some higher order numerical scheme,

preferably, full simulation.

8. INITIAL REGION OF TURBULENT FLOWS.

Turbulent shear flows develop in general from laminar flows through a complex transition process, which undergoes a series of instabilities developing out of a weak instability of the basic flow, in which initial disturbances are amplified. Subsequently by a process of bifurcation, non-linear interactions and three-dimensional distortions, leading to complex vortex structures which become stretched and pinched, and where the near flow singularity is only avoided by the action of viscosity. The extremely high, but finite, value of the local vorticity, leads to the production of Emmons spots, and the flow ultimately breaks-down to a turbulent state. The dissipation mechanism changes dramatically from one of gradient diffusion, to one involving the local generation of extremely small structures in the flow, which possess a high local instantaneous value of vorticity, many times that of the vorticity of the mean flow. As we have discussed above, the rate of dissipation in a turbulent flow is $\epsilon \approx \overline{v\omega^2}$, hence, using a similar relationship for the instantaneous dissipation, the local rate of dissipation is very high within a turbulent spot.

The initial discrete spectrum in the disturbed flow at the commencement of transition, develops into a continuous spectrum as more and more smaller scale structures are formed as a result of the cascade of instabilities, or the near catastrophic breakdown, of the initially laminar flow. The near continuous spectrum from low to high frequencies suffers a rapid decay in the region of the frequency of the dissipating eddies, referred to as the Kolmogoroff range. The near continuous spectrum developing in the later stages of transition is representative of the growth of a large number of vortex structures having a wide range of scales from the order of the flow itself down to the small dissipating eddies in the Kolmogoroff range. The rapid changes in the energy spectrum of the flow through transition leads to a change in the local mean flow structure, and thus is set up a complex interacting relationship between the convecting flow and the vortex structure convected by it. The one is entirely dependent on the other and the coupling

relationship is non-linear and subject to viscous influence both in the dynamics of the unsteady flow as well as in the viscous decay. Morkovin(22), Huerre and Monkewitz(23).

The prediction of transition imposes many problems but progress is being made. Cebecci et al.(24), Arnal and Coustols(25), Collier et al.(26), and Malik et al.(27).

9. FULLY DEVELOPED TURBULENT FLOW.

Following transition, as stated above, the energy spectrum is almost continuous and discrete frequencies are absent.

Nevertheless in all turbulent shear flows, whether free shear flows, such as wakes, mixing regions or jets, or wall-bounded shear flows, such as attached and separated boundary layers, there exists a large scale eddy structure to the flow, and which is characteristic to that flow. Such structures appear at random both in respect of space and time. They are convected by the flow and suffer distortion and interaction with the rest of the flow and ultimately decay. These large eddies provide one of the vehicles for the entrainment of irrotational fluid from outside the turbulent shear layer. The other, less important mechanism for entrainment, is the gradient diffusion which takes place along the boundary between the turbulent and non-turbulent fluid as discussed by Townsend(5) and Savill(13).

10. THE LARGE SCALE STRUCTURE.

These large scale pseudo-random eddies formed at a given station in a turbulent shear flow have similar structures and are normally referred to as coherent or organised structures. Cantwell(20). Since their structure changes from flow to flow, and they change from station to station in a given flow, as the mean flow changes and the flow develops a change in scale, it seems reasonable to assume that they are closely connected with the structure of the mean flow itself. We note, of course that the decomposition of the instantaneous flow into a mean, and a fluctuating component whose time average is zero, is just one of an infinite set of ways of describing any unsteady flow. In particular the real flow passes through a succession of states as it is convected downstream, and there can be no single realisation when it truly conforms to that designated as the mean flow. So the concept of a mean flow is artificial and yet it is the flow field measured in all mean flow experiments. Thus the question is raised whether the large scale structure as observed in the real flow, is the same as would exist in an artificial flow defined by the mean (or smoothed) flow. The answer to this question is fundamental to all modelling of turbulent flows. All computational schemes, apart from LES and Full Simulation, involve this analogy, in that the real flow is replaced by an equivalent flow having the properties of the true mean flow, but its turbulent structure is associated with that mean

flow, rather than the instantaneous flow as would exist in the real flow. Townsend repeatedly discusses this dilemma in describing the application of a simple eddy structure to modelling the Reynolds stresses. A further critical case where the structure of the turbulent flow has to be modelled with respect to a given mean flow is provided in the models of equivalent acoustic sources used to predict the far field noise radiation from turbulent flows. This is an even more critical case than the modelling of turbulence to predict the structure of the mean flow, for in the acoustic case it is not the Reynolds

stresses that have to be modelled but their space-time correlations. Thus we require the full time dependent relations for all the Reynolds stresses in the acoustic, or aerodynamic noise problem, and not simply their time averaged values as required here. But surprisingly enough the comparisons between the theoretical models, based on the mean flow analogy, and experiment show a remarkable agreement, which many assume to be fortuitous, and the entire philosophy of the use of the turbulent models based on the mean flow analogy, is still the subject of vigorous debate. But the Russian school have examined this same problem, Belotserkovskiy and Shidlovsky(28), and their conclusion is most significant. They invoke the 'Ievlev' hypothesis' (referred to by Belotserkovskiy as 'Ievlev's process') which states that by the use of 'smoothed equations', and satisfying the same boundary conditions as the real flow, the correct statistical flow parameters, which depend on the large scale turbulence, will be obtained, even though the detailed space-time patterns for the artificial flow will not duplicate any real process. Thus the evolution of the probability densities for the real flow, are equal to those obtained from solutions to the 'smoothed equations' satisfying the same boundary conditions.

It appears therefore that introducing a mean flow analogy for calculating the properties of a turbulent flow is permissible. It would also appear that in the light of 'Ievlev's hypothesis' that the large scale organised or coherent structure in a turbulent flow, is related to the eigen values and eigen functions of the basic mean flow. This is not to be taken as a proposal that all large scale structures in all turbulent flows relate to the dominant local natural frequency of these flows. In some flows, or parts of flows there is evidence to suggest that the preferred scale is that of a second harmonic, Landahl(29), Zhang and Lilley(30), whilst in other flows the characteristic scale of the large eddies appears to follow the set of sub-harmonics in their passage downstream, as found by Morris et al.(31). We should be reminded that here the dominant eigen mode is that of the equivalent mean turbulent flow, which contains the simulated background turbulent flow. All modes in this disturbed flow, and it is disturbed

because it is turbulent, arise naturally, continuously and at random in space and time, just as in the real flow. However only those modes that are both energetic, and are either near neutral or are unstable that can survive. The remainder are damped. The modes are in general of finite amplitude and, as in Rapid Distortion Theory, suffer rapid distortion under the influence of the mean strain rates, and strong non-linear interaction with the rest of the flow. The success of these analyses of the large scale structure have been related to only a few simple flows, and the entire subject is one of

great activity as well as of interest. Clearly there is need to couple these new theories of the large scale structure in turbulent flows with the results of Rapid Distortion Theory.

Sofar the structure of the large eddies has had no impact on the modelling of turbulence at the level of the Integral equations and One-Point Closure methods. Hence it is something of a mystery that such good results are sometimes obtained with methods such as the $k-\epsilon$ equation over a wide range of flows using the same turbulence model. The results of the Stanford 1980-1981 Conference led Kline to propose that since no universal model of turbulence can exist for the prediction of the characteristics of turbulent shear flows, it is best to accept that fact and to use zonal modelling, with appropriate, and separate, turbulence models with specially adjusted parameters and constants in each zone. Such modifications would, in effect, represent the influence of differences in the influence of the different large scale structures, on the structure of the remainder of the turbulence, present in the real flow in each zone. The fact that this would appear to be simply a 'fine-tuning', whereas the changes in the large scale structure as observed in the real flow, from zone to zone, are far from negligible, suggests that the large scale structure is basically the vehicle by which energy is transferred from the mean flow to the turbulence, and that the fine detail of that large scale structure are of lesser importance. Thus provided the turbulence model correctly represents this transfer of energy to the turbulence, it may be relatively unimportant to introduce a supplementary model for the large scale turbulence structure itself. However it is the large scale structure which acts to control the growth of of the mean flow as well as to control the entrainment of irrotational fluid into the bulk of the turbulent flow.

11. TURBULENT STRUCTURE.

The turbulent structure of turbulent shear flows at high Reynolds numbers is highly inhomogeneous as a result of the spreading of the turbulent flow into the surrounding ambient non-turbulent fluid. The bounding surface of the turbulent fluid is highly contorted by eddies, which according to Townsend(5) and the

experiments of Grant(11), resemble the Helmholtz instability of a vortex sheet with a growth and decay cycle. The alternation between stability and instability suggests that overall the flow is in a near-state of neutral stability, and the contortions of the bounding surface allow the entrainment rate of irrotational fluid to be self-adjusting and dependent only a constant, called by Townsend the flow constant, which is a function of the flow. Townsend and others assume the instantaneous flow to comprise a mean velocity field, $U(x)$, a large eddy motion, u' , and the main turbulent

motion, u'' . The main turbulent motion comprises all the smaller eddies down to the eddies of smallest scale responsible for the dissipation. According to Townsend, it may be assumed that the turbulence is quasi-homogeneous at the higher end of this range, down to a state of local isotropy in which the structure is near universal, which by measurement is in accord with Kolmogoroff's theory. Eddies in this lower range of scales make little contribution to the total kinetic energy of the motion. Townsend shows that it is the main turbulent motion which is exposed to the mean shear or strain rates, imposed by the mean flow gradients. It follows from applications of Rapid Distortion Theory, as described above, that the main turbulent motion possesses structural similarity, such that its contribution to the main motion is limited to only changes in the scale of length and velocity. The principal use of structural similarity in many turbulent models, such as in $k-\epsilon$, is the assumption that $\overline{-uv}$ is proportional to $\overline{q^2}$ with only minor adjustments for the relative position in the flow and the flow itself.

12. TURBULENCE IN A MOVING FRAME.

Most measurements of turbulence are based on a fixed frame analysis. In general, this gives the impression that of a random distribution of eddies crossing the observation window, and that events relatively remote from each other are statistically independent. However flow visualisation and measurements of space-time correlations at a range of laboratory Reynolds numbers show that much of the structure, especially in the larger scales, is ordered and has a longer characteristic decay time than would be apparent from a statistical analysis of the measurements. The measurements of Davies et al.(32) in the mixing region of a jet, show that the average convection speed of the turbulence is almost constant across the mixing region. The space-time correlations show that the largest characteristic time scale is found when the moving frame analysis is performed at a speed equal to the convection speed. In addition this time scale equals the inverse of the mean rate of strain $1/(dU/dy)$, as proposed above in Section.(7). Similar results have been obtained in boundary layers by

Favre(33). There appears some evidence that the characteristic Strouhal number of the turbulence in a moving frame, ω_L/T_L , is nearly constant across a mixing region, or throughout most turbulent free shear flows, and the variation of the properties of the turbulence, including the Reynolds stresses, across the mixing region is the result of the intermittency caused by flow in these regions as being alternately turbulent and non-turbulent arising from the passage of the big eddies and the entrainment of non-turbulent fluid from outside the

shear layer. Some turbulence models reflect this intermittency.

However turbulent models need to be based on the properties of the turbulence relative to the local mean flow, since the modelling must be based on the mean flow analogy discussed above. Thus the analogy will not involve the intermittency that exists in the real flow.

However turbulence models based on empirical correlations may clearly use the measured intermittency to provide the necessary data base for the varying properties of the turbulence in the given region of flow.

13. ALTERNATIVE APPROACHES.

Throughout this presentation attention has been focussed on the dynamic processes involved with turbulent mixing. It has also been stated that whereas the effects of the turbulent mixing are concentrated in the Reynolds stress tensor, with its six independent components, the combined effect of the turbulence on the mean flow is governed by the divergence of the Reynolds stress tensor, which is a force per unit volume. This force has three components only and it is the magnitude and direction of this force, which we will call the 'vortex force', which influences the development of the mean flow, rather than the influence of the separate components of the Reynolds stress tensor. Some important conclusions now arise as to the influence of the Reynolds stresses and that of the vortex force. Let us write the equations of mean motion in the following form:

$$\frac{\partial Q}{\partial t} = F - \nabla H - \nabla \text{curl} \Omega : \nabla \cdot Q = 0$$

where $F = Q \times \Omega + \overline{q \times \omega}$,

and $H = P + Q^2 + \overline{q^2}$.

We see that F can be interpreted as the overall vortex force per unit volume and $\overline{q \times \omega}$ is related to the Reynolds stresses by

the relation:

$$\overline{q \times \omega} = \nabla \overline{q^2/2} - \nabla \cdot \overline{q q}$$

The mean flow and the mean turbulent kinetic flux equations become:

$$\frac{\partial Q^2/2}{\partial t} = -\nabla \Omega^2 + Q \cdot (\overline{q \times \omega}) - \nabla \cdot (H Q - \nabla(Q \times \Omega)) \quad \text{and,}$$

$$\frac{\partial \overline{q^2}}{\partial t} = -\nabla \overline{\omega^2} - Q \cdot (\overline{q \times \omega}) - \nabla \cdot (\overline{h q} - \nabla(\overline{q \times \omega}))$$

These equations show clearly the role played by the vortex force and the Reynolds stresses. The dissipation is here represented as $\overline{v \omega^2}$ and $\nabla \Omega^2$ for the turbulent and mean flow respectively. The energy transferred from the mean flow to the turbulence is $Q \cdot (\overline{q \times \omega})$. The remaining term, when the mean flow is stationary, involves diffusion.

We see that the part of the vortex force attributed to the turbulence is $(\overline{q \times \omega})$.

The turbulent kinetic energy is included with the total energy, H, and :

$$h = p + q^2 - \overline{q^2} + q \cdot Q, \text{ is the}$$

instantaneous total energy in the turbulence. The turbulent energy equation does not include a pressure-rate of strain interaction, and the pressure enters the diffusion process only. The major contributions to the turbulent energy equation arise from the linear terms in the equations of motion for the turbulent flow. These results are for incompressible flow only and need modification when the flow is compressible. All these equations are exact and have simply been obtained by a rearrangement of the turbulent terms in the well-known Reynolds-averaged equations.

The inference is that modelling the Reynolds stress tensor, or deriving equations for the derivation of its components, may not after all be the best approach in deriving the influence of the turbulence on the characteristics of the mean flow, as well as the influence of the mean flow on the turbulence. It has been known for a long time that the Reynolds stress itself does not provide an active influence on the instantaneous properties of the turbulence. A simple example is that of the turbulent flow over a flat plate in zero pressure gradient. If we introduce the usual boundary layer approximations we find that:

$$-\overline{uv} = \int_0^y \overline{i \cdot (q \times \omega)} dy = - \int_y^\delta \overline{i \cdot (q \times \omega)} dy.$$

These relations show clearly that the Reynolds shear stress is not a primary variable of the turbulence. Experiment

shows that, in general, its mean value is a minute fraction of its peak value. It is determined entirely from the mean turbulent component of the vortex force. The turbulent component of the vortex force is dominated by the instantaneous magnitude and direction of the vorticity. Peak values in the fluctuating vorticity arise from vortex stretching and pinching, and these occur locally in the smallest scales of turbulence and arise sporadically. When they occur their contribution to the Reynolds stress is enormous, otherwise their contribution is almost negligible. Thus to attempt to model the Reynolds

shear stress terms and to attempt to interpret such modelling in physical terms is open to great difficulties. The better approach appears to be to combine the derivatives of the several Reynolds stress components into the vortex force vector $\overline{q \times \omega}$. Equations can be derived for the transport of the turbulent vortex force, which in principal are simpler than the corresponding Reynolds stress transport equations.

However here we simply wish to reinterpret the main physical components in the turbulent energy balance equation - the k-equation. There are just three groups of terms. The production, dissipation and the diffusion terms. The magnitude and direction of the turbulent vortex force is the unknown in this system of equations. The dissipation

function, $\epsilon = \overline{v w^2}$, is also an unknown, unless it is approximated in one of the forms discussed above. If however the k- ϵ method is used, we need to solve the equation for ϵ . The ϵ -equation is simply the scalar vorticity equation and the physical interpretation of the terms in that equation can be better understood than if we think of it as a transport equation for dissipation.

14. THE EXPERIENCE OF CERTAIN UK GROUPS.

(a) RAE.

Lock and Williams(34) have shown that the viscous-inviscid interaction technique is an efficient and accurate method for calculating the attached viscous flow over aerofoils. For two-dimensional attached flows the existing turbulence models appear to be satisfactory.

The prediction of separated flows and three dimensional flows presents a different picture. The viscous-inviscid interaction technique is not viable and even the most complex turbulent flow models appear to be inadequate. Accurate two-dimensional results have been achieved up to large high lift coefficients and stalling, but not when shock induced separation is involved and when large regions of separated flow exist. In three-dimensional flows it has proved possible to extend the interaction technique up to limited regions of separated flow but it appears that large separated flow regions will require solutions of the full Reynolds-averaged Navier-Stokes equations with

suitable turbulence models. It is expected that with such methodology a wide range of practical problems could be tackled including, wing tips, junction flows, shock induced separation and jet flows.

The RAE have studied the measurements and surveys by Delery(35) and Delery et al.(36) on shock wave interactions ranging from incipient to extensive regions of separation, for the purpose of testing the performance of turbulence models. Benay et al.(37) report results using an inverse boundary layer method and Dimitriades and Leschziner(38) use a

Reynolds-averaged Navier-Stokes method. RAE conclude that zero-equation models give a poor representation of viscous processes, particularly near separation. The zero-equation model most used at present for problems in external aerodynamics is the Baldwin-Lomax(39) 'mixing-length' model. Improvements in the mixing-length model can be obtained from the Johnston-King(40) model, which includes history effects, through an equation for the rate of change of the maximum shear stress. The performance of two-equation models appears to be variable and flow dependent. There are important distinctions between the high Reynolds number version using wall-functions and the low Reynolds number version which integrates the full equations to the wall. The high-Reynolds number version permits coarser grids close to the wall. Dimitriades et al. have extensively tested these models for the case of the tests by Delery. They conclude that the high-Reynolds number solution gives an excessively thick boundary layer ahead of the shock, which predicts a greater tendency towards separation, and once separated the recirculation is excessive. The low-Reynolds number solution tends to inhibit separation. All models predict levels of turbulence energy which are too small immediately downstream of the shock and values of shear stress which are too small far downstream. It is found that the full transport equations for the normal stresses should predict strong turbulence anisotropy, as found in the experiments. However the two-equation models represent the turbulence properties in terms of two scalar quantities k and ϵ . Thus these models fail to predict the turbulent anisotropy which is an important property of the real flow. Leschziner(41) suggests that the use of full Reynolds Stress Models provides a notable improvement in accuracy, but the errors are still significant. It is suggested that some of the errors are possibly the result of the pressure-strain interaction producing a tendency towards isotropy and the use of the isotropic dissipation. Currently new models, to overcome these difficulties, are being investigated. It is also hoped that certain results obtained from LES and Full Simulation calculations will assist in a more accurate determination of the pressure-rate of strain and the dissipation, to assist in their modelling in the two-equation and full

Reynolds stress models, to overcome the difficulty that these quantities cannot be directly measured in experiments.

In three-dimensional flows the problems become complicated by strong three-dimensionality in the turbulence structure and the influence of more complex regions of separation. Current versions of the Reynolds Stress Models fail to explain the lag in shear stress direction and the decrease in amplitude from that obtained in two-dimensional flows, as found in the experiments of Van den Berg et al.(42) and Bradshaw and Pontikos(43,44).

The RAE stress that improvements in turbulence modelling are vital for three dimensional flows and separated flows in two and three dimensions. To assist the development of improved methodology for turbulence models the need is for further dedicated, definitive experimental studies providing good reliable data of the flow field and in particular the measurements of the Reynolds stresses. Some of this data exists in the measurements of Van den Berg et al. and Bradshaw and Pontikos, and further data is currently being collected in the experiments on the three-dimensional GARTEUR AG07 wing.

To avoid some of problems related to reduction in the level of numerical diffusion referred to above, the QUICK scheme of Leonard(45) is being modified to include higher order upwind schemes. There is also on-going work at RAE to identify the errors caused by numerical diffusion. Support is also being given to the development of methods using LES to provide an input to the modelling of turbulence quantities that currently cannot be obtained by measurement. Finally there is work supporting the understanding and prediction of transition.

(b). UMIST.

The CFD work at UMIST is well-known and is devoted to the study of turbulent flows. The aim is the development of computer programmes which can be used for an increasing range of flows. The Group sees many problems in zonal modelling, and would prefer to continue along a more 'universal' line of development. The Group has shown improved results by moving from one-equation to two-equation eddy viscosity models, and from an eddy viscosity scheme to a Reynolds Stress Model, known as 'second moment closure'. The expectation is that second-moment closures will replace the standard k- ϵ models within the next decade, and become the 'engineering standard'.

The Group report improvements to the ϵ -equation where excessive near-wall length scales are obtained. Further improvements have been made to the ϕ_{ij2} term which are required when applied to strong swirling flows.

The Group has moved away from Algebraic Stress Models, and has more recently

concentrated on Reynolds Stress models. The number of different external and internal flows studied is very large and the experience gained in the use of these codes, and the comparison of results with experiment is not easily summarised here. In most case studies the current methods have performed well yet further improvements are needed. Reference should be made to Launder(46) and Leschziner(47) for further details of the UMIST experience on the use of their second order moment closure scheme incorporating their turbulence models.

(c). UKAEA HARWELL.

The Group, during the last decade, has worked extensively on solutions to the Reynolds-averaged Navier-Stokes equations. The current computer code, HARWELL-FLOW3D, has been used for solutions to a variety of flow problems. The standard version uses a k- ϵ model on the assumption of an isotropic eddy viscosity. For curved flows it has been found necessary to remove this restriction by including the transport equations for the Reynolds stress tensor components. Thus FLOW3D is a Reynolds Stress Model using body fitted coordinates. Typical results obtained with both an Algebraic Stress Model and the Reynolds Stress Model are found in Clarke and Wilkes(47,48).

(d). QMC.

Professor Leslie's Group have a wide experience in the use of LES for a limited range of flow geometries. Sub-grid scale modelling is by the Smagorinsky eddy viscosity model. More recently the Group has commenced work using k- ϵ and current attention is focussed on the numerical scheme and improvements in accuracy.

(e). SURREY UNIVERSITY.

Dr. Castro's Group has recently started work on flows involving large regions of separation and plans to investigate zonal modelling. The aim is to perform calculations on flows for which the experimental data is available, such as the Test Cases in the Stanford Conference(1980-1981). The computer codes will include k- ϵ and FLOW3D and comparisons will be made with results from Rapid Distortion Theory and PHOENICS. Current interest is focussed on the results from the 'straight pipe - contraction - diffuser' exercise, where a relatively simple set of flows has produced a wide variety of apparently converged solutions, using the standard k- ϵ and Reynolds Stress Models.

15. CONCLUSIONS.

The present paper sets out to examine the background and the basis for the different models of turbulence as currently used for solutions to the Reynolds-averaged Navier-Stokes equations.

The current status of the different schemes is briefly described and some of the current experience is reviewed.

The conclusion is drawn that no model of turbulence as currently employed is fully satisfactory, although many computer codes may legitimately claim to give results to 'engineering accuracy'. The need is stressed to provide means for calibrating all CFD computer codes against good, reliable, independently assessed experimental data. In addition where possible the numerical methods need to be carefully checked for errors arising from too large numerical

diffusion, which in some cases is known to mask the characteristics of the turbulence. Numerical test cases alone against time-dependent analytic solutions may also be a method to assess the performance of the numerical scheme. In all codes the errors introduced with different grids needs careful assessment.

The 'mean flow analogy' is discussed as the main basis for turbulence modelling and reference is made to its comparison with the structure of turbulence in the real flow. The 'mean flow analogy' is shown to be justified by the use of 'Ievlev's hypothesis'.

Attention is drawn to a need for a reassessment of the central role claimed in turbulence modelling for the six independent components of the Reynolds Stress Tensor. It is shown that the mean flow is controlled not by the Reynolds stresses but rather the divergence of the Reynolds stress tensor, which is a force per unit volume, and to its magnitude and direction. A further discussion leads to the introduction of the vortex force per unit volume, and its turbulent component, $q \times \omega$. It is shown that all turbulent flow models can be reduced to these derived quantities, and not only can the physical understanding of the turbulence model be improved, there appears to be an expectation that greater accuracy will be obtained in the final analysis.

The final conclusion relates to the need to replace the term eddy viscosity by a term that more adequately expresses the large scale turbulent mixing process in a turbulent flow. A simple and yet startling conclusion is that the use of eddy viscosity over the past century to provide a 'rough' description of turbulent mixing, when it is known that the process of turbulent mixing is in noway analogous to viscous diffusion, can be justified by replacing it by the term 'large eddy circulation', a quantity that has the same dimensions and numerically is of the same order of magnitude. Moreover it truly describes what large scale mixing does perform.

16. ACKNOWLEDGEMENTS.

This review could not have been completed without the discussions and advice from many quarters. The author would particularly wish to thank

Dr. Brian Williams, Dr. Michael Leschziner, Dr. Ian Castro, Dr. Ian Jones, Dr. Nigel Wilkes and Professor Leslie. They willingly gave the author advice and the benefits of their several and varied experiences with turbulence modelling and turbulence models. However the author takes full responsibility for the statements made and views expressed in the paper.

REFERENCES.

1. Reynolds.O. (1894) On the dynamical theory of incompressible viscous fluids and the determination of the criterion.
Phil.Trans.A.186 Papers 2, 535.
2. Boussinesq.J. (1877) Mem.pres.par div.savant a lacad.sci. Paris. 23 46.
3. Prandtl.L. (1925) Bericht uber untersuchungen zur ausgebildeten turbulenz.
ZAMM 5 136-139.
4. Taylor.G.I. (1935) The transport of vorticity and heat through fluids in motion.
Proc.Roy.Soc.Series A. 135 685.
5. Townsend.A.A. (1956) The structure of turbulent shear flows.
(1976) CUP.
6. Hinze.J.O. (1959) Turbulence. McGraw-Hill.
(1975)
7. Taylor.G.I. (1938) Statistical theory of turbulence.
Proc.Roy.Soc. Series A. 151 421.
8. Von Karman.Th. (1938) On the statistical theory of turbulence.
& Howarth.L. Proc.Roy.Soc. Series A. 164 192-215.
9. Batchelor.G.K (1953) The theory of homogeneous turbulence.
CUP.
10. Kolmogoroff.A.N.(1941) The local structure of turbulence in incompressible viscous fluid.
Dokl.Akad.Nauk.SSSR. 30 299-303.
11. Grant.H.L. (1958) The large eddies in turbulent motion.
J.Fluid.Mech. 4 149-190.
12. Batchelor.G.K. (1954) The effect of a rapid distortion on a fluid in turbulent motion.
& Proudman.I. Quart.J.Mech.Appl.Math. 7 83-103.
13. Savill.A.M. (1987) Recent developments in Rapid Distortion Theory.
Ann.Rev.Fluid.Mech. 19 531-575.
14. Kline.S.J., (1968) The computation of turbulent boundary layers-1968 AFOSR-IFP-Stanford Conference.
Morkovin.M.V., Sovran.G., & Cockrell.D.J. Stanford University.
15. Kline.S.J., (1982) The 1980-1981 AFOSR-HTTM-Stanford Conference
Cantwell.B.J., Comparison of computation and experiment.
Lilley.G.M. Stanford University.
16. Coustieux.J. (1986) Three dimensional and unsteady boundary layer computations.
Ann.Rev.Fluid.Mech. 18 173-196.
17. Reynolds.W.C. (1976) Computation of turbulent flows.
Ann.Rev.Fluid.Mech. 8 183-208.
18. Ferziger.J.H., (1982) (see Kline et al. (1982) pp 634-649).
Bardina.J., Allen.G.
19. Mathieu.J. (1971) VKI.Lect.Ser. 36.
20. Cantwell.B.J. (1981) Organized motion in turbulent flow.
Ann.Rev.Fluid.Mech. 13 457-515.
21. Kline S.J., (1988) Turbulence producing coherent structures
Robinson.S.K. in the boundary layer. Progress of a cooperative evaluation.
Dubrovnik.

22. Morkovin.M.V. (1988) Recent insights into instability and transition to turbulence in open-flow systems.
 ICASE Rep.88-44.
 NASA Langley Research Center.
23. Huerre P., (1990) Local and global instabilities in spatially developing flows.
 Monkewitz.P.A. Ann.Rev.Fluid.Mech. 22 473-537.
24. Cebeci.T., (1988) A three dimensional linear stability approach to transition on wings at incidence.
 Chen.H.H., Arnal.D. AGARD Conf.Proc. 438 17.
25. Arnal.D., (1984) Application de criteres bi- et tridimensionals au calcul de la transition et de la couche limite d'ailes en fleche.
 Coustols.E. AGARD CP.365 12.
26. Collier.F.S.jr (1988) Curvature effects on the stability of three dimensional laminar boundary layers.
 Malik.M.R. AGARD Conf.Proc. 438 10.
27. Malik.M.R. (1989) Effect of curvature on three dimensional stability.
 Poll.D.I.A. AIAA Journal 23 9 1362-1369.
28. Belotserkovskiy.O.M., (1986) Current problems in computational fluid dynamics.
 Shidlovsky.V.P. MIR, Moscow.
29. Landahl.M.T. (1990) On sublayer streaks.
 J.Fluid.Mech. 212 593-614.
30. Zhang.Z. (1981) A theoretical model of the coherent structure of the boundary layer in zero pressure gradient.
 Lilley.G.M. Turbulent Shear Flows. 3. 60-72.
31. Morris.F.J., (1990) Turbulent mixing in plane and axisymmetric shear layers.
 Giridharan.M.G., Viswanathan.K. AIAA (Reno) 90-0708.
32. Davies.P.D.A.L., (1963) The characteristics of the turbulence in the mixing region of a jet.
 Fisher.M.J., Barratt.M.J. J.Fluid.Mech. 15 337-367, 559.
33. Favre.A. (1983) Turbulence :space-time statistical properties and behaviour in supersonic flow.
 Phy.of.Fluids. 26 10.
34. Lock R.C., (1987) Viscous-inviscid interactions in external aerodynamics.
 Williams.B.R. Prog.Aerospace.Sci. 24 51-171.
35. Delery.J. (1981) Investigation of strong shock/turbulent boundary layer interaction in 2d transonic flows with emphasis on turbulence phenomena
 AIAA. 81-1245.
36. Delery.J., (1986) Shock-wave boundary layer interactions.
 Marvin.J.G. AGARD 280
37. Benay.R. (1987) Validation of turbulence models applied to shock-wave/boundary layer interaction.
 Coet.M.C. Delery.D. Rech.Aerosp. 1987-3.
38. Dimitriadis.K.P. (1989) Computation of shock-boundary-layer interaction with a cell vertex method.
 Leschziner.M.A. (unpublished)
39. Baldwin.B.S. (1987) Thin layer approximation and algebraic model for separated flow.
 Lomax.J. AIAA. 78-257.

40. Johnston.D.A. (1985) A mathematically simple turbulence closure model for attached and separated boundary layers.
King.L.S.
AIAA. Journal. 23 11 1684-1692.
41. Leschziner.M.A.(1989) Modelling turbulent recirculating flows by finite volume methods-current status and future directions.
Int.J.Heat and Fluid.Flow. 10 3, 186-202.
42. Van den Berg.B.(1975) Measurements in an incompressible three dimensional turbulent boundary layer under infinite swept conditions and comparison with theory.
Elsenaar.A.
Lindhout.J.
Wesseling.P.
J.Fluid.Mech. 70 127-149.
43. Bradshaw.P. (1985) Measurements in the boundary layer of three dimensional turbulent boundary layers on an 'infinite swept' wing.
Pontikos.N.S.
J.Fluid.Mech. 159 105-130.
44. Baskaran.V. (1990) Experimental investigation of three dimensional turbulent boundary layers on 'infinite' swept curved wings.
Pontikos.Y.G.
Bradshaw.P.
J.Fluid.Mech. 211 95-122.
45. Leonard.B.P. (1987) Locally modified QUICK scheme for highly convective 2D and 3D flows.
Proc.5th.Conf.on.Num.Maths.in.Laminar and Turbulent Flows. Montreal 35-47.
46. Launder.B.E. (1988) Turbulence modelling of three dimensional shear layers.
AGARD 26.
47. Clarke.D.S. (1988) The calculation of turbulent flows in complex geometries using an algebraic stress model.
Wilkes.N.S.
UKAEE Harwell R 13251.
48. Clarke.D.S. (1989) The calculation of turbulent flows in complex geometries using a differential stress model.
Wilkes.N.S.
UKAEE Harwell R 13428.

COLLABORATIVE TESTING OF TURBULENCE MODELS

Peter Bradshaw

Mechanical Engineering Department, Stanford University, Stanford, CA 94305-3030, USA

1. SUMMARY

A review is given of an ongoing international project, in which data from experiments on, and simulations of, turbulent flows are distributed to developers of (time-averaged) engineering turbulence models. The predictions of each model are sent to the organizers and redistributed to all the modellers, plus some experimentalists and other experts (total approx. 120), for comment.

An incidental result of the project is an assembly of progress reports from turbulence modellers all over the world. For present purposes, recent references to papers by US contributors are given.

2. INTRODUCTION

This project stemmed from discussions at Stanford University about a possible repeat of the 1980/81 Stanford Conference on Computation of Complex Turbulent Flows: at the 1980 meeting a set of test cases was agreed on the basis of reports by evaluators, each of whom was appointed to examine the available experimental data for a given flow type, while at the 1981 meeting the results of predictions were presented. In informal discussions at the Cornell University "Whither Turbulence" symposium in March 1989, Dr D.M. Bushnell of NASA Langley Research Center pointed out that a collaborative effort conducted by correspondence (including mailing of tapes and disks plus Fax and electronic mail) would allow better interaction, optimisation and discussion than a "sudden death" conference. (A criticism of the 1980/81 conference was that a one-week meeting was too short for thoughtful evaluation of results.) Subsequently a proposal by Peter Bradshaw (Stanford) Brian Launder (Manchester) and John Lumley (Cornell) was approved for joint funding from the US Air Force Office of Scientific Research, US Army Research Office, NASA, and the US Office of Naval Research. The aims are those of the 1980/81 conference, which was supported principally by the U.S. Air Force Office of Scientific Research - to assess and improve the art of turbulence modelling. The project is being run from Stanford University.

The project was announced in August 1989. The first stage will last until April 1991 and involves

- (1) distribution of data sets in standard form to the modellers
- (2) return of predictions to the organizers for distribution to all participants (modellers and experimenters)
- (3) return of participants' (brief) comments on the predictions, again for distribution to all participants
- (4) modification of models in the light of (2) and (3)
- (5) iteration of steps (2) to (4)
- (6) status report, provisionally entitled "Turbulence modelling - where are we?" to be presented (probably by one of the organizing committee) at the AIAA Reno meeting in January 1991.
- (7) workshop, provisionally entitled "Turbulence modelling - where are we going?" in April 1991, to consider needs for experiments and modelling.

The gap between (6) and (7) is to allow reaction by people outside the active participant group (the grant to the organizers has been much delayed, and now runs from 1 Feb. 1990 to 31 July 1991). The sponsors have agreed that this should be an international effort, with no restrictions except those involving proprietary data: any data or turbulence models resulting from the part of the project supported by US government funds would be freely available. At the time of writing there are participants from USA, Canada, England, France, the Netherlands, Norway, Sweden, Denmark, Germany (BRD), Yugoslavia, Greece, USSR, India, Australia, Japan and Korea.

The value of ongoing interaction by mail emerged even in the early stages of the project, when inspection of the first results by the organizers showed up errors in the models or numerics used by several workers (who were unanimously grateful for the information!): they were able to submit revised results. Further short-term optimi-

sation is expected, but unfortunately the length of the project – just over a year of active work – is far shorter than the four-year program the organizers proposed as the minimum to allow a worthwhile development cycle. Also, the original idea of commissioning new experiments has been abandoned, and because of the short timescale we have not tried to repeat the 1980/81 procedure of formal evaluation reports on existing data. The Data Library prepared for the 1980/81 conference still forms the basis of the test cases. Suggestions for test cases have been circulated by the organizers for comments by all Collaborators, and several new sets of data have been offered to us. As far as possible, the new test cases are being tried out, mainly at Stanford, before distribution. The evaluation of test cases will continue as part of the actual process of calculation: if different models show consistent disagreement with a given data set, then the data will be regarded with suspicion – at least by the modellers.

It is to be hoped that the present project will throw sufficient light on the current state of turbulence modelling for desirable lines of work to be identified, if not executed. Since the present organizing group is strongly biased towards Reynolds-stress modelling, contributors with other biases – or no bias at all – are especially welcome, but, to our surprise, users of Reynolds-stress models are the largest single group, outnumbering “two-equation” modellers (although some Reynolds-stress modellers say that they will use two-equation models for some test cases and two-equation models are in the majority in the results actually returned to date).

3. ORGANIZATION OF PROJECT

Participants fall into two classes (i) “modellers”, who are the originators or innovative users of turbulence models, (ii) “experimenters” who are either providers of original test data or people likely to be able to comment usefully on the results produced by the modellers. Both classes were identified initially as those who had published papers on modelling or on potentially useful experiments in about the last three years. No formal advertising has been done, but invitees have spread the word and there are now 116 Collaborators (85 modellers and the rest experimenters). 18 are from industry, 28 from government establishments and 70 from universities). The proportion from industry is small, but it is gratifying that manufacturers and consulting companies are prepared to spend money on a public-domain collaboration to improve turbulence modelling.

This total of well over a hundred participants is much larger than anticipated, and presents a severe problem in dissemination of test results: the organizers must send each of N modellers the results of all N modellers - i.e. N^2 pieces of information, each “piece” being the salient results of perhaps 50 test cases. As a result, we intend to be fairly brutal in dropping unresponsive people from the circulation list. Initially, we shall circulate only a few diagnostic results for each case, irrespective of the amount of material submitted to us: when controversies arise, larger volumes of data can be circulated ad hoc.

4. PRESENT POSITION

We began by asking all modellers to submit predictions for four “entry test cases”, namely constant-pressure (flat plate) boundary layers at a momentum-thickness Reynolds number of 10000:

- (i) skin-friction coefficient c_f at low Mach number, isothermal
- (ii) Stanton number St for low Mach number heat transfer with small temperature difference
- (iii) c_f and St for low Mach number heat transfer with absolute wall temperature equal to 6 times free stream temperature
- (iv) c_f for adiabatic wall at $M=5$ – i.e. roughly same temperature ratio as case (iii).

The object was to identify significant inaccuracies in models or numerics – and, as mentioned above, several errors have been detected and corrected.

28 modellers have so far submitted predictions for the entry test cases, and several more have been promised). Of the 28 (some of whom reported results for more than one model) there were 8 predictions with stress-transport models, one algebraic stress model, 14 “ k, ϵ ” or other two-equation models, and 4 algebraic eddy viscosity (or mixing length). 11 of the 25 were from outside the USA. All but one or two participants predicted (i) to within a few percent of the expected value of 0.0026 (most turbulence models being optimised for flat-plate skin friction), and results for St in (ii) had a standard deviation of 0.05 of the mean value, 0.00152. However results for (iii) and (iv) were more scattered, and the standard deviation of c_f at $M=5$ was 0.28 of the mean value, 0.001 (reported values ranged from 0.00061 to 0.0019). Possibly some compressible codes are not usually run above the transonic range.

Modellers were also asked to supply a one-page summary of their current research, for circulation to all participants: and so far 66 people (including some experimenters) have done so. This assembly of information is valuable in itself, and at the end of the project we shall ask participants to update their contributions for inclusion in the final report. At the end of this paper a selection of recent reference to US modelling work is given: it does *not* include all the US participants.

Distribution of data following the entry test cases is in two main stages. Early in April 1990 we distributed IBM PC disks containing nearly all the test cases from the 1981 Stanford meeting, a selection of compressible-flow data from AGAR-Dograph 315 by Fernholz et al., and a first batch of newer test cases which were offered to, or solicited by, the Organizing Committee. This first batch consisted mainly of cases that were already available to us in usable machine-readable form or required only minor editing, and comprised a "mandatory" set of test cases to be completed by serious contenders.

In the second stage, lasting until 1 August 1990, test cases requiring significant preprocessing by the organizers will be distributed when ready. Each batch of test cases will carry a deadline for receipt of results at Stanford: such deadlines are advisory rather than mandatory, but are necessary to maintain some sort of scheduling for the organizers and the modellers.

With the exception of the "entry" cases, the system of mandatory test cases used in the 1981 meeting is not being repeated: in 1981 the idea was to check the claims of model universality, but the most valuable result of that meeting has been the current attitude that *the modeller should prove his claims for range of validity* by presenting comparisons with test cases covering the full range of his model's applicability. Also, in 1981 it was essential for all queries to be cleared up during the one-week meeting: now, we have more time.

To concentrate the minds of the modellers, we have nominated "priority" test cases, covering a range of flows, for which results should be submitted to the organizers by 1 June: models which cannot deal with most of this range will be regarded as "specialized".

Clearly the art of turbulence modelling is not likely to be advanced during the project itself, but the whole point is to allow time for thought, for identification of shortcomings in the data sets,

and for correction of minor shortcomings in the models. Also, it is high time that the community tried to draw conclusions about the ranges of validity of the different models and their likely errors.

A major interest of the supporting agencies is in prediction of compressible flows (especially shock / boundary-layer interactions and/or 3-D flows): most other single-phase flows are subsets of these, and participation by workers outside aerospace, who may be interested only in low-speed flows, is of course unreservedly welcome – most turbulence data come from low-speed flows, with or without heat transfer.

5. ZONAL MODELLING AND SELECTIVE DEBUGGING

By definition, a "model" has coefficients which are evaluated within the computer program *without case-to-case adjustment by the user*. However, the "zonal modelling" concept suggested by Kline at the 1980/81 meeting implies that the coefficients may depend on the flow type, which in turn implies that the computer program must identify the kind of flow it is calculating. A model which required the user to choose the qualitative flow type (boundary layer, mixing layer, etc) from a list in the program would be acceptable in principle, but such a model would have a hard time with – for example – separation bubbles, in which the flow nominally changes from boundary layer to mixing layer and back again. We have asked Collaborators to use the same model (as defined above) for all test cases – or identify different models. Several Collaborators have pointed out that they use different codes for different types of flow (for example, a Navier-Stokes code would not be used for a boundary layer, or a compressible code for constant-density flow) but of course this should not change the empirical content of the model. We are feeling our way in dealing with numerical error. It is possible that a few of the successful predictions for constant-pressure boundary layers may have been obtained with codes that were debugged until they gave the right answer, or with models adjusted – in good faith – to compensate for finite-difference errors or plain programming errors, but we would expect such errors to show up in unexpected discrepancies in other test cases. Simple checks of mass and momentum conservation can be made as needed.

6. CONCLUSIONS

The international project on Collaborative Testing of Turbulence Models is off to a good start: there is a large discrepancy between the 85 modellers who signed up for the project and the 28 who have actually submitted results for the entry test cases by the time of writing, but the gap is likely to narrow. Even the organizers' inspection of the entry results has identified several discrepancies which have been traced to numerical errors, and as the collaboration and interaction proceeds we expect that many of the contradictions and confusions in the literature will be resolved. We hope that some improvements in turbulence modelling will be possible even during the lifetime of the present 18-month project, but the main purpose is to set the scene for a longer-term effort.

7. REFERENCES

Note: these references are NOT cited in the text.

Extended Johnson-King:

ABID, R.; VATSA, V.N.; JOHNSON, D.A.; WEDAN, B.W.: Prediction of separated transonic wing flows with a non-equilibrium algebraic model: AIAA-89-0558: 1989.

Transport equations for time scale from k , ϵ , and Monte Carlo solution of Langevin model implying Rotta-like return to isotropy:

ANAND, M.S.; POPE, S.B.; MONGIA, H.C.: Calculations of axisymmetric turbulent jets by the pdf method: 7th Sympo. on Turbulent Shear Flows, Stanford Univ.: 1989.

Main trouble is gradient model for p_v :

BERNARD, P.S.: Limitations of the near-wall k , ϵ , turbulence model: AIAA J. 24, 619: 1986.

One-equation Wolfshtein model near wall:

CHEN, H.C.; PATEL, V.C.: Near-wall turbulence models for complex flows including separation: AIAA J. 26, 641: 1988.

Useful review and new model:

CHEN, J.Y.; KOLLMANN, W.: PDF modeling of chemical nonequilibrium effects in turbulent nonpremixed hydrocarbon flames: SAND88-8605: 1988.

One equation for k , with L scaled on δ :

GOLDBERG, U.C.; CHAKRAVARTHY, S.R.: Separated flow predictions using a hybrid k - L / backflow model: AIAA-89-0566: 1989.

Modelling 2-time pdf yields time scale or length scale:

KOLLMANN, W.; WU, A.: Equation for the probability density function of velocity and scalar for turbulent shear flows: AIAA J. 27, 1052: 1989.

Wall functions mask inherent deficiencies in stress models - useful review and backstep calcs:

LASHER, W.C.; TAULBEE, D.B.: The effect of the near-wall treatment on the behavior of Reynolds-stress turbulence models for reattaching flows: 7th Sympo. on Turbulent Shear Flows, Stanford Univ.: 1989.

New pressure-strain model:

LIN, A.: On the mathematical modeling of the Reynolds stress's equations: AIAA-90-0498: 1990

Wider relevance than title suggests:

PATEL, V.C.; RODI, W.; SCHEUERER, G.: Turbulence models for near-wall and low Reynolds number flows - a review: AIAA J. 23, 1308: 1985.

Assumes that one-time p.d.f. of modified ϵ is Gaussian and has exponential correlation:

POPE, S.B.; CHEN, Y.L.: The velocity-dissipation pdf model for turbulent flows: Cornell Univ. Rept. FDA-89-06: 1989.

Poor performance of k , ϵ , and second-order models in rotating flow:

SPEZIALE, C.G.; MAC GIOLLA MHIRIS, N.: On the prediction of equilibrium states in homogeneous turbulence: J. Fluid Mech. 209, 591: 1989.

Further development of AIAA-83-1694:

VIEGAS, J.R.; RUBESIN, M.W.; HORSTMAN, C.C.: On the use of wall functions as boundary conditions for two-dimensional separated compressible flows: AIAA-85-0180: 1985.

Uses the sublayer model from AIAA-86-0213:

WALKER, J.D.A.; ECE, M.C.; WERLE, M.J.: An embedded function approach for turbulent flow prediction: AIAA-87-1464: 1987.

Slow part - odd behavior of Rotta coefficients in homogeneous strains.

WEINSTOCK, J.: Comparison of a pressure-strain rate theory with simulations: J. Fluid Mech. 205, 195: 1989.

Claims marked improvement over two-equation model for SWBL, etc.:

WILCOX, D.C.: More advanced applications of the multiscale model for turbulent flows: AIAA-88-0220: 1988.

APPENDIX – ORGANIZING COMMITTEE

P. Bradshaw, Mechanical Engineering Dept, Stanford University, Stanford, CA 94305-3030, USA:
B.E. Launder, Mechanical Engineering Dept, University of Manchester Institute of Science and Technology, Manchester M60 1QD, England: J.L. Lumley, Mechanical and Aerospace Engineering Dept, Upson and Grumman Halls, Cornell University, Ithaca, NY 14853, USA.

REPORT DOCUMENTATION PAGE

1. Recipient's Reference	2. Originator's Reference 111 AGARD-AR-291	3. Further Reference 2/8 ISBN 92-835-0625-1	4. Security Classification of Document UNCLASSIFIED						
5. Originator	Advisory Group for Aerospace Research and Development North Atlantic Treaty Organization 114 7 rue Ancelle, 92200 Neuilly sur Seine, France								
6. Title	TECHNICAL STATUS REVIEW: APPRAISAL OF THE SUITABILITY OF TURBULENCE MODELS IN FLOW CALCULATIONS 118								
7. Presented at	See Cover 2/2								
8. Author(s)/Editor(s) Various	9. Date July 1991								
10. Author's/Editor's Address Various	11. Pages 98								
12. Distribution Statement	This document is distributed in accordance with AGARD policies and regulations, which are outlined on the back covers of all AGARD publications.								
13. Keywords/Descriptors	<table> <tr> <td>Turbulence</td> <td>Mathematical models</td> </tr> <tr> <td>Turbulent flow</td> <td>Steady flow</td> </tr> <tr> <td>Flow distribution</td> <td>Unsteady flow</td> </tr> </table>			Turbulence	Mathematical models	Turbulent flow	Steady flow	Flow distribution	Unsteady flow
Turbulence	Mathematical models								
Turbulent flow	Steady flow								
Flow distribution	Unsteady flow								
14. Abstract	<p>The papers presented at a Technical Status Review on "Appraisal of the Suitability of Turbulence Models in Flow Calculations", which was held at the 66th AGARD Fluid Dynamics Panel Meeting on 26th April 1990 in Friedrichshafen, Germany, have been assembled in this report. These papers provide a status review of the activities in several of the NATO nations which is aimed at assessing the use and suitability of existing, and emerging, turbulence models in flow fields calculations. Assessments are presented for both steady and unsteady flow fields associated with a variety of problems. These problems include forced convection flow fields for both attached and separated shear layers, two-phase flows, and turbulent reacting flows in addition to flow fields driven by free convection.</p> <p>These assessments indicate that there is presently no universal turbulence model which provides acceptable results for a broad spectrum of flow problems and some doubt is expressed concerning the possibility of ever being able to develop such a model. However, some success is noted for turbulence models which were developed for and applied to problems with similar flow field characteristics. It is generally concluded that much work remains to be done to develop a more universal turbulence model which is suitable for more general applications.</p>								

<p>AGARD-AR-291</p>	<p>Turbulence Turbulent flow Flow distribution Mathematical models Steady flow Unsteady flow</p>	<p>AGARD Advisory Report 291 Advisory Group for Aerospace Research and Development, NATO TECHNICAL STATUS REVIEW APPRAISAL OF THE SUITABILITY OF TURBULENCE MODELS IN FLOW CALCULATIONS Published July 1991 98 pages</p> <p>The papers presented at a Technical Status Review on "Appraisal of the Suitability of Turbulence Models in Flow Calculations", which was held at the 66th AGARD Fluid Dynamics Panel Meeting on 26th April 1990 in Friedrichshafen, Germany, have been assembled in this report. These papers provide a status review of the</p> <p>P.T.O.</p>	<p>AGARD-AR-291</p> <p>Turbulence Turbulent flow Flow distribution Mathematical models Steady flow Unsteady flow</p>	<p>AGARD Advisory Report 291 Advisory Group for Aerospace Research and Development, NATO TECHNICAL STATUS REVIEW APPRAISAL OF THE SUITABILITY OF TURBULENCE MODELS IN FLOW CALCULATIONS Published July 1991 98 pages</p> <p>The papers presented at a Technical Status Review on "Appraisal of the Suitability of Turbulence Models in Flow Calculations", which was held at the 66th AGARD Fluid Dynamics Panel Meeting on 26th April 1990 in Friedrichshafen, Germany, have been assembled in this report. These papers provide a status review of the</p> <p>P.T.O.</p>
<p>AGARD-AR-291</p>	<p>Turbulence Turbulent flow Flow distribution Mathematical models Steady flow Unsteady flow</p>	<p>AGARD Advisory Report 291 Advisory Group for Aerospace Research and Development, NATO TECHNICAL STATUS REVIEW APPRAISAL OF THE SUITABILITY OF TURBULENCE MODELS IN FLOW CALCULATIONS Published July 1991 98 pages</p> <p>The papers presented at a Technical Status Review on "Appraisal of the Suitability of Turbulence Models in Flow Calculations", which was held at the 66th AGARD Fluid Dynamics Panel Meeting on 26th April 1990 in Friedrichshafen, Germany, have been assembled in this report. These papers provide a status review of the</p> <p>P.T.O.</p>	<p>AGARD Advisory Report 291 Advisory Group for Aerospace Research and Development, NATO TECHNICAL STATUS REVIEW APPRAISAL OF THE SUITABILITY OF TURBULENCE MODELS IN FLOW CALCULATIONS Published July 1991 98 pages</p> <p>The papers presented at a Technical Status Review on "Appraisal of the Suitability of Turbulence Models in Flow Calculations", which was held at the 66th AGARD Fluid Dynamics Panel Meeting on 26th April 1990 in Friedrichshafen, Germany, have been assembled in this report. These papers provide a status review of the</p> <p>P.T.O.</p>	

<p>activities in several of the NATO nations which is aimed at assessing the use and suitability of existing, and emerging, turbulence models in flow fields calculations. Assessments are presented for both steady and unsteady flow fields associated with a variety of problems. These problems include forced convection flow fields for both attached and separated shear layers, two-phase flows, and turbulent reacting flows in addition to flow fields driven by free convection.</p> <p>These assessments indicate that there is presently no universal turbulence model which provides acceptable results for a broad spectrum of flow problems and some doubt is expressed concerning the possibility of ever being able to develop such a model. However, some success is noted for turbulence models which were developed for and applied to problems with similar flow field characteristics. It is generally concluded that much work remains to be done to develop a more universal turbulence model which is suitable for more general applications.</p> <p>ISBN 92-835-0625-1</p>	<p>activities in several of the NATO nations which is aimed at assessing the use and suitability of existing, and emerging, turbulence models in flow fields calculations. Assessments are presented for both steady and unsteady flow fields associated with a variety of problems. These problems include forced convection flow fields for both attached and separated shear layers, two-phase flows, and turbulent reacting flows in addition to flow fields driven by free convection.</p> <p>These assessments indicate that there is presently no universal turbulence model which provides acceptable results for a broad spectrum of flow problems and some doubt is expressed concerning the possibility of ever being able to develop such a model. However, some success is noted for turbulence models which were developed for and applied to problems with similar flow field characteristics. It is generally concluded that much work remains to be done to develop a more universal turbulence model which is suitable for more general applications.</p> <p>ISBN 92-835-0625-1</p>
<p>activities in several of the NATO nations which is aimed at assessing the use and suitability of existing, and emerging, turbulence models in flow fields calculations. Assessments are presented for both steady and unsteady flow fields associated with a variety of problems. These problems include forced convection flow fields for both attached and separated shear layers, two-phase flows, and turbulent reacting flows in addition to flow fields driven by free convection.</p> <p>These assessments indicate that there is presently no universal turbulence model which provides acceptable results for a broad spectrum of flow problems and some doubt is expressed concerning the possibility of ever being able to develop such a model. However, some success is noted for turbulence models which were developed for and applied to problems with similar flow field characteristics. It is generally concluded that much work remains to be done to develop a more universal turbulence model which is suitable for more general applications.</p> <p>ISBN 92-835-0625-1</p>	<p>activities in several of the NATO nations which is aimed at assessing the use and suitability of existing, and emerging, turbulence models in flow fields calculations. Assessments are presented for both steady and unsteady flow fields associated with a variety of problems. These problems include forced convection flow fields for both attached and separated shear layers, two-phase flows, and turbulent reacting flows in addition to flow fields driven by free convection.</p> <p>These assessments indicate that there is presently no universal turbulence model which provides acceptable results for a broad spectrum of flow problems and some doubt is expressed concerning the possibility of ever being able to develop such a model. However, some success is noted for turbulence models which were developed for and applied to problems with similar flow field characteristics. It is generally concluded that much work remains to be done to develop a more universal turbulence model which is suitable for more general applications.</p> <p>ISBN 92-835-0625-1</p>

L'AGARD ne détient pas de stocks de ses publications, dans un but de distribution générale à l'adresse ci-dessus. La diffusion initiale des publications de l'AGARD est effectuée auprès des pays membres de cette organisation par l'intermédiaire des Centres Nationaux de Distribution suivants. A l'exception des Etats-Unis, ces centres disposent parfois d'exemplaires additionnels; dans les cas contraire, on peut se procurer ces exemplaires sous forme de microfiches ou de microcopies auprès des Agences de Vente dont la liste suite.

CENTRES DE DIFFUSION NATIONAUX

ALLEMAGNE

Fachinformationszentrum,
Karlsruhe
D-7514 Eggenstein-Leopoldshafen 2

BELGIQUE

Coordonnateur AGARD-VSL
Etat-Major de la Force Aérienne
Quartier Reine Elisabeth
Rue d'Evere, 1140 Bruxelles

CANADA

Directeur du Service des Renseignements Scientifiques
Ministère de la Défense Nationale
Ottawa, Ontario K1A 0K2

DANEMARK

Danish Defence Research Board
Ved Idraetsparken 4
2100 Copenhagen Ø

ESPAGNE

INTA (AGARD Publications)
Pintor Rosales 34
28008 Madrid

ETATS-UNIS

National Aeronautics and Space Administration
Langley Research Center
M/S 180
Hampton, Virginia 23665

FRANCE

O.N.E.R.A. (Direction)
29, Avenue de la Division Leclerc
92320, Châtillon sous Bagneux

GRECE

Hellenic Air Force
Air War College
Scientific and Technical Library
Dekelia Air Force Base
Dekelia, Athens TGA 1010

ISLANDE

Director of Aviation
c/o Flugrad
Reykjavik

ITALIE

Aeronautica Militaire
Ufficio del Delegato Nazionale all'AGARD
3 Piazzale Adenauer
00144 Roma EUR

LUXEMBOURG

Voir Belgique

NORVEGE

Norwegian Defence Research Establishment
Attn: Biblioteket
P.O. Box 25
N-2007 Kjeller

PAYS-BAS

Netherlands Delegation to AGARD
National Aerospace Laboratory NLR
Kluyverweg 1
2629 HS Delft

PORTUGAL

Portuguese National Coordinator to AGARD
Gabinete de Estudos e Programas
CLAFAs
Base de Alfragide
Alfragide
2700 Amadora

ROYAUME UNI

Defence Research Information Centre
Kentigern House
65 Brown Street
Glasgow G2 8EX

TURQUIE

Milli Savunma Başkanlığı (MSB)
ARGE Daire Başkanlığı (ARGE)
Ankara

LE CENTRE NATIONAL DE DISTRIBUTION DES ETATS-UNIS (NASA) NE DETIENT PAS DE STOCKS
DES PUBLICATIONS AGARD ET LES DEMANDES D'EXEMPLAIRES DOIVENT ETRE ADRESSEES DIRECTEMENT
AU SERVICE NATIONAL TECHNIQUE DE L'INFORMATION (NTIS) DONT L'ADRESSE SUIT.

AGENCES DE VENTE

National Technical Information Service
(NTIS)
5285 Port Royal Road
Springfield, Virginia 22161
Etats-Unis

ESA/Information Retrieval Service
European Space Agency
10, rue Mario Nikis
75015 Paris
France

The British Library
Document Supply Division
Boston Spa, Wetherby
West Yorkshire LS23 7BQ
Royaume Uni

Les demandes de microfiches ou de photocopies de documents AGARD (y compris les demandes faites auprès du NTIS) doivent comporter la dénomination AGARD, ainsi que le numéro de série de l'AGARD (par exemple AGARD-AG-315). Des informations analogues, telles que le titre et la date de publication sont souhaitables. Veuillez noter qu'il y a lieu de spécifier AGARD-R-*nnn* et AGARD-AR-*nnn* lors de la commande de rapports AGARD et des rapports consultatifs AGARD respectivement. Des références bibliographiques complètes ainsi que des résumés des publications AGARD figurent dans les journaux suivants:

Scientific and Technical Aerospace Reports (STAR)
publié par la NASA Scientific and Technical
Information Division
NASA Headquarters (NTT)
Washington D.C. 20546
Etats-Unis

Government Reports Announcements and Index (GRA&I)
publié par le National Technical Information Service
Springfield
Virginia 22161
Etats-Unis

(accessible également en mode interactif dans la base de données bibliographiques en ligne du NTIS, et sur CD-ROM)

NATO  OTAN

7 RUE ANCELLE · 92200 NEUILLY-SUR-SEINE

FRANCE

Telephone (1)47.38.57.00 · Telex 610 176

Telefax (1)47.38.57.99

DISTRIBUTION OF UNCLASSIFIED
AGARD PUBLICATIONS

AGARD does NOT hold stocks of AGARD publications at the above address for general distribution. Initial distribution of AGARD publications is made to AGARD Member Nations through the following National Distribution Centres. Further copies are sometimes available from these Centres (except in the United States), but if not may be purchased in Microfiche or Photocopy form from the Sales Agencies listed below.

NATIONAL DISTRIBUTION CENTRES

BELGIUM

Coordonnateur AGARD — VSL
Etat-Major de la Force Aérienne
Quartier Reine Elisabeth
Rue d'Evere, 1140 Bruxelles

CANADA

Director Scientific Information Services
Dept of National Defence
Ottawa, Ontario K1A 0K2

DENMARK

Danish Defence Research Board
Ved Idraetsparken 4
2100 Copenhagen Ø

FRANCE

O.N.E.R.A. (Direction)
29 Avenue de la Division Leclerc
92320 Châtillon

GERMANY

Fachinformationszentrum
Karlsruhe
D-7514 Eggenstein-Leopoldshafen 2

GREECE

Hellenic Air Force
Air War College
Scientific and Technical Library
Dekelia Air Force Base
Dekelia, Athens TGA 1010

ICELAND

Director of Aviation
c/o Flugrad
Reykjavik

ITALY

Aeronautica Militare
Ufficio del Delegato Nazionale all'AGARD
3 Piazzale Adenauer
00144 Roma/EUR

LUXEMBOURG

See Belgium

NETHERLANDS

Netherlands Delegation to AGARD
National Aerospace Laboratory, NLR
Kluyverweg 1
2629 HS Delft

NORWAY

Norwegian Defence Research Establishment
Attn: Biblioteket
P.O. Box 25
N-2007 Kjeller

PORTUGAL

Portuguese National Coordinator to AGARD
Gabinete de Estudos e Programas
CLAFAs
Base de Alfragide
Alfragide
2700 Amadora

SPAIN

INTA (AGARD Publications)
Pintor Rosales 34
28008 Madrid

TURKEY

Milli Savunma Başkanlığı (MSB)
ARGE Daire Başkanlığı (ARGE)
Ankara

UNITED KINGDOM

Defence Research Information Centre
Kentigern House
65 Brown Street
Glasgow G2 8EX

UNITED STATES

National Aeronautics and Space Administration (NASA)
Langley Research Center
M/S 180
Hampton, Virginia 23665

THE UNITED STATES NATIONAL DISTRIBUTION CENTRE (NASA) DOES NOT HOLD STOCKS OF AGARD PUBLICATIONS, AND APPLICATIONS FOR COPIES SHOULD BE MADE DIRECT TO THE NATIONAL TECHNICAL INFORMATION SERVICE (NTIS) AT THE ADDRESS BELOW.

SALES AGENCIES

National Technical
Information Service (NTIS)
5285 Port Royal Road
Springfield, Virginia
United States

ESA/Information Retrieval Service
European Space Agency

The British Library

Requests for microfilm
AGARD serials
AGARD Reports

Scientific and Technical
Information Service (STIS)
NASA Headquarters
Washington D.C. 20546
United States



304377++P+UL

Hampton, Virginia 22161
United States

(also available online in the NTIS Bibliographic
Database or on CD-ROM)



Printed and Published by JNL LIMITED
40 Chiswick Lane, Uxbridge, Middlesex, U.K. UB8 3TZ

ISBN 92-835-0625-1